THE EFFECT OF CRYSTALLISATION VARIABLES ON THE POWDER CHARACTERISTICS, MECHANICAL PROPERTIES AND COMPRESSION BEHAVIOUR OF DEXTROSE

THE EFFECT OF CRYSTALLISATION VARIABLES ON THE POWDER CHARACTERISTICS, MECHANICAL PROPERTIES AND COMPRESSION BEHAVIOUR OF DEXTROSE

Ian Lafferty B.Sc. (Hons)

A thesis submitted to

De Montfort University, Leicester

For the Degree of Doctor of Philosophy

December 1998

Acknowledgements

First and foremost I would like to thank my supervisors Professor M. E. Aulton and Dr. A. M. Twitchell for their guidance, advice and support. The encouragement received from others especially Dr. J. Taylor, Dr. P Taylor and Dr. G Smith was also much appreciated.

Thanks are also due to all the technical support staff in the Department of Pharmaceutical Science for their assistance and support.

Special thanks is also due to Dr. J. I. Wells, School of Pharmacy, Liverpool John Moores University for his guidance and the use of the compaction simulator and to the staff at the School of Material Science, University of Nottingham for performing the X-ray diffraction studies.

Most importantly I wish to thank my parents and family and my fiancée Danielle for their support, encouragement and understanding without which this thesis would not have been possible.

CONTENTS

PAGE

CHAPTER FIVE: RESULTS

COMPACTION BEHAVIOUR - HECKEL PLOTS

List of Figures

List of Tables

ABSTRACT

The work described in this thesis was performed to investigate the effect of altering the conditions used during the crystallisation of dextrose on its physio-chemical and mechanical properties and how these in turn altered its behaviour both during and after compaction.

Initial experiments were conducted in an effort to grow large single crystals of dextrose capable of being mechanically tested. Although a gel crystallisation technique capable of growing single crystals of dextrose was developed, the crystals proved unsuitable for testing and the gel crystallisation technique was not flexible enough to permit a wide range of crystallisation conditions to be examined.

A second set of crystallisation experiments was conducted using a small batch crystallisation unit. Batches of dextrose were crystallised by altering a wide range of process conditions such as crystallisation cooling rate, level of initial supersaturation, growth time, seed crystal size, presence of impurities and crystallisation temperature.

The effect of altering these crystallisation conditions on the physio-chemical properties of the crystals was assessed using techniques such as X-ray diffraction and Helium pycnometery. These tests showed that changes to the crystallisation conditions could influence various physical and solid-state characteristics of dextrose.

The various batches of crystalline dextrose were then compacted and the effect of altering the crystallisation conditions on the compaction behaviour of dextrose was evaluated using Heckel plots. Mechanical properties of the compacts such as tensile strength, Brinell indentation hardness and elastic modulus were determined and by mathematical treatment of the data an estimate was made of the mechanical properties of the bulk (un-compacted) crystalline dextrose.

The batch (DC48) crystallised between the temperatures of 56 and 48°C at a cooling rate of 0.5°C/h with a Supersaturation ratio of 1.3 resulted in the material best suited to use as a direct compression tableting excipient.

These experiments showed that manipulation of the crystallisation conditions could result in important changes to the behaviour of crystalline dextrose during the compaction process and to the quality of the compacts produced thus demonstrating the need for precise control of crystallisation conditions if a reproducible product is to be obtained. They also illustrated the fact that by careful control and selection of experimental variables the crystallisation process is capable of being used as a tool for the deliberate engineering of materials whose properties have been optimised to suit their intended use.

CHAPTER ONE

INTRODUCTION

1.1 General introduction

Ever since the first tablet press was introduced by Brockendon, in 1843, technological advances have continually produced machinery and materials that have increased production outputs, extended the range of materials which may be used in tablets and resulted in a wider more complex variety of products, such as modified release formulations. The basic process of subjecting a powder mass to an applied force within a confined space in order to produce a strong coherent compact has, however, remained largely unchanged.

Despite the extensive efforts of many research teams and a multitude of publications on the subject, the tableting process continues to causes many problems. These problems, such as low tablet strength and capping vary not only from product to product but also from batch to batch. There has also been an apparent inability to fully utilise the obvious advantages of the direct compression process. Overcoming these issues takes time, wastes materials and increases expenditure, ensuring that tablet development and production is a relatively slow, labour intensive process which is not easily automated. These difficulties arise mainly because there is still a lack of proper understanding about what many experts regard as the art of tablet making which continues to be reliant more on empirical knowledge than scientific theory (Rubinstein, 1987). Also the ability to predict the compression behaviour and subsequent compact quality of any formulation is very limited. Clearly, therefore, it is important to understand and quantify the fundamental material and processing properties of drugs and excipients since these parameters can affect significantly the manufacture and performance of solid dosage forms (York 1983).

A thorough understanding of the fundamental particulate and mechanical properties of pharmaceutical materials has been shown to be vital in characterising and predicting their performance when used in operations such as compaction. They can also indicate differences in the inter-molecular and inter-atomic structure of materials and their crystals (York, 1983; Hiestand and Smith, 1984; Roberts and Rowe, 1987a). Several workers (e.g. Jones 1977, 1981 and York 1992) have classified material properties into various groups.

Properties, which have been identified as being influential in determining the processing behaviour and subsequent performance of pharmaceutical powders can be classified into three, inter-related groups as shown in Table 1.1. Solid state and particulate properties are often grouped together under the term physico-chemical properties.

Table 1.1 Classification of material properties

Solid state properties	**Particulate properties**	**Mechanical properties**
Degree of crystallinity	True density	Crushing strength
Crystal habit	Bulk density	Tensile strength
Crystal hardness	Particle size	Modulus of elasticity
Polymorphism	Particle shape	Indentation hardness
Crystal imperfections	Moisture content	Yield pressure

The earliest work investigating the compression process was carried out not by pharmaceutical scientists but by researchers in the ceramic and metallurgy industries (e.g. Walker, 1924a, b, c; Jones, 1937; Bal'shin, 1938; Seelig and Wulff, 1946). With respect to pharmaceutical materials, work on the physics of the compression process began in earnest in the mid 1950's with the development of the instrumented tablet press (Huguchi et al., 1954). In the years that have followed many experimental techniques have been developed which can be used to define both the compression processes and/or assess the fundamental mechanical and material properties of tablets and tableting excipients. Examples of these include force-displacement profiles, compaction simulation studies, flexure testing and indentation testing. Consequently there has been a steady output of theories and equations which attempt to describe the compression process and the compaction behaviour of materials. The capability to predict how a single material (never mind a tablet formulation combining several materials, each with their own deformation characteristics) will behave, is however, still a major goal for pharmaceutical scientists. The problem is often further complicated by lot to lot and source to source variations of mechanical properties experienced for a particular material.

In more recent years workers such as Hiestand and Smith (1984) and Roberts and Rowe (1987b) have derived indices and ratios which combine several mechanical properties of both materials and compacts, which they suggest may be useful in bringing a predictive capability to the compression of pharmaceutical materials.

Another area of study, which has generated a great deal of interest in recent years, is the subject of crystal engineering. Here, controlled manipulation of the crystallisation process is employed to deliberately modify materials, thus ensuring they have desired or improved material properties, such as improved flowability or compressibility, "designed in". However, before these approaches can be used to universally and reproducibly manufacture materials with predictable and desirable properties and before tableting can become a more scientific and efficient process the fundamental mechanical and material properties which are influential in dictating the compaction behaviour of pharmaceutical materials must be identified, understood and quantified.

1.2 The compression process

In order to produce good pharmaceutical tablets the active ingredient (drug) must first be formulated and processed with other materials known as excipients. These are specifically chosen to produce a powder with the necessary processing properties (such as compressibility and flowability) required to cope with the demands of modern tableting equipment.

Wet granulation and direct compression are the two principle methods used to prepare a formulation for compression into tablets. The direct compression route has several advantages over the wet granulation method. The number of unit operations involved is reduced, thus saving time, increasing efficiency and leading to greater batch to batch uniformity, while the elimination of heat and solvents from the process ensures greater product stability. However, despite these advantages, wet granulation remains the most popular method in use. This is partly because until direct compression became a viable process, wet granulation was the only real alternative and so its use has become somewhat traditional with the technology and expertise already well established. The other reason for this apparent reluctance to adopt the direct compression route centres on the availability of materials, which will lend themselves to the process. Clearly the direct compression route places much more stringent

demands on the particle properties of materials than wet granulation (Armstrong; 1986).

Since the mid 1950's a substantial amount of research has been conducted in an attempt to clarify and understand the physics of the tableting process and the mechanisms involved in the compaction, deformation and bonding of pharmaceutical materials. Consequently, there has been a steady output of theories and equations describing the various processes involved in the compaction of powder systems, which have been reviewed by Wray (1992). Workers including Train (1956) and Huffine (1962) split the compaction process into several distinct stages, all of which play important roles in defining the quality of the final product.

- die filling and packing
- particle rearrangement
- deformation (elastic or plastic)
- fragmentation
- bonding
- decompression and ejection

In the following sections, each of these stages will be briefly reviewed.

1.2.1 Die filling

The compression process begins by filling the powder formulation, containing drug and other excipients, into a die cavity. In general, this is achieved by utilising the force of gravity, but the nature of the compressing device, the filling technique and material properties are all-important factors to be considered. In a single punch machine, the powder is moved over the empty die by a feed shoe and gravity directs the powder into the cavity forming a uniform powder bed. In high-speed rotary machines, the use of feed frames, which spread the powder over the die table, and the centripedial force created by the action of the machine can often result in a wedge shaped or v-shaped powder bed being formed. In research type, compression machines such as compaction simulators the die is usually manually filled which can result in the formation of a conical shaped powder bed. Ridgway-Watt (1981) using

holographic interferometry found that tablets produced from Avicel filled into a die with uniform, wedge shaped and conical packing showed differences which reflected the various deposition techniques.

Material properties, such as the shape, size, density and surface properties, all of which contribute to the flowability of a powder, are also important in determining the packing characteristics and thus the initial porosity of the powder bed. Clearly, cubic particles will fill and pack differently to long needle shaped particles, while particles with poor flow properties and a skewed range of sizes may produce a powder bed with large void areas. These material properties are also further complicated by the fact that the powder blend being compressed will generally consist of several materials each with different packing characteristics.

Woodhead and Newton (1984) used a γ-ray attenuation technique to investigate the variability of porosity within a powder bed. They showed that both the overall porosity and the local porosity were dependent on the deposition technique, used to fill the die, and on material properties. These packing characteristics are important as they define the amount of inter particulate contact during the early stages of the compaction process which has consequences for both the deformation and bonding processes.

1.2.2 Particle rearrangement

As soon as the upper punch enters the die, it exerts a compression force on the powder bed. This causes inter-particle slippage, which results in a decreased powder volume and thus closer packing of the particles. It was shown by De Baley (1972) that during this stage no force was transmitted to the lower punch, suggesting that all the applied force is initially used to overcome friction and cohesion between particles. Exactly how much force is required to cause this rearrangement is dependent on material properties, such as the shape, size and surface properties, of the powder mixture. It was shown by York (1978) that as the particle size of a powder was decreased the amount of rearrangement taking place at low compression pressures was increased. This is because the smaller particles resulted in an increased number of contact points, which therefore increased the overall frictional and cohesive forces within the powder

system. This in turn increased the porosity of the powder bed at zero pressure and so more re-arrangement was required to form a compact.

1.2.3 Deformation

As the applied force is further increased the individual particles become immobilised and the force is transmitted through inter particulate contact points to the lower punch. Areas of stress develop at these contact points and deformation of the particles takes place resulting in a change of geometry. The amount of relative deformation produced is known as the strain. The nature of this deformation can be described as either elastic, plastic or destructive, and is dependent on factors such as the rate and magnitude of the applied force, the duration of application and the material's mechanical properties.

Under relatively low compression forces, some materials behave according to Hooke's law, which states that the strain produced is proportional to the stress. Once the applied force is removed the deformation recovers completely and is described as elastic deformation. The elasticity of a material is characterised by its modulus of elasticity, which is determined from the slope of the stress-strain plot in the elastic region. The measurement of this fundamental property will be discussed later. Few if any materials however, behave 100% elastically as the inter-particle voids initially present in a powder bed cannot be recovered by the removal of the force.

For most materials, however, the linear stress-strain relationship eventually reaches a limit called the yield point and any further deformation which occurs beyond this point does not obey Hooke's law and cannot be recovered. This type of deformation is known as permanent or plastic deformation and is highly dependent on the crystal structure of the material. Several methods for characterising this property, particularly the use of Heckel plots, will be discussed in later sections of this chapter.

In reality, the powder materials used by the pharmaceutical industry have both elastic and a plastic component. Which one predominates is largely characteristic of the material and is extremely important in determining the properties of the final product.

Tablets made from very elastic materials are likely to suffer from capping or laminating faults, as there will be a large recovery of deformation, releasing energy and thus breaking bonds, when the applied force is removed. The compaction behaviour of materials which are known to behave plastically were shown to be time dependent by David and Augsberger (1977) and are thus influenced by punch velocities (Roberts and Rowe, 1985). It is therefore generally concluded that a limited elastic component and a high plastic component will result in good compact strength.

1.2.4 Fragmentation

As the applied force is further increased the powder particles can become stressed at a magnitude or rate, which exceeds the material's ability to deform, and thus they fracture (Train and Lewis 1962). Particle fracture is dependent on the distribution of flaws or cracks within a particle and is also known to be sensitive to particle size.

Fragmentation results in the generation of fresh surfaces, which then behave as new potential bonding sites. These smaller fragments may also undergo more rearrangement to fill the void spaces, so increasing the densification of the compact. They can also undergo further deformation (elastic or plastic) as previously described. The number of inter-particulate bonds and thus the strength of compacts prepared from fragmenting materials has been demonstrated to be a function of the extent of fragmentation taking place (Eriksson and Alderborn, 1995; Van Kamp, et al., 1986). Roberts and Rowe (1987a) found that some materials, such as lactose monohydrate, showed a transition from plastic behaviour to brittle behaviour as particle size was changed, while other materials such as microcrystalline cellulose, showed no transitional properties. In general, a high degree of fragmentation favours high compact strength.

1.2.5 Bonding

As the compression forces are increased still further the new material surfaces, formed as a result of deformation and/or fragmentation, come into contact with each other and form areas of bonding which impart strength and cohesion to the compact. Several theories as to how this bonding takes place have been suggested but have proved difficult to substantiate experimentally. Research including that of Turba

and Rumpf (1964), York and Pilpel (1972), De Boer et. al. (1978), and Leuenberger (1986) has, however, lead to the following mechanisms being recognised as the most relevant to the bonding of pharmaceutical particulate systems.

- cold welding
- solid bridges
- melting at contact points
- mechanical interlocking

Cold welding or cold bonding is generally believed to be the predominant mechanism of bonding in pharmaceutical compacts (Hiestand, 1978). The increasing pressure forces the particles closer together forming areas of true inter-particular contact. The interfacial energy is always less than the energies of the two surfaces and thus strong attractive forces (bonds) develop. These bonds will be similar to the internal bonds of the particles. Van der Waals forces are considered to be the most important attractive forces involved in cold welding, resulting from irregular dispersions of electrons in atoms or from asymmetry in the molecules. Other forces such as columbic attraction between charged species, covalent bonding, and hydrogen bonding may also be involved in cold bonding depending on the nature and structure of the material (Ezesobo and Pilpel, 1976; Luangtana-Anan, 1990).

Due to the high pressures experienced at the contact points melting or dissolution followed by recrystallisation can take place resulting in the formation of solid bridges between particles, which increases the strength of a compact. It has also been suggested that inter-particle friction experienced during compression may be sufficient to raise the local temperature enough to melt some tableting materials. Rankell and Higuchi (1968) using heat transfer kinetics demonstrated that the melting temperatures of typical pharmaceutical substances could be attained during compression, while York and Pilpel (1972) showed that because of the high pressures observed at the microscopic contact points, melting could occur at temperatures significantly below the actual melting point of the material. On cooling, the melt solidifies causing fusion bonding or solid bridges between particles and thus increases the strength of the compact. This mechanism could be especially important in

determining the strength of compacts prepared from materials with low specific heat capacities and poor thermal conductivity.

The mechanical interlocking theory suggests that when under compression pressure, particles deform and/or fracture and that the edges of the particles then interlock to form a mechanical bond. This type of bonding will depend on the particle shape and surface properties but is thought to provide only a minimal contribution to the overall strength of a compact.

Bonding is clearly a complex process and the contribution of each type of bond is dependent on the characteristics of the materials being compressed. It should be remembered that the bonding characteristics of one material may be totally changed by the presence of another material with completely different characteristics, and so each system must be considered separately.

1.2.6 Decompression, ejection and recovery

The decompression and ejection events and the post compression behaviour of a compact can also have a significant effect on its subsequent properties and behaviour. Once the upper punch is removed, the compact is free to recover in an axial direction and may experience some residual die wall pressure. Next the compact is ejected from the die and is now free to recover in a radial direction also. The extent to which this recovery disrupts the bonds previously formed and thus detrimentally affects the strength of the compact depends on the mechanism(s) by which consolidation was achieved. If the material was brittle and consolidated by a fragmentation process, the recovery stresses will have no effect, as the fragments cannot re-combine. Similarly, the deformation of a purely plastic material is by definition non-recoverable and therefore no bond disruption would be expected. Most real materials, however, posses some degree of elastic behaviour. This will tend to reverse any elastic deformation, and therefore, some recovery and bond disruption would be expected.

Shlanta and Milosovich (1964) reported that when some materials were held under a constant pressure the compressive stresses were observed to decreased with time. The mechanism by which this stress relaxation takes place is known as plastic flow. Over time, the applied force causes the particles to flow into

voids or spaces, so reducing the volume of the compact and thus relieving the stress. Plastic flow is thought to be an important factor in counteracting the detrimental, effects of elastic recovery.

Armstrong and Haines-Nutt (1972) defined elastic recovery (ER) using the equation:

$$ER = [(H_o - H_p) / H_p] \times 100 \qquad \text{(equation 1.1)}$$

Where H_o and H_p are the heights (or thickness) of a compact under pressure and after ejection respectively.

Stress relaxation (SR) was defined by Banguda and Pilpel (1985):

$$SR = [(H_p - H_t) / H_t] \times 100 \qquad \text{(equation 1.2)}$$

Where H_t is the height of a compact held under the maximum load for thirty seconds. The ratio of ER/SR was found to be inversely proportional to the tensile strength of compacts prepared from paracetamol / Avicel mixtures. It has also been used to predict the capping and lamination tendency.

1.2.7 Porosity - pressure relationships

Many theories and equations have been developed in an attempt to quantitatively characterise the compaction of powders in a die. These have been critically reviewed by Krycer and Pope (1982). Several workers, including Kawakita et al. (1966), Cooper and Eaton (1966) and Heckel (1961a and b) have utilised porosity - pressure relationships in order to describe the densification and consolidation of a powder bed. Of these, the Heckel treatment is by far the most widely used for pharmaceutical purposes and will be discussed in more detail later (Section 1.2.8).

The porosity (ε) of a powder system is a measure of both the inter and intra particle voids and pores and can be defined by equation 1.3:

$$\varepsilon = 1 - \rho_a / \rho_T \qquad \text{(equation 1.3)}$$

where ρ_a is the apparent density of the compact and ρ_T is the true density of the material, as normally determined by helium pycnomerty. The ratio ρ_a / ρ_T is commonly referred to as the relative density, D.

1.2.8 The Heckel equation and its applications

Heckel (1961a, b) considered the densification of metal powder to be analogous to a first order reaction and introduced the equation:

$$\ln (1/1\text{-}D) = kP + A \qquad \text{(equation 1.4)}$$

where D is the relative density at pressure P and both k and A are constants. For an ideal plastic material, a linear plot would be expected when ln (1/1-D) is plotted against compression pressure. In reality, however, deviations occur at both low and high pressures due to particle rearrangement and strain hardening respectively. A typical Heckel plot is detailed in Figure 1.1. In Heckel's work the slope of the graph, k, was intended to represent the plasticity of the material. With respect to pharmaceutical materials, k is the slope obtained from the linear portion of the Heckel plot. Hersey and Rees (1971) showed that:

$$P_y = 1/k \qquad \text{(equation 1.5)}$$

where P_y is known as the mean yield pressure of the material. This parameter has since been widely used to characterise the compaction behaviour of pharmaceutical materials. From the value of the intercept A, obtained by extrapolating the linear portion of the Heckel plot to zero pressure, a relative packing fraction D_A can be calculated using the equation:

$$D_A = 1 - e^{-A} \qquad \text{(equation 1.6)}$$

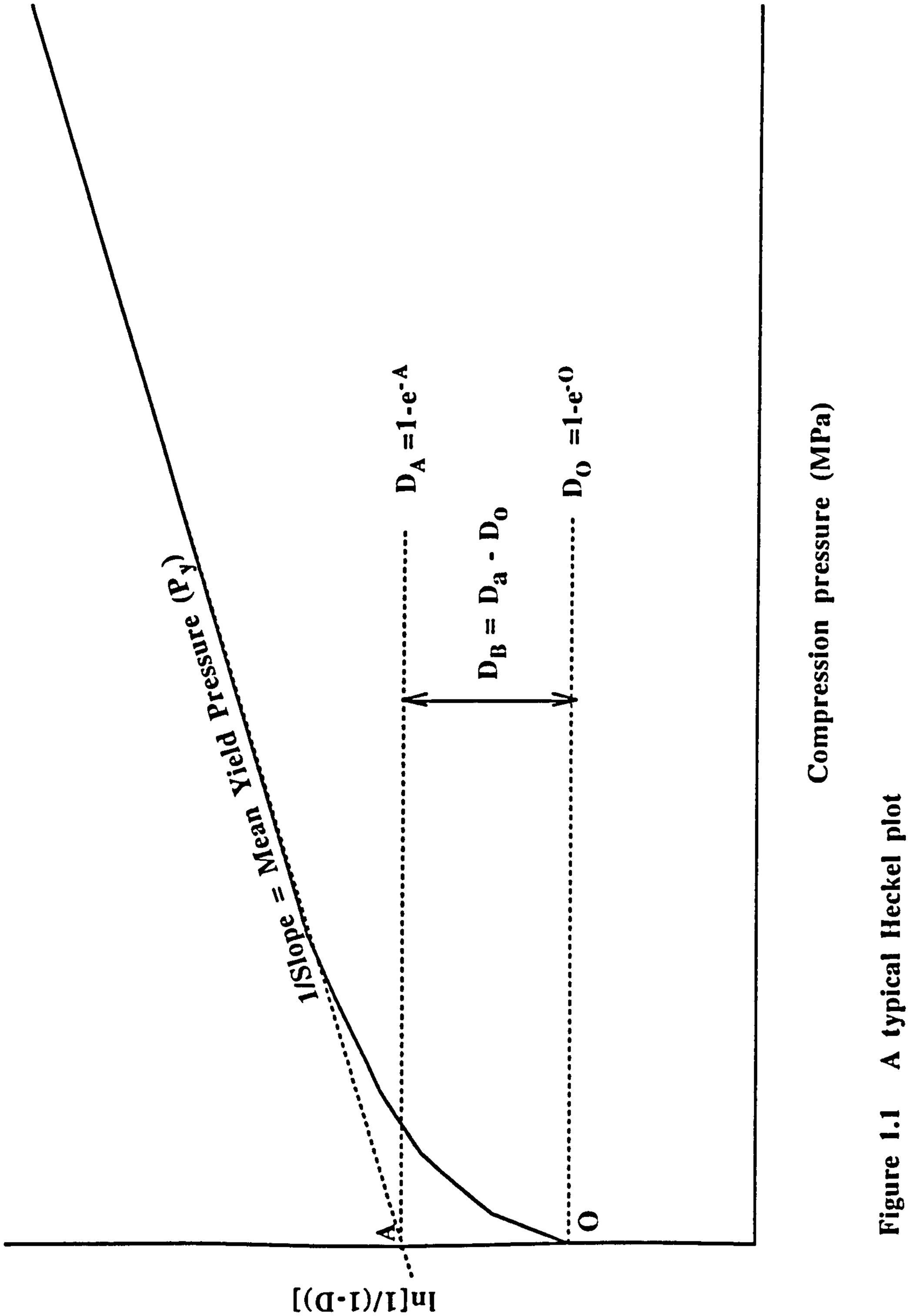

A typical Heckel plot

Figure 1.1

The value of the relative density at the point where the compression is first detected is known as D_o and thus another packing fraction, D_B, which is used in describing the amount of particle rearrangement which takes place at low compression pressures, can be calculated from equation 1.7:

$$D_B = D_A - D_o \qquad \text{(equation 1.7)}$$

The values of D_A, D_B, and D_o are in general only affected by the shape and size of the particles in the powder mixture.

Three distinct shapes of Heckel plots (Figure 1.2) representing different compaction mechanisms have been identified by Hersey and Rees (1971) and York and Pilpel (1973). Materials were categorised by compressing different particles size ranges. In type A deformation, the three lines represent materials with different initial packing densities (D_o). Consolidation occurs initially by particle slippage and rearrangement, followed by plastic deformation. Such materials (e.g. sodium chloride and microcrystalline cellulose) retain different degrees of porosity depending on their initial packing in the die, (Hardman and Lilley 1979 and M^c Kenna and M^c Cafferty 1982).

In type B deformation, the plots are slightly curved at the beginning but become coincidental after a certain compression pressure is exceeded. This type of behaviour is characteristic of materials which densify initially by fragmentation followed by plastic deformation (e.g. lactose and calcium carbonate). The coinciding of the lines corresponds to the end of the fragmentation stage. In general, the linear portion of type A plots, are steeper than that of type B plots. Therefore, materials with type A deformation behaviour, usually have a lower mean yield pressure and so are more easily deformed (i.e. they are more plastic). Type C deformation behaviour is generally associated with materials which have a very low yield pressure and a limiting porosity, (i.e. they can be compacted to zero porosity). York and Pilpel (1973) found fatty acids behaved in this way. These materials experience no rearrangement and so consolidation occurs purely by plastic flow with the possibility of melting at contact points.

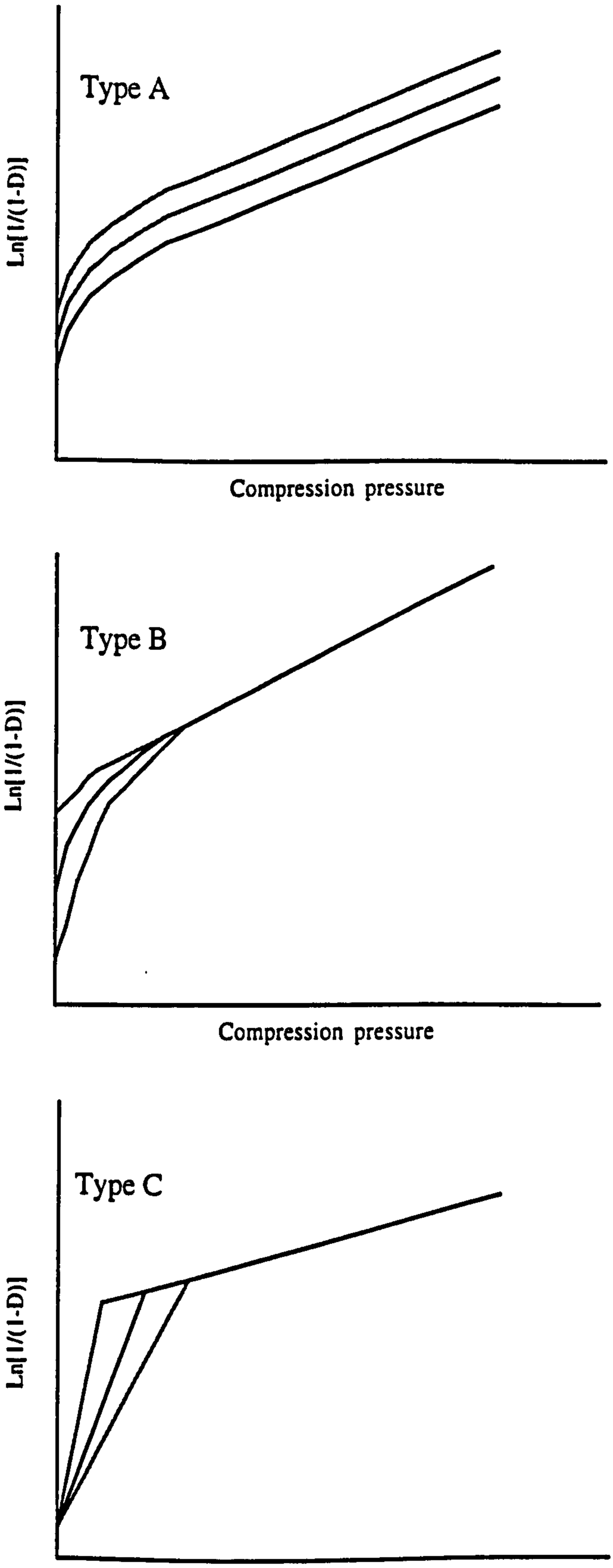

Figure 1.2 Different types of compression behaviour distinguished by the different shapes of Heckel plots

Several workers have investigated the effects of experimental variables on Heckel plots and have demonstrated their limitations in predicting compaction behaviour. Rue and Rees (1978) observed that materials such as microfine cellulose (Elcema) gave completely non-linear Heckel plots. Roberts and Rowe (1986, 1987) have shown that the predominant compaction mechanism may be a function of a material's particle size. They described how the behaviour of some materials displayed the tendency to change from brittle to ductile as their particle size was changed. York (1979) was critical of the use of Heckel plots as the results are influenced by factors such as the history of the material, the method of die filling, compaction rate, lubrication effects and the method used to determine the density of the compact.

There are two possible methods for determining yield stress values from compression studied via Heckel plots. These two approaches are generally referred to as 'at pressure' and 'zero pressure' or ejected tablet measurements, and can result in quite different values being obtained. These methods differ in the way the dimensions and thus the density of the material being studied are determined. If the Heckel plot is constructed by continually measuring the dimensions of a compact within the die as the pressure is increased, then the yield pressure value will be an 'at pressure' measurement. If a series of compacts are, however, prepared over a range of compaction pressures and their dimensions determined after ejection, then the yield pressure is clearly a 'zero pressure' measurement. There are several opinions as to which is the best method. Roberts and Rowe (1987b) suggest that if the measurements are made 'at pressure' with lubricated punches, at very slow speed and the particle size of the material is below its brittle/ductile transition point, then the yield stress obtained by using the Heckel plot will be comparable to that obtained from the indentation hardness (determined at or extrapolated to zero porosity) using equation 1.12 (see section 1.3.5).

Fell and Newton (1971) and York (1979), however, have shown that 'at pressure measurements' include an elastic component in the deformation and thus result in a falsely, low yield pressure value. Heckel (1961a, b) used zero pressure measurements but made them while the compact was still inside the die and so did not allow for full elastic recovery. Krycer and Pope (1982) reviewing the interpretation of compaction

data stated that the measurements should be made at zero pressure on an ejected compact.

Normally only that part of the Heckel plot obtained during the compression stage (increasing compression force) is employed. Duberg and Nystrom (1986), however, utilised 'at pressure' Heckel plots, obtained during both the compression and decompression stages of compaction for several materials. They divided the plots into three separate phases which they used to discuss the compaction mechanisms of the materials. A typical complete compression cycle diagram with the separate phases is shown in Figure 1.3. They evaluated the fragmentation behaviour of a material using linear regression of phase 1. The yield pressure was determined from phase 2 and was shown to reflect the total deformation ability of the material. Phase 3 was used to evaluate the elastic behaviour of the material by monitoring the change in porosity as determined by the downward slope of the decompression phase of the Heckel plot.

Paronen and Juslin (1983) suggested that by subtracting the gradient of the decompression slope obtained from the zero pressure method from that obtained by the 'at pressure' method and taking the reciprocal of that value, one would get a parameter which describes the tendency of a compact to recover elastically.

In their critical review of compact data, Krycer and Pope (1982) suggest that Heckel plots are most useful in comparing the compression of different materials, when identical experimental conditions have been used.

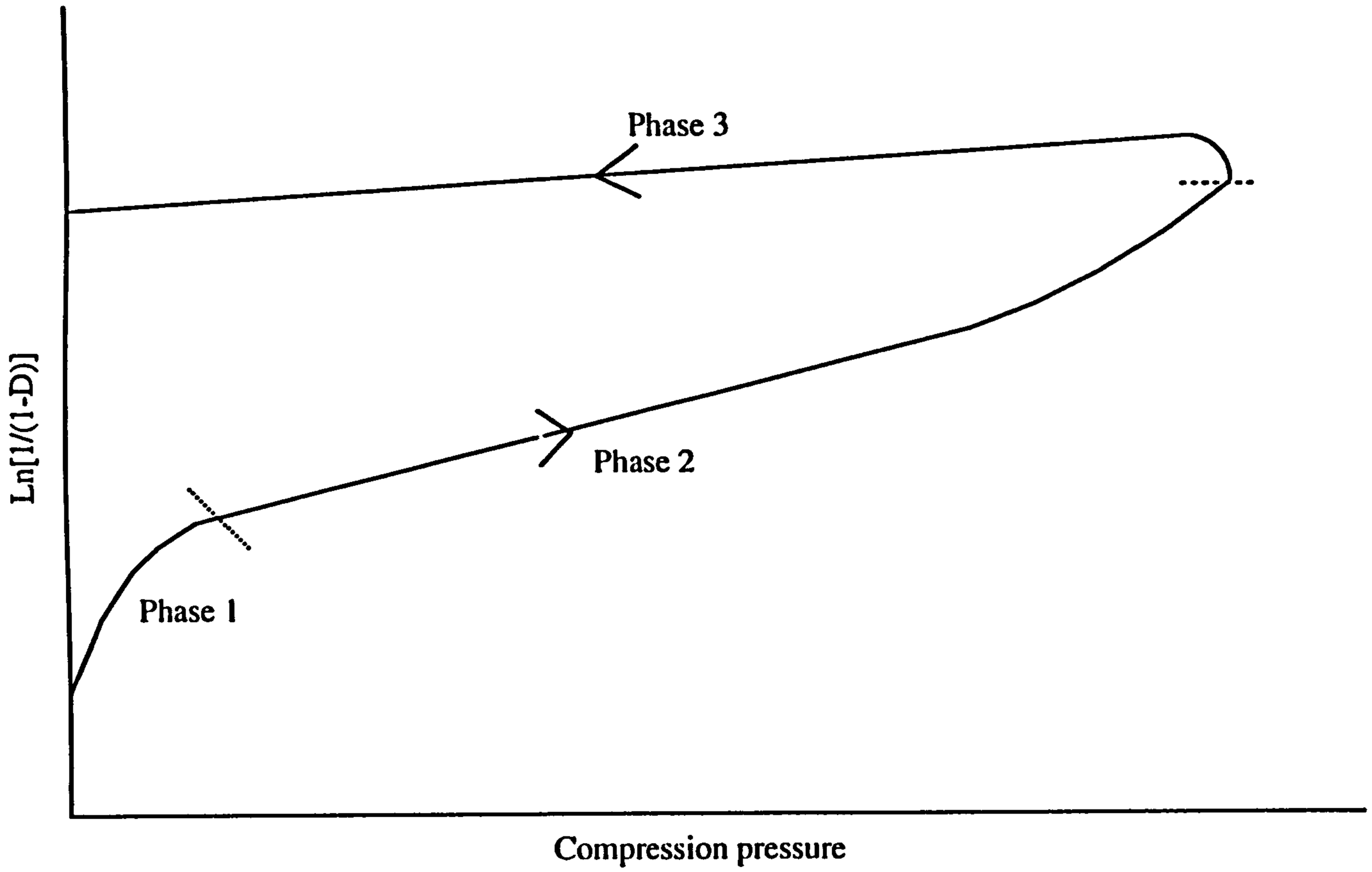

Figure 1.3 A typical complete compression cycle Heckel plot with the three phases

1.3 Mechanical properties of compacted materials

Once the tablet was introduced as a dosage form, the need to determine its mechanical properties, in order to quantify its strength and produce a uniform product, was soon recognised and a number of simple tests were introduced. In more recent years, the evaluation of the fundamental mechanical properties of pharmaceutical materials and compacts has been identified as being of critical importance. This is particularly true if the capability to predict how a specified material or mixture of materials will behave during and after compression is to be achieved. The situation however is complicated by the fact that there is often significant lot to lot variations in the physico-chemical and mechanical properties of drugs and excipients which can have serious implications for the reproducibility of the formulation and processing operations. Martino et al. (1993) and Bernabe et al. (1997) detail significant variability in the compression behaviour and physical properties of lactose between batches supplied by different suppliers and between batches from the same manufacturer.

The following parameters are considered to be the most relevant to the mechanical evaluation of pharmaceutical materials and compacts (Schubert, 1975; Roberts and Rowe, 1987a, b).

- Elastic modulus (stress/strain profiles)
- Hardness (resistance to local deformation)
- Yield stress (plasticity)
- Tensile strength (a measure of bond formation determined using diametral crushing force).

Some of the techniques used to determine the above properties will be discussed in the following sections with particular reference to those used in this work.

1.3.1 Diametral crushing force

Pharmaceutical compacts are brittle, irrespective of the consolidation mechanism by which they were formed, as fracture is not preceded by any significant deformation (Breenbaum and Brodie, 1959; Stanley, 1985). Traditionally the force required to

fracture a compact across its diameter has often been incorrectly referred to as its hardness. The crushing force or mechanical strength is a more accurate term. Diametral crushing is achieved by placing a compact between two parallel platens, one of these platens moves towards the other and applies a force across the compact until it fractures. The force required to cause the fracture is therefore referred to as the crushing force of the compact.

1.3.2 Tensile strength

The diametral crushing force of a compact is useful as an in process test used to ensure compacts have the necessary strength to withstand subsequent handling and to check product uniformity. It has been shown, however, to be dependent on the size of the compact and thus direct comparisons with compacts of different dimensions cannot be made.

The tensile strength of a compact is a much more reliable property. A compact is subjected to an applied load as in the diametral crushing strength test and provided the specimen fails in tension, the fracture load can be easily converted into tensile strength (σ_x) by the equation:

$$\sigma_x = \frac{2F}{\pi.d.t.} \qquad \text{(equation 1.10)}$$

where F is the fracture load, d is the diameter of the compact and t is its thickness. The compact is considered to have failed in tension if it has broken by a single fracture along its diameter or by a triple cleft fracture where two additional cracks appear, parallel and either side of a central fracture. The equation was first used to determine the tensile strength of pharmaceutical compacts by Fell and Newton (1968). The tensile strength values of a compact calculated using equation 1.10 may still show considerable variations, depending on the testing conditions. Variables such as the use of padding (Fell and Newton, 1970) and the rate of loading (Rees et al., 1970) have been shown to affect the results obtained. Therefore, if results are to be compared, consistent testing conditions must be used.

1.3.3 Indentation hardness

The hardness of a material has been defined as its resistance to local deformation (Tabor, 1951) and is indicative therefore of its plasticity. It is normally determined by loading a hard indenter onto the surface of the material and recording the deformation produced. The hardness of the material can then be calculated (Section 3.4.8).

Indentation testing has for many years been used in the fields of metallurgy and material science but has only been used in the area of pharmaceutical technology since around the mid 1960's. The development of micro and nano indentation equipment (which require very small loads) has allowed the mechanical properties of tablets, single crystals and films to be evaluated.

Indentation hardness is essentially a surface property but has also been related to other mechanical properties such as elastic modulus (Ridgway et al., 1969a: Aulton et al., 1974). The influence of crystal growth conditions on the hardness and elasticity of potassium crystals was studied by Ridgway and Aulton (1971). Indentation hardness studies have also been used in the evaluation of pressure transmission during compression and the density distribution in the resultant compacts. Ridgway et al., (1969b) and Aulton (1981a, b) reported that the hardness values obtained across the face of compacts varied with distance from the centre due to non uniform pressure transmission. Other workers, including Leuenberger (1982), Hiestand and Smith (1984), Jetzer (1986a, b,) and Roberts and Rowe (1991) have combined indentation hardness results with other parameters such as compression pressure, tensile strength, yield stress and porosity to derive equations and ratios which can be used to characterise and possibly predict the deformation behaviour of pharmaceutical materials.

The various techniques used to determine indentation hardness can be classified into two main groups i) static and ii) dynamic. In static testing, a small indentation is made in the surface of the material by gradually pressing a hard indenter onto the surface of the test specimen by applying a constant load for a set time. The area of the indentation is determined and the hardness calculated. In dynamic testing the indenter is usually attached to a pendulum and allowed to swing freely against the test specimen. The hardness is then calculated from the indentation depth and indenter

rebound height. Two variations of the static testing method, namely the Brinell and Vickers's tests, are the most commonly mentioned in pharmaceutical publications. These two techniques differ mainly in the geometry of the indenter. The Brinell test uses a spherical indenter, while the Vickers's test uses a pyramidal shaped indenter. For the purpose of this work the Brinell testing method was employed and will be discussed in more detail later (section 3.3.3).

Some limitations of indentation hardness measurements have been reported (Church 1984 a and b, Duncan-Hewittt and Grant 1987). For example, it has been suggested that as indentation is a point measurement, the occurrence of voids or surface irregularities could produce inaccurate results if the indent was made at these points. This is probably the cause of the high standard deviations sometimes associated with indentation measurements.

A few inconsistencies in reported indentation hardness values are evident. Roberts and Rowe (1995) point out that the values obtained by Aulton (1981a) for some pharmaceutical materials were lower than those reported by other workers. Ichikawa et al. (1988) reported a value of 523 MPa for α-lactose monohydrate crystals while Wong (1988) reported values of around 66 MPa. Leuenberger (1982) published values for sucrose compacts ranging from 1046 to 1723 MPa while Duncan-Hewitt and Weatherly (1989) reported a value of 645 MPa for single crystals of sucrose (which would be expected to give higher values than compacts).

The problem with directly comparing the results of different studies is that factors such as the history of materials, experimental conditions and the nature of the testing equipment cannot be taken into account. In the course of this work, however, all the samples were treated and tested in exactly the same way and therefore the results will at least indicate any relative differences in their hardness.

1.3.4 Elasticity

When a material is subjected to a stress in a particular direction, it will experience a corresponding change of dimensions (strain) in that direction. Within the region where a material behaves elastically and thus obeys Hooke's law, the stress and strain are related by the equation:

$$\text{Stress} = E \times \text{Strain} \qquad \text{(equation 1.11)}$$

where E is the modulus of elasticity of the material. The modulus of elasticity (elastic modulus) is a fundamental property of the material, directly related to its inter-atomic and/or inter-molecular bonding forces. It is a measure of the stiffness or rigidity of a material and has been identified as being a critical mechanical property in classifying and predicting its behaviour during and after compression. Several techniques have been employed to determine the elastic modulus of pharmaceutical materials, namely, flexure testing (four and three point beam bending) and indentation studies. In flexure testing, a rectangular beam of small thickness and width (in comparison to its length) is compacted from the material being tested. The beam is then subjected to a transverse load. The deflection of the beam at its central point is then measured, and the elastic modulus calculated. In 1984, Church and Kennerly used a four point beam bending test, where the beam was supported at two points and loaded at two points, to determine the elastic modulus, fracture stress and strain of several pharmaceutical materials. Later, Roberts and Rowe (1989) used a three point method, where the beam was supported at two points and loaded at one, and found good agreement between results obtained by both methods. It is, however, known that results can be affected by factors such as particle size and moisture content, (Kerridge and Newton, 1986; Roberts and Rowe, 1987 b; Mashadi and Newton, 1987a and 1987b; Mashadi, 1988; Bassam et al., 1988).

Generally, there is a good agreement between the elastic modulus values obtained by various workers, but some inconsistencies have been noted. For example, Mashadi and Newton (1987a) published a value of 45 GPa for Sorbitol Instant which is much higher than expected when compared with the values obtained for other sugars, such as 12.2 GPa reported for mannitol by Bassam et al. (1988). Also, Khan et al. (1988) published a value of 0.07 GPa for Avicel PH101 while Bassam et al. (1988) reported

a value of 8.7 GPa at a comparable porosity and moisture content. Roberts and Rowe (1989) demonstrated that microscopic flaws and cracks present in the beams can lead to inconsistent results and must be eliminated. Despite these inconsistencies, flexure testing has become widely used within pharmaceutical technology.

Indentation studies are mainly associated with measuring hardness but may also be employed to assess the elastic modulus of a material. In measuring hardness, it is the depth of initial indentation that is important, but for the determination of the elastic modulus it is the amount of recovery, after the indenting load is removed, that is measured. A full description of the technique is detailed in Chapter 3.

As with hardness both the Brinell and Vickers methods can be used to measure the elastic modulus. Ridgway et al. (1970), Aulton (1981a, b), and Wong (1988) all used a spherical sapphire indenter (Brinell indentation) to measure the elastic modulus of a variety of pharmaceutical crystals and compacts, while Duncan-Hewitt and Weatherly (1989a, b) used a Vickers indentation technique to evaluate the elastic modulus of sodium chloride and sucrose. As with hardness measurements, the possibility of making the indent at a point of surface irregularities or high voidage is recognised as a disadvantage of the technique. Roberts and Rowe (1995) are critical of elastic modulus values obtained by Brinell indentation techniques, as they are not in agreement with results obtained in studies using flexure testing. The difference may be due, however, to the fact that different types of elastic modulus are being measured. The most commonly referred to elastic modulus is the Young's modulus, E, which is a measure of a materials resistance to tension and is thus determined by flexure testing and Vickers indentation studies. Materials also have a resistance to compression and this is reflected by its bulk elastic modulus, K. It is this value which is measured via Brinell indentation studies which use a spherical indenter. Factors such as the rate of loading, the load, the size of the indenter and the thickness of the test specimen can also affect the results obtained. So long as identical experimental conditions are used throughout an investigation, a comparison of elastic modulus results should, however, provide a useful and meaningful study.

The relationship between elastic modulus and molecular structure has been studied by Roberts et al. (1991). They found a direct link between the inter-molecular interactions, based on the cohesive energy density (CED), and the elastic modulus of several materials as determined by a three point beam bending method. This suggests therefore, that, the elastic modulus of a material could be predicted from knowledge of its chemical structure.

1.3.5 Yield stress

The yield stress or mean yield pressure, like hardness is a measure of the resistance of a material to local deformation. For completely plastic materials, it has been shown that

$$P_y = H/3 \qquad \text{(equation 1.12)}$$

where P_y is its yield stress and H is its Vickers indentation hardness. The various methods of obtaining the yield pressure and its application have already been discussed (section 1.2.8). The lower the mean yield pressure the more easily deformed (or plastic) the material. Roberts and Rowe (1995) have reported a good agreement between values obtained experimentally and those obtained using the above equation, for certain materials.

Roberts and Rowe, (1985) studied the effects of punch velocity on the compaction properties of several pharmaceutical materials and found that it had an effect on the parameters derived from the interpretation of Heckel plots. They also observed that the extent of the effect was material dependent. For materials known to compact by plastic deformation, the yield pressure was seen to increase as the compression speed was increased, while no increase was observed for materials known to deform via a fragmentation mechanism. They introduced a strain rate sensitivity index, (SRS), which was calculated by the equation:

$$SRS = P_{y2} - P_{y1} / P_{y2} \qquad \text{(equation 1.9)}$$

where P_{y2} and P_{y1} are the fast (300 mm/s) and slow (0.033 mm/s) compression velocities respectively. This strain rate sensitivity index may be used to rank materials in order of their tendency to deform plastically.

1.3.6 Interrelationships between mechanical properties

A pragmatic approach, which would assist in the predication of compaction behaviour, was proposed by Roberts and Rowe (1987 b). It was based on the measurement of yield stresses (at pressure), the variation of that yield stress with strain rate, the indentation hardness and the elastic modulus. As previously shown, the indentation hardness (H) and the yield pressure (P_y) can be related by the equation;

$$P_y = H/C \qquad \text{(equation 1.13)}$$

where C is a constant approximately equal to three for ductile materials. For materials with an elastic component however, the relationship is much more complex, but a simplified version of this relationship was introduced by Marsh (1964).

$$\frac{H}{P_y} = 0.07 + 0.6 \quad \text{Ln}\frac{E}{P_y} \qquad \text{(equation 1.14)}$$

This equation is useful as the ratios E/P_y and H/P_y can be directly related to material behaviour.

Hiestand and Smith (1984) proposed several tableting indices which related various mechanical properties. One of these indices known as ***The Bonding Index*** is interpreted as indicating the relative survival during decompression, of the areas of true contact that are formed at maximum pressure. It is defined as the tensile strength (σ_t) divided by the indentation hardness (H)

$$\text{Bonding Index (BI)} = \sigma_t / H \qquad \text{(equation 1.15)}$$

If the indenter dwell time is very small, typically less than a millisecond, the bonding index is considered to be a worst case measurement, while indenter dwell times of 30 seconds define a best case bonding index.

1.3.7 Zero porosity

One particular problem encountered when comparing mechanical data such as indentation hardness or elastic modulus obtained from various compacted particulate systems is in the definition of the porosity at which the comparisons should be made. The porosity of the system is the main factor separating the mechanical property of the compacted specimen from the mechanical property of the material. Since pharmaceutical powders cannot be formed into solid compacts without porosity, the method used to determine the fundamental (zero porosity) mechanical property (M_o) involves the preparation of several specimens, of various porosity values and extrapolation of the specimen mechanical property (M) to zero porosity using the exponential equation

$$M = M_o \exp^{-bp} \qquad \text{(equation 1.16)}$$

where p is the porosity of the specimen and b is the gradient of the linear plot. Several workers, including Spriggs (1961) and Kerridge and Newton (1986) have used the equation to evaluate fundamental material elastic modulus. Others such as Ryskewitch (1953) and Adolfsson and Nystrom (1996) have used it to calculated fundamental material tensile strength values. The validity of these techniques is usually assessed by evaluating the linearity of the data.

1.4 Physico-chemical and derived material properties

In addition to mechanical factors, another group of properties which have been identified as being of critical importance to the behaviour of materials both during and after compression are their physico-chemical properties (Jones, 1977; York, 1992). Among this group are properties such as particle size, particle shape, particle size distribution and density which in turn affect so called derived properties such as flowability and compressibility.

1.4.1 Particle size, shape and size distribution

It has been claimed that the particle size of a material is one of the most important factors affecting its compaction behaviour (Hersey et al., 1967; Sheik-Salem and Fell, 1982). In general, the strength of a compact is seen to increase as the particle size is decreased (Vromans et al., 1985) but this is not always the case. Shotton and Ganderton (1961) claimed that when the inter-particulate bonds are very weak the compact strength is not affected by particle size. Huttenrauch (1983) reported that for materials with strong inter-particulate bonds the rule was reversed with compact strength increasing as particle size increased. The influence of the consolidation mechanism on the relationship between compact strength and particle size was characterised by Alderborn and co workers (1982, 1985, and 1988). They proposed that, for materials with a high tendency to fragment, the original particle size had little effect on the strength of a compact, while for plastically deforming materials the compact strength increased with a decreasing particle size.

For materials known to deform plastically, such as sodium chloride and potassium chloride, it has been observed that the yield pressure is independent of particle size (Hersey et al., 1973; Humbert-Droz et al., 1982). However for materials which deform by fragmentation such as lactose and calcium carbonate it has been reported that the yield pressure increases with a reduction in particle size (Hersey et al, 1973; York, 1978). Roberts and Rowe (1987a) demonstrated that for some materials a change in particle size could be responsible for a transition in deformation behaviour from brittle to ductile fracture. Clearly, the relationship between particle size and the behaviour of compacts both during and after compression is a complex one. The distribution of particle size has also been identified as being an important factor in dictating the behaviour of powder materials during and after compaction. Especially well recognised are the difficulties that arise due to a high proportion of fine material contained in a powder system. This can lead to segregation of materials and weight uniformity problems, as well as being responsible for an increased capping or lamination tendency.

The particle shape of materials is another physico-chemical property which is well recognised as being influential in affecting the compaction behaviour and mechanical

properties of pharmaceutical compacts (Alderborn, 1995). The major problem in assessing the effect of particle shape lies in the difficulty of obtaining samples of materials which are of a similar size but different geometry. Essentially this is achieved by either using different crystallisation techniques or by milling and sorting the material. It has been illustrated by several studies (e.g. Alderborn and Nystrom, 1982; Alderborn et al., 1988 and Wong and Pilpel, 1990) that the effect of particle shape is related to the consolidation mechanism. For materials which deform plastically, such as Starch 1500 and sodium chloride, it was found that a change from a regular to an irregular shape can cause a large decrease in yield pressure and a small decrease in elastic recovery. This resulted in an increased particle to particle contact area which enhanced bonding and increased the tensile strength of the compact. For materials such as lactose and di-calcium phosphate, which deform by fragmentation, the mechanical properties were found to be virtually independent of particle shape. Using Heckel analysis, York (1978) and Paronen and Juslin (1983) demonstrated that as particles become more spherical the amount of particle rearrangement occurring during compression increased.

Particle shape has also been shown to influence the uniformity of die filling. Ridgway and Scotton (1970) reported that the variation in the weight of material filled into a die increased, as the particle shape (as measured by the Heywood shape coefficient) became more irregular.

1.4.2 Material density

The density of a powder system is well recognised as an important factor in determining the behaviour of a material during operations such as mixing and tableting. Several different types of density values have been employed to characterise pharmaceutical materials, the three most common of these are defined as follows.

Poured bulk density - This is also referred to as the fluffed or apparent density. It is usually determined by pouring a known mass of material into a measuring cylinder and recording its volume. The density is then calculated by dividing the mass of the material by its volume.

Tapped bulk density - This is usually measured at the same time as the poured bulk density by subjecting the system to a predetermined number of taps or shocks. This causes the powder particles to pack more closely and thus occupies a smaller (tapped) volume. The tapped density is then calculated by dividing the mass of the material by the tapped volume.

Both the poured and tapped density are affected by factors such as particle size, size distribution, particle shape, inter particle cohesion and packing characteristics of the material.

True density - This is defined as the mass of material divided by the solid volume, which excludes all inter and intra-particle voids. It is generally measured by a technique of gas (helium) pycnometry, which calculates the solid volume by determining the amount of gas displaced by the solid. The true density is an intrinsic property of a material and is related to its crystal structure. It has therefore been used as an indirect method for evaluating differences in the degree of crystallinity between samples of the same material.

1.4.3 Moisture content

The presence of moisture (usually water) in drugs or excipients is known to cause changes in its solid state, physico-chemical and mechanical properties, affect its compression behaviour and alter the properties of the subsequent tablets or compacts. Water (or any other solvent) may be either bound (i.e. incorporated into the crystal lattice) or adsorbed (i.e. trapped in voids or loosely attached to the surface). Neumann (1953) demonstrated the influence of moisture on the flow properties of powders. He showed that as the moisture content of a powder was raised to a critical point, the angle of repose, and thus the flowability, of the powder increased. Any further increase in moisture content, however, resulted in a decrease in the angle of repose. It was later proposed that this was due to the amount of water causing a change in whether lubrication or surface tension effects predominated.

In terms of compression, Seth (1959) suggested that capping was partly caused by the lack of moisture within a granulation while sticking resulted if the granulation was too wet. It was therefore proposed that there was an optimum level of moisture, which would differ for each formulation and depend largely on the cohesive properties of the materials involved.

Jaffe and Foss (1959) found that the removal of the water of crystallisation rendered several materials that had previously produced good tablets, virtually impossible to compress successfully. They suggested that this was due to the fact that the crystal structure had been disrupted by removing the water. Shotton and Rees (1966) reported greater force transmission, lower ejection force and improved consolidation when sodium chloride was compressed in the presence of increased moisture.

Griffiths (1969) suggested that during compression of hydrated materials it was possible that moisture may be squeezed out of the particles and in combination with the high temperatures which occur at the contact points, result in recrystallisation within the compact.

The effects of moisture, however, are not universal. Several workers (e.g. Fell and Newton, 1970 and Bolhuis, 1988) have reported that anhydrous lactose forms stronger compacts than lactose monohydrate, while Wong and Aulton (1987) observed that alpha lactose monohydrate single crystals, were harder, more elastic and more brittle than single crystals of anhydrous lactose.

Armstrong and Patel (1986) illustrated the influence of altering the moisture content of both dextrose monohydrate and anhydrous dextrose. They reported that the strength and toughness of compacts prepared from both materials reached a maximum, at a critical moisture content, and then decreased if the moisture content was raised further.

1.4.4 Flowability

The ease with which a material can move from one position to another under the influence of gravity is termed its flowability and has been shown to be an important factor in operations such as tableting. Poor flow can result in an insufficient amount

of powder being filled into the die and thus lead to problems in the weight uniformity and dose uniformity of the tablet. The wet granulation process is often employed to increase the flowability of a powder system prior to compression. The flow of a material is affected by factors such as particle size, particle shape and surface cohesion between particles. One relationship for assessing the flowability of a material is known as the Hausner ratio, (HR), which is defined by the equation;

$$\text{Hausner ratio} = \text{Tapped bulk density}/\text{Poured bulk density} \qquad \text{(equation 1.17)}$$

A ratio of 1.7 or above is indicative of a very cohesive material which does not flow well, while a value of 1.2 or below indicates a very free flowing material.

1.5 Solid-state properties and their influence on the compaction process

The solid materials, which are used as pharmaceutical drugs and excipients are generally organic crystalline substances. As a result, a considerable amount of research has been aimed at evaluating their solid state properties and clarifying the influence these properties have on the compaction process. Some properties, which have been identified as being of particular importance in the design and manufacture of solid dosage forms, are listed in Table 1.2. It has been demonstrated that variations in these properties can be responsible for altering the behaviour of materials during operations such as tableting and also affect the subsequent performance of the product (e.g. Hanssen, 1970; Huettenrauch 1978; Chiou and Kyle 1979 and Bernabe et al., 1997).

As a consequence of the increasing understanding about the relationship between the solid state properties of pharmaceutical materials, their processing behaviour and subsequent performance, the concept of crystal engineering and particle design has developed. This will enable materials with enhanced handling and processing properties (e.g. flowability and compressibility) to be manufactured by deliberately designing desired properties into a material.

Table 1.2 Solid-state properties which influence the compaction process

Crystal structure

Crystal imperfections (defect and impurities)

Degree of crystallinity

Crystal habit (size and shape)

Crystal hardness

Polymorphism

1.5.1 Crystal structure

A crystalline solid is one in which the constituent structural units, be they atoms, ions or molecules are arranged in rigid geometric configuration, which is characteristic of the material. This geometric array repeats itself in a three dimensional manner resulting in a structure with long range order known as a crystal lattice.

Crystals can be classified as ionic, covalent or molecular depending on the nature of the chemical bonding and the intermolecular forces within the crystal. Pharmaceutical crystalline substances generally consist of molecular crystals composed of individual molecules. The atoms within each molecule are held together by covalent bonds and the molecules are held together by relatively weak intermolecular forces such as Van der Waals forces and hydrogen bonding.

In a molecular crystal, molecules are arranged into a unit cell which is the smallest repeating unit of the lattice structure. Unit cells are arranged into planes which make up the faces of a crystal and the angles between these faces are characteristic of the material. In 1669, Nicolaus Steno observed that the interfacial angles of different quartz crystals were always the same. This fact was later confirmed by other workers and the law of constant interfacial angles or the first law of crystallography was proposed by Hauy in 1784. Figure 1.4 shows the consistency of three different habits of a material.

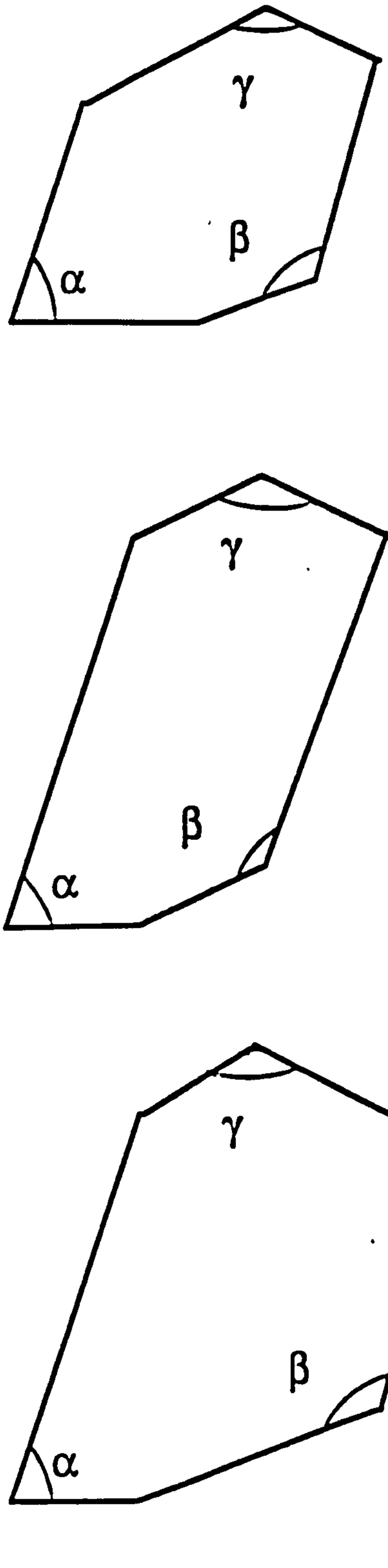

Figure 1.4 Consistency of interfacial habit for three different crystal habits. The angles α, β and γ have the same value throughout.

The unit cells of different crystal types are described in terms of their symmetry which may be about; i) a point (a centre of symmetry) ii) a line (an axis of symmetry) or iii) a plane (a plane of symmetry). Some crystals may posses several different elements of symmetry while others may posses none. All crystals of the same substance will posses the same elements of symmetry.

On the basis of their symmetry, Auguste Bravais (1811-1863) showed that only 14 different lattice types, referred to as the Bravais lattices (Figure 1.5), are possible. These 14 lattices can be further grouped into seven crystal systems based on the angles between and relative dimensions of the sides of the seven unit cells: *cubic, tetragonal, triclinic, orthorhombic, monoclinic, trigonal and hexagonal.* These seven systems can be further subdivided into classes based on whether they are primitive (P). Face centred (F), side or end centred (C), body centred (I), or rhombohedral (R). This results in 230 possible crystal forms, most of which have been observed.

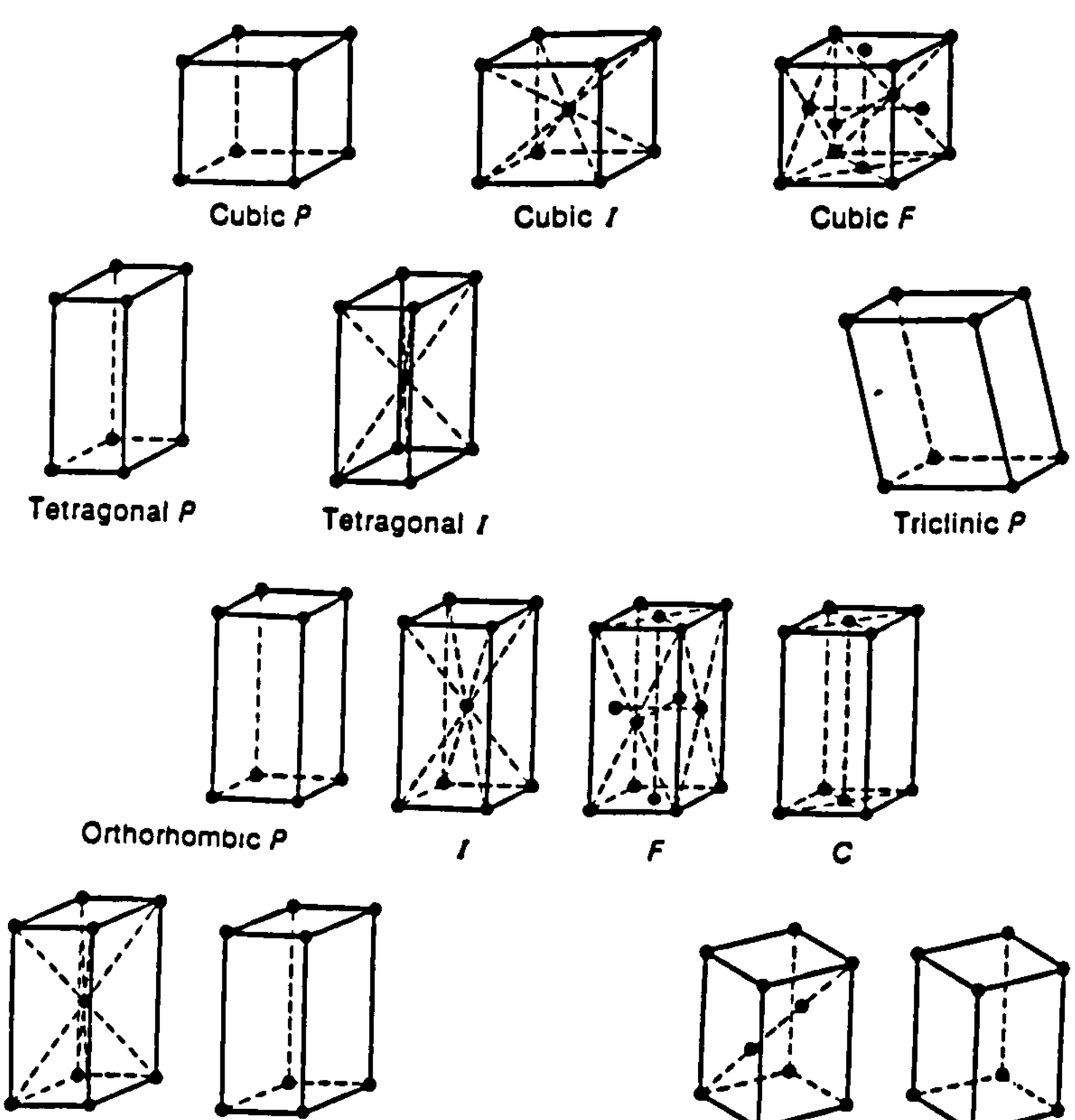

Figure 1.5 The 14 Bravais lattices

In order to describe crystals in terms of the orientation of planes, Miller indices can be used. The index of a crystallographic plane is specified by the reciprocal of the intercepts the plane makes with the three crystal axis. The procedures for determining the Miller indices of any crystal plane are:

1. Determine the intercepts
2. Find the reciprocals of the intercepts
3. Clear any fractions

Figure 1.6 below shows some examples:

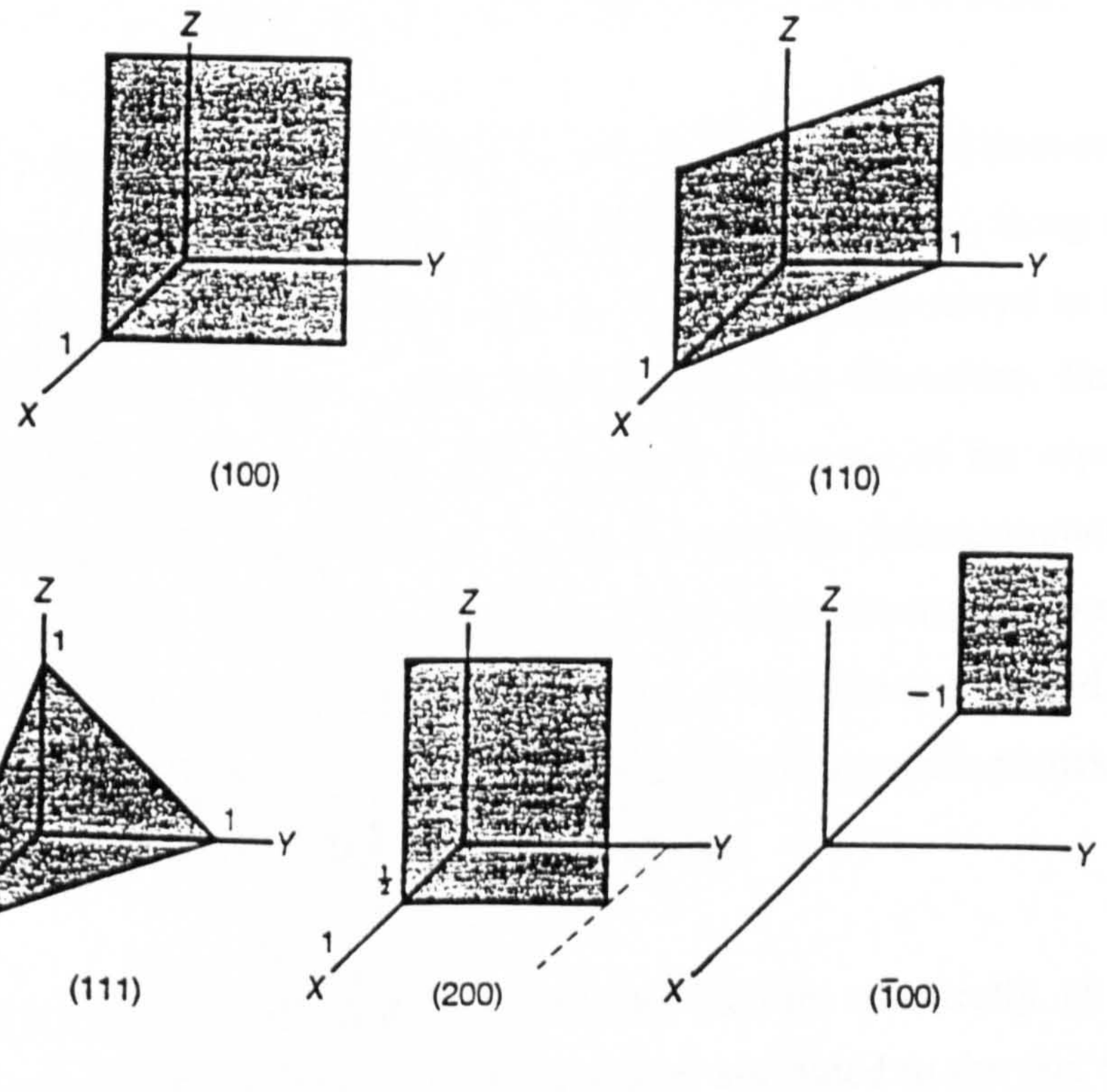

Figure 1.6 Miller indices of several crystallographic planes in a cubic crystal.

Seth (1959) was the first to report that compression behaviour of pharmaceutical substances was dependent on crystal structure. The degree of symmetry within a crystal has been shown to affect its deformation properties. Jaffe and Foss (1959) investigated the role of crystal structure on the ability of materials to form tablets. They reported that materials with cubic crystal systems could be directly compressed while materials with a rhombohedral lattice could not. This is thought to be due to the fact that the cubic crystal is isotropic (i.e. has the same properties in all directions) and so requires no special orientation of lattice planes for the relief of stress.

It has also been shown that it is possible for the crystal structure to be altered during the compression process. For an elastic material, the intermolecular forces will oppose any structural changes and restore the crystal to its original form. If, however, the intermolecular forces are exceeded, then plastic or permanent deformation takes place and if the applied stress is continued, plastic flow will occur.

The presence of slip planes and dislocations have been demonstrated to influence plastic deformation (Hess, 1978). Stepwise displacements along slip planes within aspirin crystals resulted in the displaced elements being moved in an orderly manner to a new location with equal molecular packing. Therefore, the internal packing arrangement was unchanged while the external shape of the crystal was modified. Highly symmetrical crystals such as sodium chloride possess numerous slip planes by which plastic deformation can take place and alternative mechanisms can be responsible for the deformation depending on the planes involved. For example, all planes parallel to the 110 face are potential slip planes while planes parallel to the 100 face are more likely to become cleavage planes.

Materials such as starches and cellulose deform elastically at low pressure and plastically at higher pressures, this has been attributed to the fact that these materials contain adjacent regions of crystalline and amorphous structure.

1.5.2 Crystal imperfections

Few if any crystals are perfect and any deviations, which cause a disruption in the order, are considered as imperfections or defects. In terms of molecular crystals, these imperfections are usually referred to as i) point defects ii) line defects or iii) surface defects. These defects may provide an explanation for the difficulty in producing materials with reproducible stability and mechanical properties, since batch to batch variations in the production of these materials will give rise to different concentrations of defects.

Point or zero dimension defects occur as the name suggests at specific points within the lattice. The major point defects are (**A**) Vacancies (**B**) Substitutional defects or (**C**) Interstitial defects, (Figure 1.7). In terms of molecular crystals, interstitial defects occur when a foreign material (impurity) becomes incorporated in the spaces between the molecules of the host material. If the foreign molecule actually occupies the site of a host molecule, the defect is known as a substitutional defect. A vacancy occurs when a molecule is missing from its site leaving 'a hole' in the structure. For pharmaceutical materials, interstitial and substitutional impurity defects are the most frequently encountered due to trace amounts of other chemicals being incorporated into the crystal during the crystallisation process. Bernabe et al. (1997) demonstrated the effects of such impurities on the compression capacity of lactose.

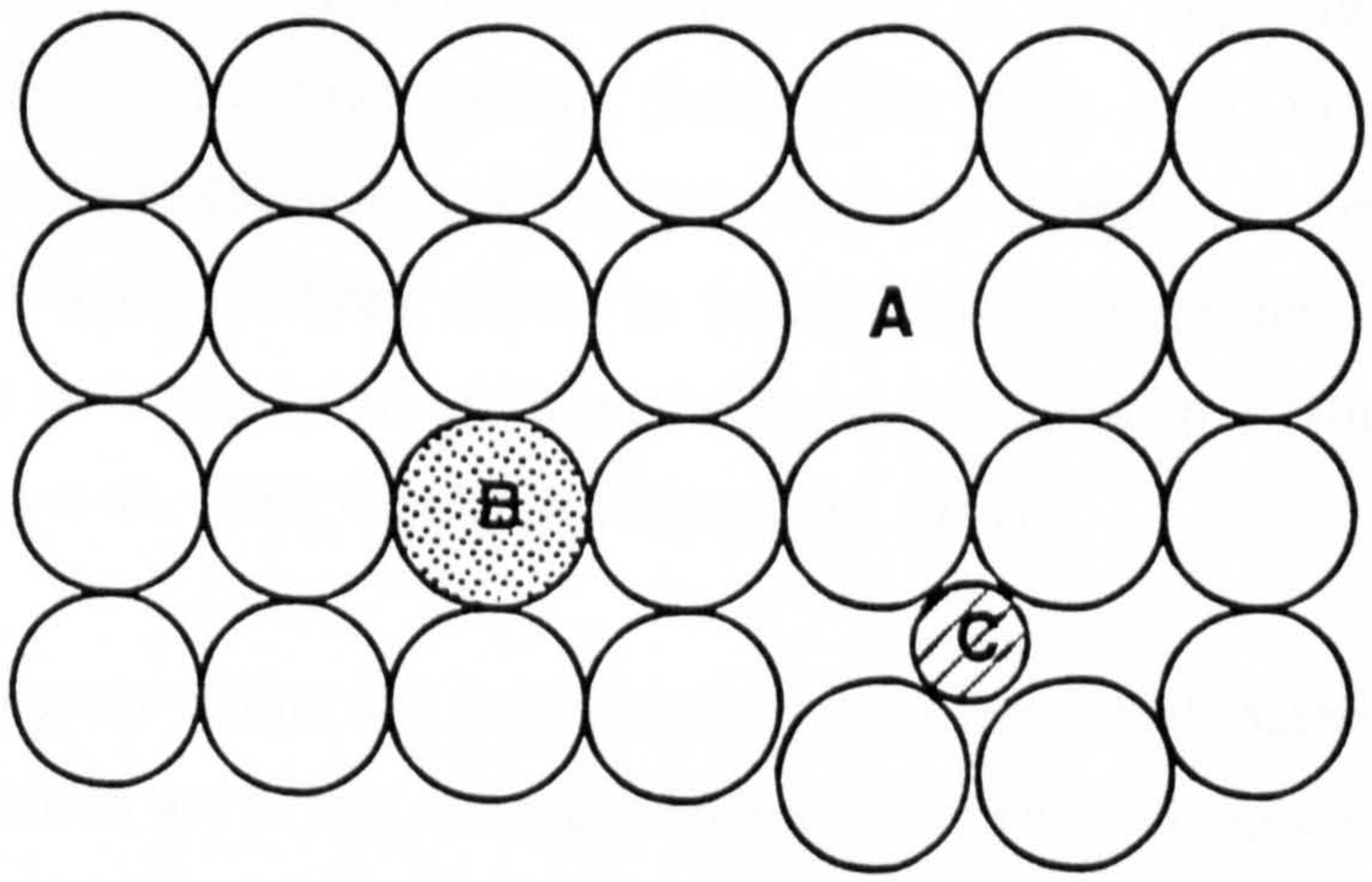

Figure 1.7 Examples of the various types of impurities.

Line or one-dimensional defects consist largely of edge and screw dislocations. Most crystals have many such defects, which are formed readily during the crystal growth process. It is the movement of these dislocations, under the influence of an applied force, that is responsible for the mechanism of plastic (non-recoverable) deformation. The presence of such defects produce areas of disorder within the crystal lattice which result in both the internal energy and the entropy of the lattice being increased producing a thermodynamically unstable and thus activated system. Huttenrauch (1978 and 1983) postulated that this activation of the crystal structure was responsible for the effects of crystal imperfections on the deformation behaviour of pharmaceutical materials.

The influence of crystal imperfections on the compression process was noted by Milosovich (1963). He suggested that a high dislocation density would in general lead to greater plastic flow of the material. Ridgway and Aulton (1971) reported that the hardness of single crystal of potassium bromide could be modified by altering the crystallisation conditions. They observed a decrease in both crystal hardness and elasticity with increasing rate of crystal growth.

Conditions of crystal growth are not the only factors which contribute to crystal defects. The nature and concentration of imperfections are extremely sensitive to even minor changes in the manufacturing process and so often vary from batch to batch. This leads to a lack reproducibility in the formulation, processing and performance of the final product. (Jones 1981, York 1983, York and Grant 1985). Pharmaceutical processing operations such as granulation, milling, drying and tableting have also been shown to induce imperfections into materials and thus influence their physico-chemical and compression properties (Huttenrauch 1977a, b; Kaneniwa et al., 1985; Otsuka and Kaneniwa, 1984).

Although great efforts are made to purify pharmaceutical materials the presence of crystal defects are in fact desirable for process such as compression. They enhance the ability of a material to deform plastically and /or fracture, which has been shown to a favourable property for tableting materials (Aulton et al., 1984).

1.5.3 Degree of crystallinity

The degree of crystallinity is a measure of the relative molecular order (or conversely a measure of the relative number of imperfections) within a crystalline material but has proved a difficult parameter to quantify. The increasing awareness of the important role, crystal imperfections play in determining the compaction behaviour of a material has, however, lead to several techniques for indirectly measuring the degree of crystallinity. This can then be used to compare and rank similar samples of the same material. It has been found, however, that the different techniques often result in very different values being obtained for the same material (Pikal et al., 1978). Table 1.3 below summarises these techniques with some specific references:

Table 1.3 Some techniques used to assess crystallinity

Technique	Reference
Solution calorimetry	Pikal et al. (1978), Grant and York (1986)
D.S.C	York and Grant (1985)
I.R. spectrophotometry	Nakai et al. (1982)
X-ray diffraction	Imaizumi et al. (1977), Black and Lovering (1974).
True density	Huttenrauch (1978), Ludlam-Brown (1989)

While several workers (e.g. Martino et al., 1993) have demonstrated a link between compressibility and the degree of crystallinity they have been unable to quantify the relationship due to the problems associated with measuring crystallinity.

1.5.4 Crystal deformation

The mechanisms of deformation of pharmaceutical bulk materials were briefly introduced in section 1.2.3. In this current section the deformation mechanisms and in particular their relationship with solid-state properties will be discussed.

1.5.4.1 Elastic deformation of crystals

As with most structures, crystals can be compressed elastically. The displacement caused by the small changes in shape and volume are proportional to the applied force and can be recovered when the force is removed. The degree of elastic compression is dependent on the elastic modulus of the crystal. Within a crystal, elastic deformation causes both bond extension and shear distortion of the bond angles as shown in Figure 8. Elastic deformation is not thought to be influenced significantly by structural changes such as the presence of defects.

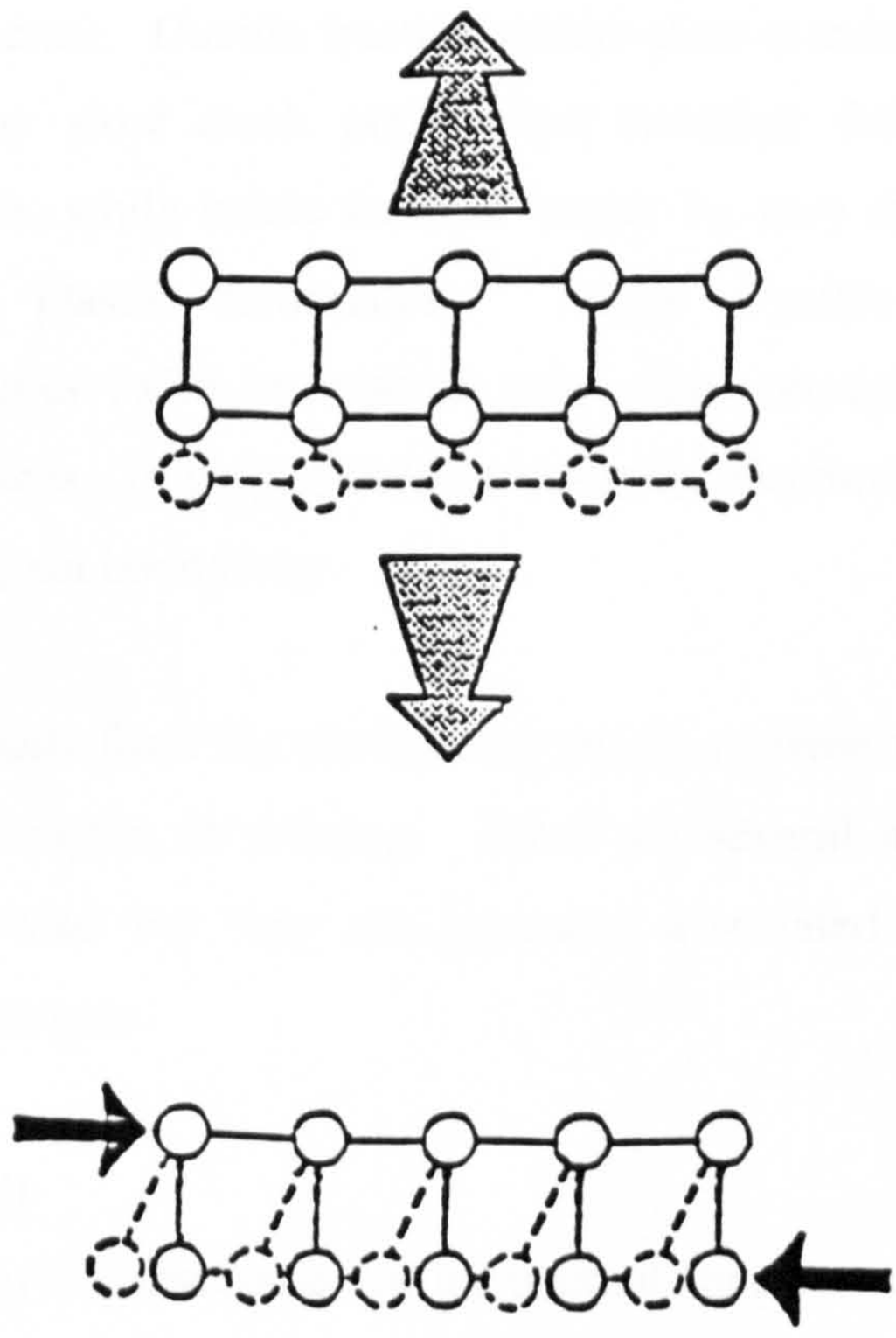

Figure 1.8 Elastic deformation causing both a) bond extension and b) shear distortion of the bond angle.

1.5.4.2 Plastic deformation of crystals

Plastic deformation in crystals takes place by displacement along slip or glide planes and is largely influenced by the crystal structure. The more symmetrical the crystal system the more slip planes that will be present and therefore the greater the degree of plasticity exhibited by the material. For the seven crystal systems, the susceptibility to plastic deformation decreases in the following order; cubic, hexagonal, tetragonal, rhombohedral, orthorhombic, monoclinic and triclinic. Hence inorganic materials such as sodium chloride which crystallise in the cubic system are usually very compressible, while organic materials which tend to crystallise in the monoclinic and orthorhombic systems are less readily compressed.

1.5.5 Fracture

In addition to elastic and/or plastic deformation, many crystals fracture when under the influence of an applied load. This breaking of the crystal is characterised as either brittle or ductile fracture. Ductile fracture occurs after extensive plastic deformation and is indicated by slow crack propagation resulting from the formation and coalescence of voids, while brittle fracture occurs by very rapid crack propagation after little or no plastic deformation. Single crystals may fracture along crystallographic planes (with or without prior displacement) leaving two crystal halves with plane faces. In polycrystalline materials, fracture can occur along either cleavage planes or grain boundaries.

Fracture usually results from the pre-existing cracks or from the formation of micro cracks during deformation or twining. There are several mechanisms, by which cracks can be initiated but they are generally associated with defects such as vacancies and dislocations.

1.5.6 Crystal habit

The habit of a crystal is a description of its external appearance. Often a material can crystallise in a variety of shapes and sizes and with a different number of crystal faces but its internal structure always remains the same. Crystal habits are often qualitatively described by names such as needle like, plate like, tabular or prismatic. Some examples of crystal habits are shown in Figure 1.9.

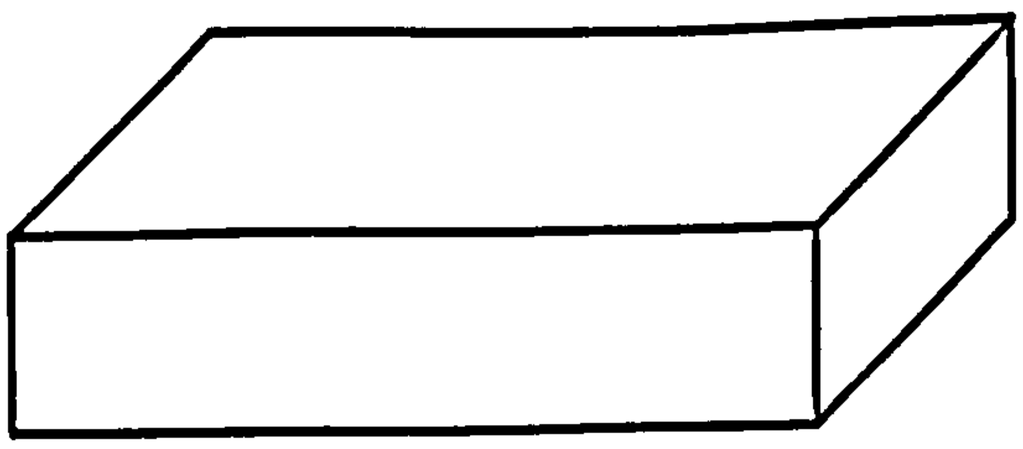

Tabular

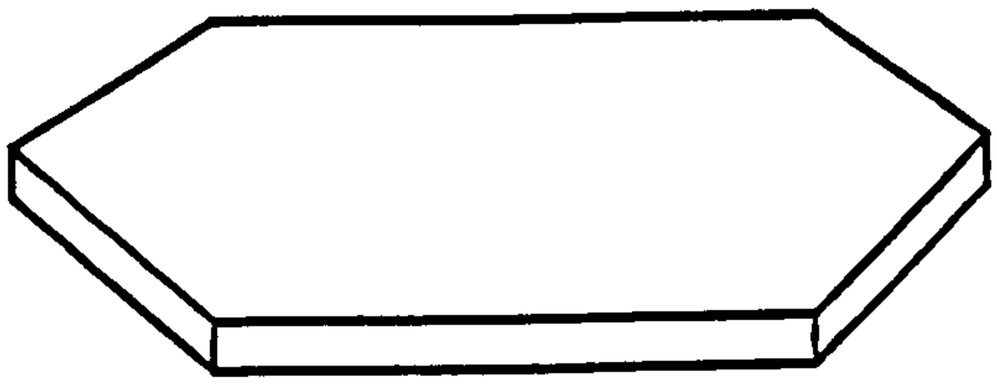

Plate

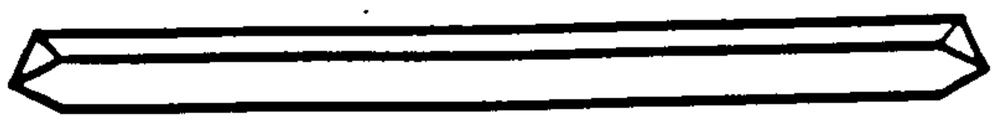

Acicular

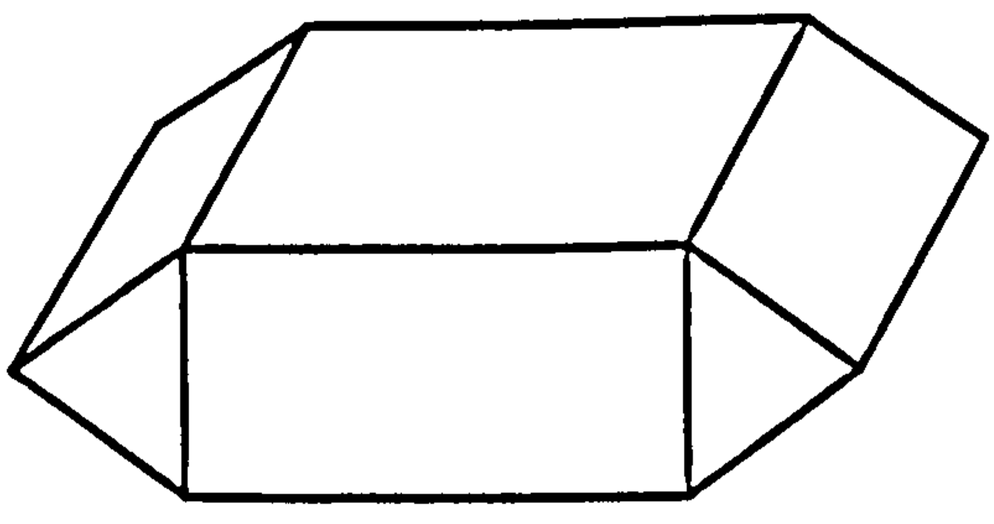

Prismatic

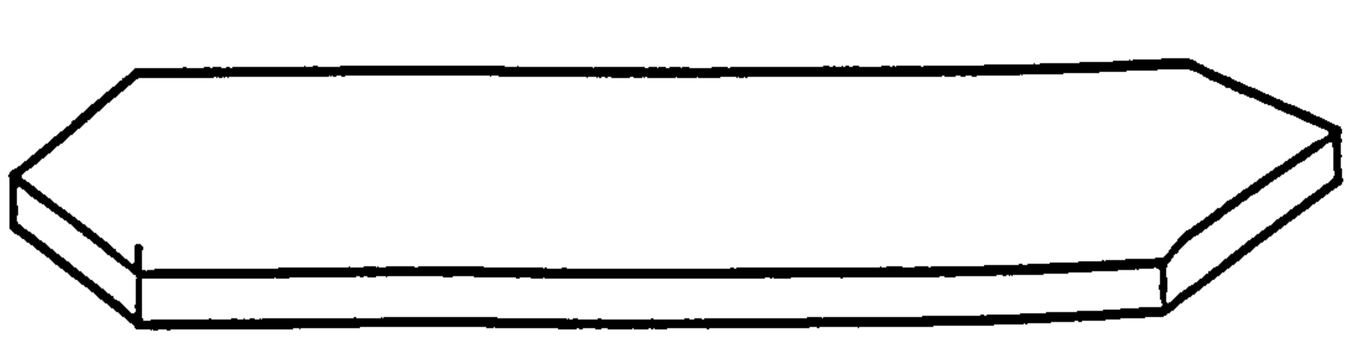

Bladed

Figure 1.9 Examples of some crystal habits.

Several techniques have been reported for quantitatively describing a crystal habit such as shape factors (Heywood, 1947) and aspect or length to width ratio (Garti and Tibika, 1980; Chow et al., 1985).

Changes in crystal habits are generally due to changes in the growing environment resulting from variations in crystallisation conditions, such as the degree of saturation, cooling rate, stirring rate, levels of impurities or changes to the crystallisation solvent (Haleblian, 1975). For example, Garti and Tibika (1980) and Marshall and York (1989) modified the habit of nitrofurantoin crystallised from formic acid mixtures. Fairbrother and Grant (1978) and Michaels and Colville (1960) demonstrated that the inclusion of additives in the crystallisation medium could reproducibly modify the habit of adipic acid crystals. Ludlam-Brown (1990) modified the habit and several other fundamental properties of ibuprofen by altering factors including cooling rate and stirring rate.

Several worker have reported enhancement of dissolution rate resulting from changes in the crystal habit of several materials (e.g. Chiou et al., 1979).

The effect of crystal habit on the compaction of pharmaceutical materials has also received considerable attention. Shell (1963) quantitatively described crystal habits by measurement of preferred orientation and related this parameter to compression characteristics. He found that the higher the 001 orientation ratio relative to the 010 orientation ratio the more compressible was the compound. Shotton and Obiorah (1973) reported interesting differences in the compaction behaviour of two habits of sodium chloride. Dendrite crystals were found to produce stronger tablets than crystals of a cubic habit. Marshall and York (1991) reported modified compaction behaviour of samples of nitrofurantoin, whose habit was previously altered by changing the crystallisation solvent.

1.5.7 Crystal hardness

As with compacted material, the hardness of a crystal is defined as its resistance to local deformation and can be measured by (micro) indentation techniques. Ridgway et al., (1969) measured the hardness of crystals of several pharmaceutical materials

and examined the relationship between crystal hardness and radial pressure during compaction. Ridgway and Aulton (1971) reported the effect of crystallisation conditions on the hardness of single potassium bromide crystals and attributed the lowering of hardness with increasing growth rate to an increase in crystal defects.

In measuring the hardness of single crystals and interpreting its significance, two factors must be given consideration. Firstly, there is the problem of growing single crystals, which possess the necessary size and perfection to facilitate handling and testing. Often the techniques used in order to achieve this may in themselves be responsible for modifying the hardness of the material. The second factor is concerned with which crystal face to measure. Crystal faces may have very different hardness values, which may in turn be affected differently by the growth conditions. Wong and Aulton (1987) and Wong (1988) found that variations in growth rate had a different influence on the hardness of two different faces of α-lactose single crystals grown in agar gel. The hardness of one face was observed to decrease with growth rate while the hardness of the other increased. This was attributed to a variation in the effect of imperfections on the different lattice planes.

1.5.8 Polymorphism

The ability of a material to crystallise with different internal structures and thus in a different crystal system is termed polymorphism, e.g. carbon as graphite (hexagonal) and as diamond (cubic). It is believed that probably all organic compounds can exist in several polymorphic forms (Haleblian and McCrone, 1969). The bioavailability, stability and processing of a material have been found to be very dependent on the choice of polymorph. Polymorphs have different internal structures, and subsequently have different energy contents. Thus, the polymorph with the lowest energy will be the most stable form. Physicochemical properties including melting point, solubility and density as well as bulk properties such as compressibility are also influenced by the polymorphic form of the material.

1.6 The Crystallisation process

Crystallisation can be defined as the removal of a solid from a solution by increasing its concentration above the saturation point in such a manner that causes the excess solid to separate from the solvent in the form of crystals. There can be few if any pharmaceutical powder materials that have not been subjected to the process of crystallisation at some stage of their manufacture. Generally, it will have been used as a means of purifying the material, but more recently, there has been an increasing awareness of its potential as a tool for manipulating and optimising various material properties. Hiestand et al. (1980) showed that crystallisation conditions could significantly alter the physical and mechanical properties of pharmaceutical substances. This can thus make the role of these materials, in processes such as tableting more predictable, reproducible and efficient.

Crystallisation is a very complex operation. Mullin (1993) describes it as a process which is highly dependent on fluid and particle mechanics, involving simultaneous heat and mass transfer in a multi-component system, where solution composition, particle size, particle shape and size distribution are continually changing.

The crystallisation process has been studied in detail by workers including Jackson (1968); Nyvlt (1971); Pamplin (1980) and Vere (1978). It can be effectively split into three main stages:

- achievement of supersaturation
- formation of crystal nuclei
- crystal growth

The following sections will briefly review the main principles of the process.

1.6.1 Solubility and saturation

The solubility of a material is defined as the maximum amount that will dissolve in a given solvent at a given temperature. When the solvent contains exactly that amount, it is said to be saturated at that temperature. If it contains less, it is undersaturated and

if it contains more, it is referred to as supersaturated. A state of supersaturation is a prerequisite for crystal growth. The idea of a solution being supersaturated may at first seem unreasonable, however this state can be achieved simply. Firstly, by making a saturated or undersaturated solution and secondly by either evaporating or cooling the solution to render it more concentrated (supersaturated) than it was at its equilibrium (saturation) conditions without causing crystallisation to occur. Supersaturation has been defined by a number of equations:

Supersaturation Ratio = C/S (equation 1.18)

Absolute Saturation or Saturation potential (Δ)= C-S (equation 1.19)

Degree of Supersaturation = C/S - 1 (equation 1.20)

where C is the concentration of the solution and S is the equilibrium or saturation concentration at a given temperature.

Ostwald (1897) identified several areas of temperature solubility diagrams, which are of particular interest to those involved in crystallisation. (see Figure 1.10 for a typical temperature solubility diagram). These regions are explained as follows:

Undersaturation or Stable Zone - In this region the solution is undersaturated and crystallisation is impossible.

Metastable Zone - Here the solution is slightly supersaturated. Crystal growth may occur if seed crystals are introduced into the solution but spontaneous crystallisation is not possible.

Labile Zone - In this supersaturated region the solution is unstable and spontaneous crystallisation is likely to occur.

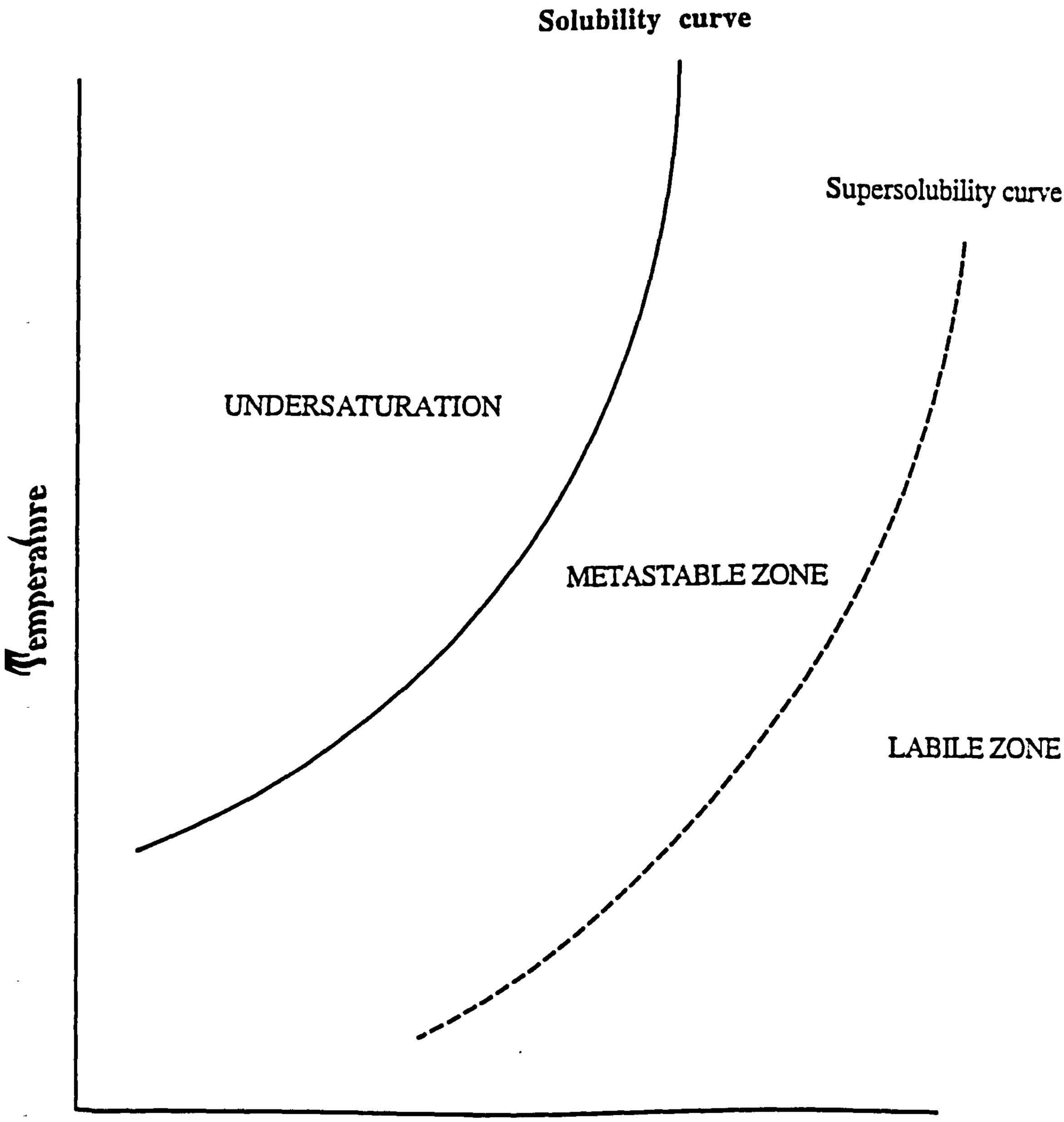

Figure 1.10 Typical solubility and supersolubility curves

Many workers since Ostwald have investigated the existence of the metastable zone and it appears that the exact position of its boundary is susceptible to factors such as agitation, overheating and the presence of impurities. It is now generally accepted that the supersolubility curve is actually a zone over which the probability of spontaneous nucleation and crystallisation increases as it approaches the labile zone.

1.6.2 Nucleation

After supersaturation has been achieved, the next step in the crystallisation process is nucleation. Here a critical number of molecules must aggregate to form a stable nucleus, which can then grow to form a crystal. There are three distinct types of nucleation involved in the crystallisation process:

- primary homogeneous (spontaneous) nucleation,
- primary heterogeneous nucleation (induced by the presence of foreign particles),
- secondary nucleation (induced by the deliberate introduction of seed crystals).

It is not always possible to determine whether primary nucleation is homogeneous or heterogeneous, but as it nearly impossible (under normal laboratory conditions) to prepare and store a saturated solution free from the influence of foreign particles such as air borne dust, it is generally accepted that the majority of primary nucleation is of the heterogeneous type.

1.6.2.1 Homogeneous (spontaneous) nucleation

Nuclei formation in a homogeneous supersaturated solution is not a foregone conclusion. Thermal motion within the solution causes the constituent molecules to continually aggregate and separate. If, however, these molecules aggregate with the correct orientation a lattice structure is built up. In some cases these lattices are so unstable that they simply breakdown and re-dissolve, but in other cases they manage to grow beyond a certain critical size where they become stable and free to undergo crystal growth. This process is essentially governed by the energetics of the system. The mathematical treatment is dealt with by several workers (e.g. Mullin, 1993) and will not be reproduced here.

The energy of a saturated solution is constant, under constant conditions of temperature and pressure, but there will be fluctuations about the mean value throughout the system and in those supersaturated regions where the energy rises to a high level, nucleation will be favoured. As already mentioned, the survival of a newly formed nuclei in the supersaturated solution will depend on its size. It will either continue to grow or re-dissolve. Whichever process occurs, the overall outcome must always result in a lowering of the overall free energy ΔG between the particle and the solute. The free energy ΔG is equal to the sum of the surface excess free energy ΔG_s and the volume excess free energy ΔG_v By considering a typical free energy diagram as shown in Figure 1.11, we can see how this critical nuclei size arises. Particles smaller than $\mathbf{r_c}$ will re-dissolve to lower the free energy of the constituent molecules while particles larger than $\mathbf{r_c}$ will overcome the energy barrier to lower their free energy, thus becoming stable and available for growth.

The magnitude of the free energy barrier and thus the size of the critical nuclei are both dependent on solubility (and therefore temperature), the degree of supersaturation and the surface to particle liquid interfacial tension (temperature dependent) (Mullin 1993).

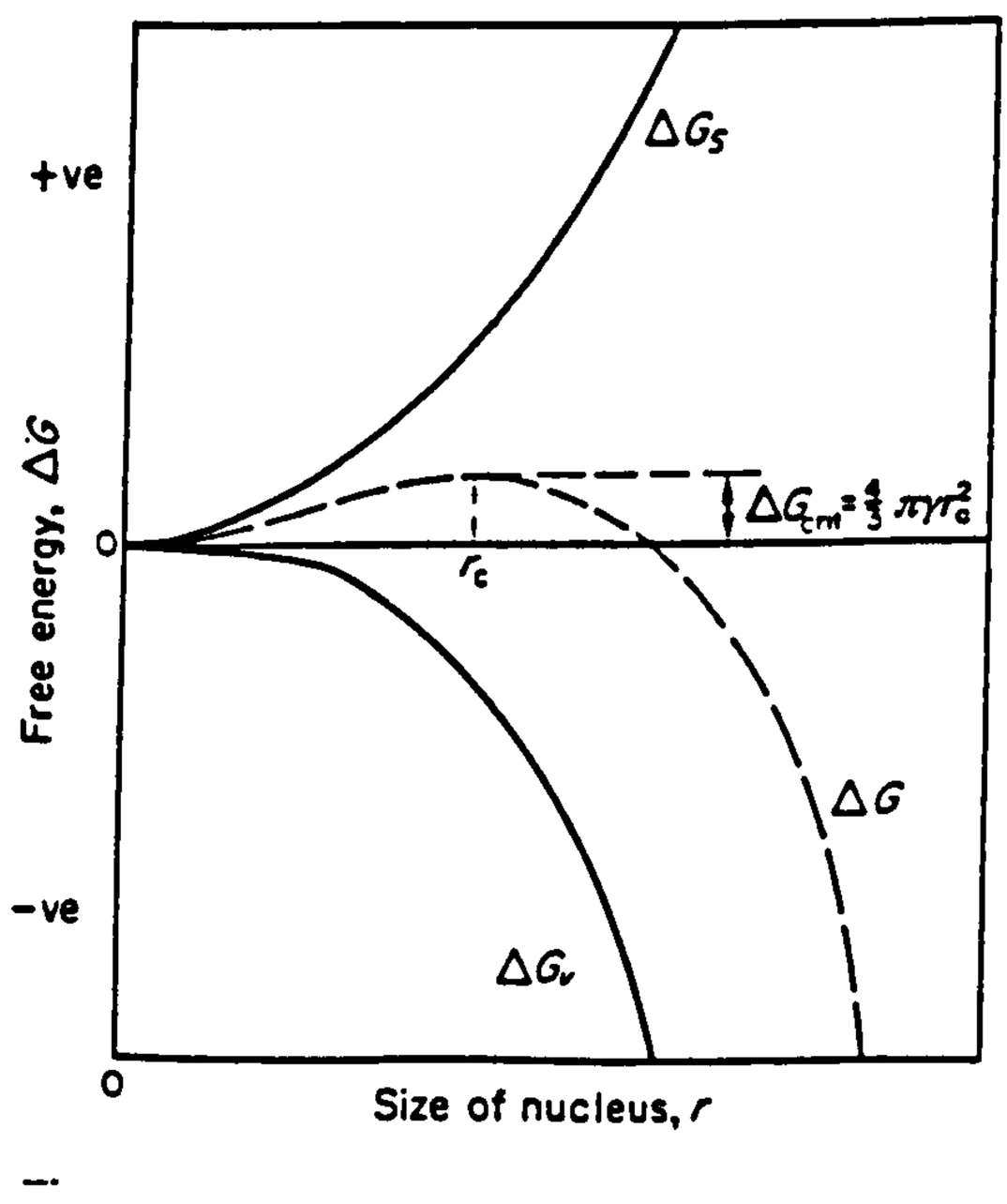

Figure 1.11 A free energy diagram explaining the phenomenon of a critical radius

1.6.2.2 Heterogeneous nucleation

If a foreign body, which is crystallographically similar to the material being crystallised is introduced into the supersaturated solution, then the free energy barrier for nucleation will be reduced and so crystal growth becomes more probable. This effect is also caused by sympathetic surfaces such as the wall of the crystalliser, which can act as a catalyst for nucleation.

1.6.2.3 Secondary nucleation

The best method for inducing crystallisation is to seed the supersaturated solution with small crystals of the material to be crystallised, or with some isomorphous crystals, if purity is not an issue. The seeds should be uniformly dispersed in the solution and with proper regulation of the conditions a high degree of control over the final product can be gained.

1.6.3 Crystal growth

Various theories exist which propose to explain the mechanism of crystal growth, but they can be broadly classified into three principle groups.

- surface energy theories
- adsorption theories
- diffusion theories

1.6.3.1 Surface energy theories of crystal growth

In recent years a surface energy factor, which describes the influence of surface characteristics on growth mechanisms, has been developed. These theories are based on the work of Gibbs (1928) who suggested that a crystal would grow in such a way so as to attain the shape which gave it the minimum surface energy. Although thermodynamically correct it can only be strictly applied to crystals of less than 2 μm (Springenberg, 1934). Wulff (1901) showed that the equilibrium shape of a crystal could be related to the free energy of the crystal faces. He suggested that the rate of growth of a crystal face was proportional to its surface energy. Although these theories still attract some attention there is no quantitative evidence to support them

and they fail to explain the effects of supersaturation and solution properties. Therefore, they are not considered to be of great significance.

1.6.3.2 Adsorption layer theories of crystal growth

The most significant contribution to the development of these theories was the work of Volmer (1939). He used a thermodynamic approach to explain the concept of crystal growth based on a consideration of the events surrounding the arrival of molecules in a solution at a growing crystal face. His model suggested that when molecules of the crystallising substance arrive at a crystal surface, they are not immediately integrated, but instead, form a loosely adsorbed layer (third phase). The thickness of this layer is certainly less than 10 nm and probably nearer to 1nm. These adsorbed molecules lose only one degree of freedom and so are free to migrate over the crystal face (surface diffusion) until they are drawn into the lattice at positions of high attractive forces known as active centres. Under ideal conditions, this stepwise build up will continue until the whole plane face is completed. If further growth is to take place on that face Volmer suggested that a monolayer island nucleus must be formed by surface nucleation (Figure 1.12). It was demonstrated that this surface nucleation can occur at lower levels of supersaturation than that required for three dimensional nucleation under equivalent conditions (Mullin, 1993). The starting point for Volmer's theory was provided by Kossel's (1934) model of crystal growth (Figure 1.13). He proposed that a crystal face is made up of moving layers or steps of mono-molecular height. Incomplete steps will contain one or more kinks. The surface may also have loosely adsorbed molecules as well as vacancies in both the surface and the steps. New molecules are most easily incorporated into the lattice at these kinks which consequently move along the step until it is eventually completed. Fresh steps are created by surface nucleation usually at the corners.

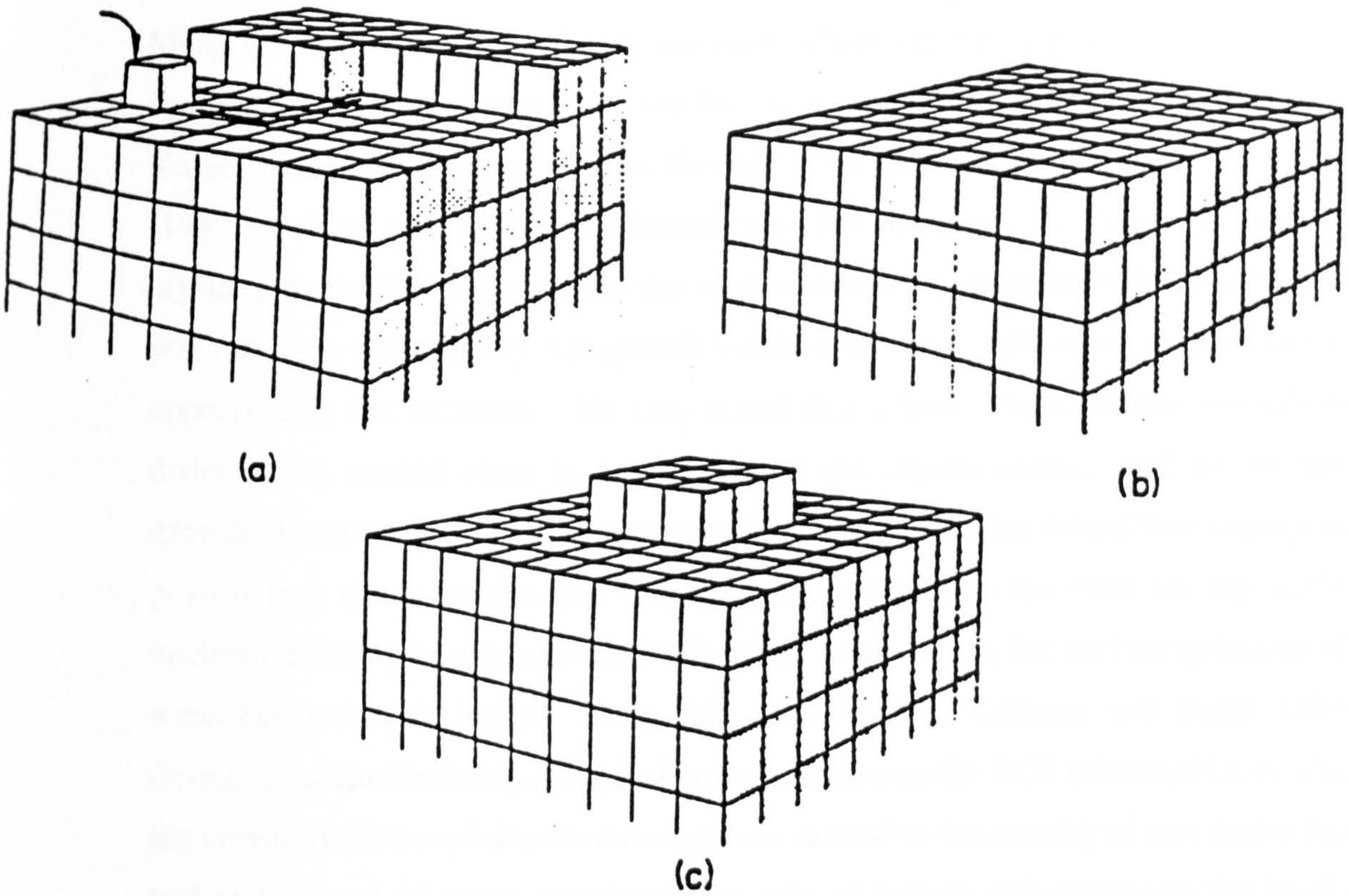

Figure 1.12 Volmer's model of crystal growth: (a) migration towards desired location; (b) completed layer; (c) surface nucleation (Mullin, 1993).

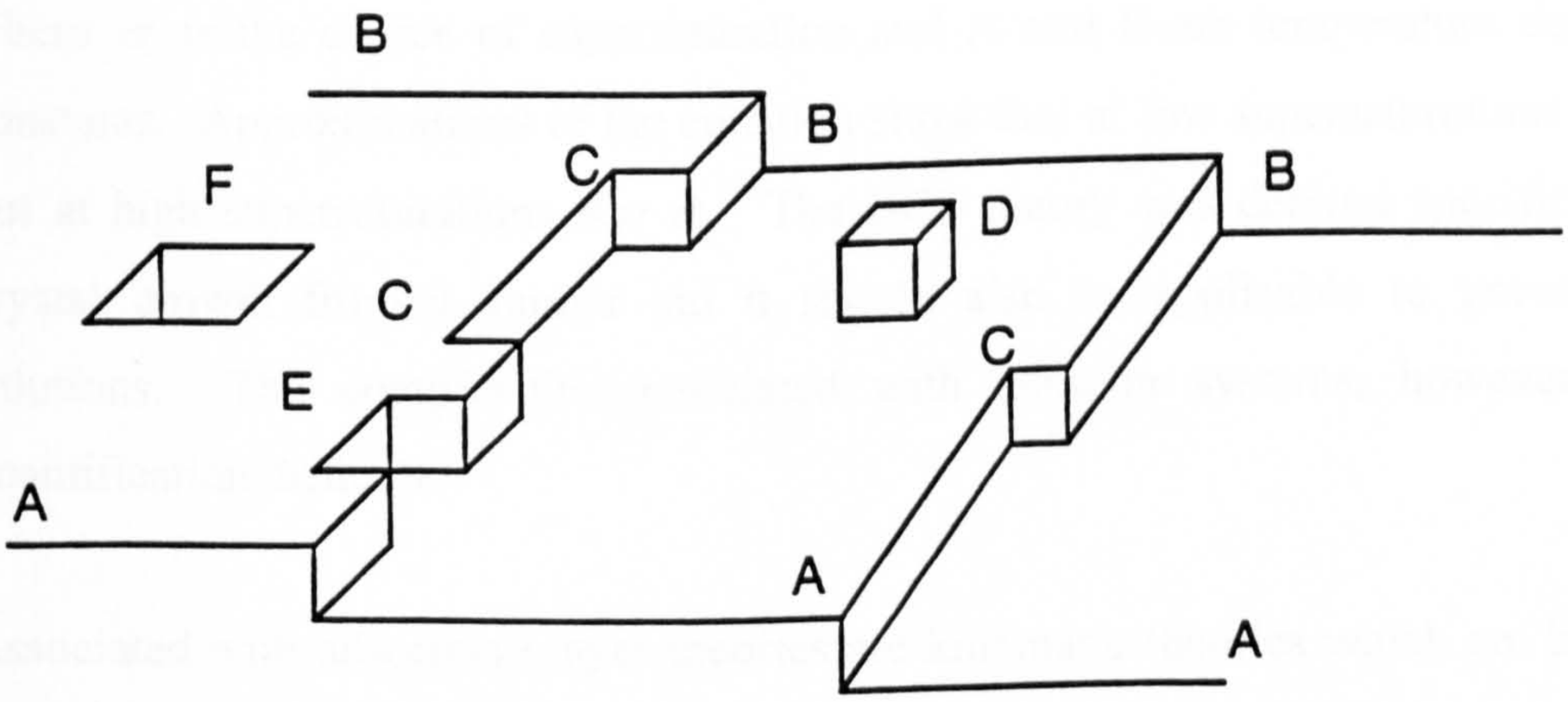

Figure 1.13 Kossel's model of a growing crystal showing flat surfaces (A), steps (B), kinks (C), surface adsorbed growth units (D), edge dislocations (E) and surface vacancies (F), (Mullin, 1993).

Many examples have been found, however, where crystal faces are seen to grow at supersaturation levels which are too low to support surface nucleation and so the Kossel model would appear to be flawed. This dilemma was solved when Frank (1949) showed that surface nucleation was not necessary to stimulate successful crystal growth. He suggested that the ideal situation represented by the Kossel model was rare as it was unlikely that growth would ever occur without some imperfections appearing in the structure. He also stated that crystal imperfections (specifically dislocations) caused steps to be formed on the crystal surface and so promoted growth. He perceived that the presence of a screw dislocation would lead to perpetual growth in a spiral fashion and thus completely removed the need for any surface nucleation, as a plane crystal face will never exist. Thus, the surface grows as if it were covered with kinks. From this basis Burton, Cabrera and Frank (1951) developed a kinetic theory of crystal growth, known as the BCF relationship, in which the curvature of the spiral near its origin was related to the spacing of successive turns and to the level of supersaturation. The rate of growth was related to the level of supersaturation by the equation

$$\text{Growth Rate (R)} = A\,\sigma^2 \tanh (B / \sigma) \qquad \text{(equation 1.21)}$$

where σ is the degree of supersaturation and A and B are temperature dependent constants. Approximations of the equation show that at low supersaturations $R \alpha \sigma^2$ but at high supersaturations $R \alpha \sigma$. The BCF theory was derived specifically for crystal growth from a vapour but it should also be applicable to growth from solutions. The complexities associated with solution systems, however, make quantification difficult.

Associated with adsorption layer theories are kinematic theories which are based on the fact that as molecules are added to kinks in a step, the step appears to move across the crystal face and thus has an apparent velocity. This velocity is dependent on the proximity of other steps as they will be competing for the same molecules to enable growth. Therefore, to obtain the maximum growth the steps must be at an optimum distance apart.

1.6.3.3 Diffusion theories of crystal growth

These theories originate from the work of Noyes and Whitney (1897) who considered that crystallisation was the reverse of dissolution and that the rate of both processes was governed by the extent of the concentration gradient between the crystal structure and the crystallisation liquor. The deposition rate was proposed to follow the relationship

$$dm/dt = K_m A (C - C^*) \qquad \text{(equation 1.22)}$$

where m is the mass of solid deposited in time t, A is the surface area of the crystal, C is the solute concentration in the liquor, C^* is the saturation concentration and K_m is the mass transfer coefficient. Nernst (1904), Miers (1904) and Marc (1908) made several minor changes to the equation. This work lead Brethoud (1912) and Valeton (1924) to suggest that mass deposition occurred by a two step process. The first step involved the transportation of solute molecules from the bulk liquor to the crystal surface while the second step involved a first order reaction where the molecules became incorporated into the crystal lattice. More recently this model has been further developed, by Nyvlt (1971), to a three stage process;

- transfer of solute molecules from the liquor to the crystal face
- movement of the molecules within the adsorption layer
- incorporation of the molecules into the crystal

He also suggested that the rate of crystallisation was determined by the slowest step and that diffusion controlled crystallisation could be accelerated by agitation of the system.

1.6.3.4 Surface entropy factor

In an attempt to resolve the various mechanisms proposed for crystal growth, Bennema and Gilmer (1973) devised a surface entropy factor, ϕ, by using computer simulated crystallisations. This surface entropy factor was essentially a measure of the molecular smoothness of the growing crystal face and the solution properties of the solvent.

They proposed that:

$$\phi = 4E / kT \qquad \text{(equation 1.23)}$$

where E is the energy gain upon formation of a solid - fluid bond at the interface, k is the Boltzmann Constant and T is the absolute temperature. They further postulated that certain growth mechanisms would only occur within specific ranges of ϕ values as a consequence of surface smoothness. They suggested that for $\phi < 3.2$ the crystal was rough and possessed many kinks, thus providing the necessary requirements for continuous, uninterrupted growth. If ϕ was between 3.2 and 5.0 they concluded that the surface was less rough but still but was still capable of promoting growth via surface nucleation. In the cases were ϕ was greater than 5.0, they claimed that the crystal surface was smooth and that a high level of supersaturation was required if surface nucleation and crystal growth was to take place.

It is now generally accepted that the various growth mechanisms can be covered by two general models.

i) The birth and spread (B & S) model, where growth is initiated by surface nucleation and predominates at moderate to high supersaturations and on rough surfaces.

ii) The BCF model, where growth progresses via the development of screw dislocations and is thought to predominate at low supersaturations.

1.6.3.5 Measuring linear crystal growth rates

There are in principle two methods for measuring crystal growth rates, direct and indirect. Direct measurements are based on either observation and measurement of the dimensions of single crystals, using some micro-imaging technique or by calculating the linear crystal growth rate by measuring increases in the mass or volume of either single crystals or the bulk product. The indirect methods are based on the evaluation of some experimental data obtained from the product such as changes in particle size distribution.

It should be remembered that the actual rate of growth of a crystal would be subject to variations throughout the course of a crystallisation. Therefore, the linear rate of growth is an average growth rate covering the entire process. The rate of crystal growth can be influenced by factors such as supersaturation levels, temperature and agitation. For example, the rate of crystal growth of sucrose has been reported to increase with agitation up to a 400 rpm. Agitation above this rate was found to exert no further effect. The rate of growth was also shown to increase in proportion to the square of the amount of supersaturation (Whitter and Gould, 1930).

Randolph (1970) proposed the following equation to describe the linear growth rate, G:

$$G = K_G S^m \qquad \text{(equation 1.24)}$$

where K_G is the growth rate constant, m is the order of growth and S is the amount of supersaturation. The growth rate constant was shown to be a function of temperature, solution purity and the degree of agitation.

1.7 Batch crystallisation by controlled cooling

As already discussed, the crystallisation of a solid from a solution can be achieved by cooling a saturated solution until it becomes supersaturated. Crystal growth can then be initiated by either spontaneous nucleation or by the introduction of seed material into the solution. The growth of crystals however, will cause the solution to begin to desaturate. Therefore, to ensure that the solution stays in a supersaturated state it must be continually cooled until a satisfactory end point is reached. Batch crystallisation experiments are conducted by placing a solution into a crystallisation vessel which allows several experimental variables to be controlled and closely resembles large scale industrial crystallisation processes. There are a large number of experimental variables that require careful control if batch-to-batch uniformity is to be achieved. Changing these variables offers the means to modify the crystallisation process so as to produce materials with different properties. The principle variables, which have been identified as being important in altering material properties, are listed below:

- rate of cooling
- degree of supersaturation
- addition of additives, impurities and solvents
- agitation (stirring) rate

1.7.1 Effect of cooling rate and supersaturation levels

The rate at which a solution is cooled controls the level of supersaturation, which in turn affects growth rates and growth mechanisms. For example, Mullin (1979) demonstrated that crystal growth rates typically increase with an increase in the degree of supersaturation, and in turn this affected crystal properties such as habit and size. Slower, and thus more controlled cooling rates, have also been shown to influence the size distribution of crystals (Mullin and Jones, 1974; Hiestand et al., 1981). Mechanical properties of crystals have also been shown to be affected by the degree of supersaturation. Ridgway and Aulton (1971) grew crystals of potassium bromide at a range of supersaturations, and observed changes in the rate of crystal growth and subsequently the hardness of the crystals. Ludlam-Brown (1989) reported

that the degree of crystallinity of ibuprofen as well as particle size, bulk density, true density and enthalpy of fusion were all influenced by changes in the cooling rate of the supersaturated solution.

The mechanism by which crystal growth takes place is also known to be sensitive to the supersaturation level and thus the rate of cooling. Slower cooling rates result in lower levels of supersaturation and this is believed to encourage spiral growth by the BCF mechanism. Faster cooling rates and therefore higher saturation levels results in growth by the B & S mechanism. Intermediate or changing levels would therefore be expected to result in a combination of growth mechanisms. It is thought that this overlap of growth mechanisms may be a major source of lattice imperfections.

1.7.2 Effect of additives, impurities and solvents on crystal growth

The effects of additives, impurities and solvents on the various properties of crystalline materials has been the subject of many studies and only a brief review will be presented here. The inclusion of surfactants in the crystallisation medium was shown to affect facial growth rates of adipic acid crystals (Michaels and Colville, 1960). The inclusion of anionic surfactants resulted in the production of needle like crystals, while the inclusion of cationic surfactants produce thin plate like crystals. It is believed that this was caused by the surfactants being adsorbed onto selective faces and once adsorbed they prevented any surface nucleation and thus growth to take place. Fairbrother and Grant (1978) also reported that the addition of alkanols to the crystallisation solvent produced adipic acid crystals in the shape of elongated rods due to adsorption onto the 110 and 100 faces, which retarded their growth rates. Chow et al. (1984, 1985) demonstrated that surface irregularities, heat of fusion, melting point density and dissolution rate of adipic acid crystals were all affected by the addition of alkanonic acids to the crystallisation solvent.

Berkoitch-Yelin (1985) proposed a set of predictive rules for the modification of crystal habits by the inclusion of additives in the crystallisation system, by considering the interactions between the solvent and solute at the crystal/solution interface.

She suggested that the adsorption of impurity molecules on a specified face retarded the growth of that face and so modified the morphology of the crystal.

The choice of solvent used in crystallisation has also been shown to play a major role in determining the shape of the final product. In a review of the subject, Davey (1982) proposed that the influence of solvents on crystal habits was due to the effects of solvents on the nucleation rates and growth mechanisms. In terms of pharmaceutical materials, e.g. nitrofurantion (Garti and Tibika, 1980), ibuprofen (Gordon and Amin, 1984) and hexamethylmelamine (Gonda et al., 1985) have all had their crystal habits modified by the use of alternative solvents. Marshall and York (1991) further demonstrated that the compaction properties of nitrofurantion were altered by crystallisation from different solvents.

1.7.3 Effect of agitation rate on crystal growth

The extent of agitation has been shown to be another important variable in the crystallisation process. Agitation principally affects the kinetics of crystal growth, and therefore can have significant consequences for the final product. The use of an agitator in a crystalliser generally results in smaller, more uniform crystals and a reduction in the growth time compared with when one is not used. The final product also tends to have a higher purity because less mother liquor is retained by the crystals after filtration and more efficient washing is possible (Mullin, 1993). Whether or not agitation intensity affects crystal growth would appear to be related to the growth mechanisms involved.

Bransom et al. (1969) observed that the rate of crystal growth of magnesium hydrates increased as the stirring rate was increased and suggested that this was due to a reduction in the width of the diffusion field. Metha et al. (1970) demonstrated that while the growth rate of sulfathiazole was dependent on stirring rate, that of methylprednisones was not. These differences can be explained by the fact that the diffusion layer is involved in the growth mechanism of magnesium hydrates and sulfathiazole, but is not involved in the growth mechanism of methylprednisones.

acid crystallised from water. He proposed that these modifications were due to alterations in the width of the metastable zone induced by changes in stirrer rate.

It is believed that the kinetics of crystal growth are affected by agitation in several ways. These are:

i) increased agitation results in an increase in the collision frequency of nuclei and thus increases the probability of secondary nucleation.

ii) increased agitation improves the homogeneity of the crystallisation liquor producing a more uniform product.

iii) Increased agitation causes more severe collisions between crystals, which in turn produces small crystal fragments. These fragments then behave as seeds, which induce further crystal growth.

The process of batch crystallisation is widely used to produce pharmaceutical materials commercially. This is mainly due to the fact the crystallising vessel can be thoroughly cleaned after each batch preventing any inter batch contamination. For this reason small scale batch crystallisations are often employed to mimic the conditions of industrial crystallisers.

1.8 Gel crystallisation of single crystals

In recent years, advances in solid state science has relied heavily on the production of single crystals which facilitate the testing procedures required to investigate the fundamental properties of materials. As a result much effort has gone into the development of growth techniques which will produce crystal specimens of suitable size, perfection and purity. One such technique being employed is that of crystal growth in gels.

The technique of growing crystals in a gel media first came to the attention of scientists in the late 1800s and enjoyed a period of popularity lasting into the 1920s. During this time, the focus of interest rested on the phenomenon of Liesegang Rings. Liesegang, a colloidal chemist and photographer who was experimenting with gels

observed that when he reacted silver nitrate with a gelatine gel impregnated with potassium chromate, regularly spaced rings of silver chromate formed in the gel. The first systematic study of the technique was made by Hatschek (1911) who included the chloride, iodide and sulphate of lead among his portfolio of crystals grown in gels. Realising that reactants could be diffused into, or dialysed from gels, led other workers such as Holmes (1926) to grow single crystals of copper and gold using a U-tube apparatus. Despite the success of these workers, however, the experiments were empirical in nature and gave little insight into the growth mechanisms involved. As a result, interest faded and the technique was largely forgotten for many years.

The requirements of the solid state scientists who required single crystals to carry out detailed investigations into the intrinsic properties of materials lead to a revival of the technique during the 1960's. The considerable progress in the study of gel crystallisation made during this period is attributed to Henisch (1968, 1970, 1971). In the years since, the emphasis has been on the growth of high quality single crystals and on extending the range of materials that can be crystallised in this way. Gel crystallisation has also been employed as a method for growing low solubility materials and organic substances, which have proved difficult to grow by more conventional methods. For example, insoluble copper halide crystals were grown in silica gel by Armington and O'Connor (1968) while Etter et al. (1986) have successfully grown single crystals of several high molecular weight organic substances.

Traditionally, crystal growth in gels was believed to involve a diffusion process. A reagent was diffused into the gel, which decreased the solubility of the solute in the saturated gel, or reacted with another reagent incorporated into the gel and thus induced nucleation and crystal growth. An alternative method which has been successfully used to grow single crystals of lactose (Wong, 1988) involves the gelling of a saturated solution followed by cooling to induce nucleation and crystallisation. This is very much the same as crystallisation from an aqueous solution but the gel offers several advantages such as providing a means of controlling nucleation density.

The principle function of the gel is believed to be the suppression of nucleation (Henisch, 1968). Since the crystals within any one system compete with one another

for solute, their ultimate size is obviously related to the number of crystals present. Suppression of the nucleation density by the gel therefore limits the number of crystal and so enables larger crystals to be grown before the supersaturated solution becomes depleted. The ability of any gel to suppress nucleation is related to its structure and is generally considered to be a direct function of its pore size distribution. In many cases, it has been reported that increasing the density of the gel (and thus decreasing the pore size) has resulted in a greater degree of nucleation suppression. For example, Patel and Roa (1978) showed that an increase in the density of silica acid gels decreased the nucleation density. The structure of many gels and therefore their ability to control nucleation are known to be affected by factors such as pH and the age of the gel. Another function of the gel is in the provision of a steady controlled environment free from convection currents and concentration gradients. It also supports the growing crystals in a three dimensional structure which yields to its growing faces but exerts no significant forces upon it.

Crystal growth in a gel appears to occur in one of two ways. Hanoka (1969) and Patel and Roa (1977) illustrated the situation where a cusp like cavity forms around the crystal. This cavity behaves as a womb around the crystal with the cusp wall acting as an osmotic membrane, which permits the addition of solute into the womb. Therefore, the crystal is surrounded not by a gel but by a solution whose solute concentration is equal to that at the surface of the crystal. In other instances, it has been demonstrated that the crystal is in direct contact with the gel and therefore growth must have proceeded via diffusion of solute through the gel media (Lefaucheaux et al., 1981 and 1982). It has been found that this mechanism can, however, lead to gel being incorporated into the crystal (Nickl and Henisch 1969).

In recent years, pharmaceutical scientists have been eager to relate the intrinsic properties of materials to their bulk behaviour. They have therefore required large single crystals which are suitable for the evaluation of mechanical properties such as hardness and elasticity. Wong (1988) described a technique of gel crystallisation, which used agar gel to successfully grow large single crystals of lactose monohydrate and anhydrous lactose.

A degree of caution should, however, be used when interpreting the data obtained from single crystals grown by gel crystallisation, especially if it is to be related to the bulk behaviour of the material. The crystallisation conditions used to grow these single crystals are very different to those used to produce the material commercially and may significantly affect its physical and chemical properties and its subsequent behaviour in operations such as tableting.

1.9 Aims and objectives

The interrelationships between the material properties (e.g. solid state and mechanical) of pharmaceutical excipients and their subsequent behaviour during operations such as tableting are well recognised (e.g. Jones 1977, 1981; York 1983, 1992). Inter batch and source to source variation of these properties are still, however, largely uncontrolled and result in many of the problems associated with tablet production.

Most pharmaceutical excipients are organic in nature and have undergone crystallisation either as a part of their manufacture or as a purification step. The crystallisation process has been identified as being the origin of some material property variations but has also been shown to be a useful tool in deliberately manipulating material properties with the aim of optimising their behaviour during pharmaceutical operations (van der Voort Maarschalk 1998). However, it is clear that the links between the fundamental material and mechanical properties of pharmaceutical materials and their compaction characteristics must be identified and quantified before a predictive capability can be introduced into this approach.

The specific aim of this work therefore, was to investigate the effect of altering crystallisation process variables on the material properties of dextrose, its behaviour during compaction and the mechanical characteristics of its compacts.

Initial work was to focus on the batch production of dextrose using a range of crystallisation conditions and on the development of a technique for growing single crystals of dextrose suitable for mechanical testing.

A detailed study was carried out to evaluate the effect of altering the crystallisation conditions on the physiochemical properties of dextrose. The various batches could then be compacted and the compaction behaviour characterised. The mechanical properties of the compacts were then determined and the results used to assess the fundamental mechanical properties of the crystalline batches of dextrose.

Dextrose was chosen for this work for a number of reasons. It has been identified as a viable pharmaceutical excipient suitable for use as a direct compression filler but has never gained the popularity of lactose and thus the amount of previous studies on its material properties and compression behaviour is relatively small. Also, while it is chemically similar to lactose, it possesses different crystal habits and has markedly different solubility. It is therefore hoped that it will prove to be a good model producing data which can be both compared with and differentiated from the known properties and behaviour of lactose. This in turn may help to elucidate the role of crystallisation variables in controlling the physiochemical, mechanical and compaction properties of pharmaceutical excipients.

CHAPTER TWO

CRYSTALLISATION OF DEXTROSE

2.1 General introduction

This chapter is divided into three main sections. Firstly it lists all the materials employed in this study and presents a brief review of dextrose with particular reference to its solubility, crystal morphology, industrial crystallisation and pharmaceutical usage, as relevant to this work. The second section details the experimental procedures used to grow single crystals of dextrose using a gel crystallisation technique. These crystals, however, proved unsuitable for mechanical testing. The third section, is concerned with the experimental techniques and procedures used to produce batches of dextrose. These were subsequently used to investigate the effect of batch crystallisation variables on the solid state, particulate and compression properties of dextrose and the mechanical properties of its compacts.

2.2 Growth of single crystals of dextrose monohydrate

In order to test and characterise the fundamental mechanical properties of dextrose monohydrate, single crystals of a suitable size and perfection were required. The growth of single crystals of dextrose from aqueous solutions has been reported previously but the crystals were small and too fragile for handling or mechanical testing (Grerrta and Berglund, 1989). Following suggestions made after research on the fundamental mechanical properties of lactose monocrystals (Wong 1988), the technique of gel crystallisation was utilised as it had shown potential as a method capable of yielding large single crystals with a high degree of perfection.

For this work, a system based on the use of Carbopol 940 gel was employed. An extensive literature search revealed no record of any attempts to grow single crystals of dextrose by gel crystallisation techniques.

2.3 Materials

All the materials used in this work were general purpose laboratory grade.

Dextrose anhydrous (BDH Chemicals, Poole UK)

Dextrose monohydrate (BDH Chemicals, Poole UK)

Carbopol 940 (BDH Chemicals, Poole UK)

Lactose anhydrous 940 (BDH Chemicals, Poole UK)

Sucrose 940 (BDH Chemicals, Poole UK)

Micrcocrystalline cellulose (Avicel PH101) (FMC, Philadelphia, USA)

Magnesium stearate (BDH Chemicals, Poole UK)

Ethanol (FSA, Loughborough, UK)

Acetone (FSA, Loughborough, UK)

Sodium hydroxide (FSA, Loughborough, UK)

2.3.1 Dextrose

Dextrose ($C_6H_{12}O_6$), also referred to as D-glucose, is a naturally occurring monosaccharide widely found in all plants and animals. It is generally available in three forms, alpha monohydrate, alpha anhydrous and beta anhydrous, the latter being the least common.

Although known to exist for a long time, the first attempts at commercial production were not reported until the beginning of the nineteenth century. Several significant modifications to the process were made during the following century, most notably by Kirchoff (1811), Behr (1881), Wagner (1906) and Porst et al.(1924). However it was not until the 1920s when a series of detailed investigations into the process was undertaken by Newkirk (1924, 1925, 1939) that the process became commercially viable. Essentially the process used commercially today has changed little since then. The work of Newkirk was, however, concerned mainly with the establishment of an efficient and practical manufacturing process with little consideration given to the effects of crystallisation variables on the material properties.

Detailed information on the crystal forms of dextrose was first reported by Beck (1889). The monohydrate crystallises in the monoclinic system and forms thin plate like crystals of hemimorph development (Figure 2.1). Often at one end of the crystal, one (010) face is present instead of two (110) faces (as shown by the dotted line). The anhydrous form crystallises in the rhombic system and appears as a slightly elongated prism with hemihedral end surfaces (Figure 2.2).

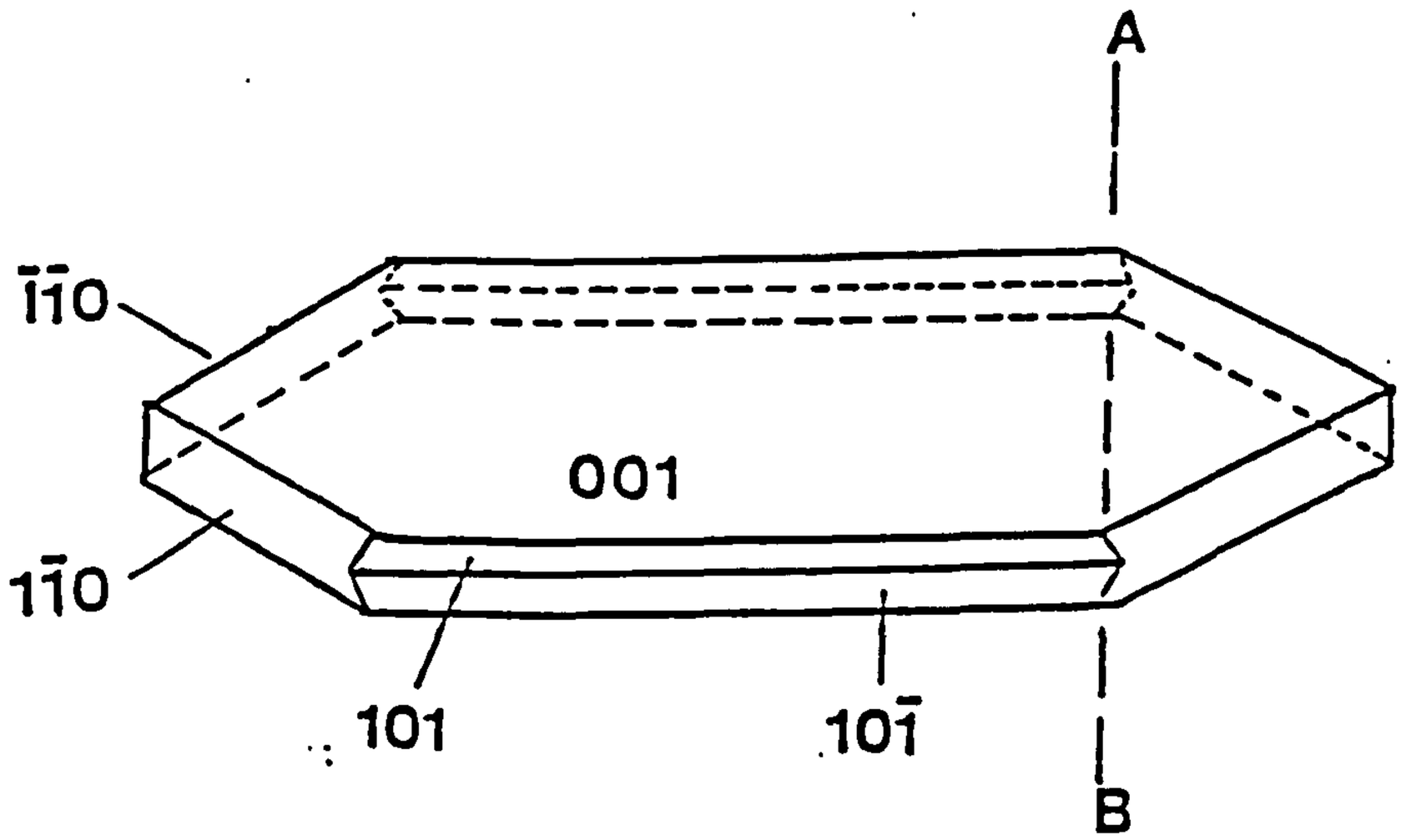

Figure 2.1 Crystal habit of dextrose monohydrate

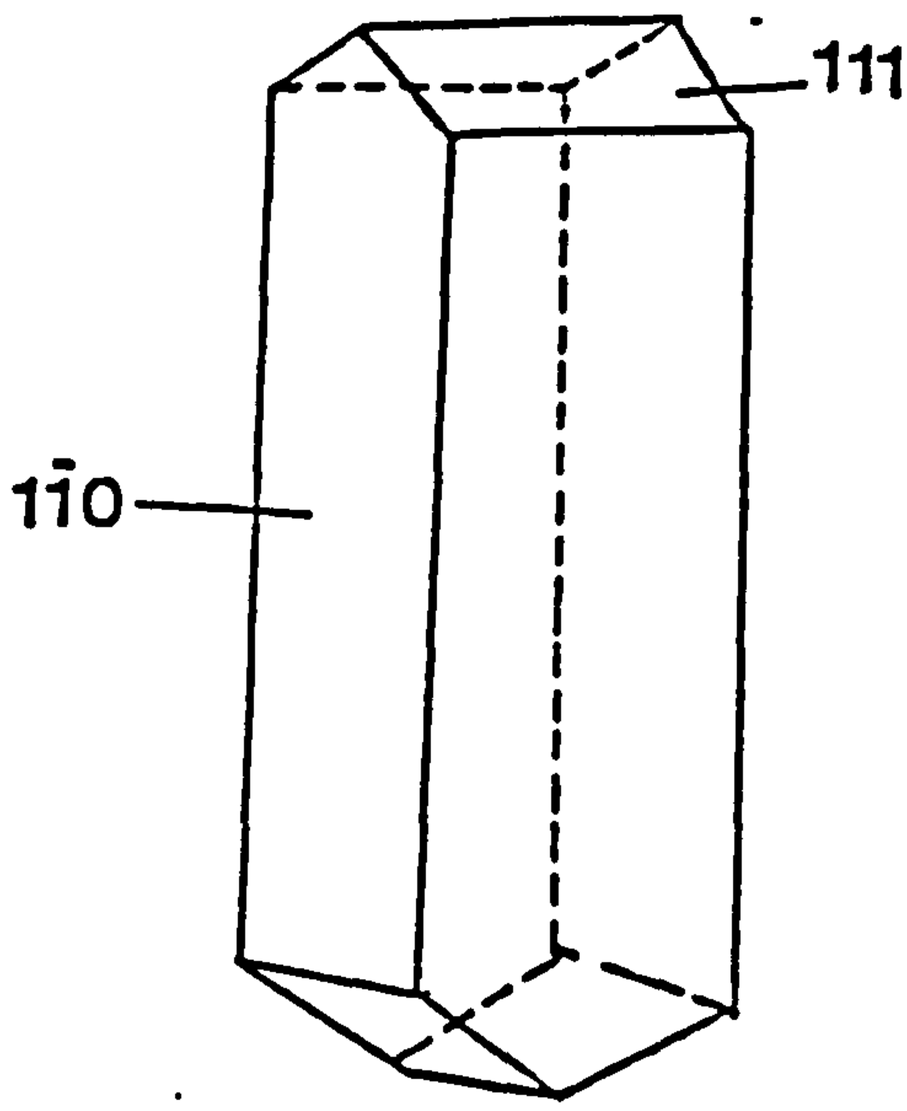

Figure 2.2 Crystal habit of anhydrous dextrose

The solubility of dextrose in water has been comprehensively studied over a wide range of temperatures by Jackson and Silbee (1922) and Young (1957). An aqueous solubility curve is shown in Figure 2.3. A hydrate/anhydrous transition point exists at approximately 50°C. Anhydrous dextrose will crystallise above this temperature and dextrose monohydrate will crystallise below it. A second order polynomial equation was found to fit the solubility/temperature data over the 30-60°C temperature range:

$$Y = 0.083X^2 - 1.833X + 100.00 \qquad \text{(equation 2.1)}$$

Where X is the temperature in °C and Y is the amount of dextrose required to produce a saturated solution.

Crystallisation of carbohydrates is often complicated by the presence of tautomers that, although closely related, are distinct molecular entities. When dextrose is dissolved in water, it immediately undergoes a partial stereo-chemical transformation from the alpha form to the more soluble beta form. The rate of this $\alpha \rightarrow \beta$ transformation is known to be dependent on the temperature of the solution. At equilibrium conditions the situation can be represented by the reaction equation:

$$\underset{\text{crystals}}{\alpha - dextrose} \Leftrightarrow \underset{\text{Supersaturated solution}}{\alpha - dextrose} \Leftrightarrow \beta - dextrose \qquad \text{(equation 2.2)}$$

The final solubility % therefore is not that of α-dextrose in water but in a solution of β-dextrose. At relatively low temperatures, dextrose crystallises from aqueous solutions in the α-hydrated (monohydrate) form, although an equilibrium solution contains approximately 40% α-dextrose and 60% β-dextrose. During crystal growth therefore, the β-form must transform to the α-form and it is the speed of this $\beta \rightarrow \alpha$ transformation, which is the rate determining step for the rate of growth of dextrose. Also the presence of the β form retards the rate of crystallisation, as would any foreign material (impurity). The temperature solubility curve for dextrose shown in Figure 2.3 has a transition point at 50°C. Below this point dextrose crystallises as the monohydrate and above it crystallises as the anhydrous material. The solubility of

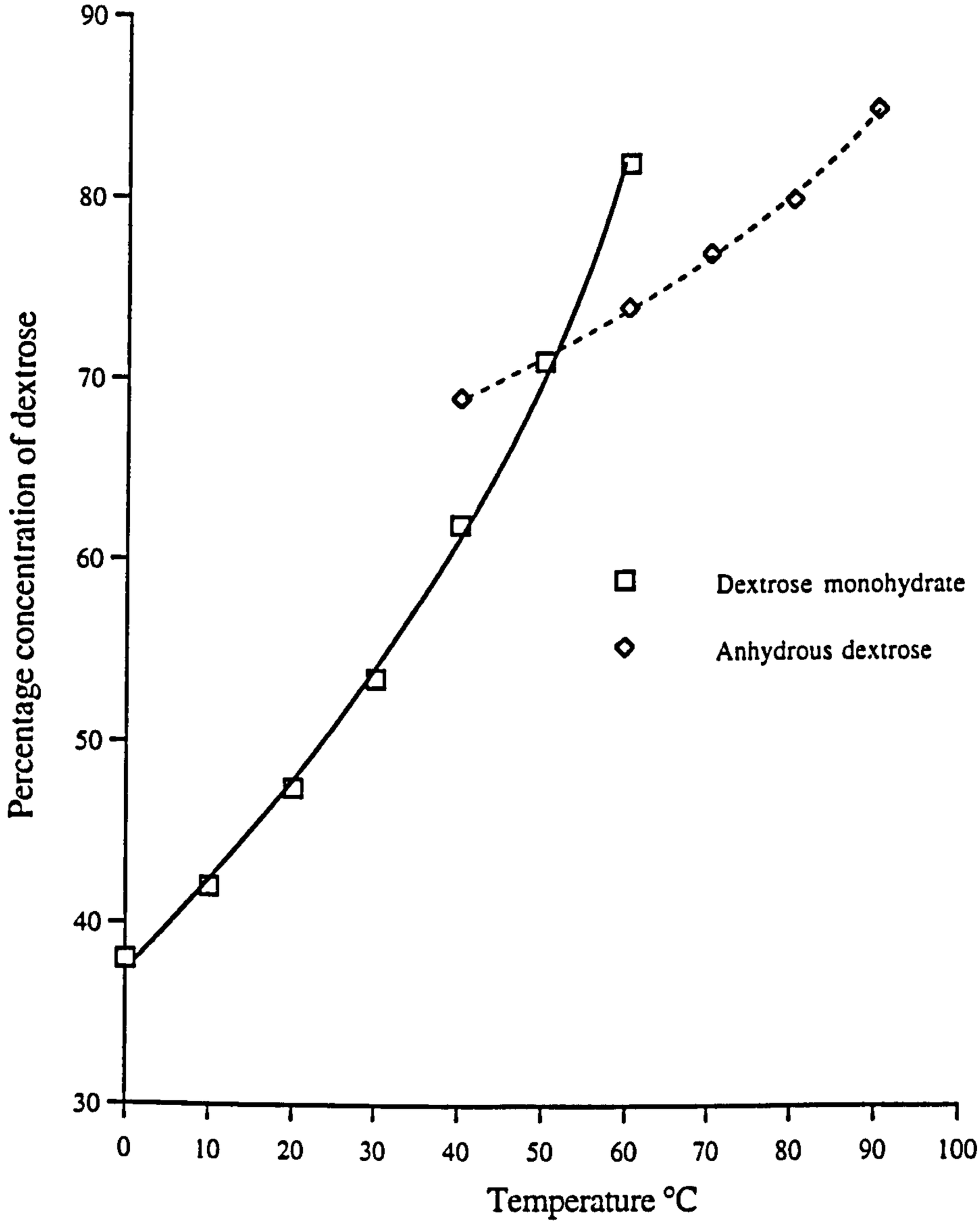

Figure 2.3 Aqueous solubility curve for dextrose (data from Mullin, 1993)

the β form is least at temperatures approaching the boiling point of the aqueous solution and this form is therefore crystallised at temperatures above 90°C. The rate of crystallisation of dextrose and other carbohydrates in the temperature range 0 to 30°C was studied by Whitter and Gould (1930). They reported that the rate increased with increasing temperature, probably due to an increase in the rate of the $\beta \rightarrow \alpha$ transformation, while it decreased with time due to decreasing supersaturation.

It was proposed by Edwards (1982) that the growth of dextrose crystals was a two stage process. Firstly a solute molecule had to diffuse from the bulk solution to the crystal surface and secondly it had to orientate itself into a position on the crystal lattice. He concluded therefore that the linear rate of growth could be diffusion controlled or surface reaction controlled.

2.3.2 Commercial production of dextrose

Alpha dextrose monohydrate manufacture begins with the acid hydrolysis of starch (usually cornstarch) followed by purification, concentration by evaporation and finally crystallisation (and recrystallisation if a higher purity product is required). The crystallisation is carried out by slowly cooling a supersaturated solution of dextrose, from a temperature of approximately 40°C to approximately 30°C with constant agitation over a period of several days. Crystallisation is induced by the inclusion of up to 25% of the previous batch, as seed crystals. When approximately 60% of the solute has crystallised the resulting magma is centrifuged and the last traces of mother liquor are washed off. The wet crystals are then dried in a stream of hot air to remove all but the water of crystallisation (theoretically 9.1%).

The crystallisation of alpha dextrose monohydrate is strongly influenced by the presence of the beta isomer. The rate of crystallisation is firstly limited by the slow transformation in solution of the more soluble beta isomer to the less soluble alpha isomer. Secondly, the beta isomer in an equilibrium solution behaves as an impurity or a foreign material, which slows the rate of crystallisation and can affect the habit of the resulting alpha monohydrate crystal.

Anhydrous alpha dextrose can be obtained by drying the monohydrate material. A better product is, however, obtained if the crystallisation is carried out as described for

α–dextrose monohydrate but at a temperature above 50°C. Again the magma is centrifuged and the crystalline material washed, filtered and dried in a stream of warm air to produce crystals which this time have a moisture content of less than 1%.

2.3.3 Pharmaceutical applications of dextrose

In pharmaceutical terms, dextrose is commonly used as a tablet filler or diluent. Duvall and Joshy. (1965) evaluated the use of dextrose in direct compression systems and found that it many respects dextrose was comparable to the more commonly used sprayed dried lactose. Henderson and Brono (1970) compared the properties of dextrose with two well known direct compression agents, spray dried lactose and anhydrous lactose USP. They concluded that the compression characteristics of dextrose were superior to that of the lactose sugars, producing stronger and less friable tablets.

Patel (1986) examined the effect of moisture content on the compressional properties of anhydrous dextrose and dextrose monohydrate. For anhydrous dextrose, they reported an increase in tensile strength and tablet toughness as the moisture was increased up to a limiting value of approximately 8.9% after which there was a rapid decrease in both parameters. The yield force, as measured from Heckel plots, was observed to decrease as the moisture content was increased indicating an increase in plastic character. For dextrose monohydrate, any change in the moisture content from its nominal value of approximately 9.1% was seen to decrease both the tensile strength and tablet toughness. When both materials had the same, moisture content the material that was originally anhydrous was always found to produce stronger and tougher compacts. These findings were attributed to the way in which the water was held on the material. In the hydrated anhydrous dextrose the moisture was only loosely attached and so could behave like a lubricant, increasing the plasticity of the system and thus aiding compression. In the monohydrate material, the moisture was tightly locked within the crystal lattice, and therefore, could not contribute to bond formation.

2.3.4 Carbopol 940

Carbopol resins are hydrophilic, water soluble, crosslinked, acrylic acid polymers. When they are dispersed in water, they partially swell and when neutralised with a water soluble base they swell completely causing a dramatic increase in viscosity. The resins vary in molecular weight, degree of crosslinking and molecular structure. These differences are responsible for the specific rheological characteristics and thickening efficiency of each resin.

In the experiments conducted to grow single crystals of dextrose using a gel crystallisation technique, Carbopol 940 was used, as it offered several distinct advantages over other gels which had previously been reported. It produced a sparkling clear gel, which made visual and photographic observations less troublesome. It produced a very viscous gel on neutralisation that was stable over the range of temperatures and pHs expected in the experiments to be conducted. The viscosity of the gel could be decreased by over neutralisation so allowing crystals to be easily recovered. Also its chemical structure is different from dextrose thus minimising the possibility of the gel being incorporated into the growing crystals as was the case in the work by Wong (1988), where lactose crystals were grown in agar gel.

2.4 Growth of single crystals in Carbopol gels

2.4.1 Carbopol gel preparation for crystal growth

Preparation of a Carbopol gel containing a supersaturated solution of dextrose was initially hindered the hydrophilic nature of the dry Carbopol resin and the viscosity of the saturated dextrose solutions. If the dry Carbopol powdered resin was directly added to an aqueous supersaturated solution of dextrose or to water itself, it formed agglomerates, the surfaces of which solvated quickly, creating a viscous layer which inhibited further wetting and dissolution of the dry interiors. This resulted in defects such as an inconsistent viscosity and the presence of partially wet agglomerates, which looked like "fish eyes", being incorporated into the gel. The problem was overcome by dry blending the Carbopol resin with the dextrose before preparing the saturated solution. Further difficulties caused by the viscosity of the solutions were

greatly reduced by the careful selection and use of filters. The final method used to prepare all the gel systems was as detailed below.

1) After weighing, the dextrose (anhydrous) and the Carbopol resin were blended together, first by mixing using a Turbula mixer for two minutes on medium speed, and then by passing the mixture through a 1 mm sieve.

2) The powder mixture was then slowly added to the required amount of heated distilled water with constant, stirring using an overhead stirrer and was maintained at the saturation temperature overnight, to ensure complete dissolution.

3) Any water lost due to evaporation was replaced and the solutions were filtered using a hot, sintered glass N°1 filter with a vacuum (to remove any un-dissolved material).

4) The saturated system was gelled by the drop wise addition of 2 M sodium hydroxide solution with constant stirring, until a pH = 7.0 ± 0.2 was achieved (the pH meter calibration self adjusted to account for elevated temperature). . Stirring was continued for 20 minutes to ensure thorough mixing.

5) The gel was then transferred to sealed containers, before being cooled to, and maintained at, various temperatures by the use of thermostatically controlled water baths.

This was the standard method used for the crystallisation of single crystals by the gel growth technique, any variations made from this method are detailed in the relevant sections.

2.4.2 Determination of saturation level required for crystallisation

Saturated dextrose solutions containing Carbopol resin at two different levels were prepared according to the method described in section 2.4.1. The amounts of materials used were as shown in Table 2.1. Portions of each gel were then cooled at a rate of 1.0°C/h to various temperatures. The gels were then maintained at these temperatures (using water baths) and observed over a two week period.

Table 2.1 Amount of material used to prepare saturated dextrose solutions at various temperatures (as calculated using equation 2.1)

	40°C	50°C	60°C
Dextrose (anhydrous)	160g	215g	289g
Water	200g	200g	200g
Carbopol 940*	0.72g 3.60g	0.83g 4.15g	0.98g 4.89g

* The two levels of Carbopol 940 are equivalent to 0.2%$^{w}/_{w}$ and 1.0%$^{w}/_{w}$ respectively.

2.4.2.1 Results and observations

Solutions Saturated at 40°C

Crystallisation Temperature	Carbopol Concentration 0.2% $^{w}/_{w}$	Carbopol Concentration 1.0% $^{w}/_{w}$
20°C	Several clusters of crystal aggregates formed which grew into each other.	A few small crystal aggregates formed near the surface of the gel but did not grow
30°C	A few very small crystal aggregates formed and grew very slowly.	No crystals observed

Solutions Saturated at 50°C

Crystallisation Temperature	Carbopol Concentration 0.2% $^{w}/_{w}$	Carbopol Concentration 1.0% $^{w}/_{w}$
20°C	Completely crystallised after less than 24 hours	A few very small aggregates formed near the surface of the gel but did not appear to grow
30°C	Small aggregates of crystals formed at first but the system was completely crystallised after 3 days.	No crystals observed
40°C	A few small aggregates were visible which grew slowly.	No crystals observed

Solutions Saturated at 60°C

Crystallisation Temperature	Carbopol Concentration 0.2% $^{w}/_{w}$	Carbopol Concentration 1.0% $^{w}/_{w}$
20°C	Completely crystallised after less than 4 hours	One aggregate formed and grew
30°C	Small aggregates of crystals formed at first but the system was completely crystallised after 24 hours	A few small aggregates formed but did not seem to grow
40°C	A number of aggregates formed and grew until the system was completely crystallised after 5 days	No crystals observed
50°C	No crystals observed	No crystals observed

2.4.2.2 Discussion

Carbopol gel demonstrated potential as a media for the gel growth of dextrose crystals. While no single crystals were observed in the experiments, microscopic examination of the small crystal aggregates formed did show the presence of several crystals growing from a central point. Figure 2.4, is a micrograph of these crystal aggregates suspended in 0.2% $^{w}/_{w}$ gel saturated at 40°C and cooled to 20°C. The experiment also indicated that supersaturation at 40°C and cooling of the saturated gel by between 10 and 20°C is more than sufficient to cause nucleation. Greater levels of supercooling caused a greater degree of nucleation and faster crystal growth. It is also evident that the concentration of the gel plays an important role in controlling nucleation density and crystal growth rate. Even at high levels of supersaturation, there was little or no nucleation or crystal growth in the systems with the more concentrated gels.

Figure 2.4 Crystal aggregates formed in 0.2% $^{w}/_{w}$ gel at 20°C with a saturation temperature of 40°C (X 10)

2.4.3 Determination of gel concentration required for crystal growth

In order to determine the optimum gel concentration required for the growth of single crystals of dextrose monohydrate a series of experiments were conducted. Solutions of dextrose incorporating Carbopol gel concentrations of 0.2, 0.4, 0.6, 0.8 and 1.0 % $^{w}/_{w\ were}$ prepared by the standard method (section 2.3.2) at a saturation temperature of 40°C. The gels were then cooled and maintained at temperatures of either 20°C or 30°C and observed over a period two weeks.

2.4.3.1 Results and observations

0.2% $^{w}/_{w}$ Carbopol gels - The gels at both temperatures were of low viscosity and lots of small crystalline aggregates formed within hours. The systems were completely crystallised after 48 hours (i.e. the entire system had become solid).

0.4% $^{w}/_{w}$ Carbopol gels - In the gel cooled to 20°C a large number of small polycrystalline aggregates formed within 24 hours. In the gel cooled to 30°C no crystals were observed.

0.6% $^{w}/_{w}$ Carbopol gels - The gel at 20°C produced several polycrystalline aggregates after one week (Figure 2.5a). In the gel cooled to 30°C no crystals were visible

0.8% $^{w}/_{w}$ Carbopol gels - The gel cooled to 20°C produced a number of tiny single crystals, which grew into aggregates after a few days, (Figure 2.5b.). The gel at 30°C contained no visible crystals.

1.0% Gels - In the gel at 20°C a number of very small crystals were visible using the microscope (X10) but these did not appear to grow. The gel at 30°C did not yield any crystals.

2.4.3.2 Discussion

The above experiment indicates that the concentration of Carbopol can be employed as a means of controlling the amount of nucleation and crystal growth that takes place. A Carbopol concentration of 0.8% $^{w}/_{w}$ appears to be the optimum level for supporting crystal growth while limiting nucleation. Another set of experiments was clearly required to optimise the growth conditions.

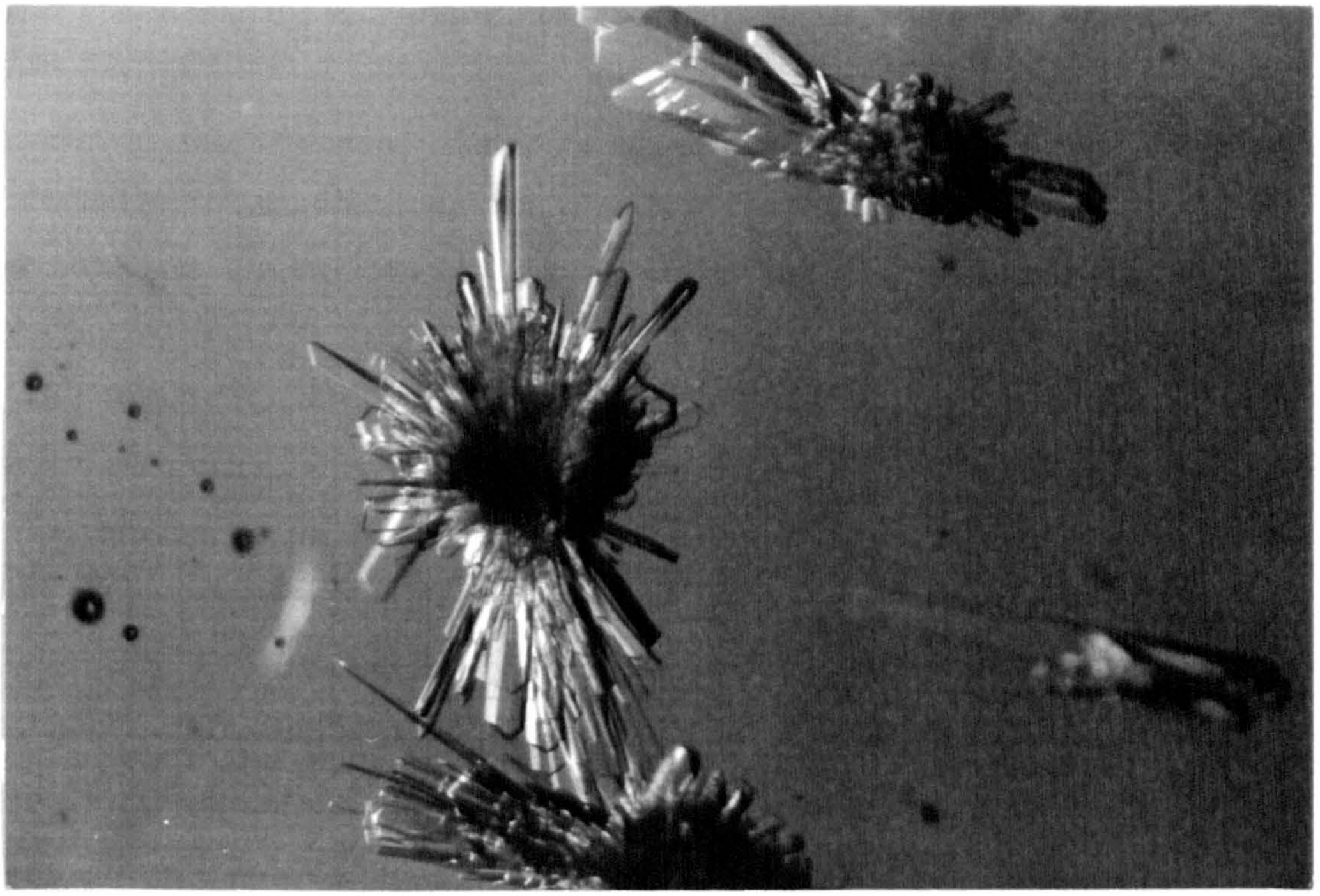

Figure 2.5a A crystal aggregate formed in 0.6% $^{w}/_{w}$ Carbopol gel cooled to 20°C (X10)

Figure 2.5b Crystals formed in a 0.8% $^{w}/_{w}$ Carbopol gel cooled to 20°C (X10)

2.4.4 Determination of optimum temperature for crystal growth

After considering the data from the previous experiments, another series of tests were conducted to optimise the conditions for nucleation and crystal growth. Using the standard method, saturated solutions were prepared at 40°C containing 0.8 $\%^{w}/_{w}$ Carbopol 940. Samples of the saturated gel were then maintained at 22, 24, 26, 28 and 30 °C and observed regularly over a period of three weeks.

2.4.4.1 Results and observations

As had been indicated in the previous experiments, the nucleation density was found to be dependent on the crystallisation temperature and indeed this would be expected as the temperature is, in reality, being used to control the degree of supersaturation. The density of nucleation clearly decreased as the crystallisation temperature was increased. At 22°C only a mass of polycrystalline aggregates were formed, while at 24°C there was a mixture of aggregates and single crystals, however these were so numerous that they quickly formed large clusters growing into each other. At 26°C, only single crystals were present but they were too crowded to allow room for much growth. At 28°C, there were a lot less single crystals and in the main, these continued to grow as single crystals (see micrographs in Figures 2.6a and b). These gels also, however, tended to become overcrowded after a few days, as new nuclei continued to appear and grow leading to crystals with a variety of sizes. At 30°C, no crystals were observed.

2.4.4.2 Discussion

In general it appears that nucleation can be controlled by careful selection of the growth conditions. A Carbopol 940 gel concentration of 0.8$\%^{w}/_{w}$ in combination with the correct temperature has been shown to be capable of providing a suitable environment for the limited nucleation and growth of single dextrose monohydrate crystals. As observed in the previous experiment, nucleation continued to oCcur in the gel maintained at 28°C, eventually overcrowding the system and depleting the saturated solution thus hindering the growth of large single crystals, but at a temperature of 30°C no nucleation occurred. It therefore seemed reasonable to assume that by, first cooling the gel to 28°C and maintaining it there for a specified

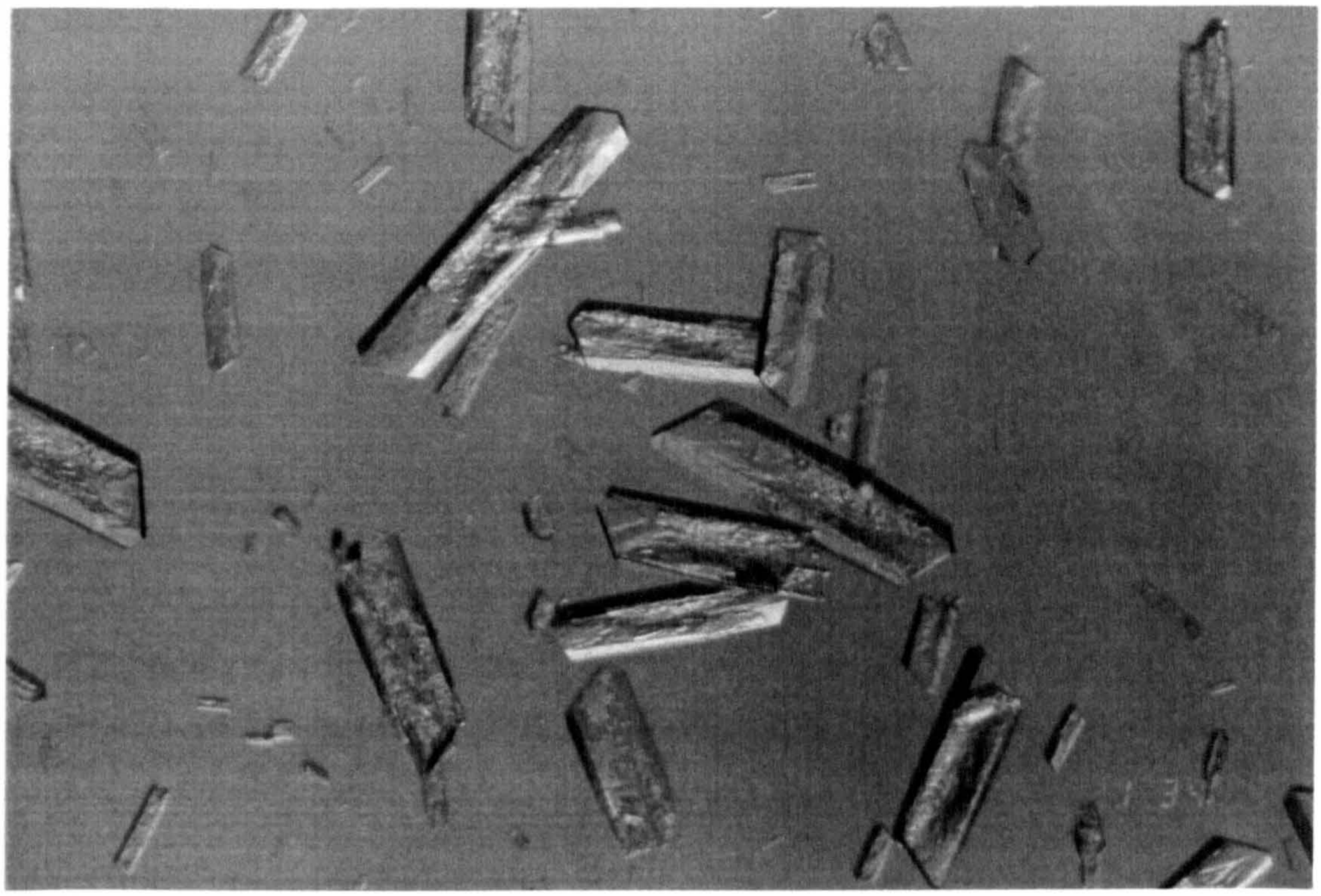

Figure 2.6a Single crystal grown in a 0.8% $^{w}/_{w}$ Carbopol gel at 26°C for 5 days (X10)

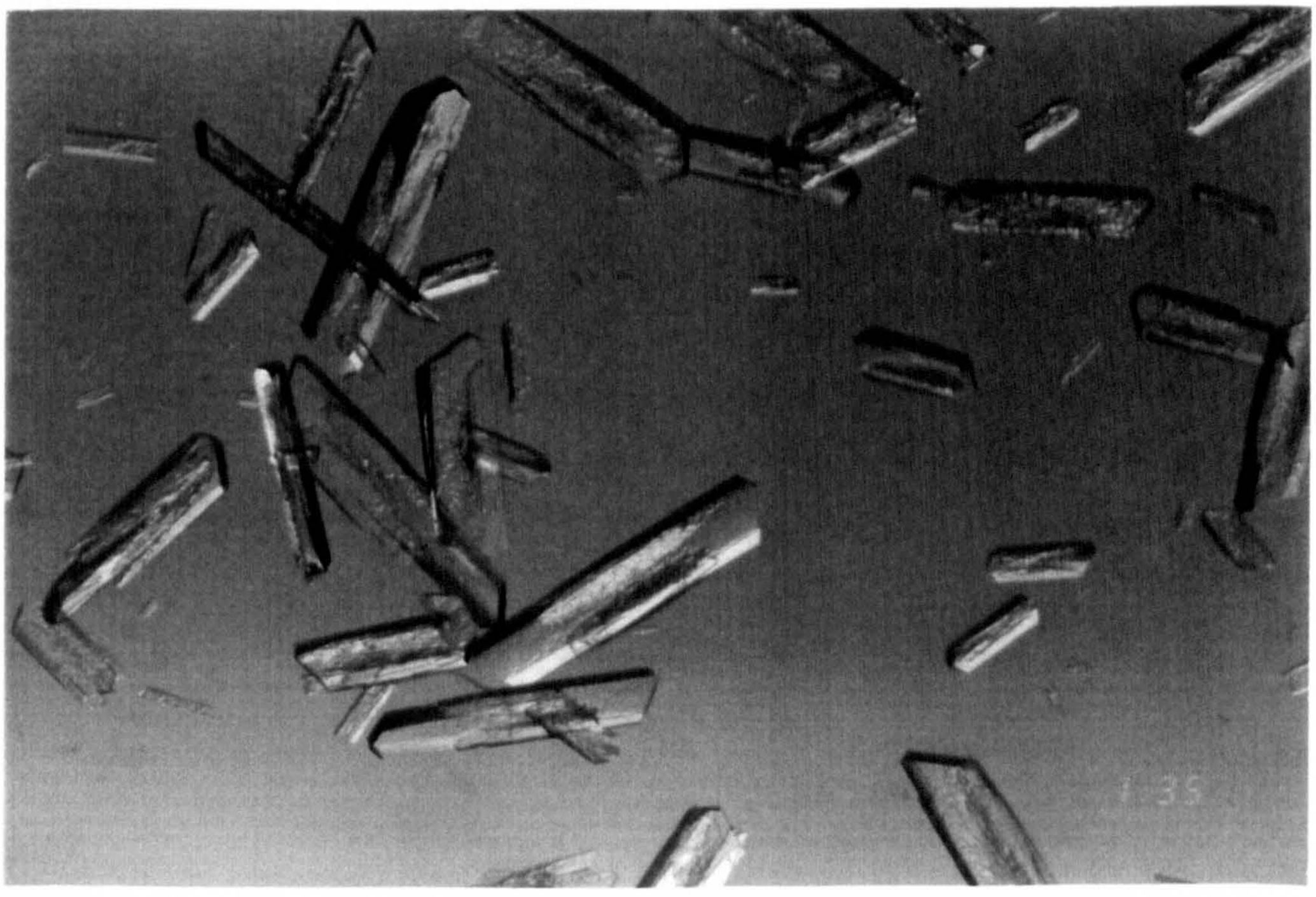

Figure 2.6.b Single crystals grown in a 0.8% $^{w}/_{w}$ Carbopol gel at 28°C for 8 days (X10)

time, nucleation would occur. Then by heating the gel to above 30°C further nucleation would be inhibited leaving the stable nuclei free too grow into large single crystals. This approach was tried in the following experiments.

2.4.5 Growth of single crystals using temperature controlled nucleation

Following the results of the above experiments another saturated gel containing 0.8%$^{w}/_{w}$ Carbopol 940 was prepared at 40°C by the standard method. It was then divided into portions of 200ml which were slowly cooled to a temperature of 28°C at which they were maintained for 24, 48, and 72 hours, to induce nucleation. The gels were then gently heated to 31°C at which temperature they were maintained and observed.

2.4.5.1 Results and observations

Single crystals were seen to be suspended in all the gels and appeared to be growing, but very slowly. There was no significant difference in the nucleation density between the gels maintained at 28°C for 24 and 48 hours, but the gel that was held at 28°C for 72 hours did have a lot more crystals present and soon became overcrowded with crystals growing into each other. Figures 2.7 (a-d) shows several photomicrographs of the crystals suspended in the gel. They can be seen to have the characteristic habit of dextrose monohydrate as shown in Figure 2.1a, but many appear to be in fact twin crystals, as lines of inter growth are visible.

2.4.5.2 Discussion

After a period of 3 weeks it became obvious that the crystals were no longer growing even though the gel was not overcrowded and the saturated solution was clearly not depleted. At this point the crystals were between 4 to 7mm in length, and it was decided to harvest and characteristic these crystals.

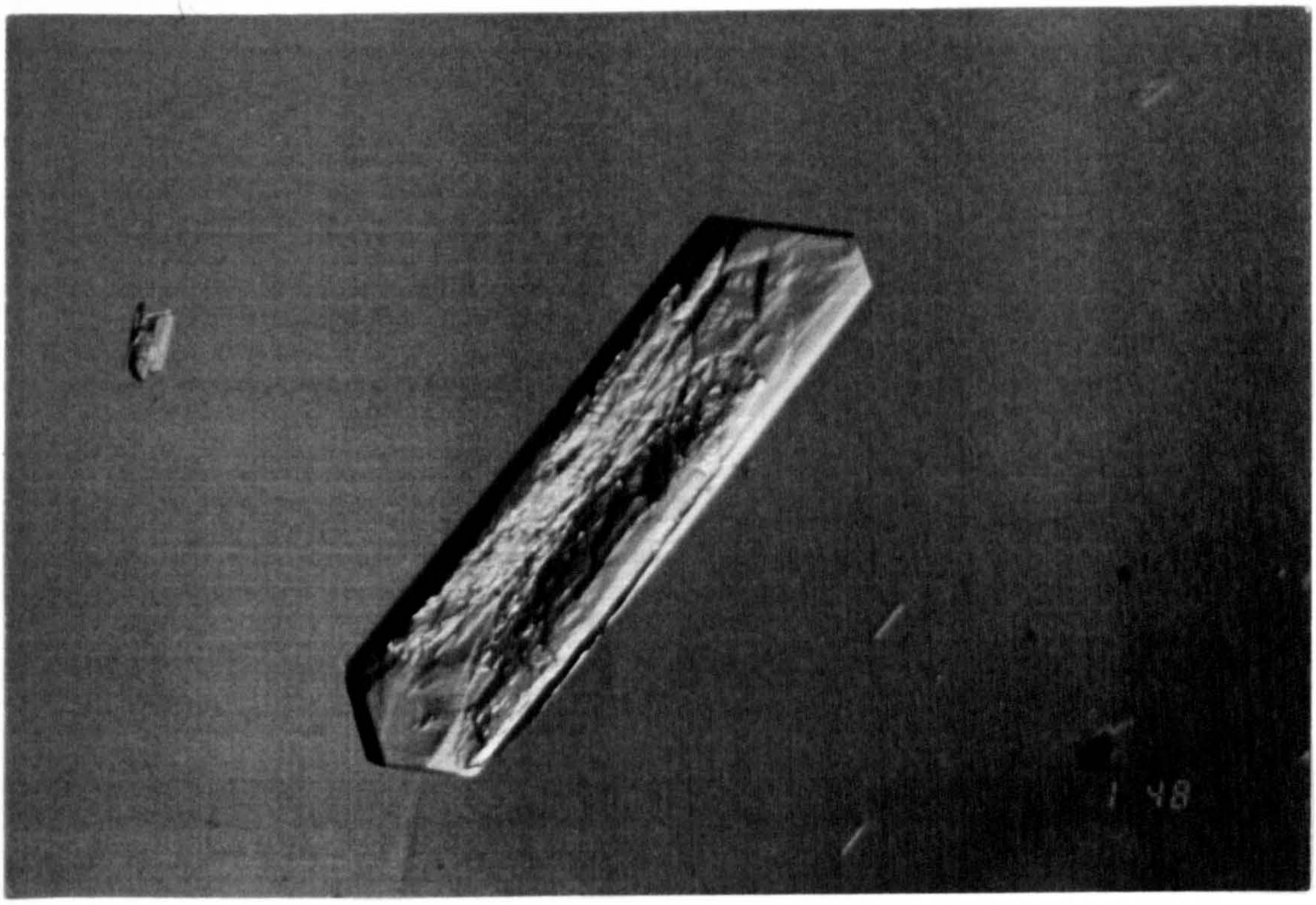

Figure 2.7a Single crystals of dextrose grown in a 0.8% $^{w}/_{w}$ Carbopol gel (X10)

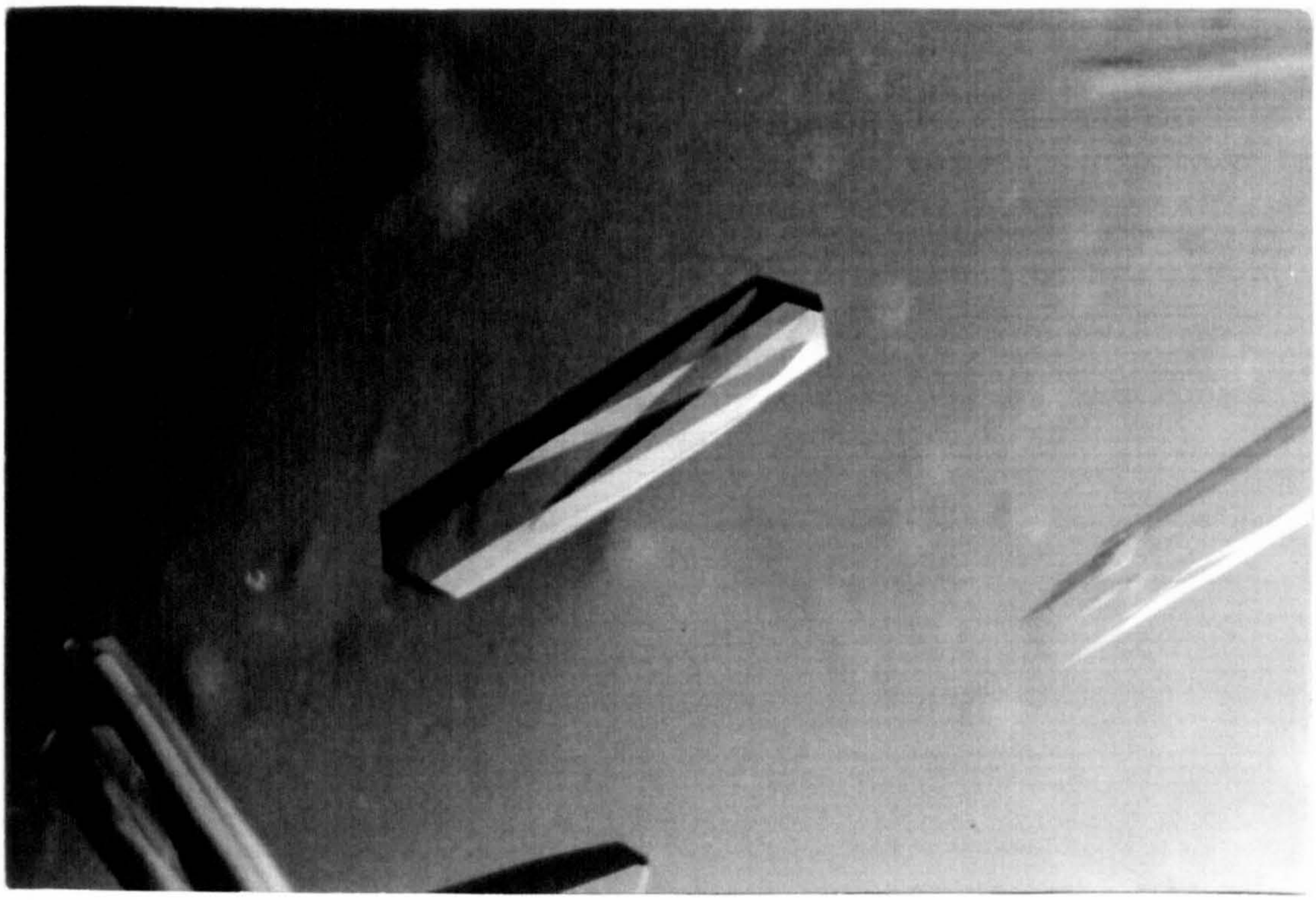

Figure 2.7.b Single crystals of dextrose grown in a 0.8% $^{w}/_{w}$ Carbopol gel (X10)

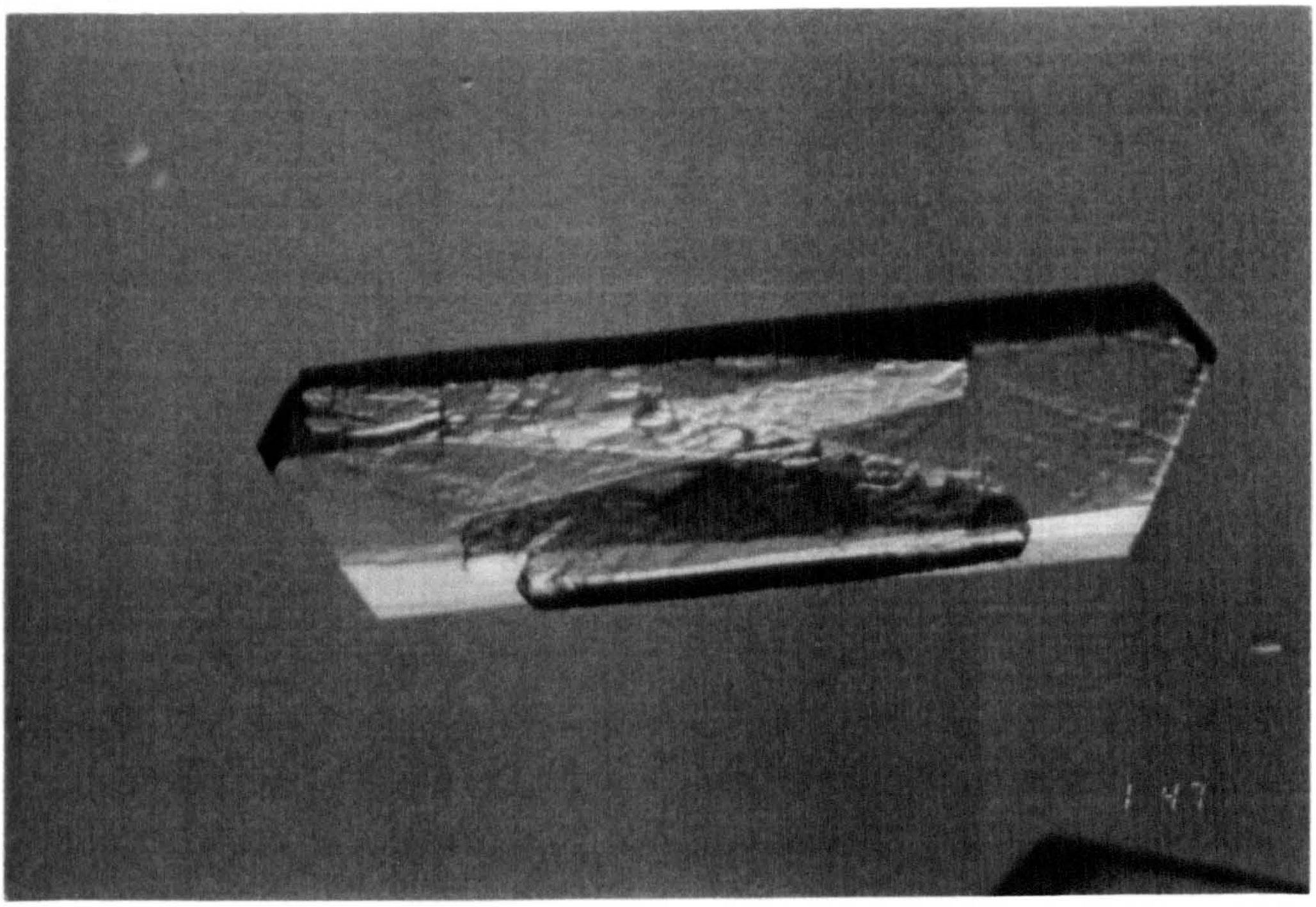

Figure 2.7 c Single crystals of dextrose grown in a 0.8% $^{w}/_{w}$ Carbopol gel (X10)

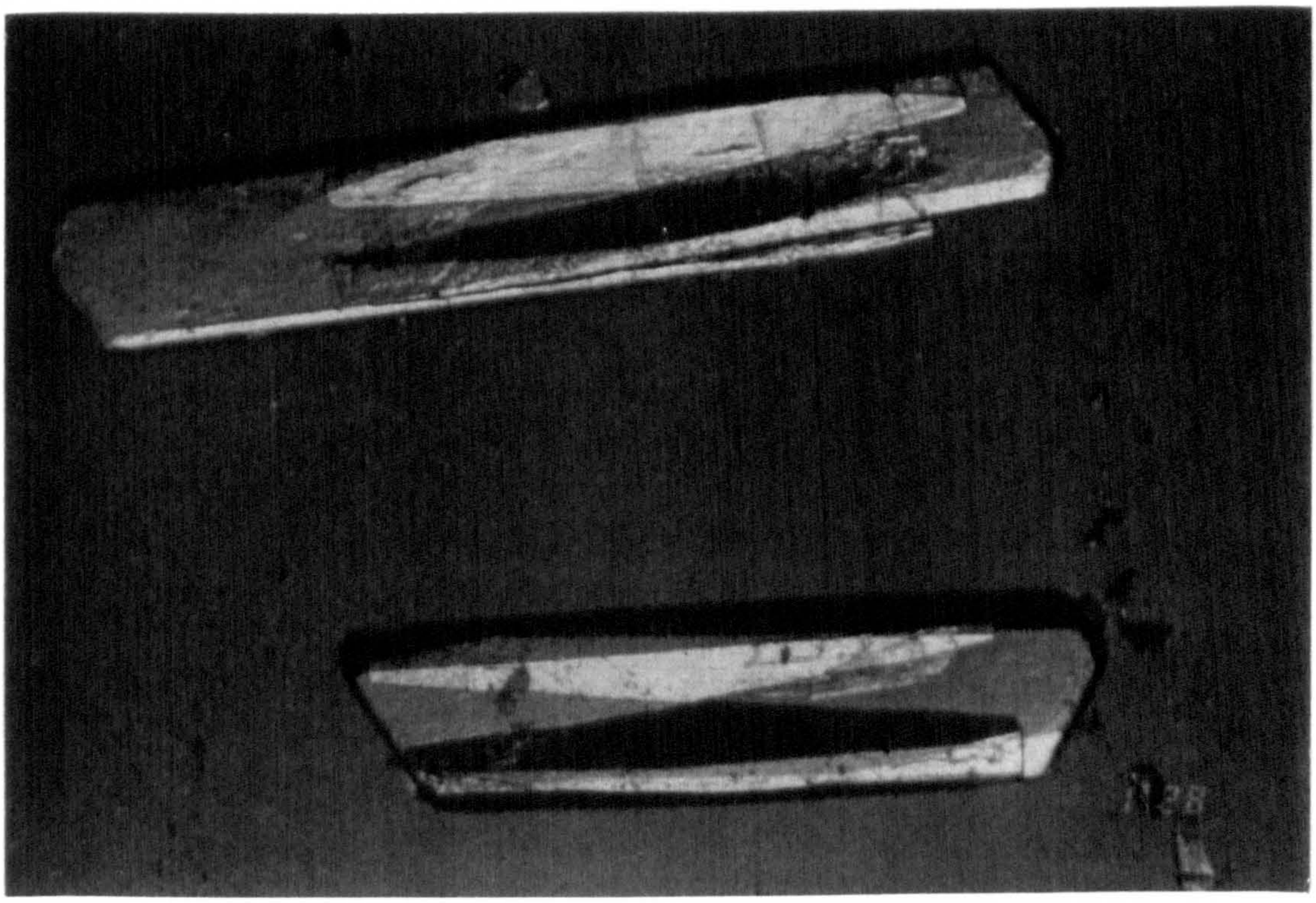

Figure 2.7.d Single crystals of dextrose grown in a 0.8% $^{w}/_{w}$ Carbopol gel (X10)

2.4.6 Harvesting single crystals

To remove the crystals from the gel, the technique of over neutralisation of the Carbopol gels was employed. A few drops of concentrated sodium hydroxide solution was added to the gel and gently mixed, causing its viscosity to decrease so permitting the now thinner gel to be decanted off. The crystals however, still required washing to remove the last traces of the gel from their surfaces. Several washing solutions were tried to determine which one was the most effective:

i) water
ii) ethanol
iii) mixtures of ethanol and water

Due to the high aqueous solubility of dextrose, washing the crystals with water, even when ice cold, completely dissolved the crystals. Washing with ethanol was also unsuccessful, causing a white precipitate to form. This was probably due to traces of dextrose in the gel being crystallised out due to its low solubility in ethanol. After trying various combinations of ethanol in water, a cold solution of 80% ethanol was found to be the most effective. The crystals were washed by gently swirling in the ethanol/water solution and filtering through a Buchner filter fitted with Whatman N°4 filter paper and a vacuum. The crystals were then dried at 35°C for 24 hours.

2.4.7 Characterisation of single crystals

The single crystals obtained by the gel growth technique were subjected to DSC analysis to confirm their identity, and purity. Samples of dextrose monohydrate and Carbopol 940, as supplied were also tested to provide standards. The DSC analysis was carried out using a Perkin Elmer DSC-2 analyser with sealed aluminium pans and the following operational conditions:

$Temp_{min}$	25°C
$Temp_{max}$	225°C
Heating Rate	10°C/min
Cooling Rate	320°C/min
Range	10 mcal/s

The DSC curves obtained are shown in Figures 2.8 a, b, and c.

The similarity of these thermographs would appear to confirm that the single crystals obtained by gel crystallisation are dextrose monohydrate. They also indicate, but do not conclusively prove the absence of gel in the crystals grown by gel crystallisation. Further analytical techniques such as H.P.L.C., however, would be required to confirm this.

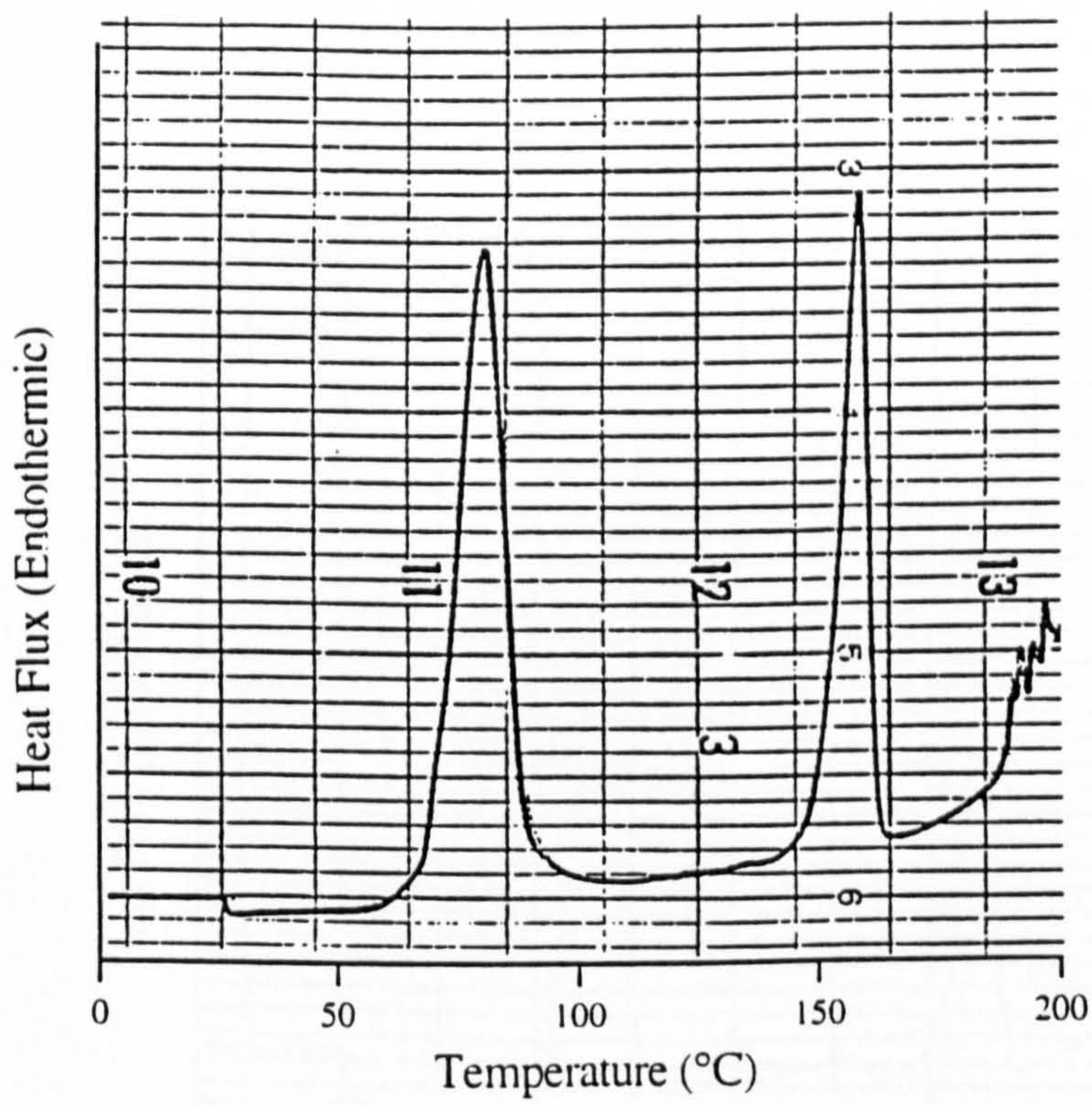

Figure 2.8a DSC thermograph of dextrose monohydrate (BDH)

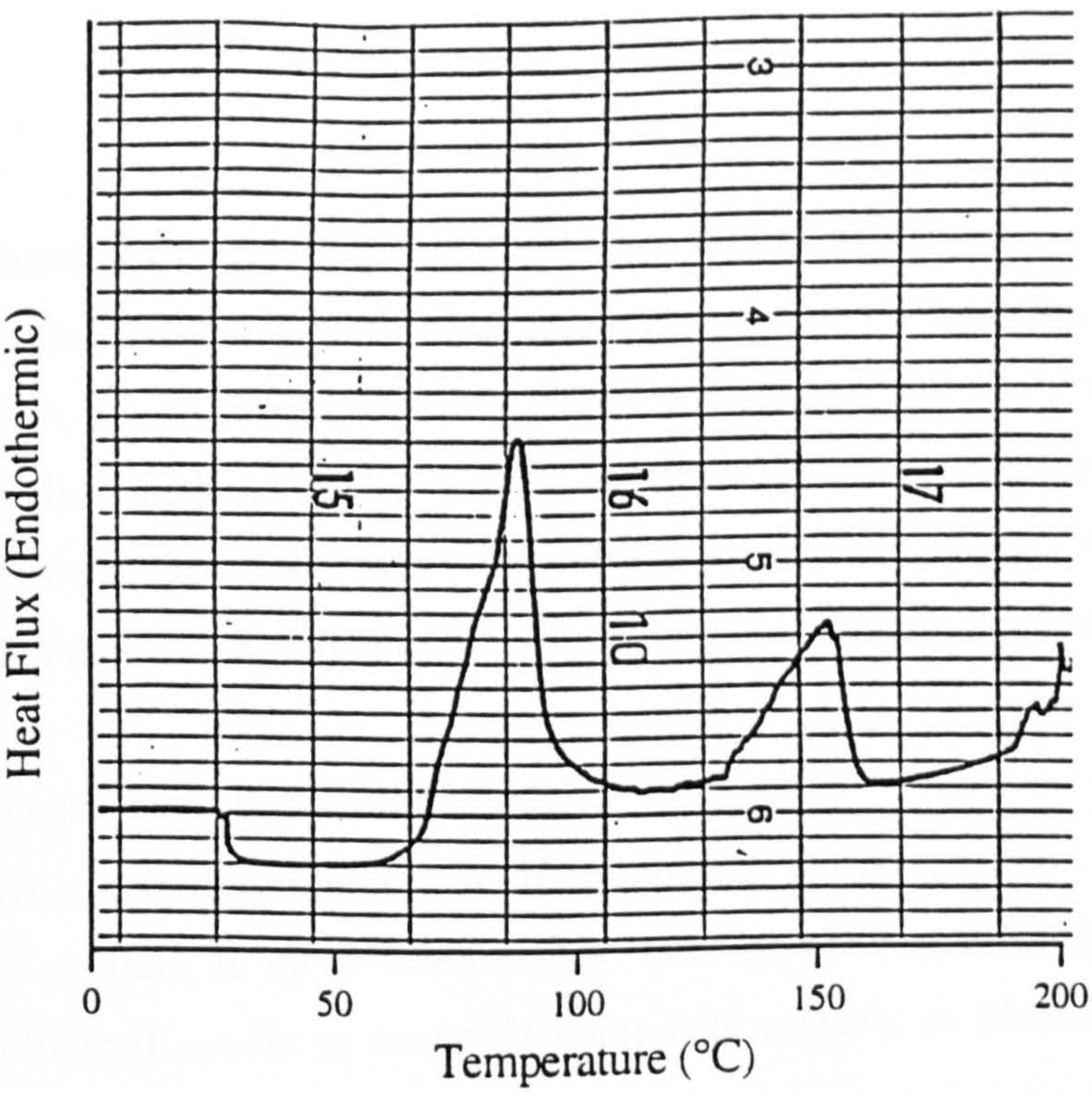

Figure 2.8b DSC thermograph of dextrose monohydrate (BDH) spiked with a 10% $^{w}/_{w}$ sample of Carbopol 940 gel

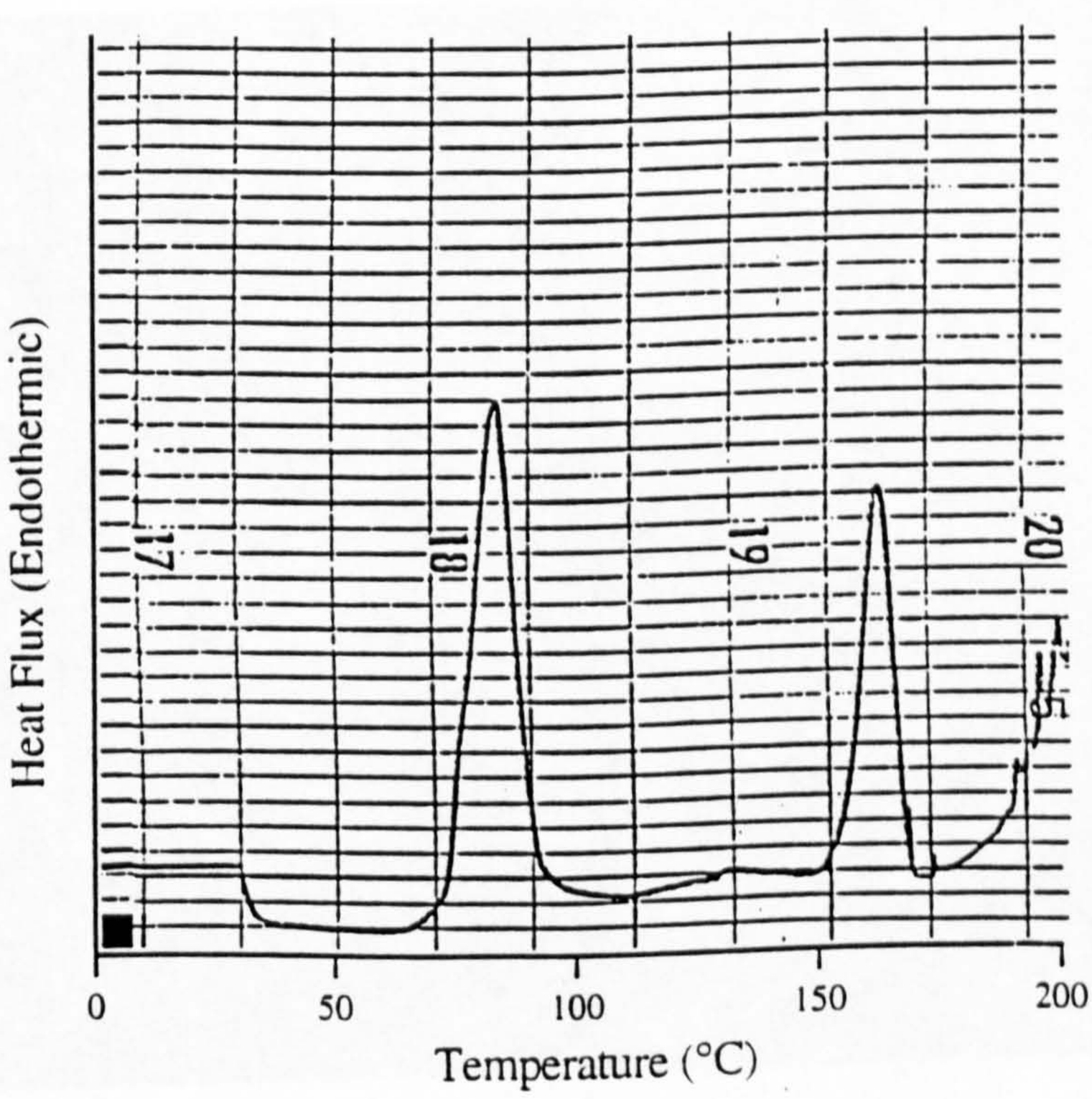

Figure 2.8c DSC thermograph of the single crystals obtained by gel crystallisation

2.4.8 Growth of larger single crystals from seeded solutions

In order to facilitate the growth of larger single crystals the technique of seeding was employed. A saturated gel containing 0.8%^{w}/w Carbopol 940 was prepared at 40°C as previously described and cooled to 31°C. Crystals which had already been grown and harvested (see section 2.4.6) were then introduced into the new gel and maintained at 31°C so that they could grow further without any spontaneous nucleation occurring.

2.4.8.1 Results and observations

The results of this experiment were disappointing. Although some growth did occur producing crystals of up to 20mm, they were of poor quality, (Figure 2.9). The crystals obtained appear to resemble composite crystals as identified by Dean and Grotterfried (1974) when dextrose was crystallised from seeded aqueous solutions.

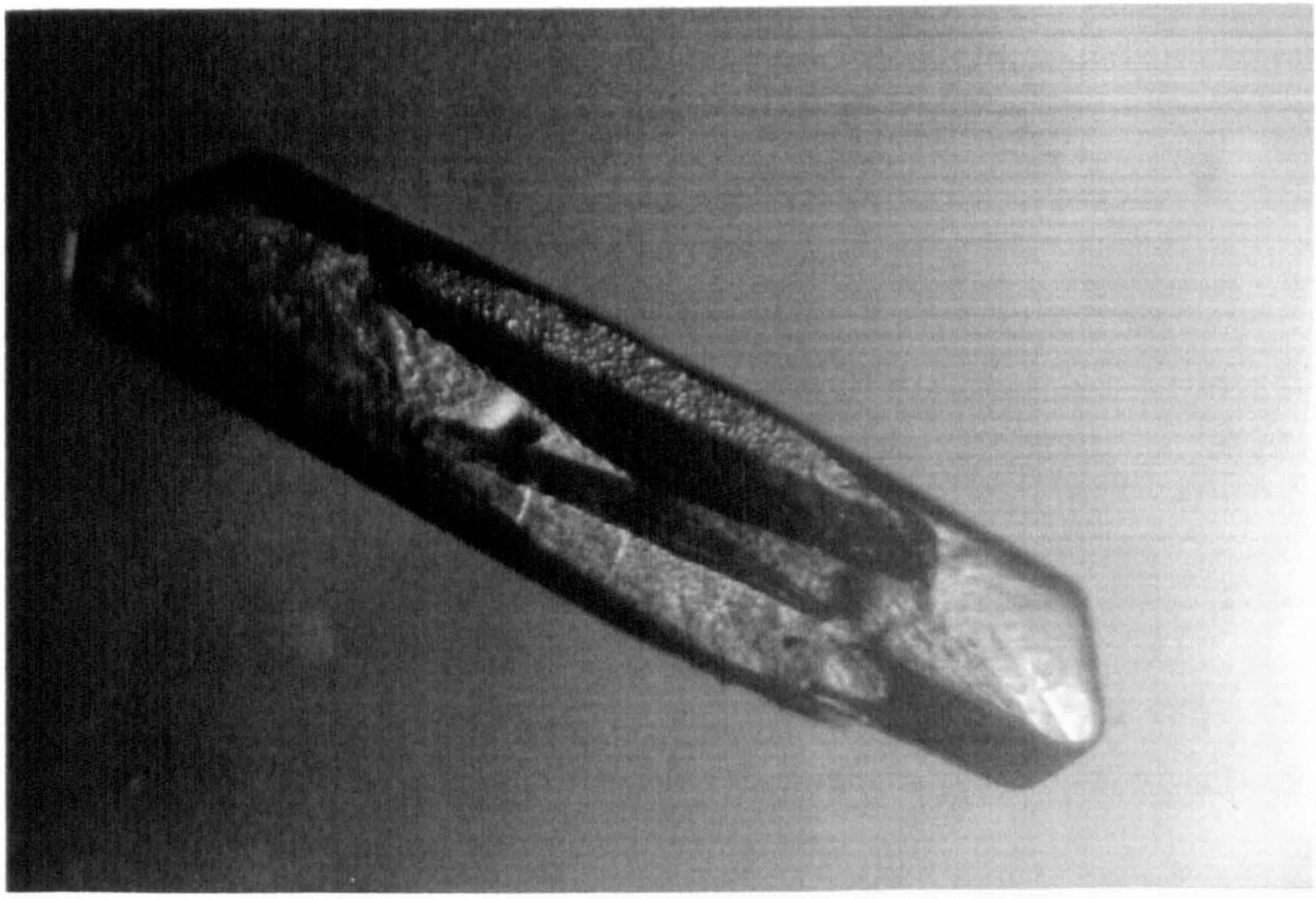

Figure 2.9 Crystals grown by seeding a 0.8% $^{w}/_{w}$ Carbopol 940 gel (X10)

2.4.9 Effect of pH on the growth of single crystals

All of the above experiments were carried out by neutralising the gel to a pH of 7.0 ±0.2. In order to eliminate the possibility that pH was interfering with crystal growth, a saturated gel containing 0.8% $^{w}/_{w}$ Carbopol 940 was prepared as before but was adjusted to a pH of 5.4 ±0.2 (the viscosity of Carbopol 940 was not affected) which is equivalent to the pH of an aqueous solution of dextrose, saturated at 40°C and cooled to 30°C. No improvement in crystal growth however, was observed.

2.4.10 Influence of cooling rate on the growth of single crystals

In previous experiments, the saturated gels were slowly cooled to their nucleation temperature, the rate being approximately 1.0°C/h. In this experiment, a gel was prepared as before, but was cooled to 28°C at a rate of approximately 10°C/h and maintained there for 24 hours, before being heated to 31°C. As in previous experiments, crystal growth did occur, but the crystals lacked perfection and consisted mainly of long thin needles as shown in Figure 2.10.

Figure 2.10. Crystals of dextrose grown in a 0.8% $^{w}/_{w}$ Carbopol gel cooled at 10°C /h (X10)

2.4.11 Overall evaluation of single crystal growth experiments

The above series of experiments demonstrated that Carbopol gel has potential as a crystal growth media. The growth of single crystals of dextrose monohydrate, however, had only limited success with crystals of up to 7 mm in length being formed. The optimum conditions appearing to be saturation at 40°C, cooling the solution to 28°C, to induce nucleation before raising the temperature to 30°C for crystal growth. It should be noted that during the above experiments, problems were encountered with regards to reproducibility, but this seems to be a commonly experienced phenomenon in the field of experimental crystallisation. Each experiment was conducted between three and five times and the results presented above are those that were most consistently observed.

Although single crystals of dextrose monohydrate were obtained, they were found to be unsuitable for mechanical testing as had been planned. This was partly due to the slender plate-like crystal habit of dextrose monohydrate, which yielded very thin and thus fragile crystals whose mechanical properties could not be examined, using the equipment available. This problem in handling crystals of dextrose monohydrate was also reported by Grerrta and Berglund (1990).

Another problem experienced was the slow speed of crystallisation and the limited extent of crystal growth. After about two weeks, the single crystals appeared to stop growing although the saturated gel system could not have been exhausted. It is believed that the reasons behind this lie in the chemistry of dextrose solutions. When crystalline dextrose is dissolved in water it undergoes a partial sterochemical transformation into the alpha form, producing an equilibrium solution containing the two isomers in a ratio of 40% alpha dextrose and 60% beta dextrose. The final solubility is therefore that of dextrose, not in water but in a solution of beta dextrose. This has two major effects on the crystallisation of dextrose monohydrate. Firstly, the transformation in solution from the more soluble beta form to the less soluble alpha form is slow and imposes a limit on the rate of crystallisation. Whittier and Gould, (1930) investigating the speed of crystallisation of several carbohydrates, found that dextrose had the slowest speed of crystallisation with a velocity

constant of $K= 2x10^{-5}$ m/s at 30°C as compared to lactose and sucrose with values of $K= 15x10^{-5}$ m/s and $K= 60x10^{-5}$ m/s respectively.

Secondly, the beta dextrose acts as an impurity retarding and ultimately inhibiting the crystallisation of alpha dextrose monohydrate. It is believed that in the case of gel crystallisation therefore, growth of large single crystals of dextrose monohydrate is hindered by the presence of the beta isomer.

It should also be noted that these experiments produce many crystals which appeared to be single but which, on closer examination, were seen to be in fact twin crystals with areas of inter growth clearly visible. This is known to be a problem encountered with many carbohydrates crystallised in static conditions (Mullin, 1993).

In an attempt to overcome the problem of limited growth, a method of removing crystals from a gel which had reached equilibrium, and placing them in a fresh saturated gel was tried. This proved unsuccessful, however, as the crystals that grew lacked perfection and appeared to be composite crystals as identified by Dean and Grotterfried (1974). It is suggested that if a method such as dialysis, or perhaps chemical separation, could be developed to remove the beta isomer from the saturated gel and so shift the equilibrium, then growth of the alpha isomer would not be inhibited. This is, however, beyond the scope of this project.

The aim of the above experiments was to produce single crystals of dextrose monohydrate of suitable size and perfection to facilitate the testing of its fundamental mechanical properties such as surface hardness and deformation characteristics. In view of the problems encountered and the time constraints on the project, it is judged that the chemistry and physical shape of dextrose monohydrate renders it a difficult material for gel crystallisation and the subsequent mechanical testing of large single crystals. Also, due to the strict experimental conditions required it would not be possible to examine the effect of crystallisation variables such as cooling rate on the mechanical properties of the crystals.

2.5 Bulk crystallisation of dextrose

Dextrose monohydrate was recrystallised from aqueous solutions as a model system to observe the influence of various crystallisation variables such as cooling rate and initial supersaturation levels on the physicochemical properties of the final crystalline product. The material obtained was also used to examine the effect of those variables on the compression properties of dextrose and the mechanical properties its compacts.

Batches of dextrose were crystallised under carefully controlled conditions to investigate the following:

i) effect of cooling rate
ii) effect of saturation level
iii) effect of crystal growth time
iv) effect of crystal seed, particle size
v) effect of additives
vi) effect of crystallisation temperature
vii) effect of crystal growth rate

Some of these variables are inter-related and in some cases it was possible to use the same sample of material to investigate more than one variable.

2.5.1 Design and construction of a programmable batch crystallisation unit

In order to accurately control and investigate the influence of the crystallisation conditions a small scale batch crystalliser unit was designed and constructed (the design was a modified version of that described by Ludwin-Brown (1989)). The main requirements of such a unit were:

1) An accurate means of generating various temperature/time profiles in order that the influence of variables such as cooling rate and crystallisation temperature could be studied.

2) A crystallisation vessel with a capacity of $2dm^3$ to enable sufficient yields to be produced in order to facilitate subsequent testing.

3) A method for continuously monitoring the temperature/ time profiles was required.

The crystallising vessel (Figure 2.11) was constructed from 3 mm borosilite glass to minimise corrosion and surface effects which may have interfered with the crystallisation. It consisted of a jacketed vessel, 400mm in length with an internal diameter of 80mm and an outer diameter of 100mm, thus producing a vessel with a capacity of $2dm^3$. Inlet and outlet ports allowed the heat transfer liquid (water/anti freeze), to be circulated around the jacket via a heater/chiller circulator unit.

A discharge valve consisting of a tapered PTFE plunger operated by a screw mechanism was built into the base of the vessel. An overhead variable speed motor was used to drive a glass stirrer with twin impellers that provided agitation of the crystallising system. The speed of the motor was monitored using an optical tachometer. Thermostatic control of the system was provided by a heater/chiller thermocirculator (Model 05CTV, Conair/Churchill) the power output of which was determined by an integrated Eurotherm 818 programmable microprocessor (Eurotherm Ltd). This facilitated accurate generation and control of desired temperature/time profiles and provided a continuous digital display of all operating conditions. Profiles could be either linear or consist of up to eight different cooling/ heating ramps linked in series. The microprocessor had time lag and tuning functions that ensured that the temperature profiles were followed to $\pm 1°C$.

A K-type Duplex thermocouple acted as a temperature probe for the system and provided a temperature output to a calibrated chart recorder

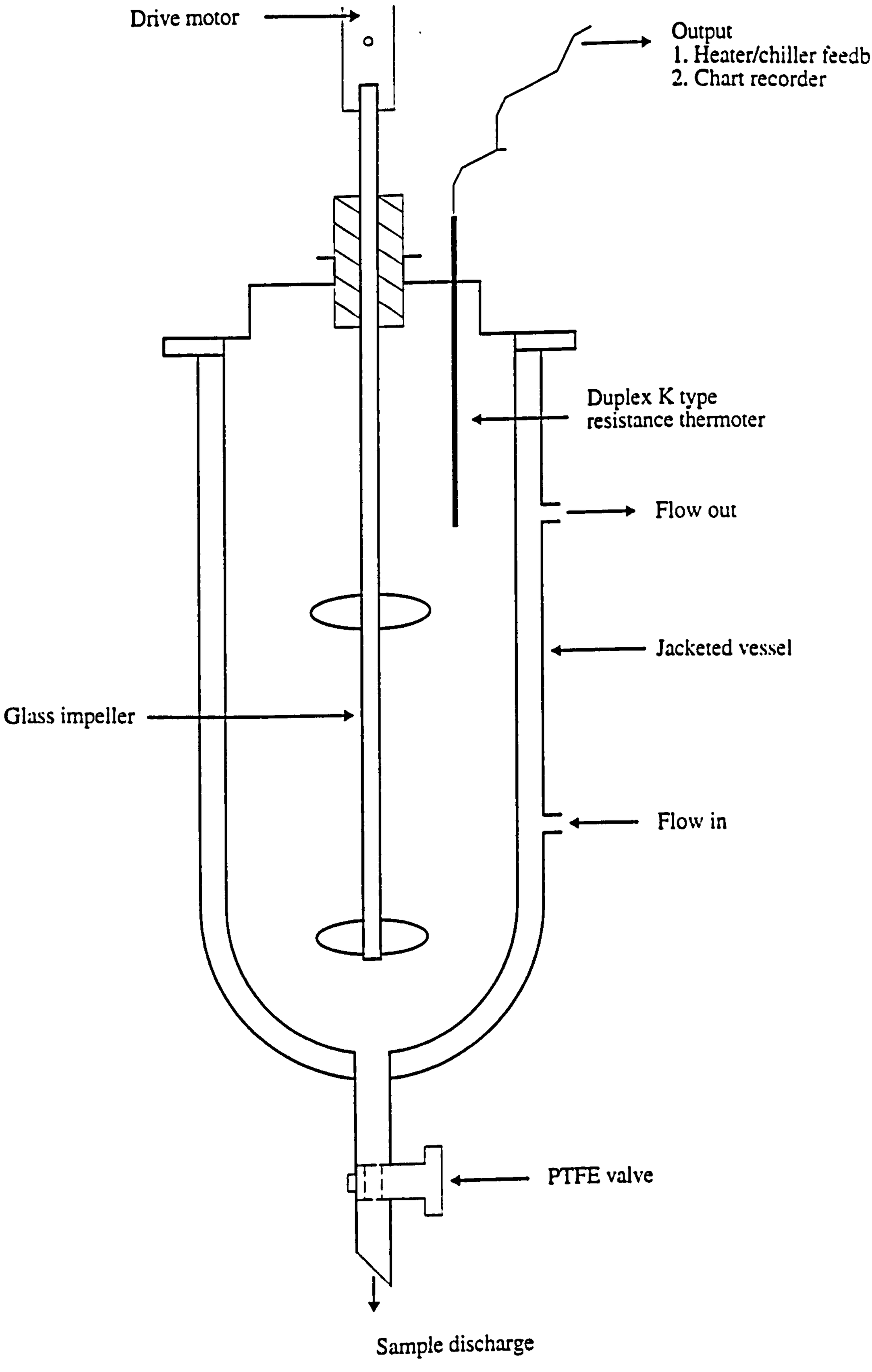

Figure 2.11 Diagram of the batch crystalliser

2.5.2 Equipment testing

The small scale batch crystallisation system was tested to determine its accuracy over the operating conditions required. The vessel was filled with 2 dm^3 of water to simulate the presence of a supersaturated dextrose solution. The heater/chiller unit was set to cool from 50°C to 20°C at two cooling rates, i) 0.5°C/h and ii) 50°C/h. These cooling rates represented the minimum and maximum cooling rates expected to be used in the experimental work. Temperature/time profiles were logged by the chart recorder and are shown in Figures 2.12 and 2.13 respectively.

As can be seen from the temperature/time profiles the unit achieved both of the required linear cooling rates. The only flaw being the slight overshoot of 1° C below the minimum temperature in the 50°C/hr cooling curve (due to the speed of cooling). However, this deficiency was not viewed as being significantly detrimental in this present work.

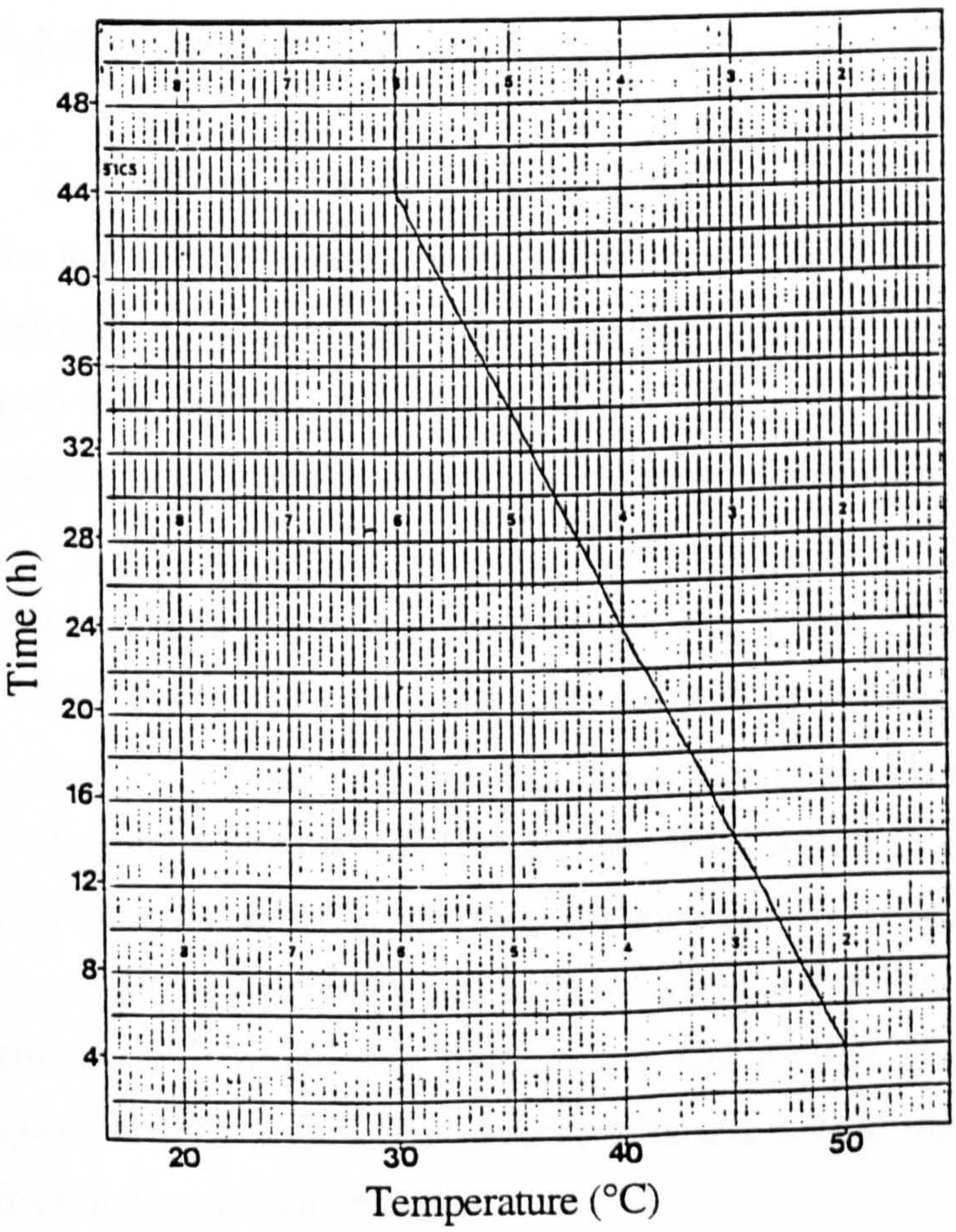

Figure 2.12 Chart recording of the experimental cooling rate tested at 0.5°C per hour

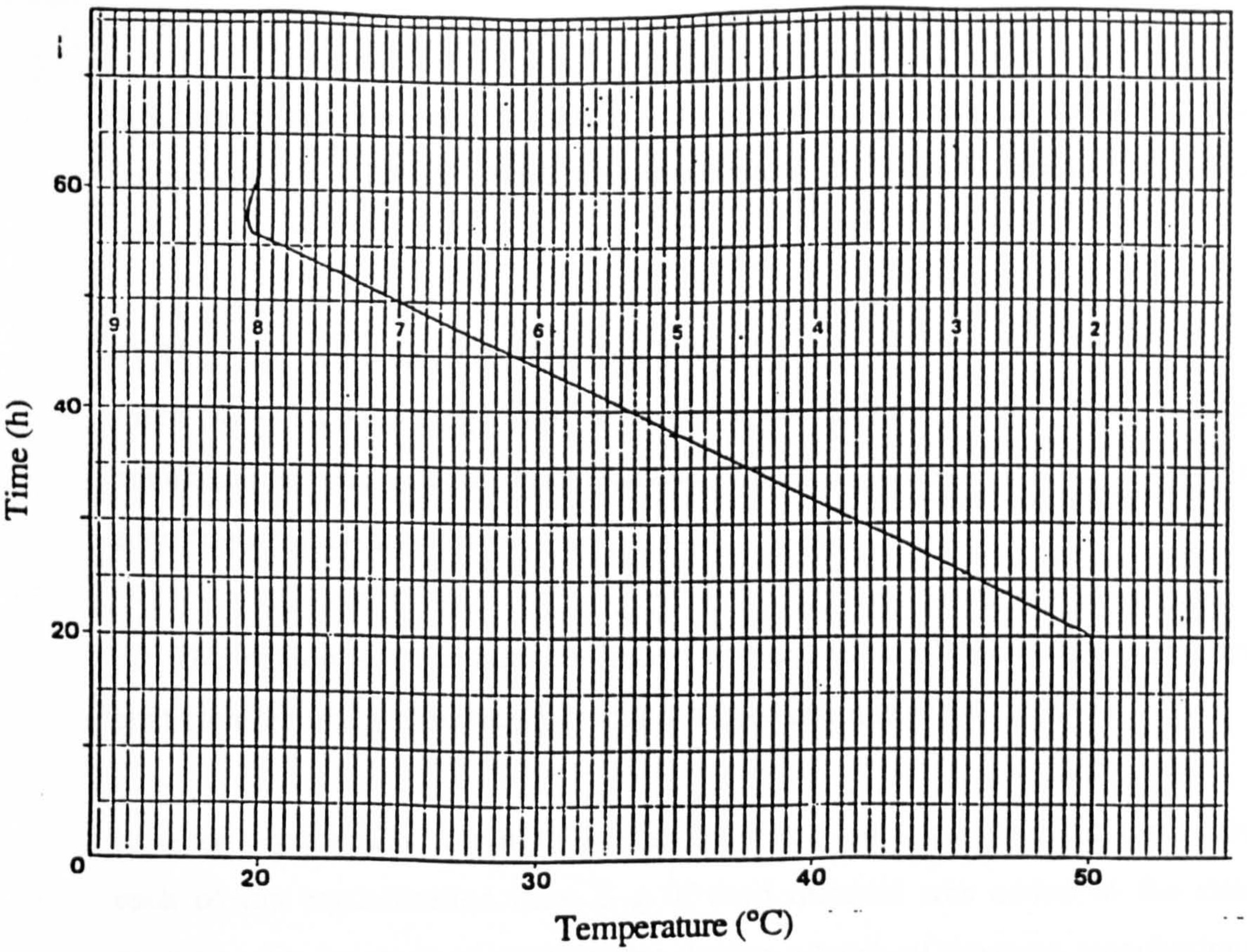

Figure 2.13 Chart recording of the experimental cooling rate tested at 50°C per hour

2.5.3 Crystallisation method development

In order to carry out subsequent physicochemical, compression and mechanical testing on dextrose or its compacts it was necessary that the batch crystallisation process produced a dry powder product which could be used directly, without the need for processes such as milling which would interfere with the properties of the material.

The main difficulty associated with the process is the successful isolation of a dry finely divided crystalline product from its viscous mother liquor. Initial attempts using several washing and filtering techniques were abandoned as at best they produced a wet sticky mass of crystals that dried into large aggregates. The problem was overcome by using a centrifuge to separate the crystallised product from the majority of the mother liquor followed by washing and filtering before drying. The standard method, which was used to produce all the materials employed in the subsequent testing is described below, with the details particular to each variable described in the relevant sections.

i) Saturated solutions were prepared by dissolving the appropriate amount of dextrose (anhydrous) in distilled water at approximately 0.5-1.0 °C above the saturation temperature.

ii) The saturated solutions were then filtered under vacuum, using a sintered glass filter No.4, before being transferred to the crystallising vessel. The solution was maintained at the saturation temperature for 15 minutes to ensure that saturation conditions had been achieved.

iii) The solutions were then cooled at a specified rated using the programmable heater/chiller unit while being constantly stirred at a rate of 500 rpm.

iv) Seed crystals were added to the saturated solution at a specified temperature. In each of the crystallisation runs, 3 g of seed material was added to the saturated solution. The seeds were obtained by sieving a batch of dextrose monohydrate and selecting a specific size range. With the exception of one study the sub 45 μm size range was used in all the crystallisation procedures.

v) Once the cooling programme was complete the crystallised material and mother liquor were discharged from the crystallisation vessel and transferred to polyethylene centrifuge vessels. They were centrifuged at 800 rpm for 5 minutes, using a MSE 18 centrifuge, which had a temperature control facility. The temperature was set at 0.5°C above the minimum crystallising temperature to ensure no further crystallisation took place.

vi) On removal from the centrifuge, the viscous mother liquor was decanted off and the crystallised product washed and filtered. Initial washing was carried out using an ice cold 80% solution of ethanol in water followed by two more washings using a 90% ethanol in water mixture. Preliminary experiments had shown this procedure to be the most efficient for washing the crystalline material without causing any dissolution, which would affect the yield and possibly the surface properties of the material. Filtering was carried out using a sintered glass N°2 filter under vacuum.

vii) The crystalline material was then placed on drying plates and dried at 30°C to a constant weight. After partial drying the powder was placed in a 2.0 mm sieve and gently agitated for 10 minutes to break up any aggregates.

viii) The yield was determined and the crystalline material stored in airtight containers in a dessicator at room temperature.

2.5.4 Bulk crystallisation experiments

2.5.4.1 Investigating the effect of cooling rate and initial supersaturation levels

As already discussed in chapter one, the rate of cooling and the degree of supersaturation have been identified as factors which can affect crystal growth and material properties. Therefore, the series of experiments described below, were carried out in order to investigate the effect of these variables on the physicochemical, mechanical and compression properties of dextrose.

The amount of dextrose required to produce a solution with an initial supersaturation ratio of 1.3 at 30°C was calculated using the polynomial equation constructed from the solubility data (equation 2.1). Solutions that were saturated at 38.5°C were prepared by dissolving 3140 g of anhydrous dextrose in 2000 ml of distilled water (157g/100 ml) at 39°C. The solutions were then transferred to the crystallisation vessel where they were maintained at a temperature of 38.5°C and a stirring rate of 500 rpm for 15 minutes to ensure saturation conditions had been reached. The cooling unit was programmed to cool the solutions to 30°C and the seed crystals were added at 38°C. At the end of the cooling cycle the liquor containing the crystalline material was collected and treated as described in the standard method (section 2.5.3). Batches of dextrose were crystallised at linear cooling rates of 0.5, 1.0, 10.0, 30.0 and 50.0°C/h.

The crystallisations at 0.5 and 50 °C/h were repeated with solutions that were saturated at 43 °C (180g/100ml), and thus produced an initial supersaturation ratio of 1.5 when cooled to 30°C. The solutions were transferred to the crystallising vessel and maintained at 38.5°C for 30 minutes before the cooling program was commenced

and the seed crystals added at 38°C. The crystallised material was collected and washed when the cooling cycle reached 30°C as previously described.

2.5.4.2 Investigating the effect of crystal growth time

Due to the wide range of cooling rates used in the previous experiments, significant differences in crystal growth times occurred. For example, the batch prepared at 0.5°C/h had a total growth time of 16.0 hours (from addition of seed crystals) while the batch prepared at 50°C/h had a growth time of less than 40 minutes. Therefore, the effect of this factor was examined by crystallising solutions with a supersaturation of 1.3 (prepared as described in section 2.15.1) at two linear cooling rates of 1.0 and 30.0 °C/h and maintaining the solutions at 30°C until a total growth time of 16.0 hours was attained before the material was recovered.

2.5.4.3 Investigating the effect of seed crystal particle size

The size of the seed material used to induce nucleation is potentially a significant factor in determining the size of the final product. In order to investigate the effect of seed size on crystallised dextrose, the crystallisation carried out at 0.5°C/h from 38.5 to 30°C (as described in section 2.15.1) was repeated but the seed material was obtained by selecting the 63-90 μm size range rather than the sub 45 μm size range that had been used in all other crystallisations

2.5.4.4 Investigating the effect of additives

As mentioned in chapter one, the presence of additives in crystallisation solutions have been reported as influencing factors such as crystal habit and the subsequent compression behaviour of crystalline materials. In the commercial production of dextrose (and carbohydrates in general) it is not uncommon for trace amounts of other carbohydrates to be present.

To examine the effects of these impurities on the various material properties of dextrose, batches of dextrose were crystallised from solutions that contained small amounts of either lactose or sucrose. Saturated solutions of dextrose where prepared at 38.5°C, as before but also included 2.5 % $^{w}/_{w}$ of either anhydrous lactose or sucrose.

The crystallisation was then carried out as previously described at a linear cooling rate of 0.5°C/h.

2.5.4.5 Investigating the effect of crystallisation temperature

Up to this point, all crystallisations were carried out by cooling supersaturated solutions from 38.5°C to a temperature of 30°C. This temperature range was chosen as it was believed to be approximately that used in the commercial production of dextrose monohydrate and could be easily maintained without the environmental temperature being a factor.

To examine the role of crystallisation temperature in determining the various physico chemical properties of dextrose and its influence on the compression behaviour and mechanical properties of dextrose compacts, a series of crystallisations were carried out using several different temperature ranges.

The polynomial equation (equation 2.1) derived from the solubility graph in section 2.21 was used to calculate the appropriate amount of dextrose required to produce solutions which had a supersaturation ratio of 1.3 when they reached their final temperature. The solutions were prepared and crystallised by the standard method. The seed crystals were added at 8°C above the final temperature and the solutions were all cooled at a linear cooling rate of 0.5°C/h. The crystallisation temperature ranges (from addition of seed material) examined were, 38-40, 48-40, 53-45, 56-48 and 59-51°C.

2.5.4.6 Investigating the effect of crystal growth rate

The effect of crystal growth rate on the properties of a material has been outlined in Section 1.6. The previous crystallisations carried out at the different temperatures produced batches with a wide range of yields, which indicated that the crystal growth rate was affected by the temperature of the system even though all other variables including the supersaturation ratio were constant. The theoretical yield of a crystallisation process is known to be related to the supersaturation ratio and the absolute supersaturation (Mullin, 1993).

From the results of the previous experiments carried out at the various temperatures, the growth rates (as measured by the batch yields) were related to the absolute supersaturation (supersaturation potential) ΔC (as defined by equation 1.19). A graph was constructed of ΔC versus batch yield as shown in Figure 2.13 and the relationship between ΔC and the batch yield found to be linear. It was therefore concluded that if ΔC was kept constant for crystallisations conducted at various temperatures, batches of a constant yield and therefore constant linear crystal growth rate would be obtained. Another series of crystallisations was therefore carried out using the same temperature ranges as before but with the degree of supersaturation of each solution adjusted so as to produce a ΔC value of 62 g/100 g of water (as was the case for the batch prepared at 53 – 48°C). This was thus expected to produce batch of a relatively constant yield. For each temperature, three batches were prepared and the yields ranged from174 to 182 g.

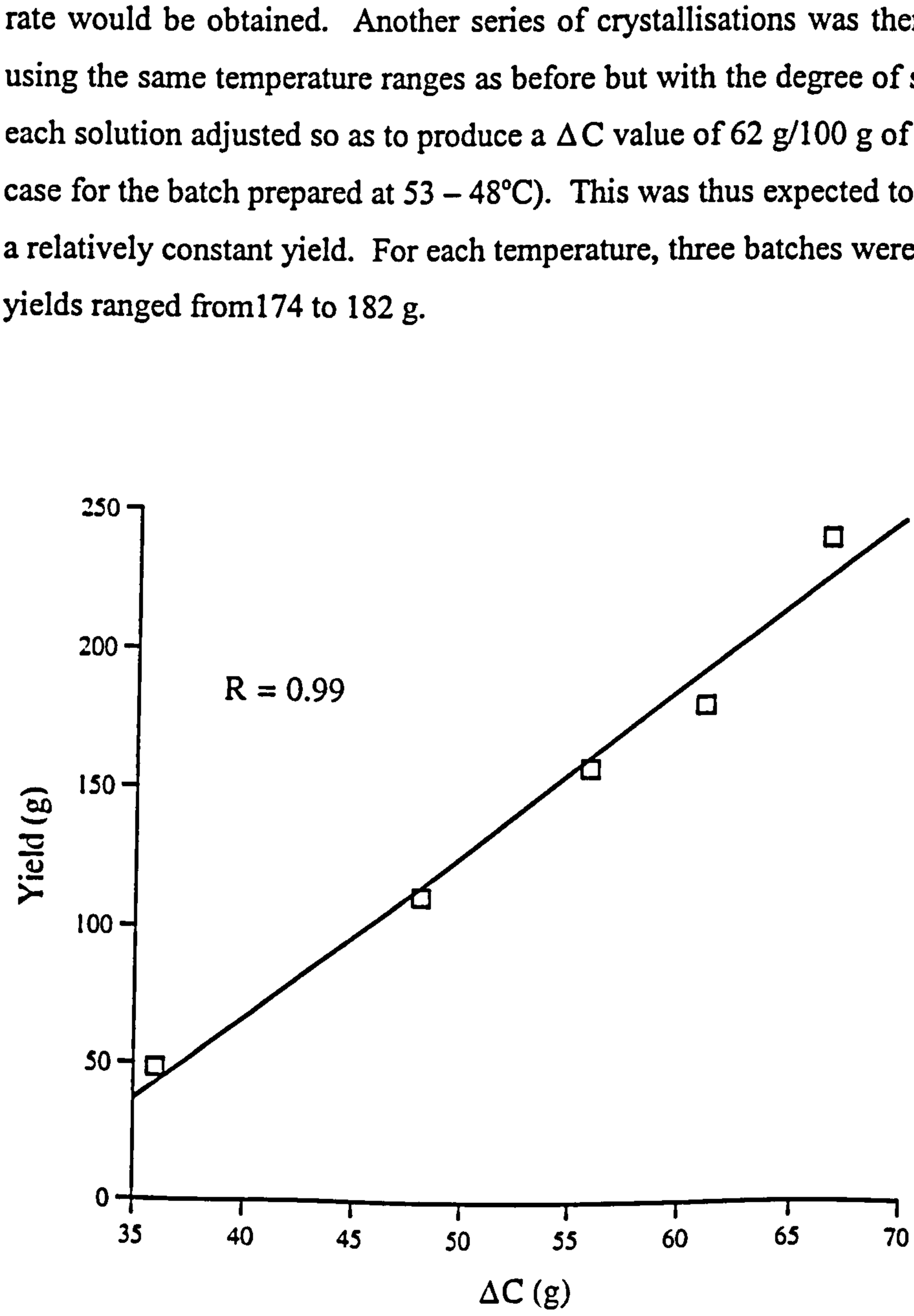

Figure 2.13 Graph showing the relationship between the batch yield size (n=3) and ΔC

2.6 Batch identification codes

To simplify identification of the various batches, each crystallisation condition was given a code as detailed below. Unless otherwise stated all batches were prepared at 38-30°C, with an initial supersaturation ratio of 1.3 and at a cooling rate of 0.5°C/h using sub 45 μm seed crystals.

D05	Cooling rate = 0.5°C/h
D1	Cooling rate = 1.0°C/h
D10	Cooling rate = 10.0°C/h
D30	Cooling rate = 30.0°C/h
D50	Cooling rate = 50.0°C/h
D1T	Growth time extend for a total of 16 hours, cooling rate = 1.0°C/h
D30T	Growth time extend for a total of 16 hours, cooling rate = 30.0°C/h
DX05	Seeded using 3 g of crystals in the 63 to 90 μm size range
DS15	Supersaturation ratio was 1.5, cooling rate = 0.5°C/h
DS15/50	Supersaturation ratio was 1.5, cooling rate was 50°C/h
DLac	2.5% $^{w}/_{w}$ lactose monohydrate added to the saturated dextrose solution
DSuc	2.5% $^{w}/_{w}$ sucrose added to the saturated dextrose solution
DC40	Temperature range was 48 - 40°C
DC45	Temperature range was 53 - 45°C
DC48	Temperature range was 56 - 48°C
DC51	Temperature range was 59 - 51°C
DR30	Temperature range was 38 - 30°C supersaturation ratio was 1.6
DR40	Temperature range was 48 - 40°C supersaturation ratio was 1.5
DR45	Temperature range was 53 - 45°C supersaturation ratio was 1.4
DR51	Temperature range was 59 - 51°C supersaturation ratio was 1.1

CHAPTER THREE

EXPERIMENTAL METHODS AND EQUIPMENT

3.1 Introduction

This chapter describes the various methods and equipment used to determine and evaluate the effect of the crystallisation variables on the solid state characteristics, physicochemical properties, the compression behaviour of dextrose and the mechanical properties of its compacts.

3.2 Assessment of solid-state properties

Several techniques are commonly used to determine the crystal structure of materials and assess the relative degree of crystallinity. Two of these techniques, x-ray diffraction and helium pycnometry have been employed in this study.

3.2.1 X-ray diffraction

X-ray diffraction is a powerful technique used for the study of crystal structure. When a monochromatic beam of x-rays are incident on a crystalline solid they are diffracted in all directions by the atomic nuclei in the crystal lattice. In some circumstances these beams are in phase and therefore reinforce each other to form diffracted beams. This diffraction will only occur when the conditions of Bragg's law are satisfied. Bragg's law is described by equation 3.1:

$$n\lambda = 2d \sin \theta \qquad \text{(equation 3.1)}$$

where n is an integer defining the order of reflectance, λ is the wavelength of the incident x-ray beam, d is the distance between the planes in the crystal lattice and θ is the angle at which the incident x-ray beam strikes the crystal.

By use of appropriate equipment, the diffracted x-rays are detected and a unique x-ray powder pattern, consisting of a series of peaks at various scattering angles, is created for every crystalline form of a compound. The technique has thus become an invaluable tool for distinguishing between different polymorphic forms of the same material. It has also been used to identify the solvated and anhydrous forms of compounds.

Another widely reported application of x-ray diffraction is the assessment of the degree of crystallinity of a compound. Several methods for interpreting powder patterns for this purpose have been reported (e.g. Nakai et al., 1982; Imaizumi et al., 1977; Black and Lovering, 1974; Ryan 1986) but all are essentially based on a comparison of the intensity ratios of selected peaks. Absolute values of crystallinity can be determined by the use of appropriate standards but even in the absence of such standards, the rank ordering of materials is possible. The number of peaks, the amount of peak splitting and the width of the peaks can also be used to compare the crystallinity of samples of similar materials. Several factors such as particle size and preferred particle orientation can however, significantly affect the intensities of the diffraction peaks.

In this study the x-ray diffraction patterns were determined for a selection of the crystallised samples at the Department of Materials Engineering and Materials Design at the University of Nottingham. The measurements were made on a Siemens D500 x-ray diffractometer using Cu Kα radiation (λ = 1.5406 nm) at 40 kV and 20 mA. All the samples tested were from the 45-63 μm size range to minimise the particle size effects. Prior to testing, the powder samples were packed into a 1 cm diameter sample holder to a depth of 2 mm. The diffraction patterns and the diffraction data obtained were then assessed qualitatively by comparison with each other and with reference diffraction data listed in the JCPDS[1] library.

3.2.2 True density (helium pycnometry)

The true density of crystalline materials reflects their molecular packing and can provide a relative measure of crystallinity when used to rank materials with a similar crystallographic structure (Huttenrauch, 1978; Ludlam-Brown, 1989). In this instance, an increase in true density indicates a decrease in the number of dislocations and thus an increase in the degree of crystallinity. If the crystallography structure is not exactly the same then changes in true density simply imply that the structure has changed but cannot be used to rank materials.

[1] Joint Committee for Powder Diffraction Studies

The true density was measured by the technique of helium pycnometry, which determines the volume of irregular shaded particles using the classical gas relationship.

True density measurements were determined five times on each of three samples for every batch of crystalline dextrose using a calibrated multi-volume pycnometer (Micrometrics USA, Model 1305). A known amount (approx. 5 g) of material was placed in a calibrated 35 cm^3 holder and the chamber purged several times. The pressures values under two sets of test conditions were recorded. The volume and thus density of the sample was then determined using a software program supplied with the equipment.

While both x-ray diffraction and true density have both been used to determine the degree of crystallinity it has been shown by Suryanarayanan and Mitchell (1985) that there is often little or no correlation between the results obtained by the different techniques.

3.3 Evaluation of physico-chemical properties

3.3.1 Particle size analysis

The importance of particle size has already been discussed in Section 1.4.1. However, due to factors such as shape, it is a difficult property to define precisely and thus the value quoted is dependent on the method used for sizing. Throughout this study particle sizing was carried out by sieve analysis and therefore the particle sizes reported are more accurately referred to as the sieve equivalent diameter, which is the diameter of a sphere which just passes through the same square mesh sieve as the irregular particle.

A known amount of material was sieved using a stack of pre-weighed sieves with apertures in the size range 45-355 μm in a $\sqrt{2}$ progression. Each sample was sieved for 15 minutes using a Fritsch mechanical sieve shaker set at an amplitude of 0.5 mm. At the end of each test, the amount of material retained on each sieve was determined. The data obtained has been presented as both the percentages retained on each sieve

size and as the cumulative percentage oversize. From the cumulative percentage oversize graph, the 50% point was used to determine the mass median diameter of the material (useful for comparison between batches). Each batch of material was sieved three times and the average results used.

3.3.2 Bulk density

Both the poured and tapped bulk density values are bulk material properties and are defined as the ratio of the mass to volume. Comparison of results from similar samples can indicate changes in the material packing characteristics and can also be used to evaluate flow properties via determination of the Hausner ratio as described in section 1.4.4. A Hausner ratio of greater than 1.7 indicates a cohesive material with poor flow properties while a ratio of 1.2 or less is obtained for free flowing materials.

To determine the poured bulk density a known weight of material was poured into an appropriately size graduated measuring cylinder, held at an angle of approximately 45° to the horizontal (BS 1460). The cylinder was then placed gently upright and the poured volume of the material recorded. The poured density could then be calculated. The cylinder was then placed onto the platform of a tap density volumeter and tapped up and down at a speed of approximately 40 taps per minute for 1000 taps. The tapping caused the powder to consolidate and pack more tightly so reducing the volume. The tapped volume was noted and the tapped bulk density calculated.

3.3.3 Moisture content

The moisture content of each sample was determined by placing a known weight in a vacuum oven at 45°C and 800 bar until no further weight loss was recorded. Three samples of each crystallised batch were tested and the mean result calculated.

3.4 Evaluation of mechanical properties

In order to facilitate the evaluation of mechanical properties such as indentation hardness, elastic modulus and tensile strength, the crystallised batches of dextrose were compressed into compacts suitable for testing. Thus, it was strictly the mechanical properties of the compacts that were directly measured. It has been shown (Kerridge and Newton, 1986; Roberts and Rowe, 1991) that such data can be extrapolated to zero porosity by use of the exponential relationship proposed by

Spriggs (1961) and the similar equation proposed by Ryskewtich (1962) as used by Adolfsson and Nystrom (1996). These zero porosity values can be considered as a measure of the material property, free from contributions due to the porosity of the compacts.

3.4.1 Preparation of compacts for mechanical testing

Mechanical testing was conducted using compacts of the crystallised dextrose, as single crystals of dextrose suitable for testing could not be obtained at the range of crystallisation conditions being investigated. From the particle size analysis studies the 63-90 μm size fraction from each of the crystallised batches was isolated and used to prepare all the compacts unless otherwise stated.

Compacts were prepared on a universal testing instrument (Monsanto T10) in compression mode using a round 6 mm diameter flat faced F-type punch and die set supported in Perspex housing. The universal testing instrument consisted of a controllable crosshead fitted with a calibrated 10 kN compression load cell and an upper platen. A lower platen was supported in a fixed position to a solid platform. The instrument was programmed to move the upper platen towards the lower platen at a crosshead speed of 10 mm/s until a specified compression force was attained. The lower punch and die were placed in the housing and positioned in the centre of the lower platen. The die wall was pre-lubricated with a 4%$^{w}/_{w}$ solution of magnesium stearate in acetone prior to each compression. The die was then manually filled with 100±2 mg of crystalline material. The upper punch was placed in position, the compression sequence started and the compression force monitored. When the required compression force was attained the pressure was immediately released and the upper platen returned to its starting position. The upper punch was removed and the compact ejected using a hydraulic press. The lower surface of each compact was marked for future reference. The compacts were then stored in an airtight container at room temperature for at least 48 hours before testing.

3.4.2 Tensile strength testing

The tensile strength of the compacts was determined by measuring the diameteral crushing strength and using the equation of Fell and Newton (1968) as detailed in section 1.3.2 (equation 1.10).

The dimensions of five compacts prepared at each compression force were determined to an accuracy of 0.01 mm using a digital micrometer. The diameteral crushing strength of the compacts was determined using the CT40 crushing strength tester with a crosshead speed of 2 mm/s. Only the results obtained from compacts, which failed in tension, were used to calculate tensile strength values.

3.4.3 Elastic recovery

The percentage elastic recovery of each compact was determined as previously described in Section 1.2.6 using equation 1.1:

$$ER = [(H_t - H_e)/H_o] \times 100$$

where H_o is the thickness of the compact immediately after ejection and H_t is the thickness 48 hours after ejection.

3.4.4 Indentation studies

The technique of indentation testing has for many years been used to evaluate the hardness of metals, but since the 1960s it has also found several applications within the field of pharmaceutical technology. It is now a recognised technique for assessing the mechanical properties of tablets, single crystals and films. In general, the method consists of pressing a hard indenter onto the surface of the test material, by applying a constant load for a set time, and monitoring the deformation, it produces. The amount and nature of the deformation is defined by the fundamental mechanical properties of the test material such as hardness.

In terms of pharmaceutical materials, indentation was initially used to evaluate the hardness of tablets and used equipment which had been designed for testing metal samples (e.g. Spangler and Kaelin, 1945 and Nutter-Smith, 1949). It was concluded, however, that the loads required for these testers (typically 1 kg or greater) were too

large for tablet work. They often caused the sample to fracture or produced a poorly defined indentation, the diameter and thus depth of which was difficult to measure accurately. Throughout the 1960's and 70's several indentation testers were developed which required much smaller loads (typically 5-25 g). These were referred to as micro-indentation testers. Ridgway et al. (1969) used a Leitz micro-hardness tester with a Vickers indenter fitted to a microscope which permitted the accurate measurement of the indent produced. Another type of tester, the ICI pneumatic micro-indentation apparatus (Research equipment, London, Ltd) used by Ridgway et al. (1969) consisted of a 1.55 mm diameter spherical (Brinell) indenter and used loads of between 4-8 g. A further advantage of this tester was that the vertical movement of the indenter was monitored by a pneumatic amplifier. The depth of indentation and the amount of recovery after the load was removed, could therefore be directly recorded onto a calibrated chart recorder, eliminating errors due to the difficulties experienced in measuring the diameter of indentations though a microscope. Further developments of this apparatus used a displacement transducer to monitor the displacement of the indenter permitting the output to be recorded on a voltmeter, chart recorder or a data logger. In more recent years equipment which requires even smaller loads (typically 0.01-0.1 g) has been developed, these are known as nano-indentation testers (Pollock, 1992).

Despite the obvious advantages of these techniques, such as the possibility of testing very small samples (e.g. single crystals) and the ability to put the equipment into a cabinet, in which the environmental conditions can be controlled, there are also two main criticisms of micro and nano indentation techniques as used to evaluate the mechanical properties of pharmaceutical materials and compacts. The first disadvantage arises because pharmaceutical compacts are generally not entirely homogenous systems, containing many areas of inter particle voids. Indentation is essentially a point measurement and thus if the test is made by indenting onto a void area then an inaccurate result will be recorded. This is probably the reason for the relatively large scatter of results often observed from a particular sample. It is therefore important to test a large number of samples and average the results. The second criticism of indentation testing is concerned with the very small loads employed in micro and nano indentation, which produce very small indentations (typically 1-5 μm). It is essentially therefore only a measure of the surface properties

of the test sample, which may not be representative of the bulk and can be affected by forces such as shear during compression. Therefore, it should be ensured that the indentation produced is sufficient to overcome the problems associated with surface irregularities.

3.4.5 Theory of indentation testing

The principles and theories concerned with the technique of indentation testing have been comprehensively covered by a series of papers edited by Blau and Lawn (1985), and only a brief introduction with particular reference to spherical (Brinell) indentation will be present here in order to support the experimental work which follows.

The type of indentation produced during a test is dependent on the nature of the material being tested. Ideal elastic materials will deform according to classical Hertz theory, which proposed that the diameter, d, of the indentation formed by a spherical indenter is described by equation 3.2:

$$\frac{d}{2} = \frac{3}{4} Fr.\left[\frac{1-\sigma_1}{E_1} + \frac{1-\sigma_2}{E_2}\right] \qquad \text{(equation 3.2)}$$

Where F is the applied pressure, r is the radius of the indenter, E_1 and E_2 are the elastic (Young's) moduli of the test material and the indenter respectively and σ_1 and σ_2 are the Poisson ratios of the test material and the indenter respectively. When the indenter load is removed, the deformation will recover completely.

For ideal plastic materials, no deformation will occur until the critical yield stress (Y) is reached when plastic flow takes places by the deformation of specific crystallographic planes. In this case, the indentation hardness (H) is related to the yield pressure by the equation:

$$H = cY \qquad \text{(equation 3.3)}$$

where c is a constraint factor determined by the geometry of the indenter and the interfacial friction. When the indenter is removed, the impression formed remains intact.

Real materials however have both elastic and plastic components. For ideal elastic solids, deformation occurs initially by elastic deformation according to its elastic modulus and then once the yield stress is reached plastic deformation takes place at a constant flow stress. When the load is removed the elastic component of the deformation recovers but the plastic deformation remains. While studying Vickers indentation, Marsh (1964) found that the indentation hardness (H) could be related to the ratio of the elastic (Young's) modulus of elasticity (E) to the yield stress (Y) by the semi empirical equation (equation 1.14) previously described in section 1.3.6.

$$\frac{H}{Y} = 0.07 + 0.61 Ln \frac{E}{Y}$$

For materials such as polymers, he found that E/Y was in the order of 10-25 and H/Y was between 1.5-2.0 corresponding to the behaviour of a very elastic material. For metals, the ratio E/Y was greater than 150 and H $\approx$ 3Y corresponding to the behaviour of a rigid-plastic material. This, however, assumes that the yield stress remains constant. With real materials, the yield stress is seen to increase as a result of plastic deformation. This effect is referred to as work hardening. Therefore, when an indentation is made in such a material, the indentation process itself produces an increase in the yield pressure. Elastic-brittle materials can undergo fracture during the elastic deformation stage if a critical tensile stress is produced. The released elastic strain energy must be sufficient to provide the surface energy required for crack propagation. The amount of energy released is related to the diameter of the indentation and consequently the smaller the indentation, the larger the stress required to cause cracking.

Three principle mechanisms of indentation have been proposed (Samuels, 1985):

- cutting mechanisms
- elastic mechanisms
- compression mechanisms

Only the later two are relevant to spherical indentation and will be discussed here.

3.4.6 Mechanisms of spherical indentation

a) Elastic mechanism

The elastic mechanism (illustrated in Figure 3.1) was advanced by Shaw and DeSalvo (1970). They suggested that:

1. The plastic deformation beneath the indenter occurs by the sinking of a plastic zone
into the material.

2. The surrounding elastically strained zone decreases in volume (increases in density) to account for the volume of the indentation.

3. During unloading, a second phase of plastic deformation occurs which is opposite in direction and smaller in volume than the loading plastic deformation. This induces internal stresses that maintain the indentation.

In constructing their model, they assumed that the form of the plastic zone beneath the indention was similar to a line of constant stress and that the surface of the material adjacent to the indentation remained flat. Little or no experimental support exists for this mechanism.

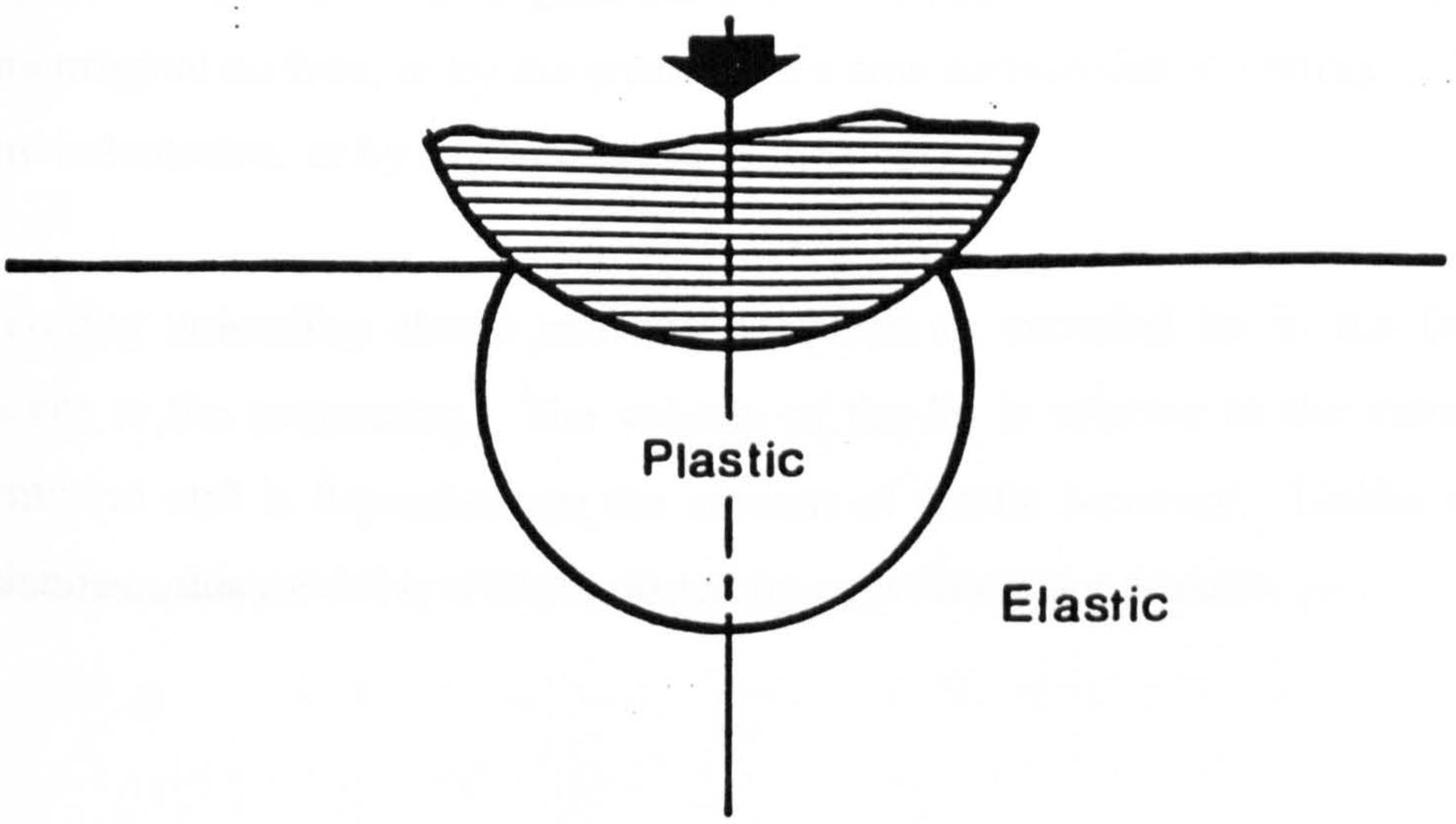

Figure 3.1 Model of the elastic mechanism of indentation proposed by Shaw and DeSalvo (1970).

b) Compression mechanism

The compression model of indentation was proposed by Mulhearn (1959). Figure 3.2 is an illustration of the mechanism. The continuous line is the elastic-plastic boundary. The broken lines represent several hypothetical shells of plastic deformation. The compression model suggests that:

1. Deformation of the test material takes place by the radial compression of hemispherical shells, which are centred (for all practical purposes) at the point of indentation. The magnitude of the strains in the shells decreases progressively as the elastic-plastic boundary is approached.

2. Differences in the deformation pattern due to the geometry of the indenter are confined to the region close to the indentation (shaded area). Within this region relatively large plastic deformation occurs.

3. The indentation surface is formed by the original test surface area folding down. Therefore, the indentation surface is mostly made up of original surface, which has been pressed vertically downwards. The surface area of the indentation is however, a few percent larger than the original surface. This extra surface is created by stretching of the original surface, or by the creation of a new surface due to cutting at the corners of the indentation, or by a combination of the two.

4. During unloading elastic recovery produces an extruded lip in the free surface adjacent to the impression. The volume of the lip is relative to the volume of the indentation and is dependent on the amount of elastic recovery. Unlike the elastic mechanism, this model is well supported by experimental evidence.

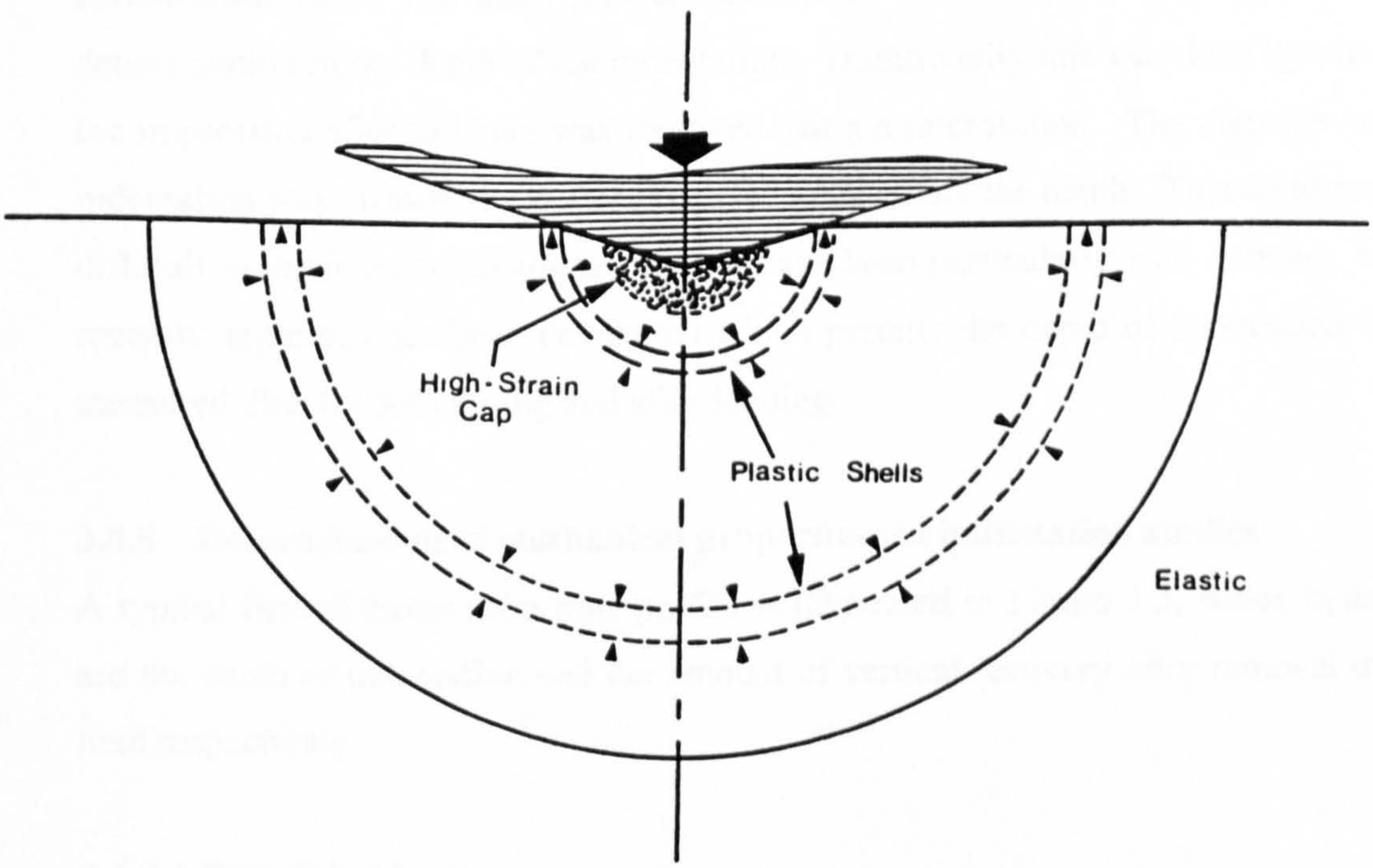

Figure 3.2 An illustration of the compression mechanism of indentation proposed by Mulhearn (1959). The circular continuos line is the elastic-plastic boundary. The broken line indicates several hypothetical plastic shells, and the arrows indicate the directions of straining of the shells.

3.4.7 Factors which influence indentation studies

The indenter -The main specifications for the indenter are that it is hard, with respect to the test material, that its geometry is perfect and that its surface is smooth and has low friction.

The loading device - The main requirement is that the load is applied smoothly with a minimum of stepwise loading. Several methods are available such as dead loading, magnetic loading, spring loading or pneumatic loading.

The test specimen - The surfaces should be uniform and homogenous. If the specimen is very thin, for example a film, then the substrate to which it is attached may influence the measured values.

Indentation size - The main problem associated with indentation studies is in the determination of the depth of the indentation. Traditionally this was done by viewing the impression after the load was removed using a microscope. The diameter of the indentation was measured and this was used to calculate the depth. This often proved difficult as the indentation edges may not have been particularly well defined. More recently apparatus has been developed which permits the depth of indentation to be measured directly both during and after loading.

3.4.8 Determination of mechanical properties via indentation studies

A typical Brinell indentation time profile is illustrated in Figure 3.3, where h_1 and h_2 are the depth of indentation and the amount of vertical recovery after removal of the load respectively.

3.4.8.1 Brinell hardness

The indentation hardness of a material is determined from the applied force and the area of the test material that can support that load. The general equation therefore is

$$\text{Hardness number} = \frac{\text{Applied load}}{\text{Area of indentation}}$$

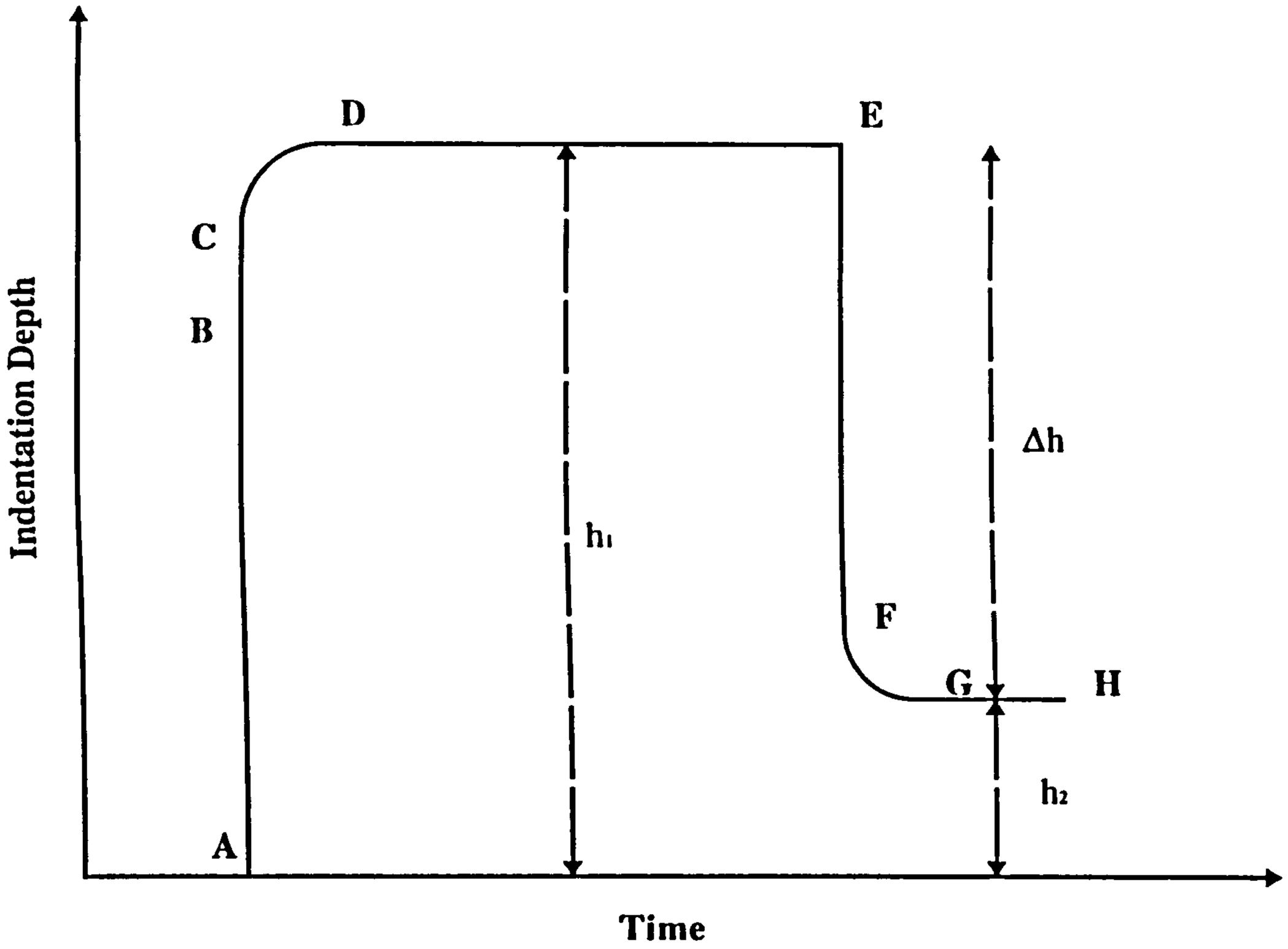

AB Elastic deformation

BC Instantaneous plasticity

CD Anelastic deformation

EF Elastic recovery

FG Anelastic recovery

HA Permanent indentation

Figure 3.3 A typical indentation depth vs. time profile with a description of the various stages

Figure 3.3 A typical profile of Brinell indentation depth variance with time

The Brinell hardness (HB) is calculated using equation 3.4.

$$HB = \frac{2F}{\pi D\left[D - (\sqrt{D^2 - d^2})\right]} \qquad \text{(equation 3.4)}$$

where F is the applied force, D is the diameter of the spherical indenter and d is the diameter of the impression under load. The diameter of the impression is determined after the load is removed and although the depth of the impression decreases due to elastic recovery, the diameter of the impression does not change.

In instruments that can directly measure the depth of the indentation this equation can be simplified to equation 3.5

$$HB = \frac{F}{\pi D h_1} \qquad \text{(equation 3.5)}$$

Where the applied force F is in Newtons, the diameter of the indenter D and the depth of the indentation h_1 are in meters the Brinell hardness is calculated in Pascals.

3.4.8.2 Elastic modulus

Development of apparatus, which could directly measure the depth of indentation and the vertical recovery after load removal, has enabled the use of indentation to evaluate the elasticity of materials.

In Brinell (spherical) indentation the change in the shape of the impression when the load is removed is illustrated in Figure 3.4 where r_1 and r_2 are the radius of the indentation under load and after the load is removed respectively. From the classical theory of Hertz, Tabor (1951) derived the following equation

$$d = 2.2\left[\frac{F}{2}.\frac{r_1 r_2}{r_1 - r_2}\left\{\frac{1}{E_1} + \frac{1}{E_2}\right\}\right]^{0.33} \qquad \text{(equation 3.6)}$$

where E_1 and E_2 are the elastic modulus of the test material and the indenter respectively. From this equation Ridgway et al., (1970) derived a simplified equation (equation 3.7) for calculating the elastic modulus of materials by indentation studies.

$$E = K \times \frac{F}{\Delta h \sqrt{h_1}} \qquad \text{(equation 3.7)}$$

where h_1 is the depth of indentation, Δh is the depth of recovery when the load is removed and K is a constant associated with the dimensions of the indenter. Detailed derivation of the equation and determination of the constant can be found in Appendix 1.

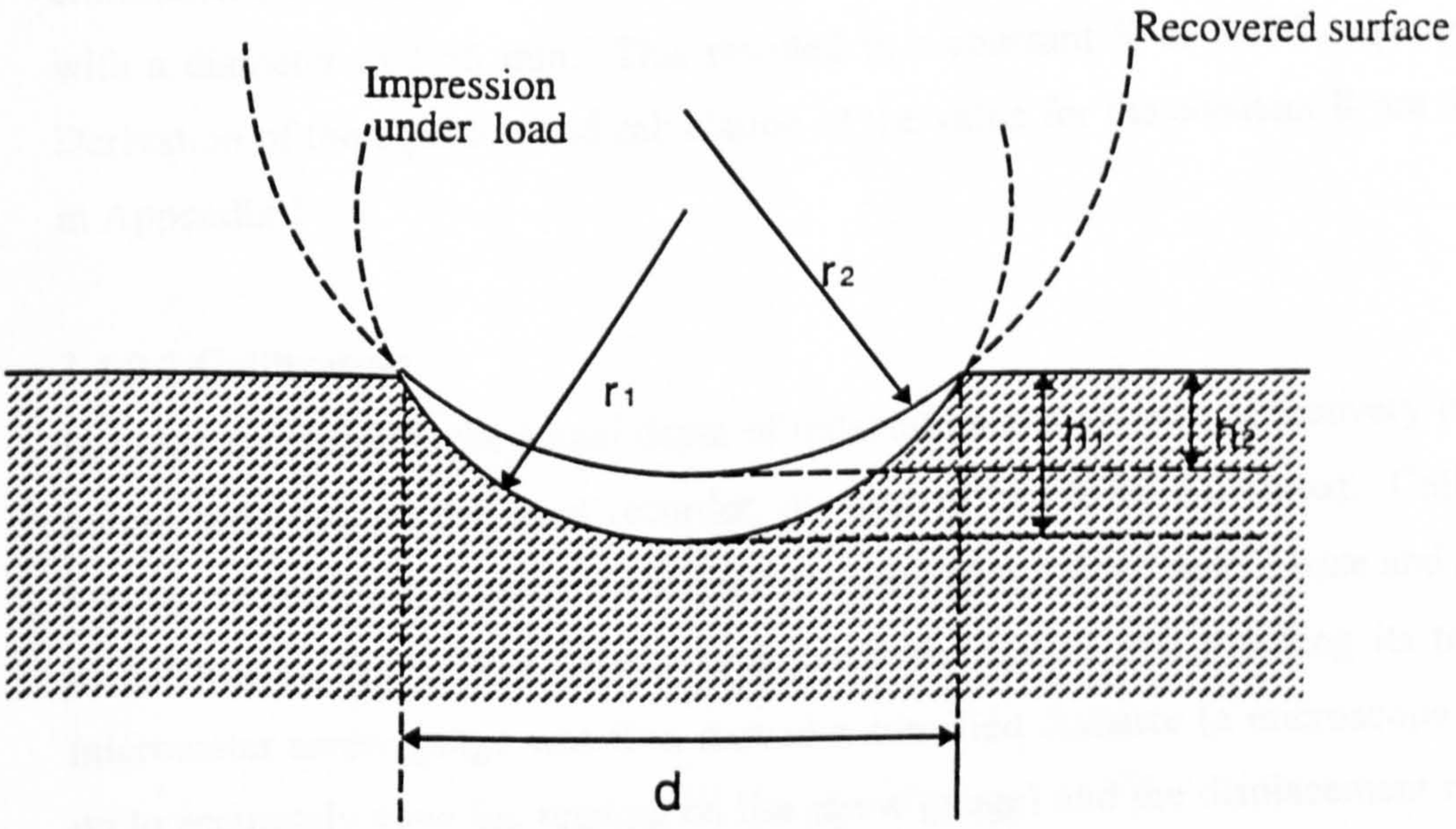

Figure 3.4 The geometry of spherical indentation

3.4.9 Experimental

3.4.9.1 Apparatus

For this work a vertical-displacement indentation tester based on a design previously described by White and Aulton (1980) was used (Figure 3.5). The apparatus consisted of a rigid steel frame onto which was fixed an aluminium block with two vertical holes. Through one hole ran a stainless steel shaft supported by a set of ball bearings, onto the bottom of which various indenter tips could be applied. The second hole supported a linear variable differential transducer, which monitored the movement of the indenter by means of a small side arm attached to the indenter shaft. The output from the LVDT was amplified and recorded directly onto a chart recorder. The load was applied to the top of the indenter shaft by means of a pneumatic controlled platform, which could be used to lower and raise a specified weight. The test sample was placed underneath the indenter tip supported on a solid adjustable stage. During this study, the apparatus was placed onto a solid marble table, which eliminated any vibrational fluctuations. The indenter tip used was a sapphire sphere with a diameter of 1.55 mm. This resulted in a constant K of 8.593 (equation 3.9) Derivation of the equation and calculation of the value for the constant K are detailed in Appendix 1

3.4.9.2 Calibration

In order to determine the actual depth of indentation and amount of recovery from the output produced on the chart recorder, the system had to be calibrated. Calibration was carried out in *situ* using a micrometer screw gauge fixed onto a base and secured in position so that it was directly underneath the LVDT and touching its tip. The micrometer screw gauge was then moved a specified distance (a microscope was set up to accurately view the reading on the screw gauge) and the displacement recorded by a chart recorder. A series of readings were conducted and a calibration curve constructed (see Figure 3.6). Each distance was measured five times and the average deflection recorded (a variation of less $\pm$ 0.05 μm was observed). The actual depth of indentation or amount of vertical recovery in μm could therefore be calculated by measuring the deflection on the chart recorder in mm and dividing the value by 2.3. For example, a deflection on the chart recorder of 23 mm was equivalent to an indentation depth of 10 μm.

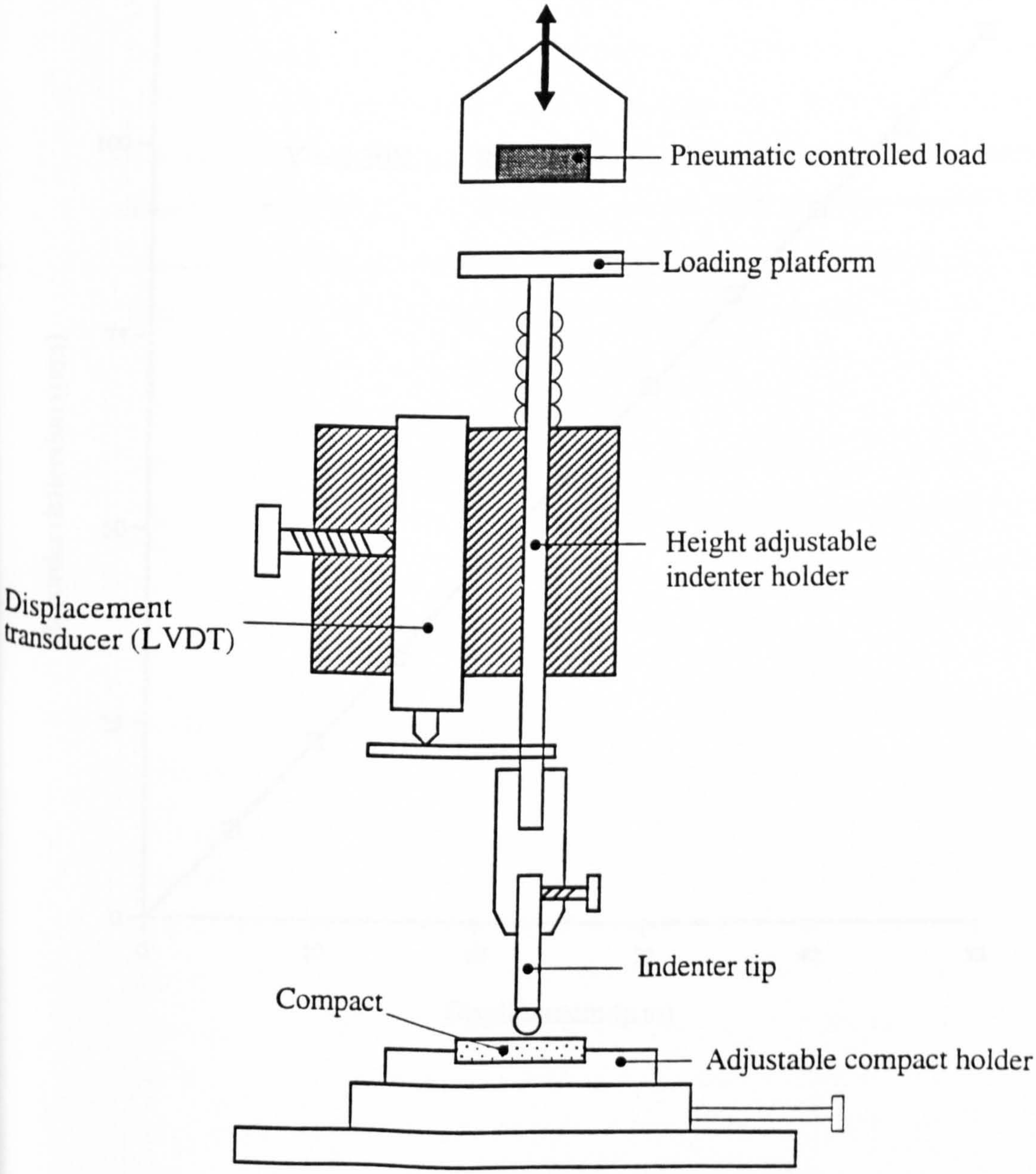

Figure 3.5 Simplified diagram of the indentation apparatus used in this work

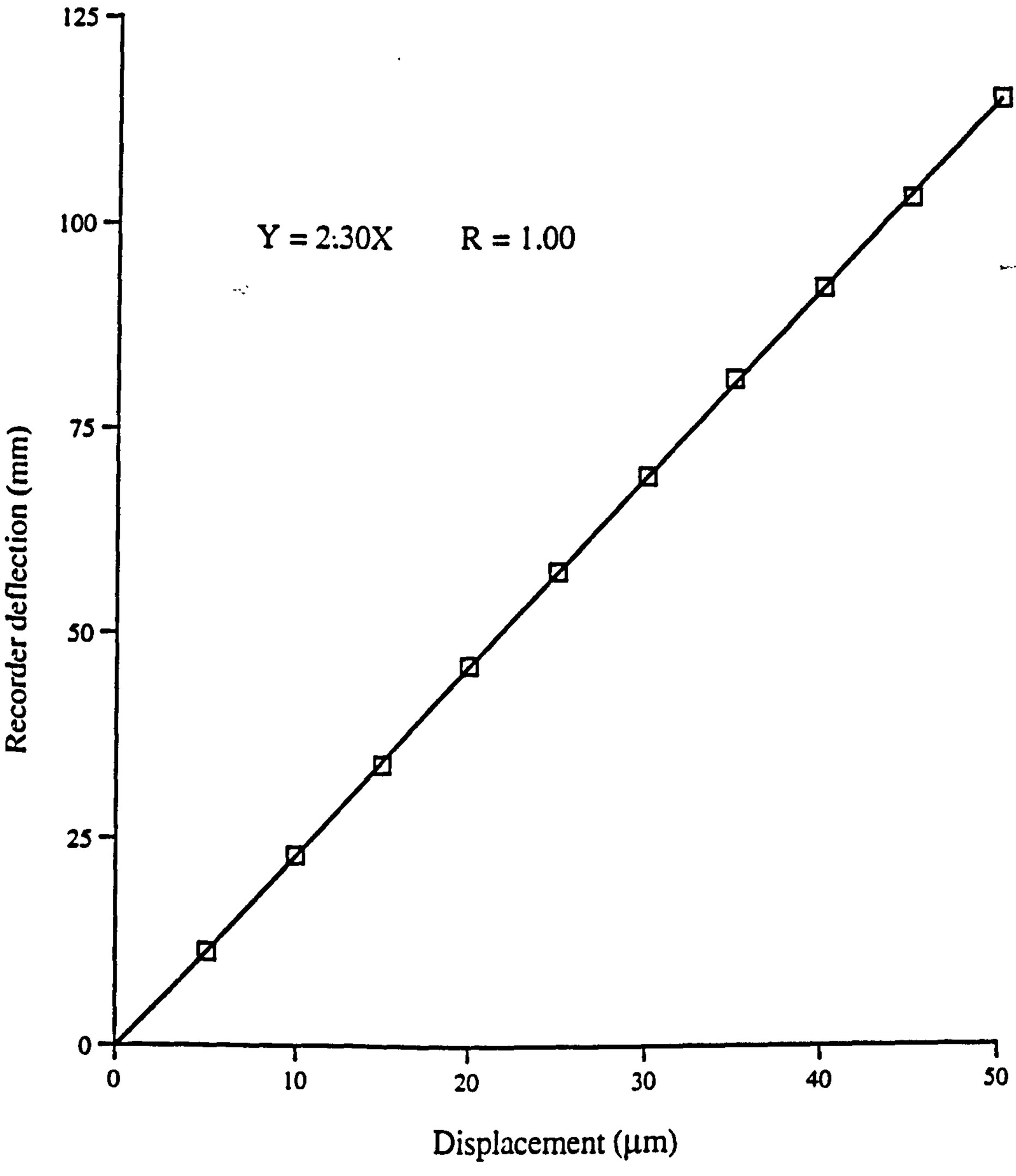

Figure 3.6 Calibration curve for the indentation apparatus

3.4.9.3 Indentation testing of dextrose compacts

A load of 1N was placed onto to the pneumatically controlled platform. The test sample was placed onto the testing stage (the face which had been adjacent to the upper punch during compression was placed facing upwards) and secured in position so that the indentation would take place in the centre of the compact. The static height of the indenter was adjusted so that the indenter tip was just in contact with the surface of the test compact. The transducer was positioned to produce a reading within the working range of the chart recorder. The chart recorder was then started and the load placed smoothly onto the indenter shaft platform using the pneumatic control. The load was applied for a set time of 30 seconds before the weight was removed using the pneumatic control. The movement of the indenter was recorded directly onto the chart recorder. The compact was removed and a new one placed in position. The test was repeated on 8-10 compacts prepared at each compression force.

3.5 Porosity of compacts and extrapolation of data

The percentage porosity of the compacts was calculated from equation 3.8:

$$\% \text{ Porosity} = [(V - Vo)/V] \times 100 \qquad \text{(equation 3.8)}$$

where V is the actual volume of the compact and V_o the volume of the material at zero porosity (calculated from the true density). The dimensions and weight of all the compacts were determined at least 48 hours after compression. The logarithm of the various mechanical properties were plotted as a function of % porosity according to the exponential equations proposed by Ryskewitch (1962) and Spriggs (1961) (Section 1.3.7). The plots were then extrapolated to zero porosity in order to determine the fundamental Brinell hardness and elastic modulus. The linearity of the plots and thus the validity of their extrapolation were confirmed by using a least squares regression analysis to determine a linear correlation coefficient (r). The statistical significance of the values obtained was checked using statistical tables for correlation coefficients (Lindley and Scott, 1995).

3.6 Compaction studies using the compaction simulator

The compaction behaviour of the crystallised batches of dextrose was further investigated by preparing compacts using a high speed compaction simulator at John Moores' University of Liverpool. This instrument permitted the punch pressures and displacements to be continually monitored during the entire compaction process, resulting in the generation of "at pressure" Heckel data and allowed the effects of varying the compaction rate to be examined.

3.6.1 The Compaction simulator

The compaction simulator used in this study has been described previously by Bateman (1988). It consisted of three basic sections:

The load frame - This consists of four vertical columns which support the upper and lower hydraulic actuators on which are located the upper and lower punches and a central platform which houses the die and the LVDTs which monitor the displacement of the punches.

The power pack - This consists of an oil reservoir at high pressure and an electric pump which produce the energy to move the actuators.

The control unit - This consists of the transducer amplifiers, the display units, a microcomputer which is used to pre-program and control the movement of the actuators and a mainframe computer for data capture and analysis.

The calibration procedures for the LVDTs, the load cells and the determination of the correction factors for the elasticity of the punches and the machine are part of the operational software and have been fully detailed by Bateman (1988). These procedures were carried out at the beginning and end of each day.

3.6.2 Compression

Compression was carried out on the compaction simulator fitted with a 12.5 mm diameter round flat-faced punches. A sawtooth displacement-time profile was programmed into the system. The output of the data points was sent via the microcomputer to the control valves on the hydraulic actuators. This signal regulated the flow of hydraulic fluid, which in turn controlled the displacement of the actuators and thus the upper and lower punches.

In this limited study, only the effect of compaction speed was examined. All compressions were carried out at a maximum compression force of 10 kN. Four compacts were produced at each of three compression rates of 10, 60 and 140 mm/s. Prior to each compression, the die was cleaned with acetone and pre-lubricated with $4\%^{w}/_{w}$ magnesium stearate in acetone. The die was manually filled with 400 ± 5 mg of crystallised material for each compact. During compression, the load and displacement of both the upper and lower punches were monitored to an accuracy of 0.05 kN and 12 μm respectively. After ejection, the compacts were stored in an airtight container at room temperature for 48 hours before the weight was measured to ± 0.1 mg and the dimensions of the compact were measured using a digital micrometer to ± 10 μm.

3.6.3 Data analysis

The data generated for each compaction was captured by the mainframe computer in ASCII format and assigned a file name. These files were then copied onto a floppy disc so that the data could be edited using a personal computer and Minitab software. The data were later converted to Microsoft Excel format for analysis. The values of weight, thickness, diameter and true density were input to a spreadsheet and the data manipulated to calculate Heckel numbers, generate Heckel plots, and porosity/pressure curves. After examination of the Heckel curves, linear regression was carried out on the 30 to 60 MPa portions of each plot and the yield pressure calculated from the reciprocal of the slope. The densification factors D_A, D_B and D_o where also determined as described in Section 1.2.8.

3.6.4 Tensile strength of compacts

The tensile strength of the compacts was determined from the force required to fracture compacts by diameteral compression on a motorised tablet hardness tester (Schleuniger, model 2E, Zurich, Switzerland). The tensile strength was calculated according to the equation 1.10 (Fell and Newton, 1970) as described in section 1.3.2.

3.6.5 Elastic recovery of compacts

The elastic recovery of the compacts was assessed as previously described in Section 3.6, according to equation 1.1 (Armstrong and Haines-Nutt, 1972), where the initial thickness of the compact was the thickness at maximum compression force and the final thickness was recorded no sooner than 48 hours after ejection.

Elastic recovery was also assessed by determining the difference between the mean yield pressure values obtained by the "at pressure" and the "zero pressure" methods and by evaluating the increase in the porosity of the compacts during the decompression phase of the compression cycle as described by Duberg and Nystrom (1986) and Paronen (1987).

CHAPTER FOUR

SOLID-STATE AND PARTICULATE CHARACTERISATION OF DEXTROSE CRYSTALS

4.1 Introduction

This chapter presents the results of the solid state and particulate characterisations described in Chapter 3. These studies demonstrate the effect of crystallisation conditions on the physicochemical properties of dextrose crystallised from aqueous solutions by the controlled cooling of supersaturated solutions. In some cases, it has been considered appropriate to duplicate the results from a batch in more than one table or graph in order to make the comparison between related batches of dextrose easier. The results are discussed in terms of the effect that the various crystallisation conditions had on a particular physicochemical property. Refer to Section 2.6 for an explanation of batch identification codes.

4.2 Effect of crystallisation conditions on the linear crystal growth rate of dextrose crystals

The effect of varying the crystallisation conditions on the linear crystal growth rates of dextrose are detailed in Tables 4.1 to 4.6. The rate of growth has been shown to influence the number of dislocations and defects and in turn affect its ability to form compacts (section 1.6.3). The growth rate has been determined by dividing the batch crystallisation yield (minus the initial 3 g of seed material) by the total crystallisation time.

4.2.1 Effect of crystallisation cooling rate

The crystallisation times and the linear crystal growth rates of the batches prepared at a range of cooling rates are shown in Table 4.1. As the cooling rate was increased through the range 0.5, 1.0, 10.0, 30.0 and 50.0°C/h for batches with an initial calculated supersaturation ratio of 1.3, the linear crystal growth rate steadily increased from 3.03 g/h to 35.44 g/h. This trend was also observed for the two batches prepared at an initial supersaturation ratio of 1.5 (i.e. DS05 and DS50). In this case, when the crystallisation cooling rate was increased from 0.5 to 50.0°C/h the growth rate increased from 9.04 g/h to 58.56 g/h.

This increase in linear crystal growth rate with increasing crystallisation cooling rate is possibly due to the fact that, at faster crystallisation cooling rates, the system reaches its maximum level of supersaturation much more quickly. Therefore, there is a greater thermodynamic driving force for nucleation and crystal growth.

Table 4.1 Effect of crystallisation cooling rate on the batch yield and linear crystal growth rate of dextrose

Batch	Cooling Rate (°C/h)	Crystallisation Time (h)	Yield (g)	Growth Rate (g/h)
D05	0.5	16.0	48.44	3.03
D1	1.0	8.0	45.32	5.67
D10	10.0	0.8	13.28	16.60
D30	30.0	0.27	7.22	26.74
D50	50.0	0.16	5.67	35.44
DS05*	0.5	16.0	141.70	9.04
DS50*	50.0	0.16	6.37	58.56

* Initial supersaturation ratio S = 1.5. In all other batches S = 1.3.

4.2.2 Effect of initial supersaturation ratio

The effect of changing the level of initial supersaturation on the linear crystal growth rate of dextrose crystals was examined by comparing several sets of crystallised material which were prepared under similar conditions, except for the level of initial supersaturation. The data obtained were presented in Table 4.2.

In each case, the batch of dextrose prepared from the supersaturated solution with the highest calculated initial supersaturation ratio had the fastest linear crystal growth rate. For example, the batches D05, DS05 and DR30 were all prepared by cooling supersaturated solutions from 38°C to a final crystallisation temperature of 30°C at a cooling rate of 0.5°C/h but they had calculated initial supersaturation ratios of 1.3, 1.5 and 1.6 respectively. This rise in the initial supersaturation ratio resulted in linear crystal growth rates of 3.03, 9.04 and 11.04 g/h being attained. This same trend of increased linear crystal growth rate with increased initial supersaturation ratio was also observed for the other sets of batches which were prepared at various crystallisation temperature ranges with different initial supersaturation ratios.
Clearly therefore, the degree of supersaturation plays a major role in determining the linear crystal growth rate of dextrose crystals from aqueous solutions.

These data would appear to be in agreement with the finding of Burton et al. (1951). They suggested that crystal growth rate was related to supersaturation ratio (section 1.6.3.2) and with the concentration gradient between the solute (crystals) and the crystallisation liquor as proposed by the various diffusion theories of crystal growth. The higher the level of supersaturation, the more crystal nuclei will be formed and so the greater the rate of growth as there are more surfaces available for growth.

Table 4.2 Effect of initial supersaturation ratio on the batch yield and linear crystal growth rate of dextrose

Batch	Crystallisation Temperature (°C)	Saturation Ratio	Yield (g)	Growth Rate (g/h)
D05	38-30	1.30	48.44	3.03
DS05	38-30	1.50	144.70	9.04
DR30	38-30	1.60	176.60	11.04
D50*	38-30	1.30	5.67	35.44
DS50*	38-30	1.50	9.37	58.56
DC40	48-40	1.30	111.64	6.98
DR40	48-40	1.50	176.28	11.02
DC45	53-45	1.30	158.21	9.89
DR45	53-45	1.40	177.92	11.12
DR51	59-51	1.10	176.51	10.84
DC51	59-51	1.30	245.44	15.15

*These batches were prepared at a cooling rate of 50°C/h. All other batches were prepared at a cooling rate of 0.5°C/h.

4.2.3 Effect of crystal growth time

The effect of extending the time available for crystal growth was examined by crystallising dextrose in the same manner as batches D1 and D30 (i.e. cooling solutions with an initial supersaturation ratio of 1.3 from 38°C to 30°C at rates of 1°C/h and 30°C/h respectively) but instead of immediately removing the material from the crystalliser when a temperature of 30°C was reached, the system was held at 30°C (with constant agitation) until a total growth time of 16 hours had been attained.

In both instances the batches with the extended growth times have, as would be expected, greater yields but the linear growth rates were less than for the corresponding batch without the extra growth time (Table 4.3).

The explanation for this effect again concerns the levels of supersaturation encountered in the solution throughout the crystallisation. Although the growth rates quoted are linear growth rates the true rate of crystal growth will not be constant for the entirety of the process. As the final crystallisation temperature is approached, the supersaturation ratio and thus the crystallisation driving force will reach a maximum value. However, as the extra time proceeds more material crystallises out of solution and so the supersaturation ratio decreases, resulting in a lowering of the growth rate. It is likely that it this depletion of the supersaturated solution that causes the linear rate of growth of batches D1T and D30T to be less than that of their corresponding batches, D1 and D30 respectively.

Table 4.3 Effect of crystal growth time on the batch yield and linear crystal growth rates of dextrose

Batch	Cooling Rate (°C/h)	Crystallisation Time (h)	Yield (g)	Growth Rate (g/h)
D1	1.0	8.0	45.32	5.67
D1T	1.0	16.0	79.81	4.99
D30	30.0	0.27	7.22	26.74
D30T	30.0	16.0	277.84	17.37

4.2.4 Effect of seed crystal, particle size

In the course of this work, the majority of crystallisations have been carried out by seeding the supersaturated solutions with crystals of dextrose monohydrate (3.0 g) selected from the sub 45 μm size range. To investigate the effect of changing the particle size of the seed crystals one set of batches were prepared using seed crystals selected from the 63 to 90 μm size range. The effect of this change, on the linear crystal growth rate of dextrose in detailed in Table 4.4.

A reduction in the yield and thus the linear growth rate is observed for the dextrose crystallised using the larger seed crystals. This may be due to the fact that, as the seeds were larger there would have been a reduction in the number of seeds available (as the same weight was used), therefore the ability of the seeds to induce further nucleation would have been reduced (as this is dependent on the number of seeds) and so there would have been a reduction in the number of surfaces available for growth.

Table 4.4 Effect of seed crystal, particle size on the batch yield and linear crystal growth rates of dextrose

Batch	Seed Size (μm)	Yield (g)	Growth Rate (g/h)
D05	<45	48.44	3.03
DX05	63-90	29.65	1.85

4.2.5 Effect of additives

The effect of including trace amounts of other carbohydrates (i.e. lactose and sucrose) in the supersaturated solutions of dextrose was investigated. The influence of this variable on the linear growth rates of dextrose is presented in Table 4.5.

As the data show, inclusions of another carbohydrate in the crystallisation solution slows the linear rate of crystal growth. The presence of another carbohydrate in the crystallisation system acts as an impurity and retards crystallisation probably by selectively adsorbing onto various sites (e.g. kinks or steps) of a growing crystal thus inhibiting further growth of that face.

Table 4.5 Effect of additives on the batch yield and linear crystal growth rates of dextrose

Batch	Additive	Yield (g)	Growth Rate (g/h)
D05	None	48.44	3.04
DLac	Lactose	30.33	1.88
DSuc	Sucrose	36.21	2.26

4.2.6 Effect of crystallisation temperature

The influence of the temperature range over which the crystallisation of dextrose was carried out, on the linear crystal growth rate was examined. The solutions were saturated at a range of temperatures and cooled at a rate of 0.5°C/h. Seed crystals were added at 8°C above the final crystallisation temperature of 30, 40, 45, 48, and 51°C. In one set of experiments, all the batches had a calculated initial supersaturation ratio of 1.3 (batches D05, DC40, DC45, DC48, DC51) while in another set the initial supersaturation ratios were adjusted (section 2.15.5) to produce batches of dextrose with a constant linear crystal growth rate (batches DR30, DR40, DR45, DC48, DR51). The effect of temperature on the yields and linear growth rates of dextrose are detailed in Table 4.6.

From the data it is evident that, for the batches with the constant initial supersaturation ratios, the batch yields and the linear rate of crystal growth increase as the temperature range is increased, rising from a rate of 3.04 g/h for batch D05 prepared at 38-30°C, to a rate of 15.34 g/h for batch DC51 prepared at 59-51°C. This temperature effect is probably a function of several factors. Firstly, the rate of nucleation is known to be temperature dependent (section 1.6.2). The greater the temperature, the higher the free energy of the system, and thus the greater the probability of nuclei reaching the critical size required for survival which increases the potential for crystal growth due to the increased number of surfaces available. Secondly, the solubility of dextrose increases with temperature and although all the solutions were prepared with the same initial supersaturation ratio of 1.3, the saturation potential (C-S) (i.e. the difference between the solubility at the saturation temperature and the solubility at final crystallisation temperature) increases, with temperature. For example, the solubility of dextrose (per 100 g of water) at 30°C is 120 g and with an initial supersaturation ratio of 1.3 the saturation concentration was 156 g giving a supersaturation potential of 36 g. Similarly the solubility of dextrose (per 100 g of water) at 51°C is 225.7 g and with a calculated initial supersaturation ratio of 1.3 the saturation concentration was 293.4 g giving a supersaturation potential of 67.7 g. This increase in the supersaturation potential is known to increases the rate of diffusion controlled crystallisations (section 1.6.3).

The second of set of batches were prepared with varied initial supersaturation ratios, which were calculated as detailed in section 2.15.5 in order to produce dextrose at a range of temperatures but with a constant growth rate. The growth rates of this series of batches ranged from 11.02 to 11.11 g/h, which was considered to be constant for the purpose of this study.

Table 4.6 Effect of temperature on the batch yield and linear crystal growth rate of dextrose

Batch	Crystallisation Temperature (°C)	Saturation Ratio	Yield (g)	Growth Rate (g/h)
D05	38-30	1.30	48.44	3.04
DC40	48-40	1.30	111.64	6.98
DC45	53-45	1.30	158.20	9.89
DC48	56-48	1.30	177.81	11.11
DC51	59-51	1.30	245.43	15.34
DR30	38-30	1.60	176.60	11.04
DR40	48-40	1.50	176.28	11.02
DR45	53-45	1.40	177.92	11.12
DR48	56-48	1.30	177.81	11.11
DR51	59-51	1.10	176.51	11.03

4.3 Effect of crystallisation conditions on the crystal habit of dextrose

At the end of each crystallisation a sample of the material obtained was viewed under a microscope and photographed. Significant (visible to the eye) changes in crystal habit were noted in several cases.

Figure 4.1 is a photomicrograph (X10) of crystals from batch D05 (cooled at a rate of 0.5°C/h from 38-30°C with an initial supersaturation ratio, S of 1.3). The crystals obtained are seen to have the characteristic habit of dextrose monohydrate crystals as detailed in section 2.2.1.

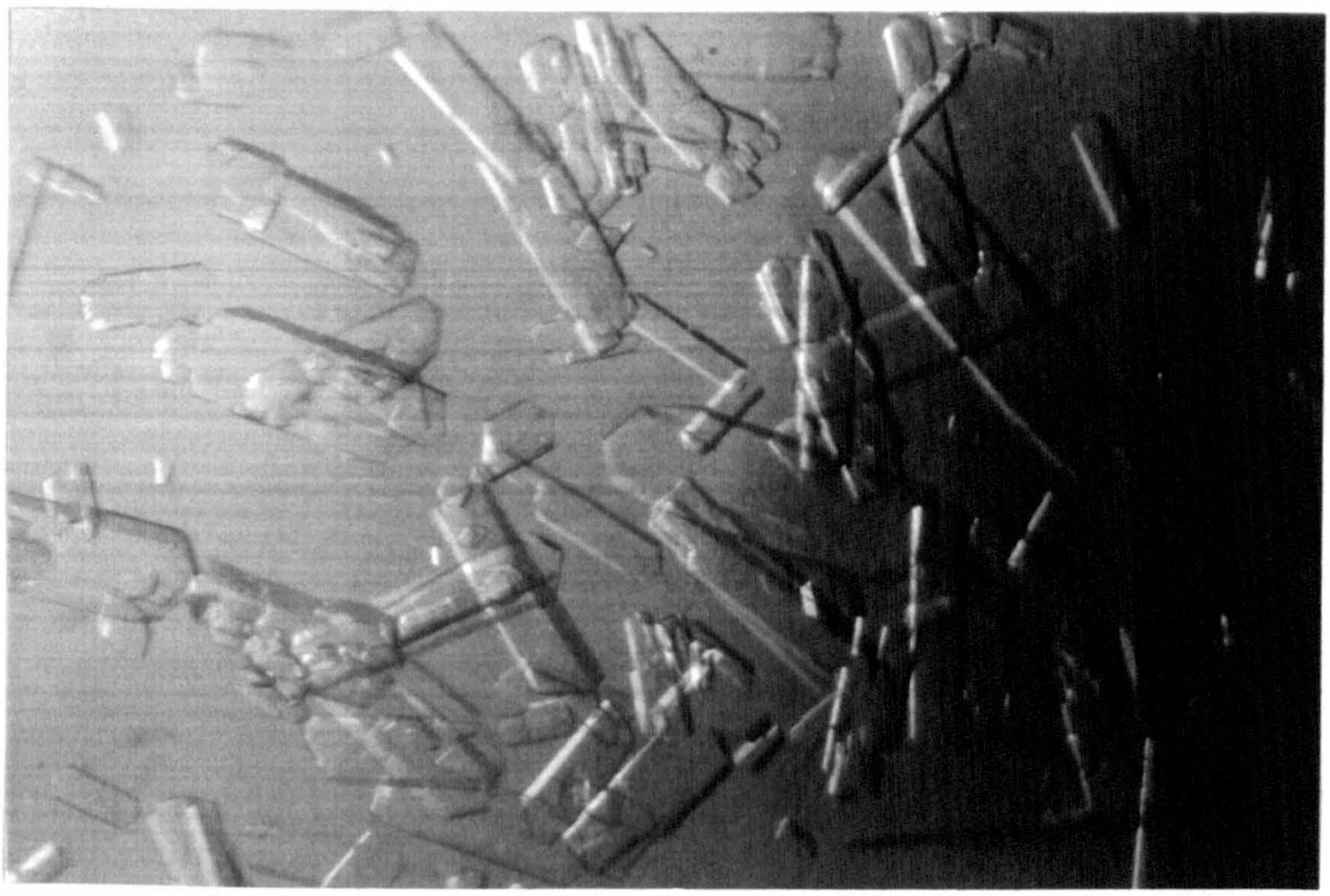

Figure 4.1 Photomicrograph (X10) of crystals from batch D05

The only factors that were observed to have an effect on the crystal habit of dextrose were the inclusion of additives and the temperature of crystallisation. Alteration of crystal habit by inclusion of additives has been widely researched and documented (section 1.5.6). The addition, of sucrose, batch DSuc (Figure 4.2) or lactose, batch DLac (Figure 4.3) to the supersaturated solutions of dextrose is seen to cause marked changes in the morphology of the dextrose crystals obtained.

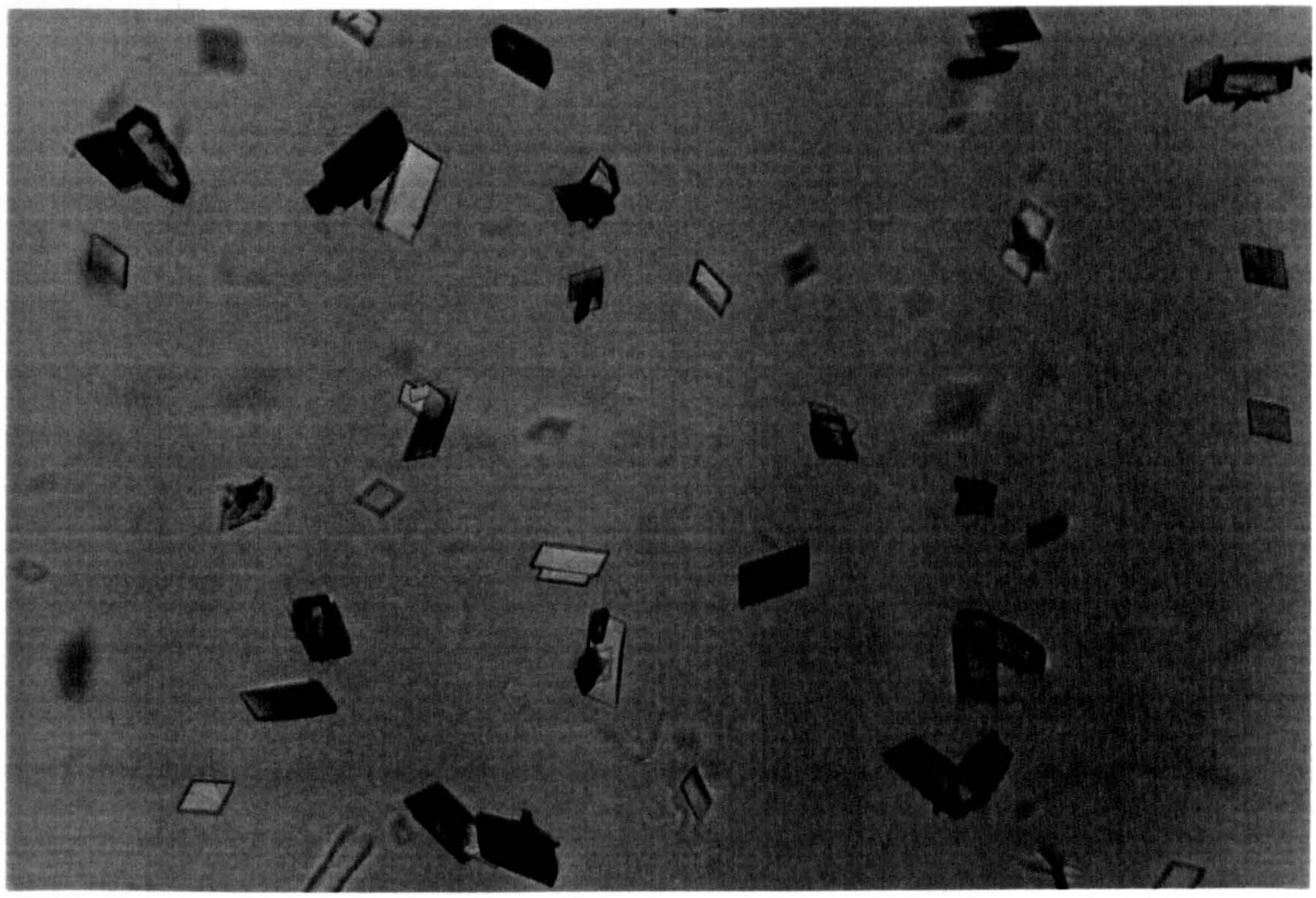

Figure 4.2 Photomicrograph of crystals from batch DSuc (X10)

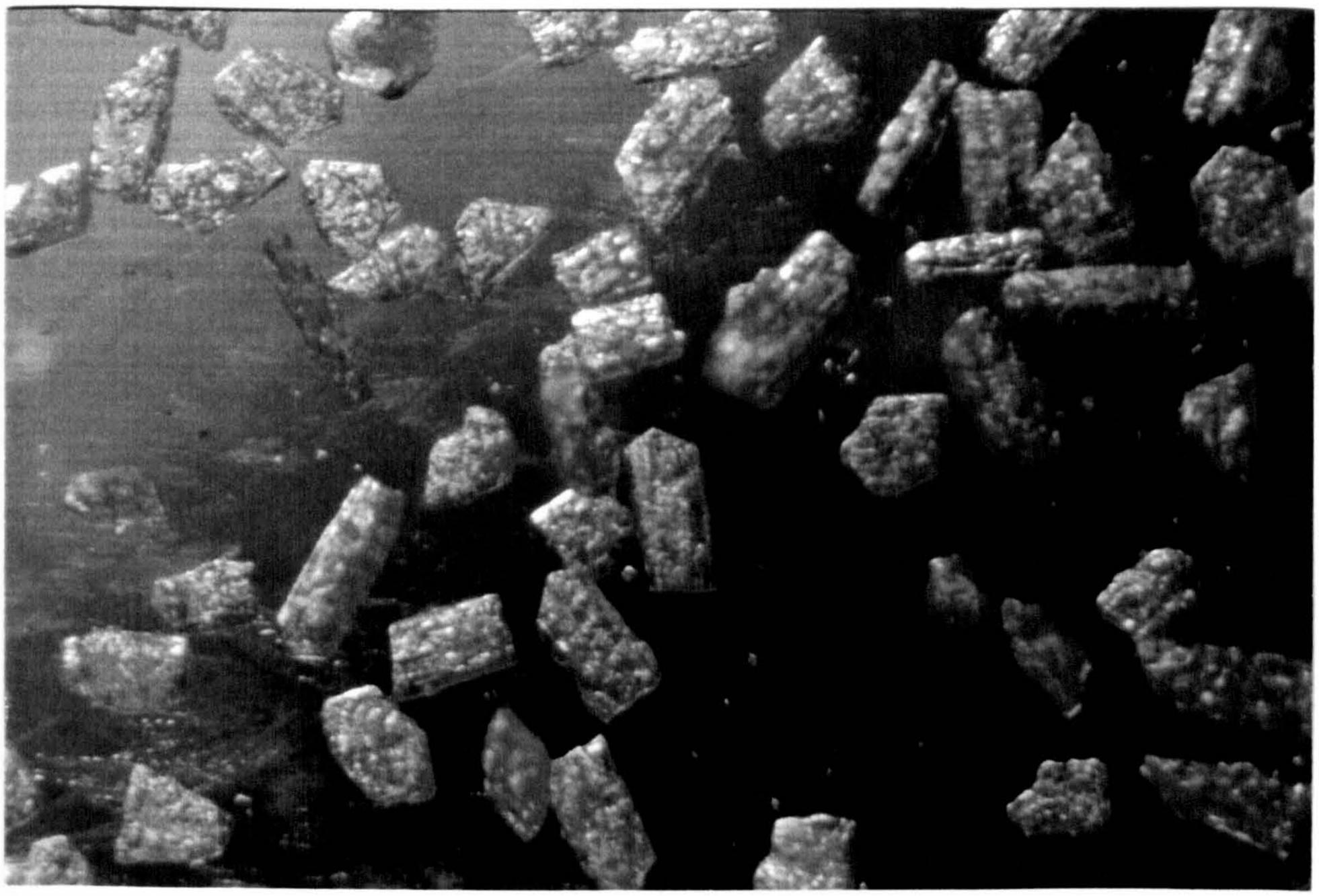

Figure 4.3 Photomicrograph of crystals from batch DLac (X10)

These changes occur because the additive (impurity) is often absorbed onto the growing crystal face and retards further growth of that face.

Other factors such as the rate of cooling and the initial supersaturation ratio probably had subtle effects on the crystal habit. It appeared that these factors caused the length to width ratio of the crystals to decrease and increases in the initial supersaturation ratio may also have changed the crystal surface properties with the faces appearing rougher. However to establish if these effects were real would have required a detailed image analysis study which was outside the scope of this project.

Changes to the temperature of crystallisation were also observed to cause significant changes to the crystal habit of dextrose. When the crystallisation was carried out over the 59-51°C temperature range the habit of the crystals obtained changed from the plate-like habit obtained for batch D05 (Figure 4.1) to a more prismatic habit (Figure 4.4) which is characteristic of anhydrous dextrose (section 2.2.1). The crystals from the batches DC40 and DC45 were similar to those of batch DO5 while those of batch DC48 (Figure 4.5) were a mixture of both monohydrate and anhydrous crystal habits.

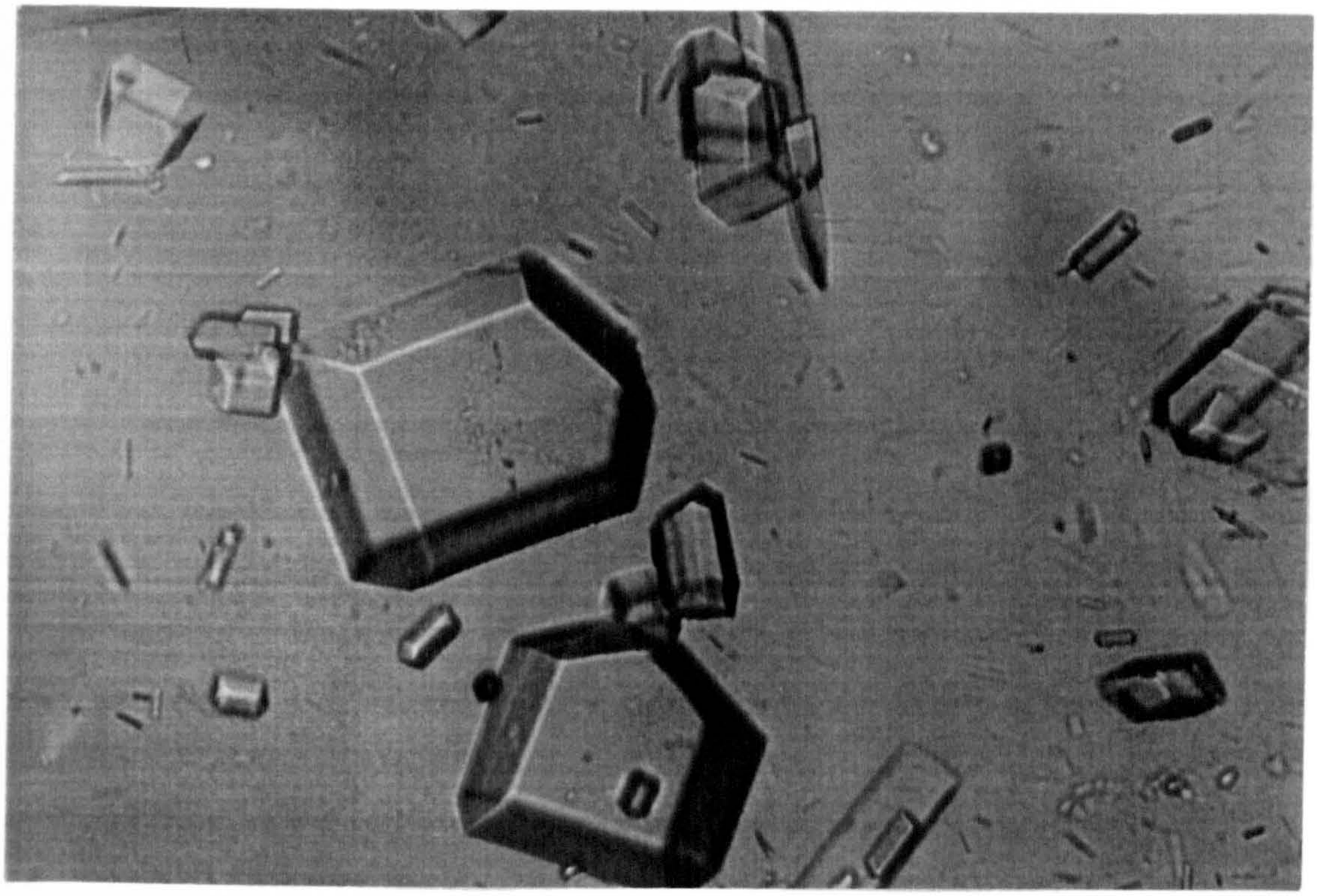

Figure 4.4 Photomicrograph of crystals from batch DC51 (X10)

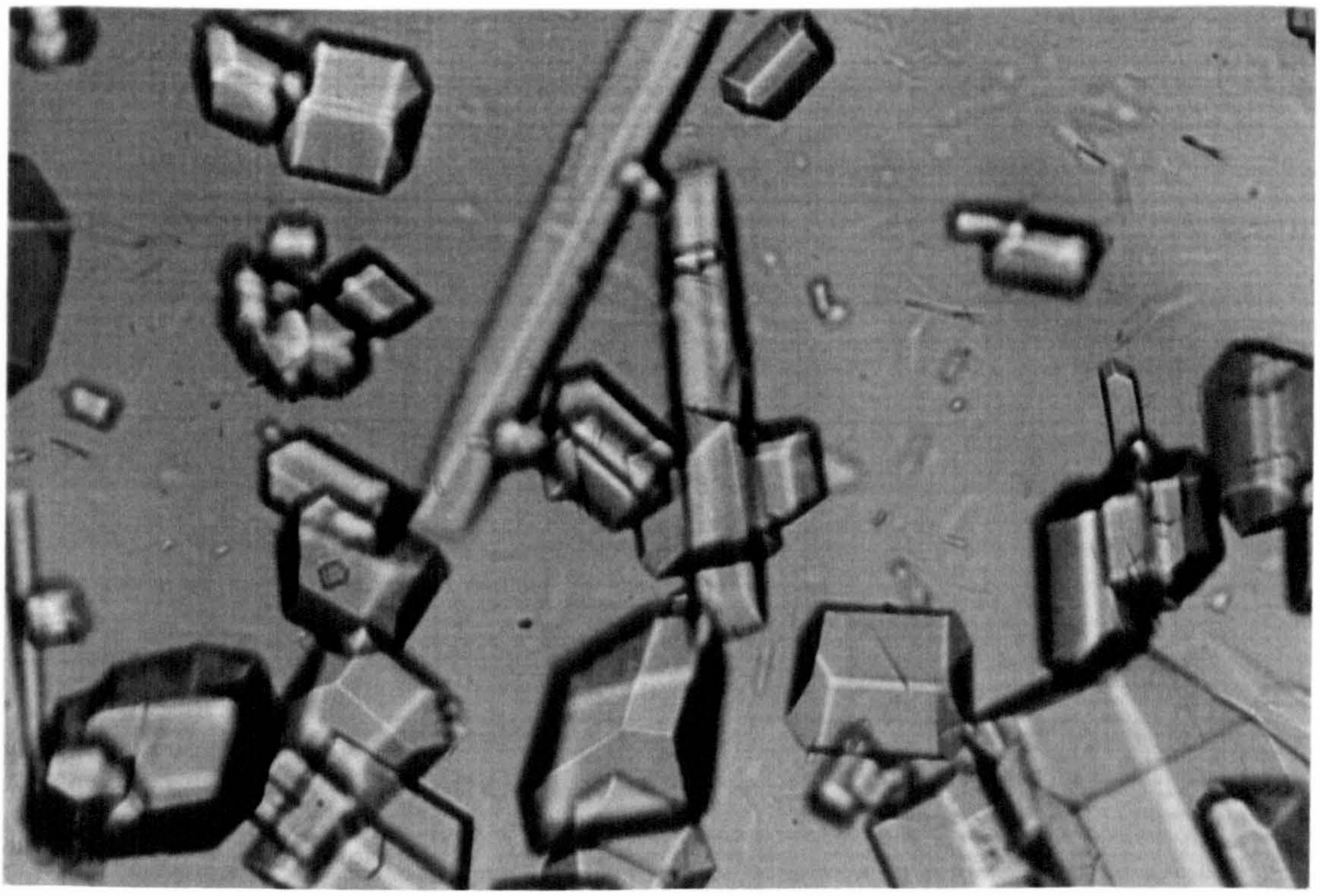

Figure 4.5 Photomicrograph of crystals from batch DC48 (X10)

4.4 Effect of crystallisation conditions on the true density of dextrose

As already discussed in chapter one, true density values are a reflection of the intermolecular structure of a material and can be used as an indicator of changes in the degree of crystallinity or crystal structure. The effect of altering the various crystallisation variables on the true density values of dextrose crystallised from aqueous solutions is detailed in the following sections.

4.4.1 Effect of crystallisation cooling rate

As the crystallisation cooling rate is increased through the range 0.5, 1.0, 10, 30 and 50°C/h a decrease in the true density values is observed (Table 4.7). The mean values were found to be significantly different at a probability level of 95% when compared using analysis of variance (ANOVA). A similar trend was also obtained for batches DS05 and DS50, both of which had initial supersaturation ratios of 1.5 and were cooled at rates of 0.5 and 50°C/h respectively.

All these samples should be crystallographically similar and therefore the true density results should be a good relative measure of the degree of crystallinity of these samples. The steady decrease in the true density values along this series would appear to indicate that a change (decrease) in the degree of crystallinity might be taking place as the cooling rate is increased. This corresponds with the finding of section 4.1 in which the increased cooling rates were reported to result in increased growth rates. As the growth rate increases it is reasonable to assume that the number of imperfections present in the lattice would increase and thus a decrease in the order or degree of crystallinity would be expected.

Table 4.7 Effect of crystallisation cooling rates on the true density values of dextrose

Batch	Cooling Rate (°C/h)	Crystallisation Time (h)	True Density (g/cm^3)	S.D. (g/cm^3)
D05	0.5	16.0	1.5207	0.0012
D1	1.0	8.0	1.5187	0.0015
D10	10.0	0.8	1.5157	0.0031
D30	30.0	0.27	1.5117	0.0015
D50	50.0	0.16	1.4863	0.0053
DS05*	0.5	16.0	1.5407	0.0025
DS50*	50.0	0.16	1.5333	0.0042

Initial supersaturation Ratio S = 1.5. For all other batches S = 1.3.

4.4.2 Effect of initial supersaturation ratio

The effect of varying the calculated initial supersaturation ratio of batches crystallised under a variety of conditions is displayed in Table 4.8. The data clearly indicate that the true density of a material is susceptible to changes in the supersaturation level of the crystallising system. For example, consider batches D05, DS05 and DR30, which were crystallised under identical conditions except for their initial supersaturation ratios of 1.3, 1.5 and 1.6 respectively. This rise in supersaturation ratio resulted in increasing true density values of 1.5207, 1.5407 and 1.5443 g/cm^3. Analysis of variance showed that these mean values were significantly different at the 95% probability level. The same effect was also recorded for the other sets of batches. Student t-tests showed that the differences between each set of these values were significant at the 95% probability level except for those of batches DC45 and DR45. An increase in the level of supersaturation therefore appears to lead to an increase in the true density of dextrose crystallised from aqueous solutions. These results demonstrate that by altering the level of supersaturation the crystal structure and possibly the number of crystal imperfections can be changed/controlled.

Table 4.8 Effect of initial supersaturation ratio on the true density of dextrose

Batch	Crystallisation Temperature (°C)	Supersaturation Ratio	True Density (g/cm^3)	S.D. (g/cm^3)
D05	38-30	1.30	1.5207	0.0012
DS05	38-30	1.50	1.5407	0.0025
DR30	38-30	1.60	1.5443	0.0015
D50*	38-30	1.30	1.4863	0.0053
DS50*	38-30	1.50	1.5383	0.0021
DC40	48-40	1.30	1.5224	0.0026
DR40	48-40	1.50	1.5257	0.0006
DC45	53-45	1.30	1.5270	0.0035
DR45	53-45	1.40	1.531	0.0010
DC51	59-51	1.30	1.5630	0.0026
DR51	59-51	1.10	1.552	0.0040

* These batches were prepared at a cooling rate of 50°C/h. All other batches were prepared at a cooling rate of 0.5°C/h.

The true density values obtained would appear to imply that at higher levels of supersaturation more ordered growth of dextrose crystals, with less imperfections, takes place (as the true density values increase). This, however, contradicts the previous findings (section 4.2) which associated increased supersaturation with faster growth rates. These in turn are generally expected to increase the number of lattice defects and thus result in a lowering of the degree of crystallinity which would be reflected in decreasing true density values. However, it must be remembered that true density values can only be used to rank samples that are crystallographically similar. This situation would therefore suggest that other factors, which predominated over the effect of growth rates, were at work and lead to the observed increase in the true density values. As mentioned in section 1.6, the mechanism of crystal growth may be

influenced by variations in the supersaturation level of the system. It was proposed that at high levels of supersaturation the B&S mechanism, which involves surface nucleation, will predominate, while the BCF model, in which growth proceeds via screw dislocations was expected to be the principal mechanism at lower levels of supersaturation. It is therefore probable that different mechanism were responsible for the growth of dextrose crystals from aqueous solutions which had different levels of supersaturation and thus caused changes in the structure or the degree of order within the crystal lattice which in turn resulted in true density values changing as observed.

The seemingly contradictory effect of raising the supersaturation levels on the true density of dextrose may also been explained by considering the proposal by Randloph (1970). He suggested that crystal growth occurred via a two step process: i) nucleation and ii) particle orientation onto a growing crystal face. As discussed in section 1.6.2 the rate of nucleation is dependent on the level of supersaturation and thus the batches with the higher initial supersaturation ratios will have a higher nucleation density and therefore a higher growth rate (as seen in section 4.2) due to a greater population of growth units. The second step in the growth process, (i.e. the particle orientation) may be slowed down due to the increased viscosity of the solution at the higher supersaturation levels, thus reducing the number of lattice imperfection and leading to the increased true densities.

4.4.3 Effect of crystal growth time

The difference in the true density values between batches D1 and D1T and between batches D30 and D30T as detailed in Table 4.9 were found not to be significant at the 95% probability level using a t-test. The linear growth rates for these batches as reported in section 4.2 showed that extending growth time increased the growth rates and so would have been expected to cause a reduction in the degree of crystallinity. However, as in the previous section several other significant factors including the level of supersaturation and growth mechanism are also at work, making comparisons of crystallinity using true density data difficult for these particular batches.

Table 4.9 Effect of crystal growth time on the true density of dextrose

Batch	Cooling Rate (^{o}C/h)	Crystallisation Time (h)	True Density (g/cm^3)	S.D. (g/cm^3)
D1	1.0	8.0	1.5187	0.0015
D1T	1.0	16.0	1.5206	0.0020
D30	30.0	0.27	1.5117	0.0015
D30T	30.0	16.0	1.5147	0.0057

4.4.4 Effect of seed crystal, particle size

The influence of altering the size of the seed crystals from less than 45 μm to between 63 and 90 μm is detailed in Table 4.10. Increasing the seed size caused reduction in the true density of the material produced from 1.5207 to 1.5127 g/cm^3. The difference was found to be significant at the 95% probability level using a t-test. This reduction in true density corresponds to the lowering of the linear crystal growth rate as reported in section 4.2.2. However, as discussed previously growth rate is not always the predominating factor and it is likely that the variation in true density is also (if not entirely) due to the fact that the bigger seeds, (which consist of random fragments of crystals), will make up a much larger part of the new crystals which have grown on to the surface of the seeds. More imperfections will, therefore be present and thus a lowering of the true density results.

Table 4.10 Effect of seed crystal particle size on the true density of dextrose

Batch	Seed Size (μm)	True Density (g/cm^3)	S.D. (g/cm^3)
D05	<45	1.5207	0.0012
DX05	63 - 90	1.5127	0.0025

4.4.5 Effect of additives

The data presented in Table 4.11 illustrate the effect of incorporating small amounts of lactose or sucrose into the crystallisation system on the true density of dextrose.

In both instances, a significant change (as determined by a student t-test) was observed in the true density of the material produced. This demonstrates that when trace amounts of either of these carbohydrates are included in the crystallisation system of dextrose they alter the structure of the dextrose crystal, indicating that they are incorporated into the lattice as impurities.

Table 4.11 Effect of additives on the true density of dextrose

Batch	Additive	True Density (g/cm^3)	S.D. (g/cm^3)
D05	None	1.5207	0.0012
DLac	Lactose	1.5553	0.0041
DSuc	Sucrose	1.5540	0.0026

4.4.6 Effect of crystallisation temperature

The effect of changing the temperature of crystallisation was investigated and the effect of this variable on the true density of the crystalline material produced was determined. The data obtained are displayed in Table 4.12.

Consider first the batches prepared with the constant initial supersaturation ratio of 1.3 (batches. D05, DC40, DC45, DC48 and DC51). It is clear that as the crystallisation temperature range is raised there is an increase in the true density of the of the material with the most significant difference occurring for batches DC48 and DC51 which were crystallised by cooling to final temperatures of 48 and 51°C respectively. At first these results appear to contradict the growth rate data which showed an increase in growth rate with increasing temperature (section 4.2.6) and would thus be expected to cause a lowering of the true density (if the samples were all crystallographically similar). It is therefore likely that the samples are structurally different and so the true density values cannot be used as a relative measure of crystallinity but simply as indicators of change. Several factors are contributing to the effect observed. The first factor concerns the solubility of dextrose, which increases with temperature. This in turn will lead to a lowering of the interfacial tension between the solute and the growing crystal face (section 1.6) which will make it easier for new growth units to properly orientate themselves onto the growing surface resulting in an increased order. However, the extent to which this factor influences the true density of the material is likely to be significant only for the batches D05, DC40 and possibly DC45.

Table 4.12 Effect of crystallisation temperature on the true density of dextrose

Batch	Crystallisation Temperature (°C)	Saturation Ratio	True Density (g/cm^3)	S.D. (g/cm^3)
D05	38 - 30	1.30	1.5207	0.0012
DC40	48 - 40	1.30	1.5224	0.0026
DC45	53 - 45	1.30	1.5270	0.0035
DC48	56 - 48	1.30	1.5485	0.0026
DC51	59 - 51	1.30	1.5630	0.0026
DR30	38 - 30	1.60	1.5443	0.00015
DR40	48 - 40	1.50	1.5257	0.0006
DR45	53 - 45	1.40	1.5310	0.0010
DC48	56 - 48	1.30	1.5485	0.0040
DR51	59 - 51	1.10	1.5520	0.0018

For the other two batches (and possibly batch DC45 to some extent) a much more likely reason for the change observed in the true density values lies in the transition point (which is located at approximately 50°C) on the temperature/solubility curve of dextrose (section 2.2.1). It is known that below 50°C the monohydrate form crystallises from aqueous solutions while the anhydrous form is obtained from crystallisations conducted above 50°C. Therefore, in these batches some or all of the growth will have been as the anhydrous crystal form. In batches DC48 and DC45 the crystals will have transformed (at least partially) into the monohydrate form when the temperature dropped below 50°C. Therefore, the relatively large changes observed in the true densities are indicative of the crystal structure changing form the monohydrate form to the anhydrous form. With little or no molecules of water present the crystal lattice will be more tightly packed and thus the true density is increased (relative to the other batches) as seen for batch DC51.

Consider now the batches prepared at the similar constant linear growth rates. It is evident that there is no straightforward trend running throughout the series, which would support the view that more than one factor was responsible for the variations in

the true density of dextrose, crystallised from these aqueous solutions. As already discussed above the most significant change in true density is observed for the batches crystallised at the two highest temperatures due to the fact that much or all of the crystallisation was conducted above the temperature/solubility transition point and so the material will possess some degree of anhydrous crystal structure. The other point of interest is that the true density of batch D05 is greater than that of DC40, despite the fact that the previous set of batches showed an increase in the true density when the crystallisation temperature was raised. The only major difference between these two batches (besides the temperature of crystallisation) is the level of supersaturation, and as was observed previously (section 4.3.1) the higher the initial supersaturation ratio the higher the true density of the material produced. These results would therefore appear to support this view.

4.5 Effect of crystallisation conditions on the x-ray diffraction patterns of dextrose

A small selection of the crystallised samples was sent for x-ray diffraction studies at the Department of Material Science, Nottingham University. The aim was to ascertain whether x-ray diffraction could detect any differences between the samples and to establish if the diffraction data could be used to quantify changes in the relative degree of crystallinity between the various samples.

The x-ray diffraction patterns obtained are reproduced in Figures 4.6 to 4.11. The d-spacing values of the major peaks (those peaks which were at least 20% of the strongest peak) from the samples are recorded in Table 4.13 in order of intensity. Reference data for dextrose monohydrate and dextrose as detailed in the JCPDS library are also included in Table 4.13. It should be noted however, that there is no information on the preparation conditions used to obtain the reference samples and the wavelength used for the reference samples (1.5418 nm) was slightly different, compared to that used for the samples being studied (1.5406 nm).

The first point to note is that large variations in the peak intensities were obtained from repeat tests on the same batch of material probably due to preferred orientation effects. It was therefore decided that the data could not be used to determine relative degrees of crystallinity by comparison of peak intensities. A continuation of this limited diffraction study for all the crystalline samples was not therefore considered to be useful.

By comparing the experimental data with the reference data it can be seen that the crystallised samples D05, D50, DR30, DC45 and DC48 all contain peaks at similar d-spacing values to the reference sample, namely those at 4.69, 4.39, 3.15, and 2.18 nm. These correspond to the strongest peaks in all the diffraction patterns at 2θ values of 9.17, 20.06, 28.26 and 42.48°. By closely observing the patterns and the data for batches D05, D50 and DR30 it is seen that the number of significant peaks is increased when either the crystallisation cooling rate or the initial supersaturation ratios are increased. This suggests that the degree of order within the crystal lattice is decreasing, which is in agreement with the true density and crystal growth rate data previously reported.

Table 4.13 X-ray diffraction data (d-spacing) obtained from the crystallised samples and from the JCPDS library

d-spacing (nm)							
Dextrose hydrate (JCPDS)	**D05**	**D50**	**DR30**	**DC45**	**DC48**	**DC51**	**Anhydrous Dextrose (JCPDS)**
4.69	9.34	9.39	4.75	9.39	4.25	4.34	4.30
4.39	4.74	3.12	9.37	3.12	3.12		3.13
3.15	3.12	4.76	3.12	4.76	9.40		
9.61	2.23	2.23	2.23	2.23	4.76		
2.18	3.17	4.45	4.44	4.44	4.34		
2.87	2.87	2.87	3.18	4.34	4.44		
3.90	4.44	3.85	2.87	2.87	2.42		
	3.85	2.41	2.42	2.41	5.96		
		3.18	3.86	3.18	5.90		
		6.83		6.82	6.81		
		3.01		3.86	3.46		
				3.17	2.23		
					2.87		
					3.86		
					3.02		
					3.19		

When comparing the patterns and data from batches D05, DC45, DC48 and DC51 (those batches with final crystallisation temperatures of 30, 45, 48 and 51°C respectively) several effects are evident. Firstly, it is clear that the pattern and data obtained for batch DC51 is similar to the reference data for anhydrous dextrose with only one major peak being detected at a d-spacing of 4.34 nm. Secondly, by observing the x-ray patterns it can be seen that as the temperature of crystallisation is decreased the peak at 4.34 nm which corresponds to a 2θ value of 20.94° gradually decreases in significance (compared to the other peaks) forming a doublet in sample DC45 and almost completely disappearing in batch D05. Another significant feature

is that the pattern for batch DC48 appears to be the most disturbed with a multitude of equally intense peaks suggesting a relatively disordered system. This may be due to the material having some monohydrate and some anhydrous character as it was crystallised across the solubility transition point for dextrose, above which it crystallises in the anhydrous form and below which it crystallises in the monohydrate form.

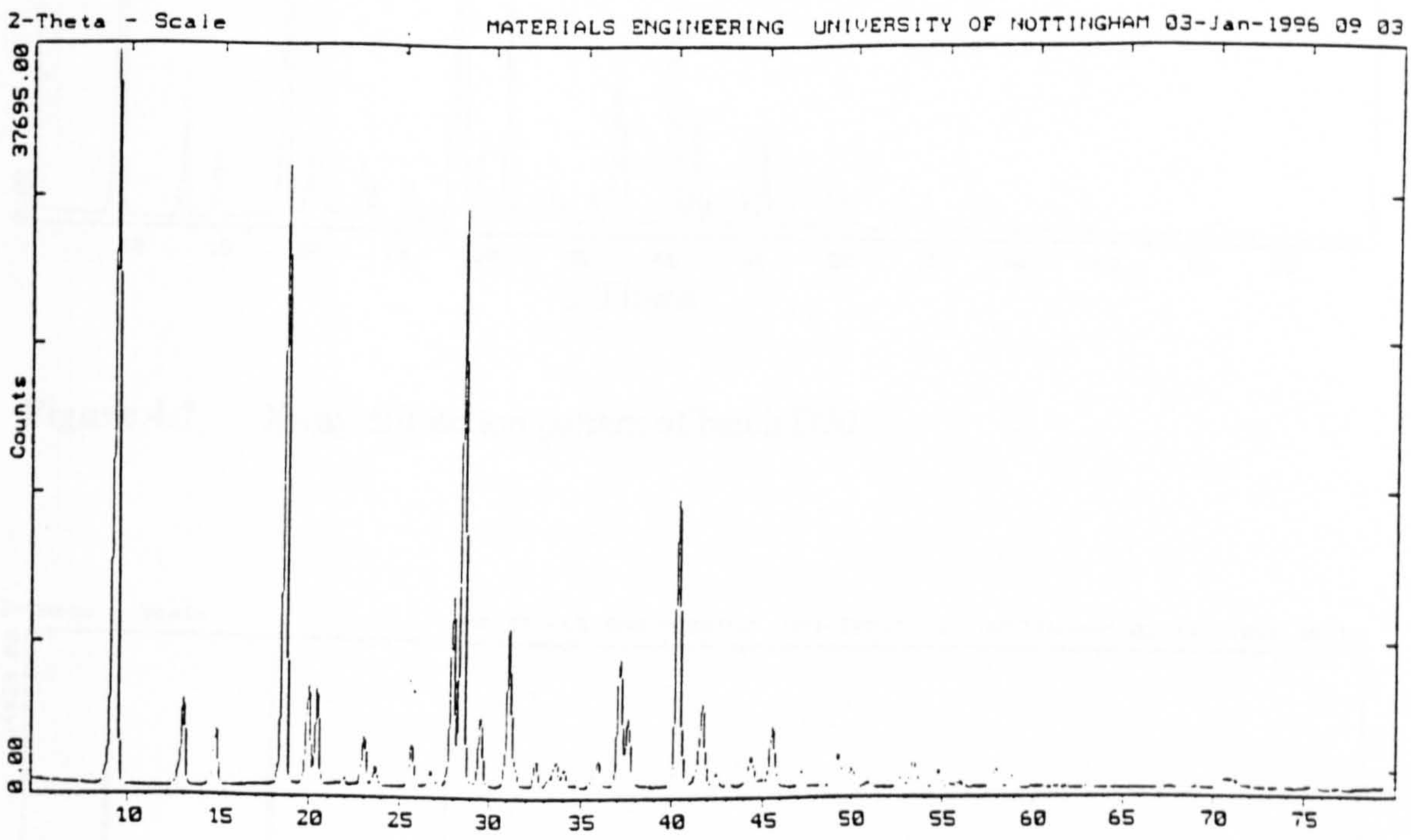

Figure 4.6 X-ray diffraction pattern of batch D05

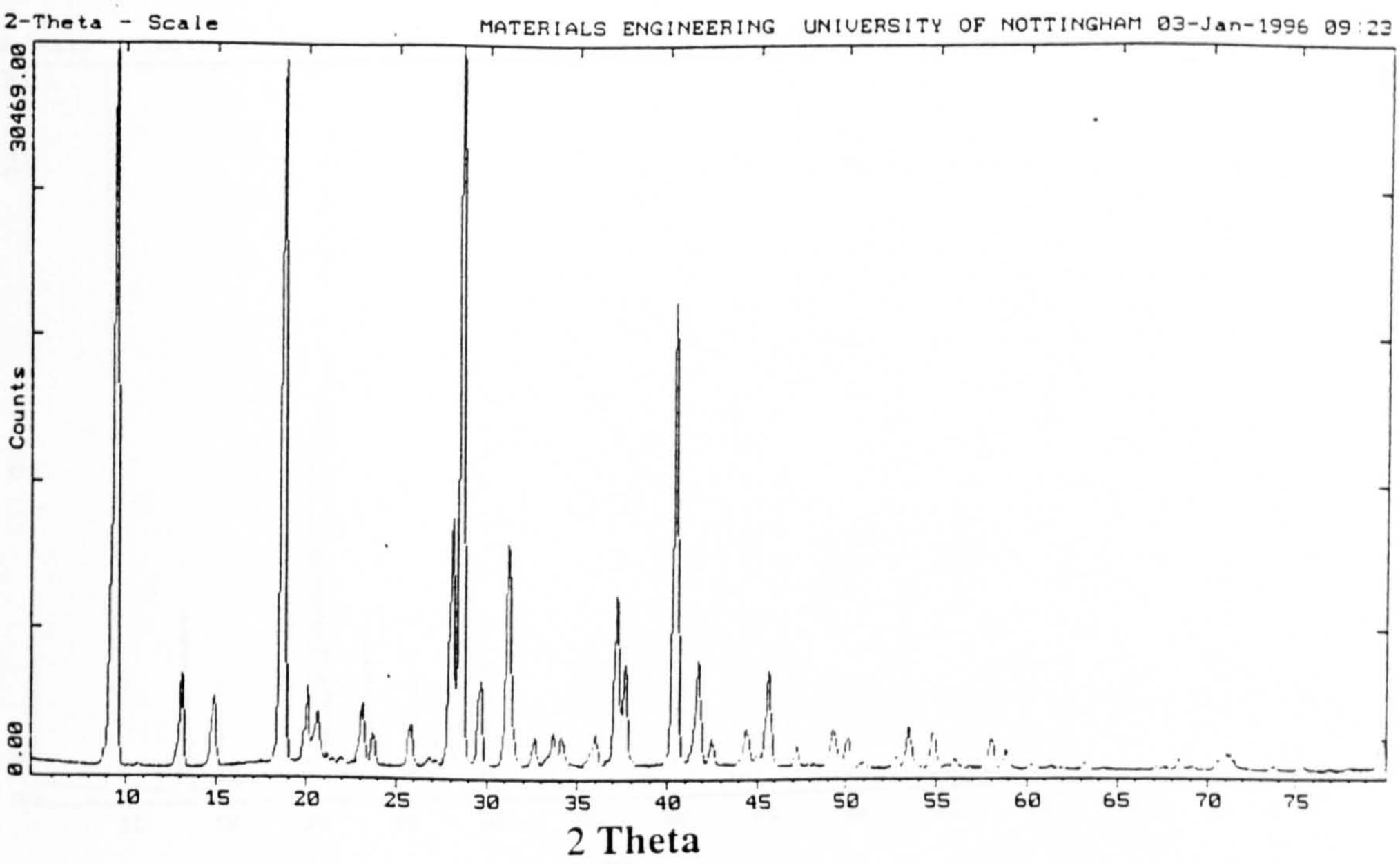

Figure 4.7 X-ray diffraction pattern of batch D50

Figure 4.8 X-ray diffraction pattern of batch DR30

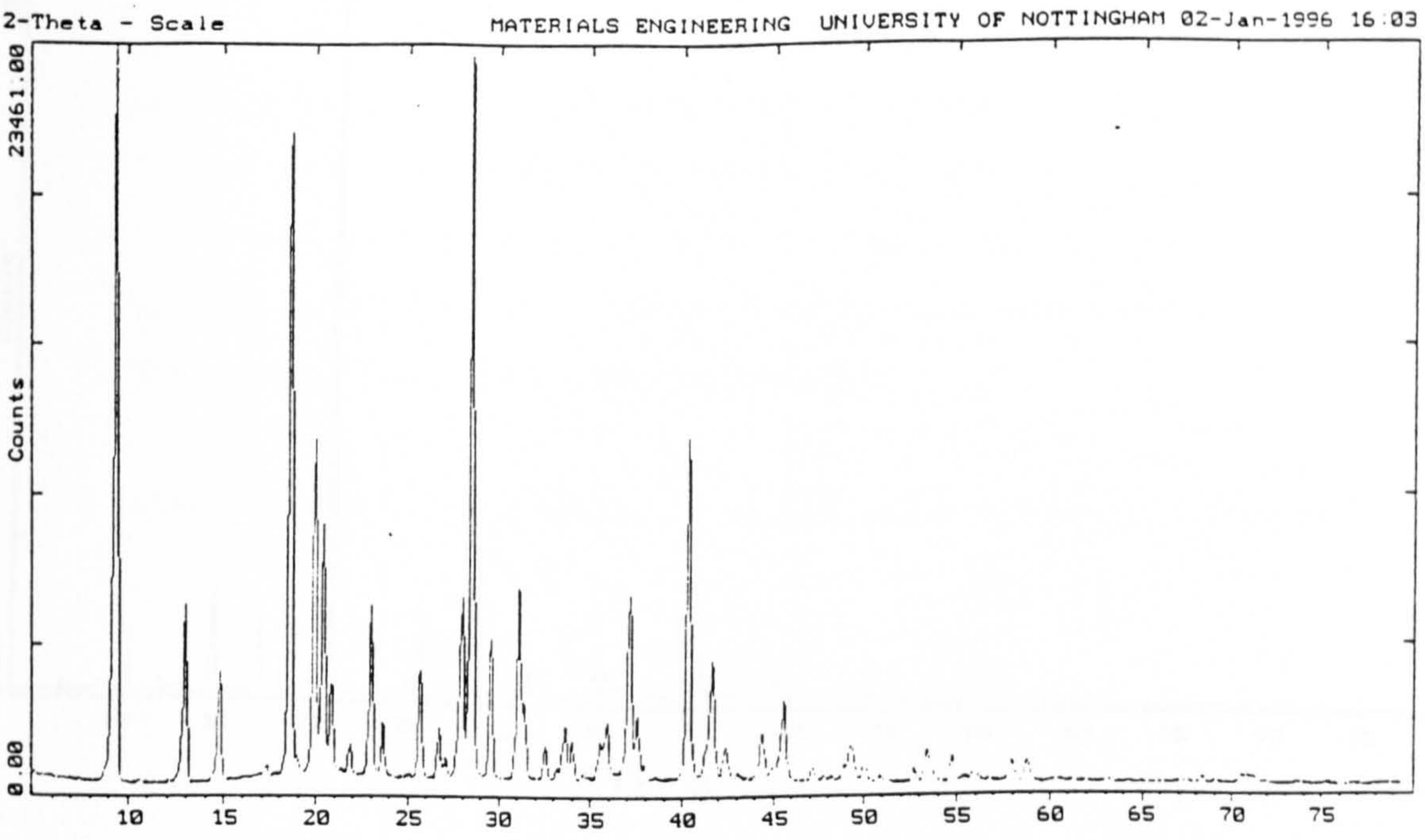

Figure 4.9 X-ray diffraction pattern of batch DC45

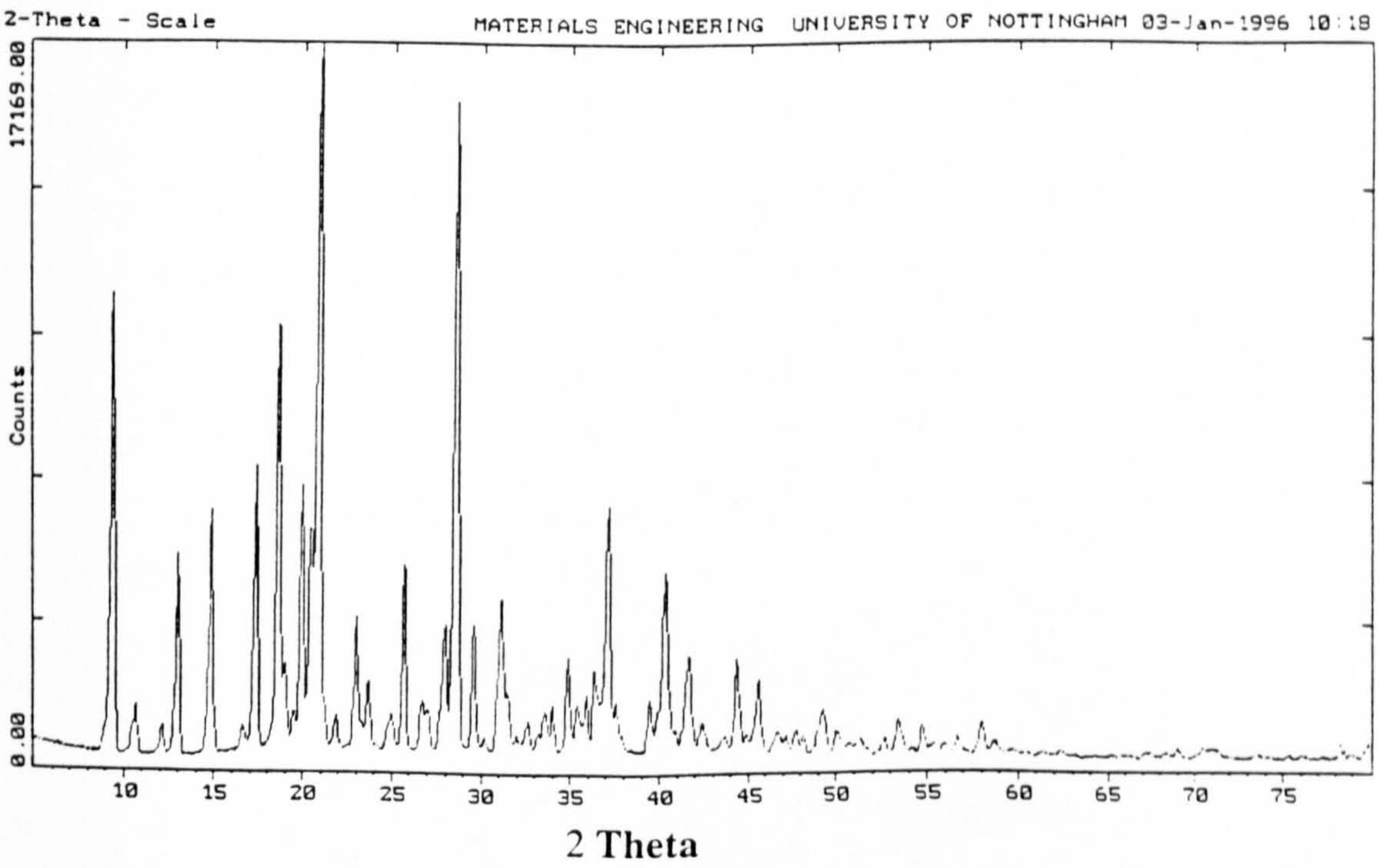

Figure 4.10 X-ray diffraction pattern of batch DC48

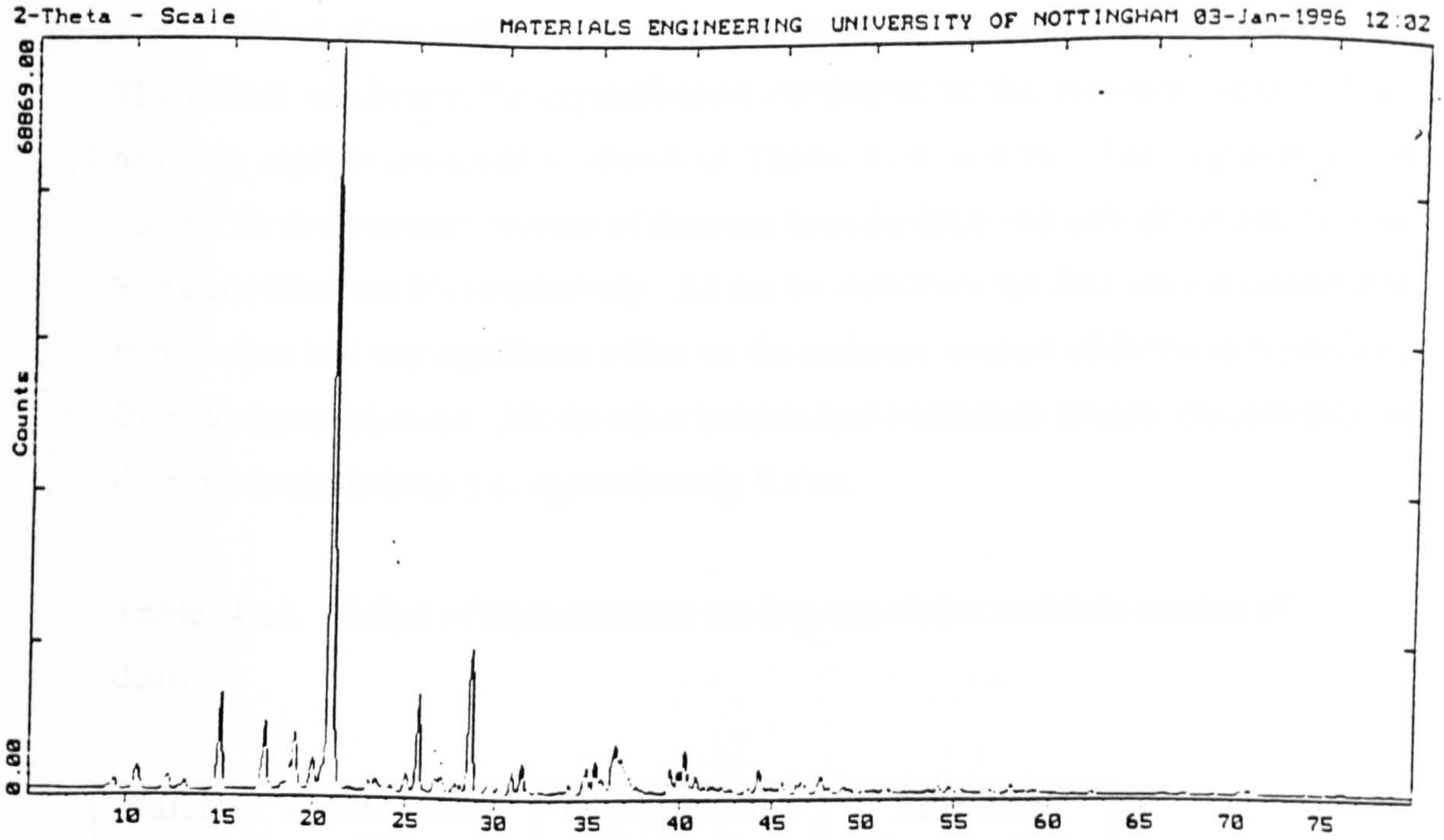

Figure 4.11 X-ray diffraction pattern of batch DC51

4.6 Effect of crystallisation conditions on the moisture content of dextrose

The effects of altering the crystallisation conditions on the moisture content of the dextrose crystals produced is shown in Tables 4.14 to 4.19. The literature values quoted for the moisture content of dextrose monohydrate and anhydrous dextrose are 9.1% and less than 1% respectively. As can be seen from the data, only crystallisation temperature had any significant effect on the moisture content of dextrose crystallised from aqueous solutions. All the other batches had a moisture content characteristic of dextrose monohydrate (i.e. approximately 9.1%).

Table 4.14 Effect of crystallisation cooling rate on the moisture content of dextrose

Batch	Cooling Rate (°C/h)	Crystallisation Time (h)	Moisture Content (%)
D05	0.5	16.0	9.14
D1	1.0	8.0	9.18
D10	10.0	0.8	9.09
D30	30.0	0.27	9.10
D50	50.0	0.16	9.12
DS05*	0.5	16.0	9.11
DS50*	50.0	0.16	9.16

* Initial saturation Ratio S = 1.5. For all other batches S = 1.3.

Table 4.15 Effect of initial supersaturation ratio on the moisture content of dextrose

Batch	Crystallisation Temperature (°C)	Saturation Ratio	Moisture Content (%)
D05	38-30	1.30	9.14
DS05	38-30	1.50	9.11
DR30	38-30	1.60	9.14
D50*	38-30	1.30	9.12
DS50*	38-30	1.50	9.16
DC40	48-40	1.30	8.69
DR40	48-40	1.50	8.63
DC45	53-45	1.30	6.99
DR45	53-45	1.40	5.89
DC51	59-51	1.10	0.61
DR51	59-51	1.30	0.38

* These batches were prepared at a cooling rate of 50°C/h. All other batches were prepared at a cooling rate of 0.5°C/h.

Table 4.16 Effect of crystal growth time on the moisture content of dextrose

Batch	Cooling Rate (°C/h)	Crystallisation Time (h)	Moisture Content (%)
D1	1.0	8.0	9.18
D1T	1.0	16.0	9.11
D30	30.0	0.27	9.10
D30T	30.0	16.0	9.10

Table 4.17 Effect seed crystal particle size on the moisture content of dextrose

Batch	Seed Size (μm)	Moisture Content (%)
D05	<45	9.14
DX05	63-90	9.04

Table 4.18 Effect additives on the moisture contents of dextrose

Batch	Additive	Moisture Content (%)
D05	None	9.14
DLac	Lactose	9.09
DSuc	Sucrose	9.13

From the results presented in Table 4.19 is clear that as the temperature of crystallisation is increased the moisture content decreases from a value of 9.1% which is indicative of dextrose monohydrate to a value of less than 1% which is characteristic of anhydrous dextrose. These results therefore confirm that as the crystallisation temperature is increased towards the temperature/solubility transition point for dextrose at 50°C so the nature of the crystals changes from monohydrate to anhydrous.

Table 4.19 Effect of crystallisation temperature on the moisture content of dextrose

Batch	Crystallisation Temp' (°C)	Saturation Ratio	Moisture Content (%)
D05	38-30	1.30	9.14
DC40	48-40	1.30	8.69
DC45	53-45	1.30	6.99
DC48	56-48	1.30	4.73
DC51	59-51	1.30	0.38
DR30	38-30	1.60	9.14
DR40	48-40	1.50	7.93
DR45	53-45	1.40	5.89
DC48	56-48	1.30	4.73
DR51	59-51	1.10	0.61

4.7 Effect of crystallisation conditions on the particle size of dextrose

The following sections present the data obtained from the particle size analysis testing as detailed in section 3.3.1. The cumulative percentage graphs were used to determine the mass median diameter (MMD) while the bar charts give a better appreciation of the changes in the size distribution.

4.7.1 Effect of crystallisation cooling rate

From Figure 4.12 it can be seen that as the crystallisation cooling rate is steadily increased from 0.5 to 50.0°C/h for the series of batches D05, D1, D10, D30 and D50 the particle size decreases, with the mass median diameter dropping from 114 to 82 μm. From Figure 4.13 it can also be seen that increasing the crystallisation rate causes the size distribution to progressively become more evenly distributed and become skewed towards the lower size range. A similar but less dramatic, effect was also observed for the two batches DS05 and DS50 prepared at crystallisation cooling rates of 0.5 and 50°C/h respectively.

The changes in particle size and size distribution are due to the reduction in time for crystal growth arising from the increased cooling rates. Since the crystals had less time to grow, there are thus a greater number of crystals existing at the smaller sizes.

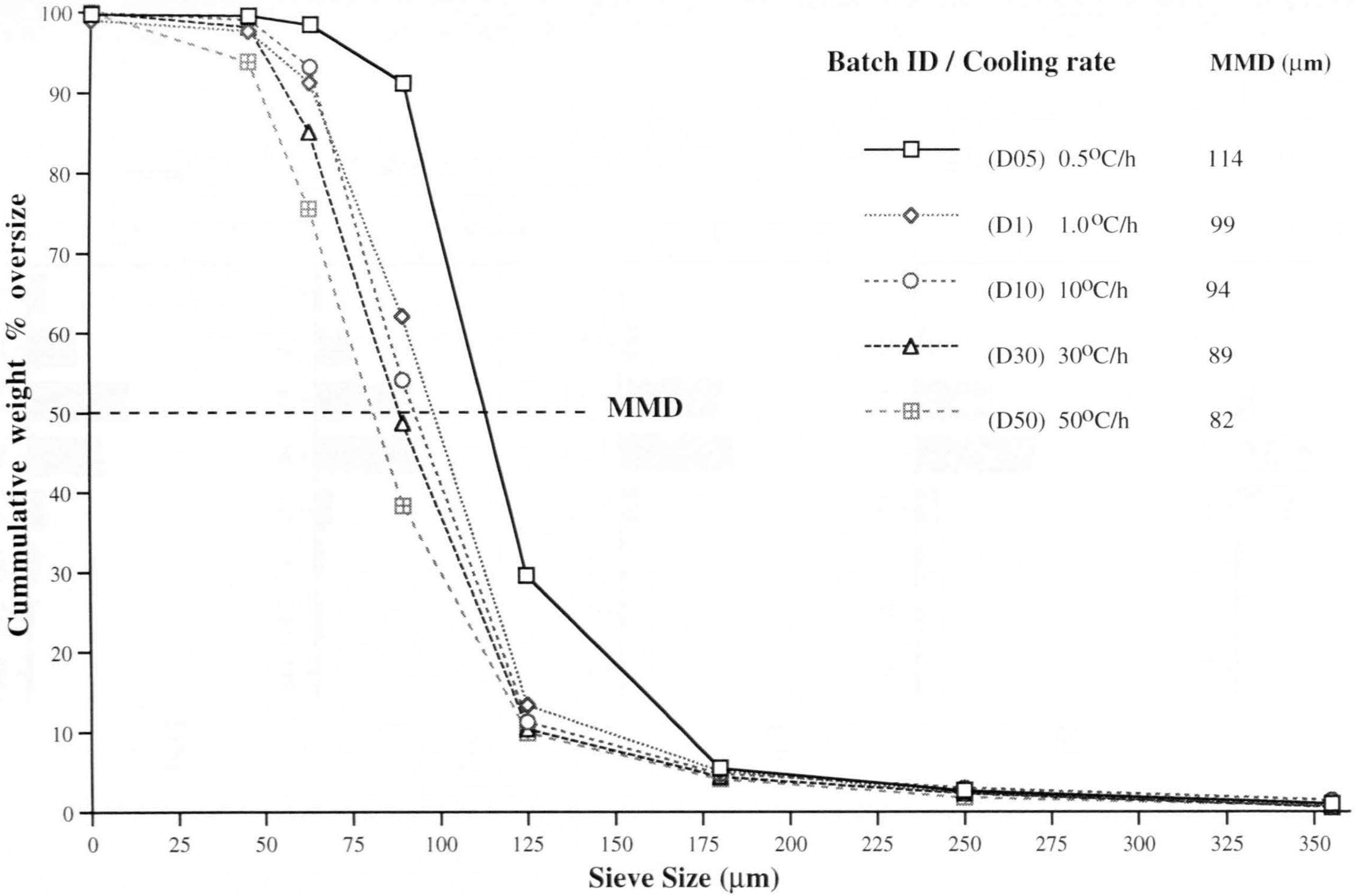

Figure 4.12 Effect of crystallisation cooling rate on the particle size distribution and mass median diameter (MMD) of dextrose

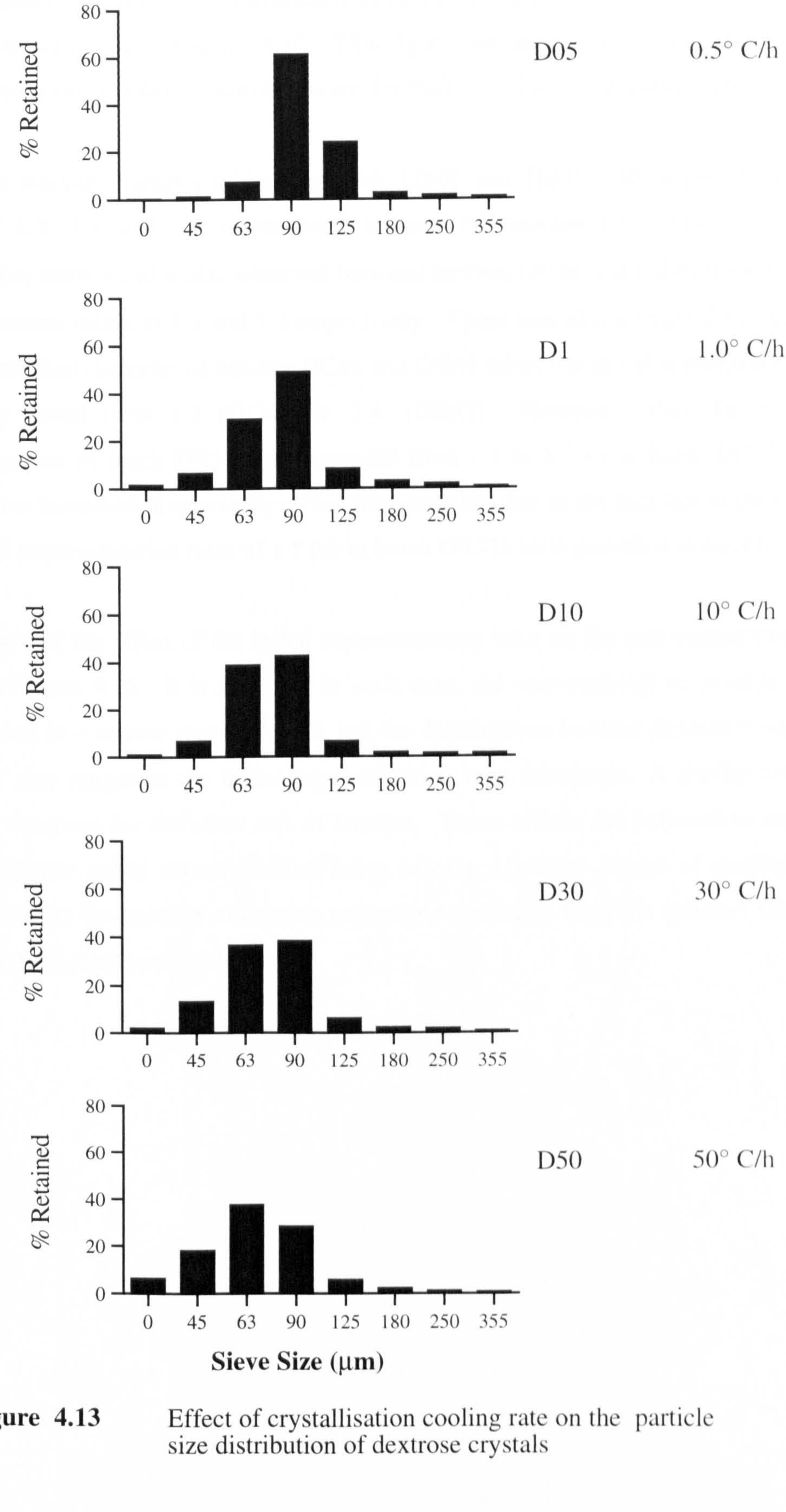

Figure 4.13 Effect of crystallisation cooling rate on the particle size distribution of dextrose crystals

4.7.2 Effect of initial supersaturation ratio

The influence of initial supersaturation ratio on the particle size of crystallised dextrose is presented in Figures 4.14. This figure compares several sets of batches crystallised under similar conditions except for their initial supersaturation ratios.

The mass median diameter of batches D05, DS05 and DR30 with supersaturation ratios of 1.3, 1.5 and 1.6 respectively is seen to decrease from 114 to 87 to 84 μm. The same trend is also observed between batches DC40 and DR40 with initial supersaturation ratios of 1.3 and 1.5 respectively. There was also a slight decrease in the mass median diameter of batches DC45 and DR45 when the initial supersaturation ratio was raised from 1.3 (DC45) to 1.4. (DR45) However, when the initial supersaturation of batch DR51 was increased from 1.1 to 1.3 as in batch DC51 the particle size increased dramatically. This was probably due to the fact that at the very low initial supersaturation ratio of 1.1 (as in batch DR51) little growth was possible.

An example of the effect of the initial supersaturation ratio on the size distribution is shown in Figure 4.15. It is seen that in each case, the vast majority of crystals are concentrated in a narrow range of sizes, but the distributions become skewed towards the lower size ranges as the initial supersaturation ratio increases. A similar effect was also observed for the other sets of batches. These effects are believed to result from the higher initial supersaturation ratios causing a greater degree of nucleation which increases the number of crystals competing for solute from the solution which in turn leads to smaller crystals.

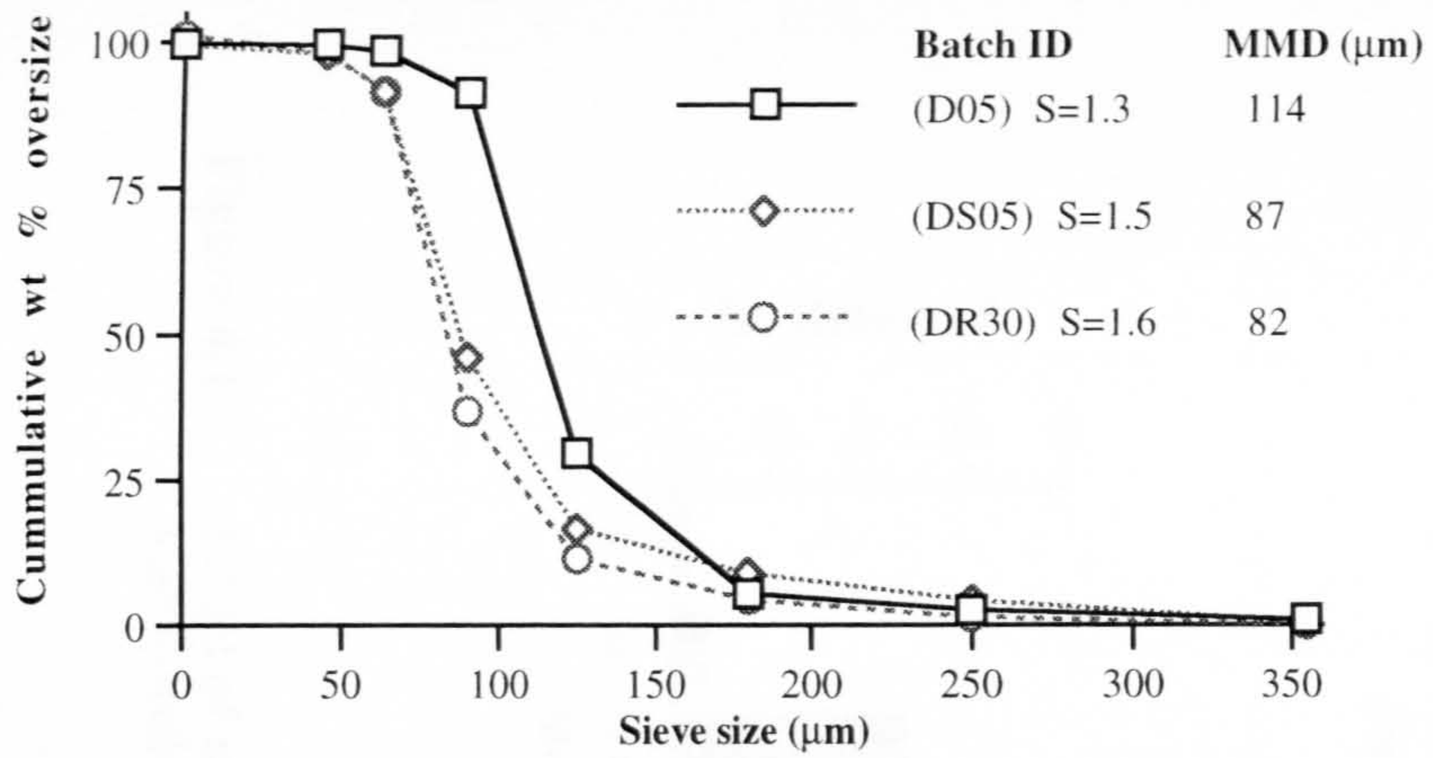

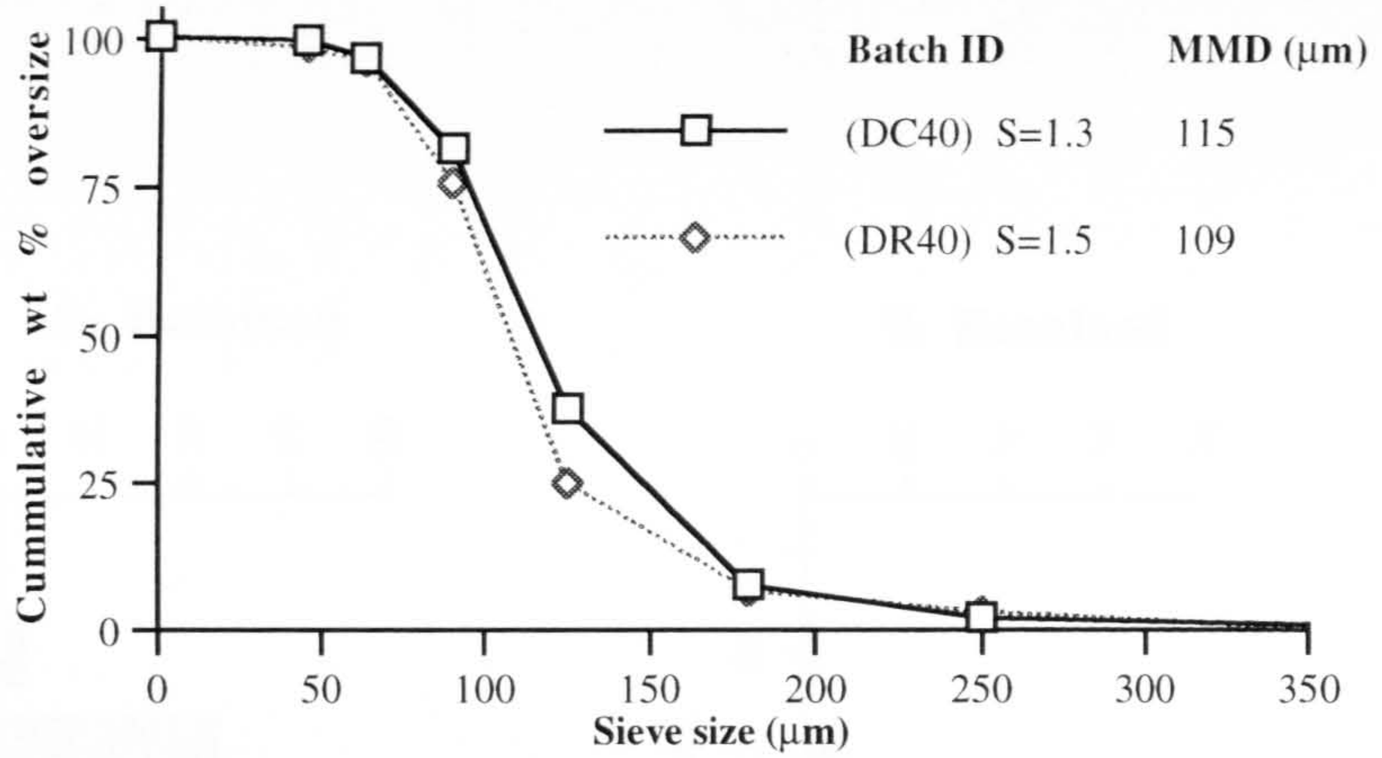

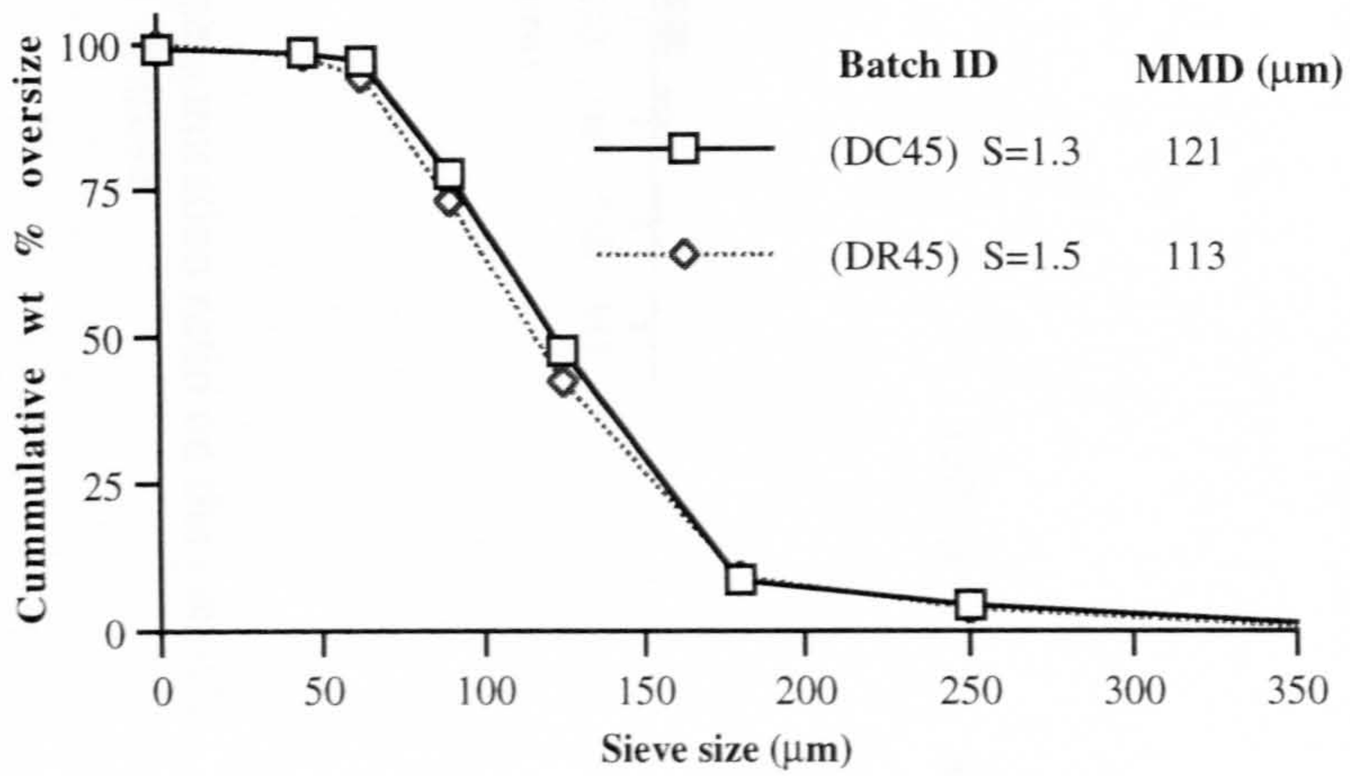

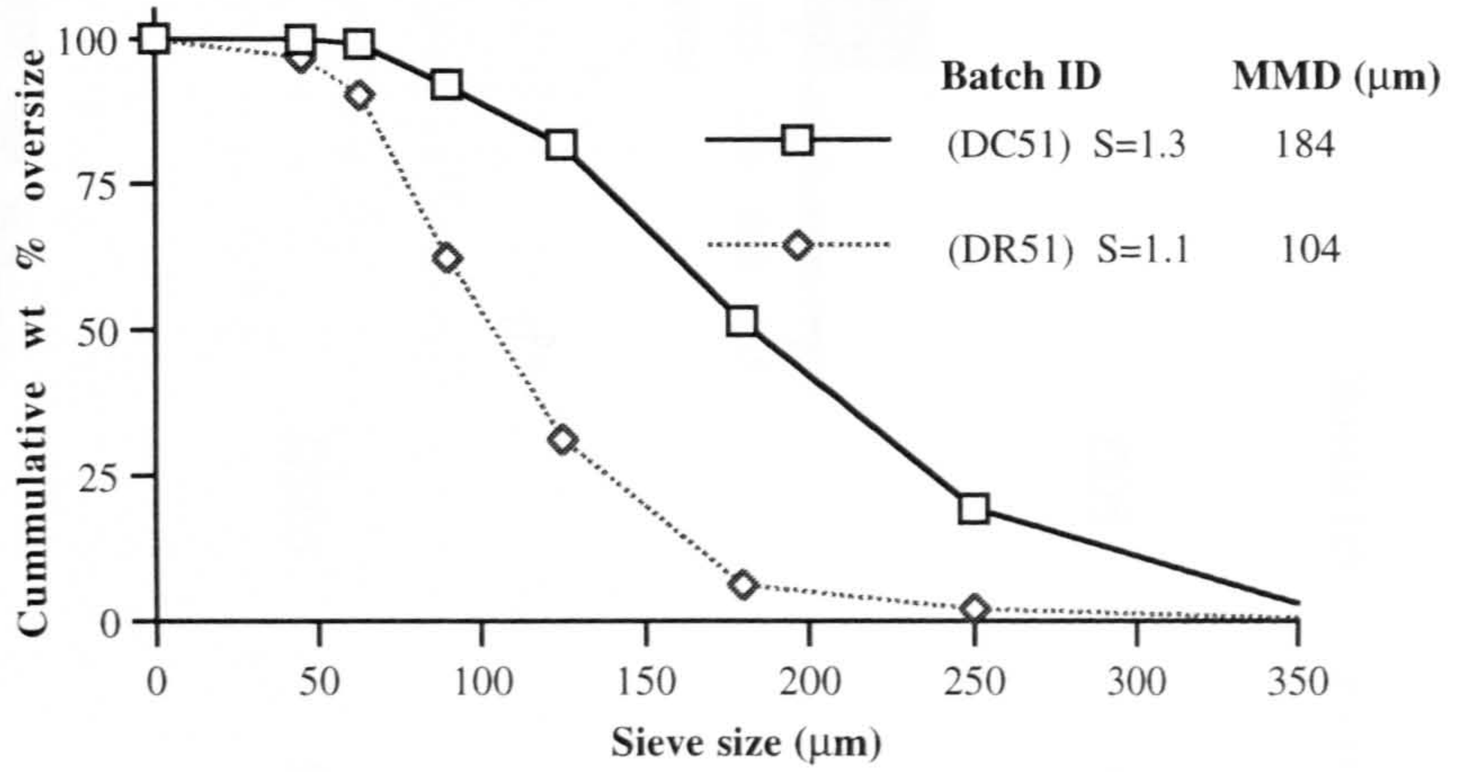

Figure 4.14 Effect of initial supersaturation ratio on the particle size distribution and mass median diameter (MMD) of dextrose

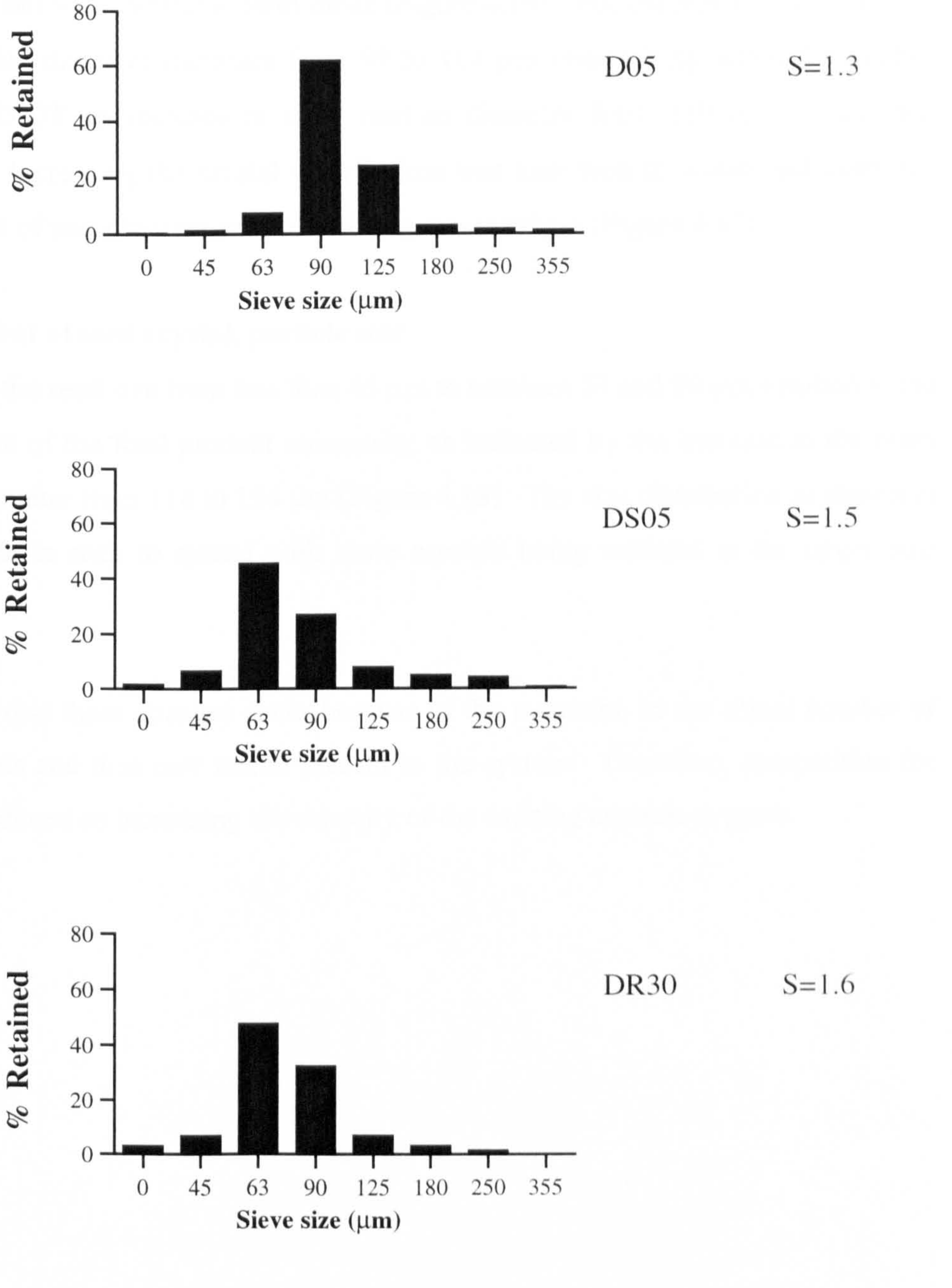

Figure 4.15 Effect of initial supersaturation ratio on the particle size distribution of dexrose

4.7.3 Effect of crystal growth time

Not surprisingly as the growth time is extended the particle size of the material increases relative to the corresponding batch which was prepared under similar conditions but with shorter growth times (Figure 4.16). For batches D1 and D1T the mass median diameter increases from 99 to 104 μm respectively while for batches D30 and D30T an increase in mass median diameter from 119 to 127 μm was observed. Increasing the crystal growth time was also seen to widen and skew the distribution of particle sizes towards the larger size ranges (Figure 4.17).

4.7.4 Effect of seed crystal, particle size

Increasing the seed size from less than 45 μm to between 63 and 90 μm resulted in the particle size of the final product increasing, as indicated by the increase in the mass median diameter from 114 to 134 μm (Figure 4.18). The size distribution as shown in Figure 4.19, is seen to spread with more crystals being retained at the larger size ranges.

It is likely that these changes occur because of the reduction in the actual number of seed crystals and thus new nuclei present in the system. Therefore, competition for solute is reduced so increasing the capacity of the existing crystals to grow.

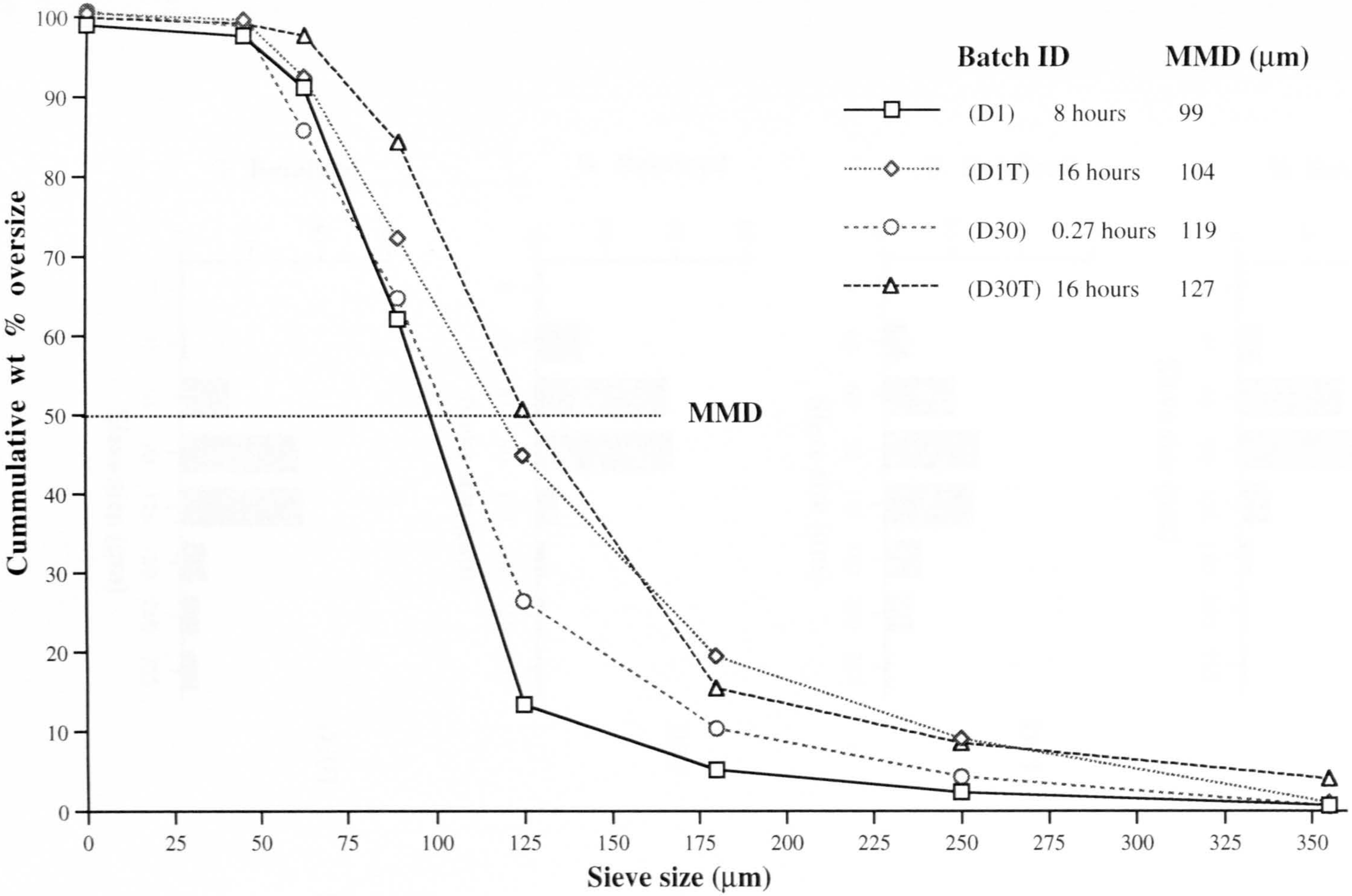

Figure 4.16 Effect of crystal growth time on the partticle size distribution and mass median diameter (MMD) of dextrose

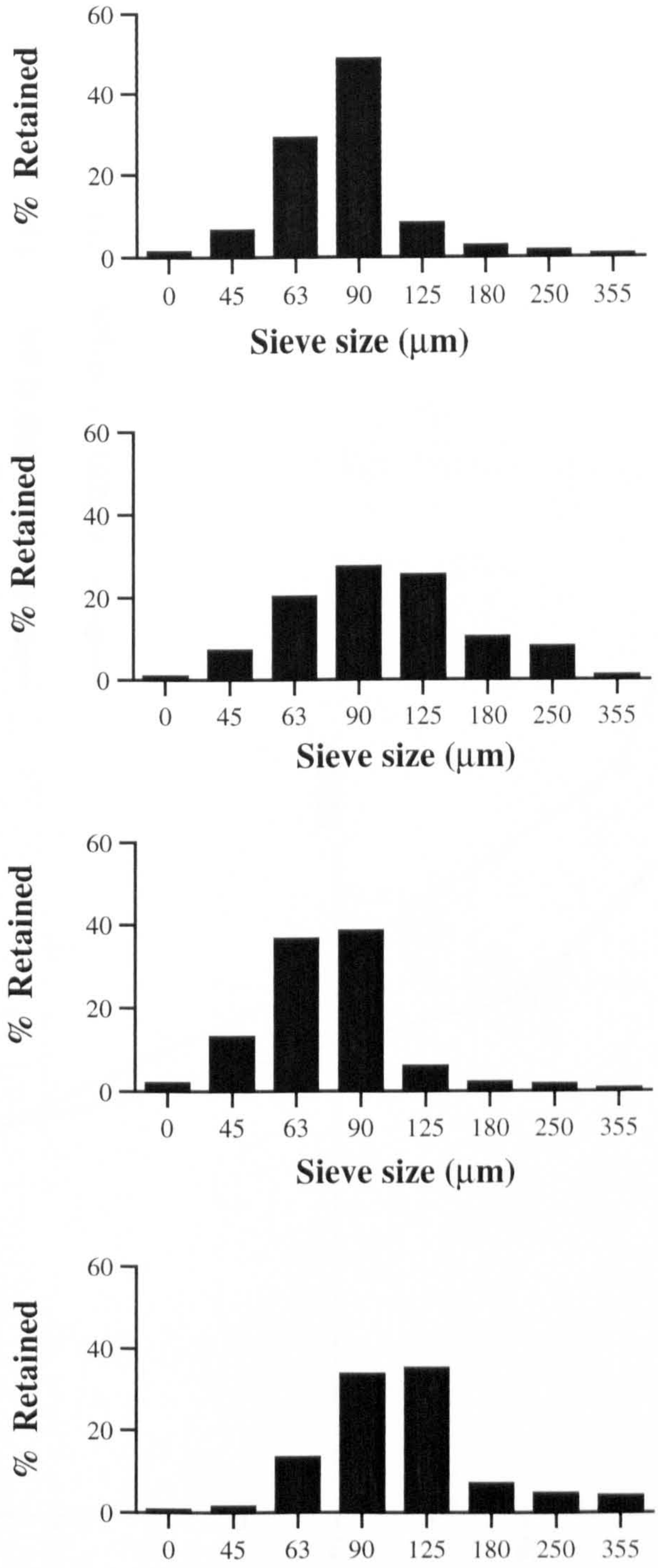

Figure 4.17 Effect of crystal growth times on the particle size distribution of dextrose

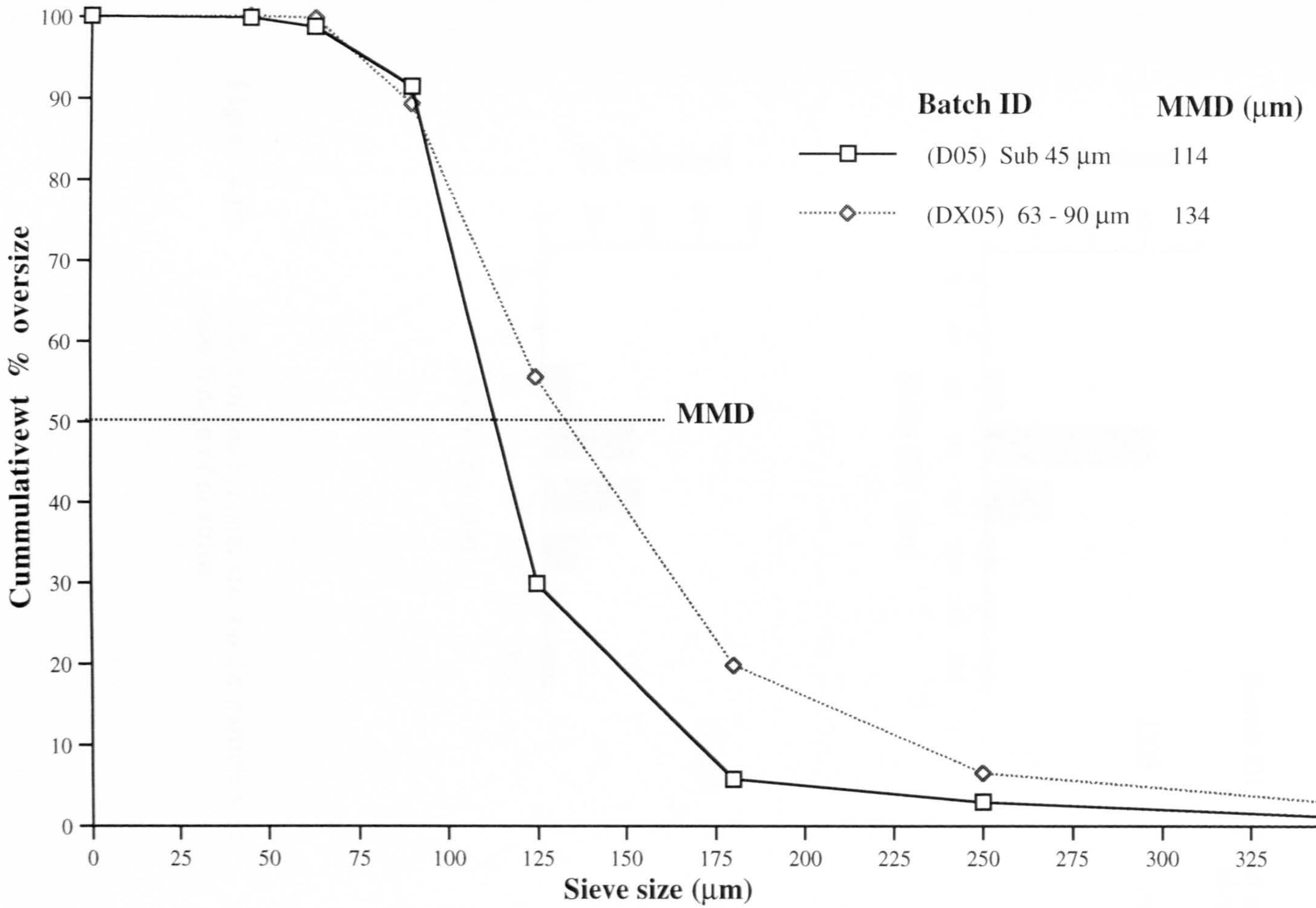

Figure 4.18 Effect of seed crystal size on the particle size distribution and mass median diameter (MMD) of dextrose

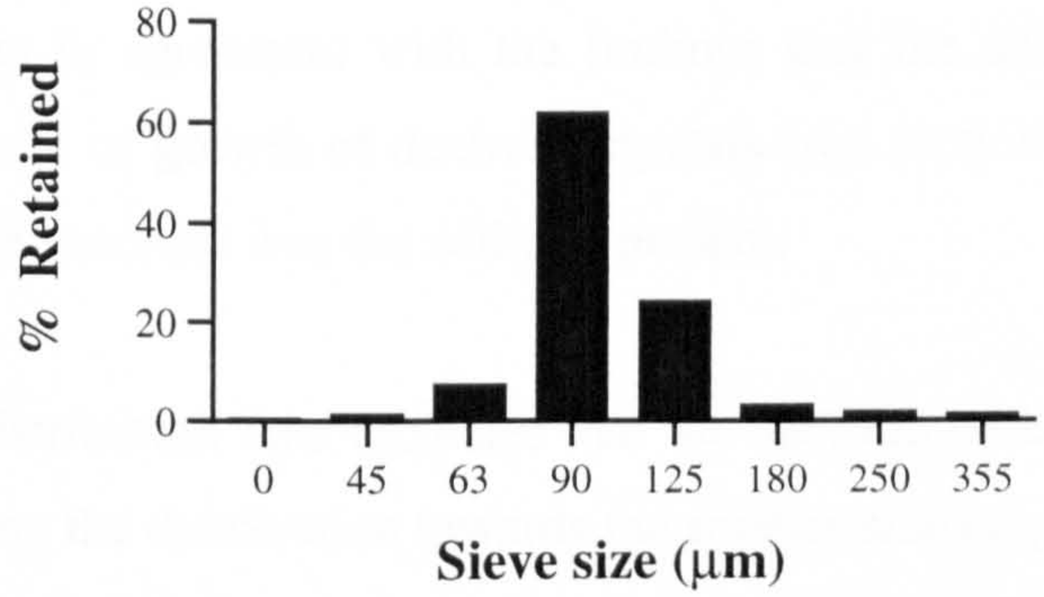

Batch ID	Seed particle size
D05	Sub 45 μm
DX05	63-90 μm

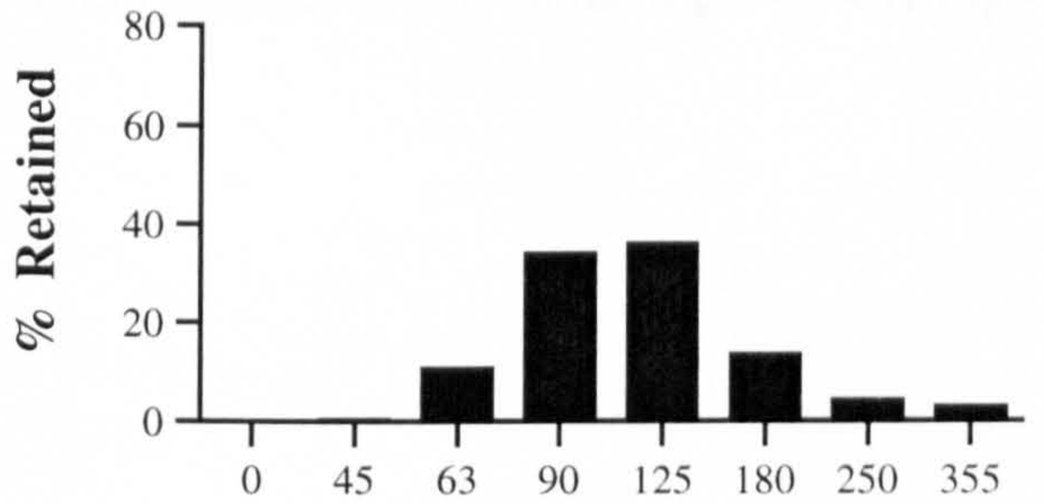

Figure 4.19 Effect of seed crystal size on the particle size distribution of dextrose

4.7.5 Effect of additives

Compared with batch D05 (crystallised without the presence of additives), the particle size of the crystals is seen to decrease when either lactose (batch Dlac) or sucrose (batch Dsuc) are added to the system (Figure 4.20). Adding lactose reduces the mass median diameter from 114 μm to 100 μm while adding sucrose reduced it to 87 μm. This data is in agreement with the findings that the addition of lactose or sucrose slows the rate of growth of dextrose crystals (see section 1.7.2) with a greater effect evident when sucrose was the additive present.

The size distribution data indicates that the addition of lactose had little effect other than skewing the distribution towards the smaller size ranges with most of the crystals being concentrated in only two size ranges (Figure 4.21). The addition of sucrose however markedly changed the shape of the size distribution graph which is probably a reflection of the changes in crystal habit previously reported (section 4.3).

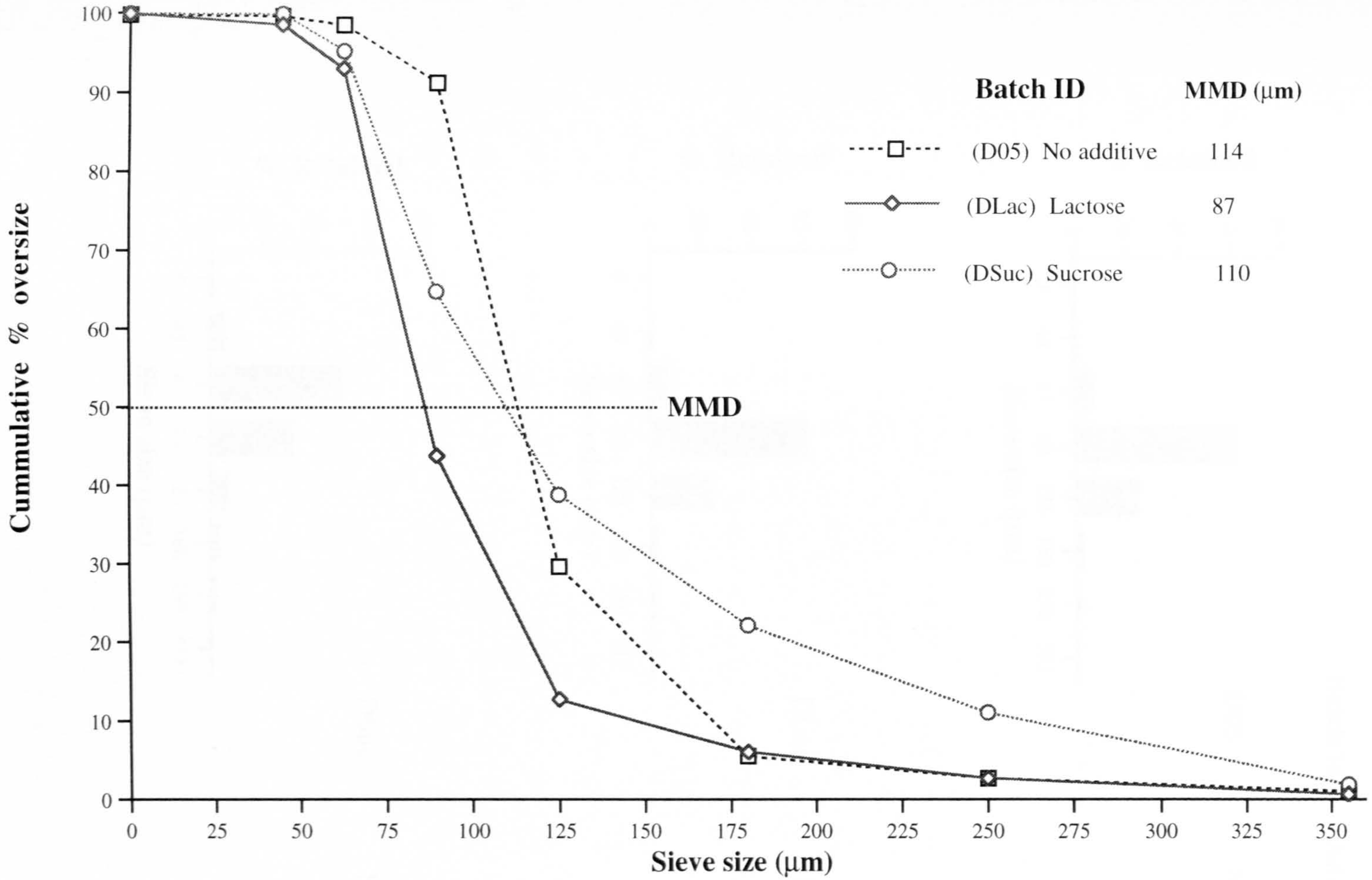

Figure 4.20 Effect of additives on the particle size distribution and mass median diameter (MMD) of dextrose

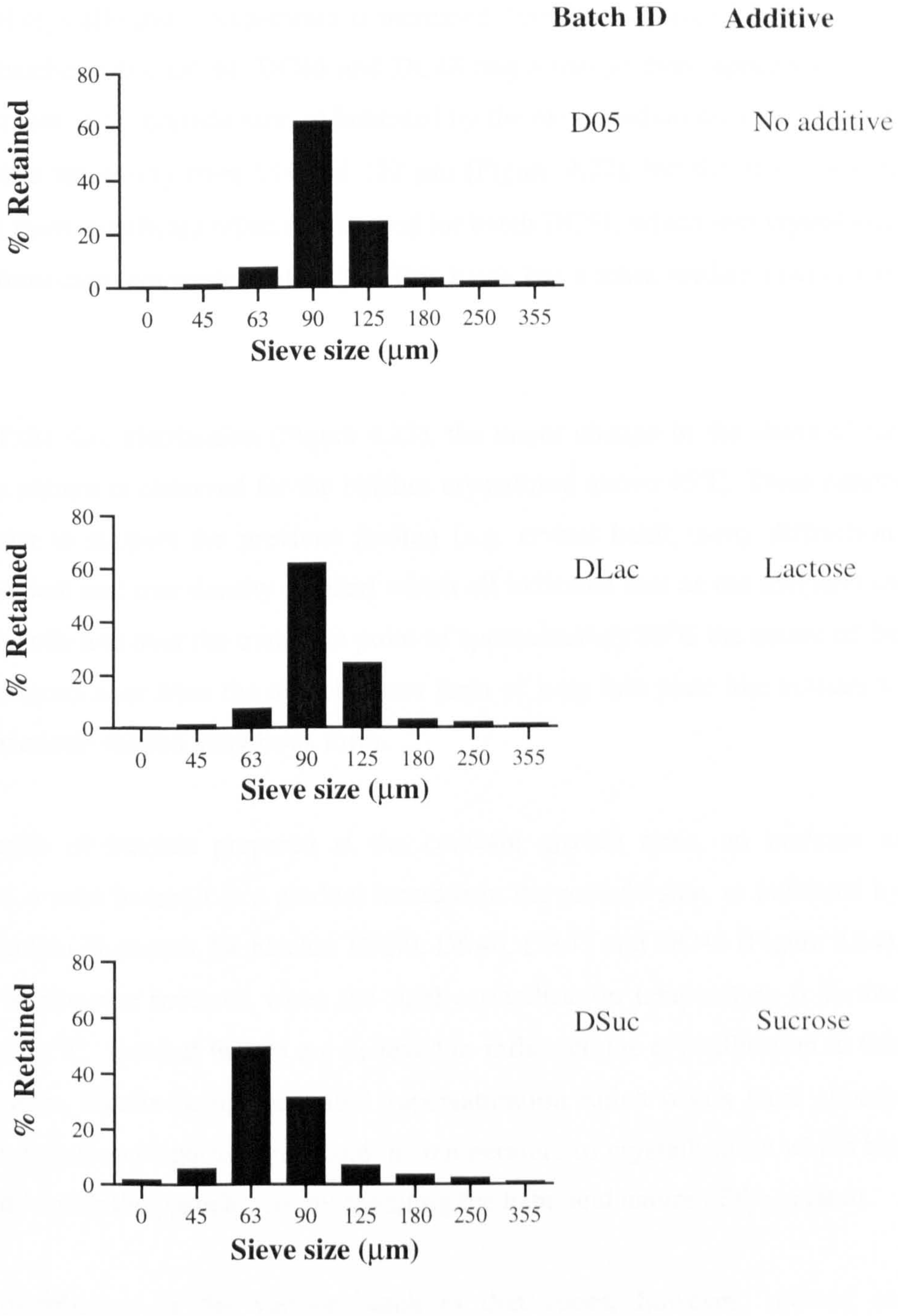

Figure 4.21 Effect of additives on the particle size distribution of dextrose

4.7.6 Effect of crystallisation temperature

Consider firstly, the batches prepared with the constant supersaturation ratio of 1.3. As the final crystallisation temperature is increased through the range 30, 40, 45 and 48°C (for batches D05, DC40, DC45 and DC48 respectively) there appears to be a general increase in the particle size, as indicated by the mass median diameter (MMD) of the crystals increasing from 114 and 122 μm (Figure 4.22), but the effect is very small. The most significant effect is observed for batch DC51, which was crystallised above the transition temperature of 50°C. This batch has a mass median diameter of 184 μm.

In terms of the size distribution (Figure 4.23), the major change in the shape of the distribution pattern is observed for the batches crystallised above 45°C. These results would appear to support the previous finding (e.g. crystal habit, x-ray diffraction, moisture content and true density studies) which all indicated that as the temperature is raised towards and over the transition point of approximately 50°C the nature of the crystals produced alter from the monohydrate form of long thin plate like crystals to the more prismatic shaped anhydrous form.

For the series of batches prepared at the constant growth rates, an increase in temperature is seen to result in a gradual increase in the particle size, as indicated by the mass median diameters for batches DR30, DR40, DR45 and DC48 (Figure 4.24). The trend is however reversed when the final crystallisation temperature is further increased to 51°C. Several factors are believed to influence the crystallisation in this series, the main factors being the initial supersaturation ratios which have already been shown to influence particle size, and the temperature of crystallisation which has been shown to alter the particle size by changing the habit and nature of the crystals.

The size distribution of the various batch in this series, however, showed no significant change in their basic shape but became more widely distributed as the temperature was increased (Figure 4.25).

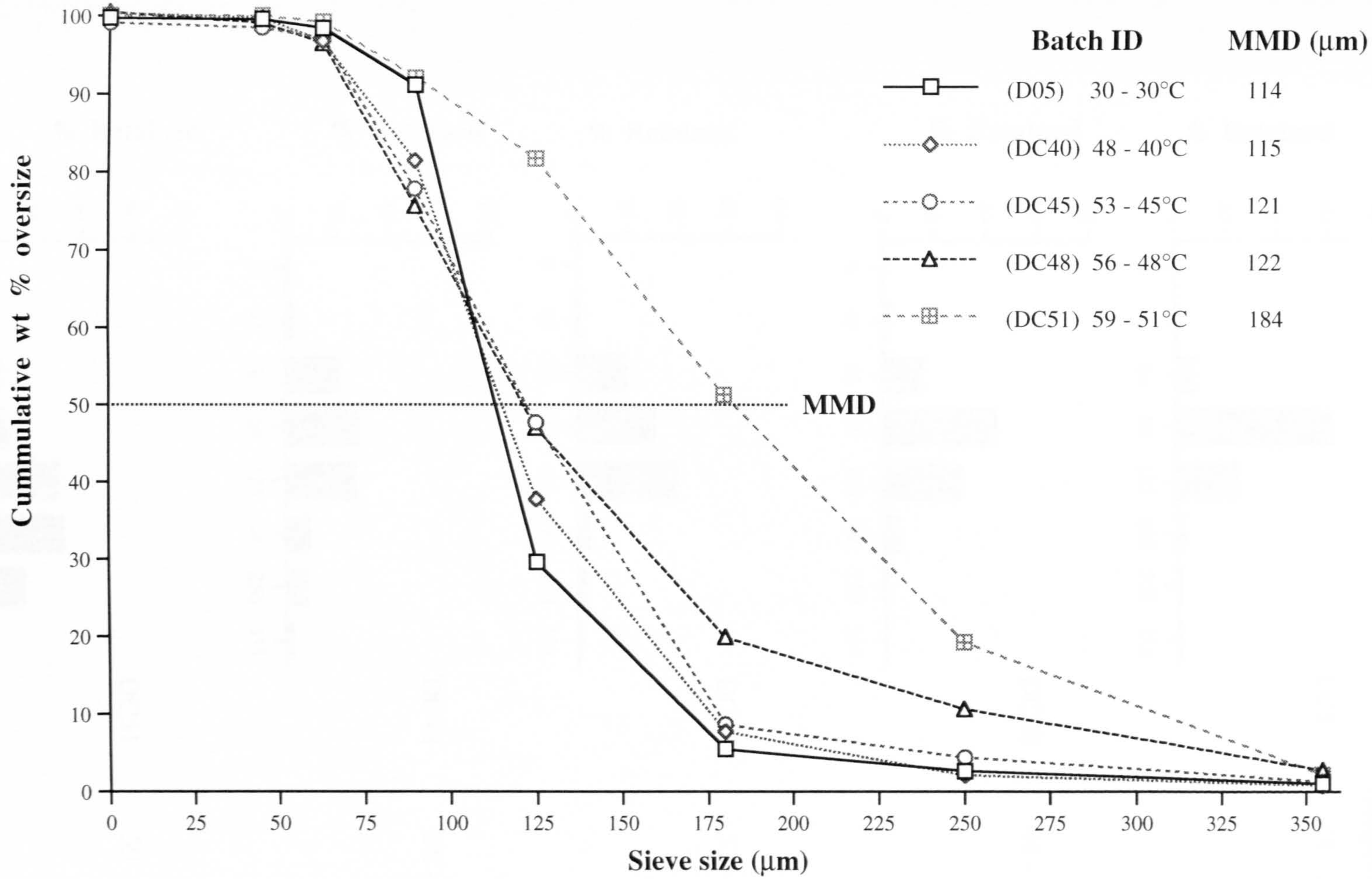

Figure 4.22 Effect of crystallisation temperature on the particle size distribution and mass median diameter (MMD) of dextrose (constant initial supersaturation ratio of S = 1.3)

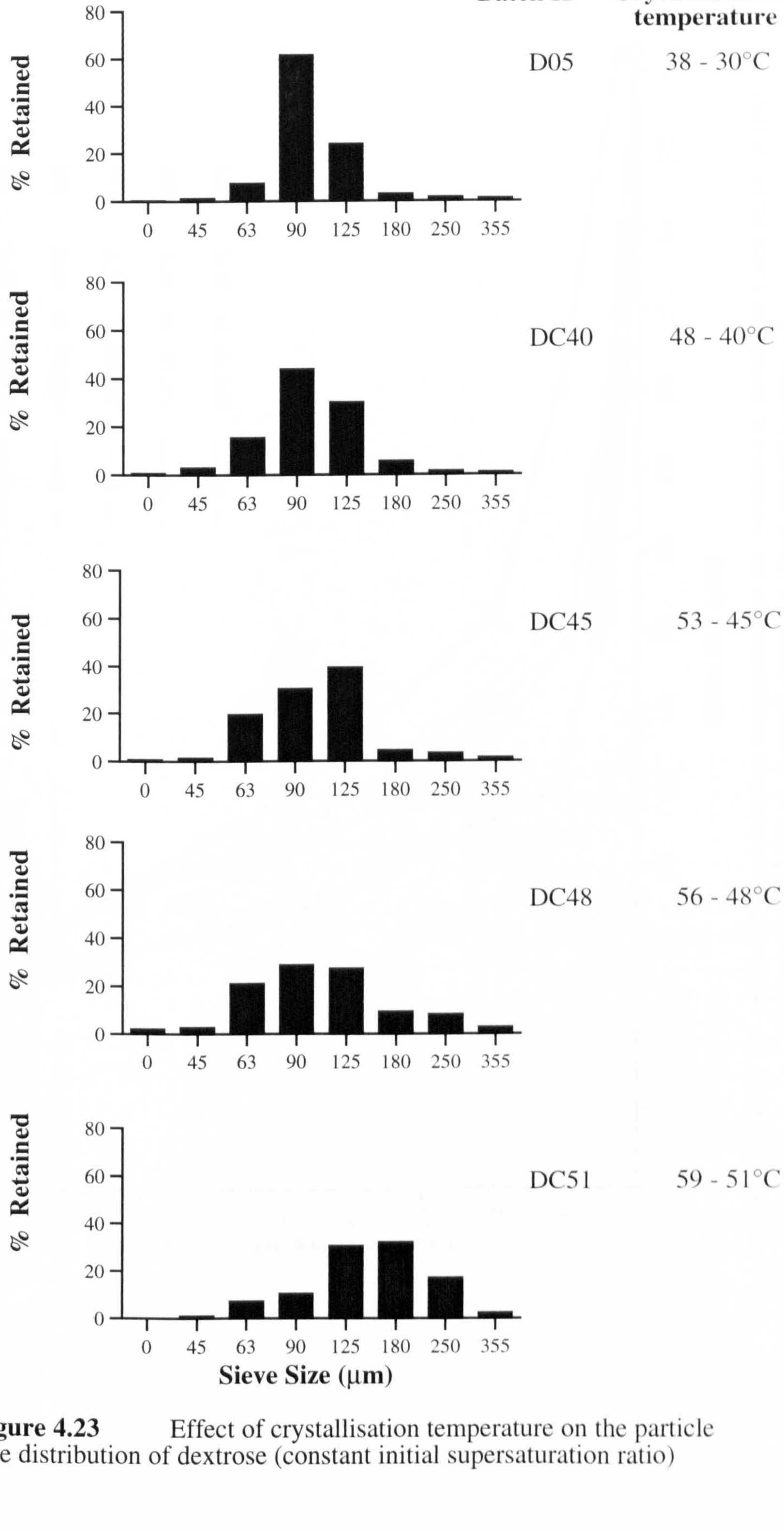

Figure 4.23 Effect of crystallisation temperature on the particle size distribution of dextrose (constant initial supersaturation ratio)

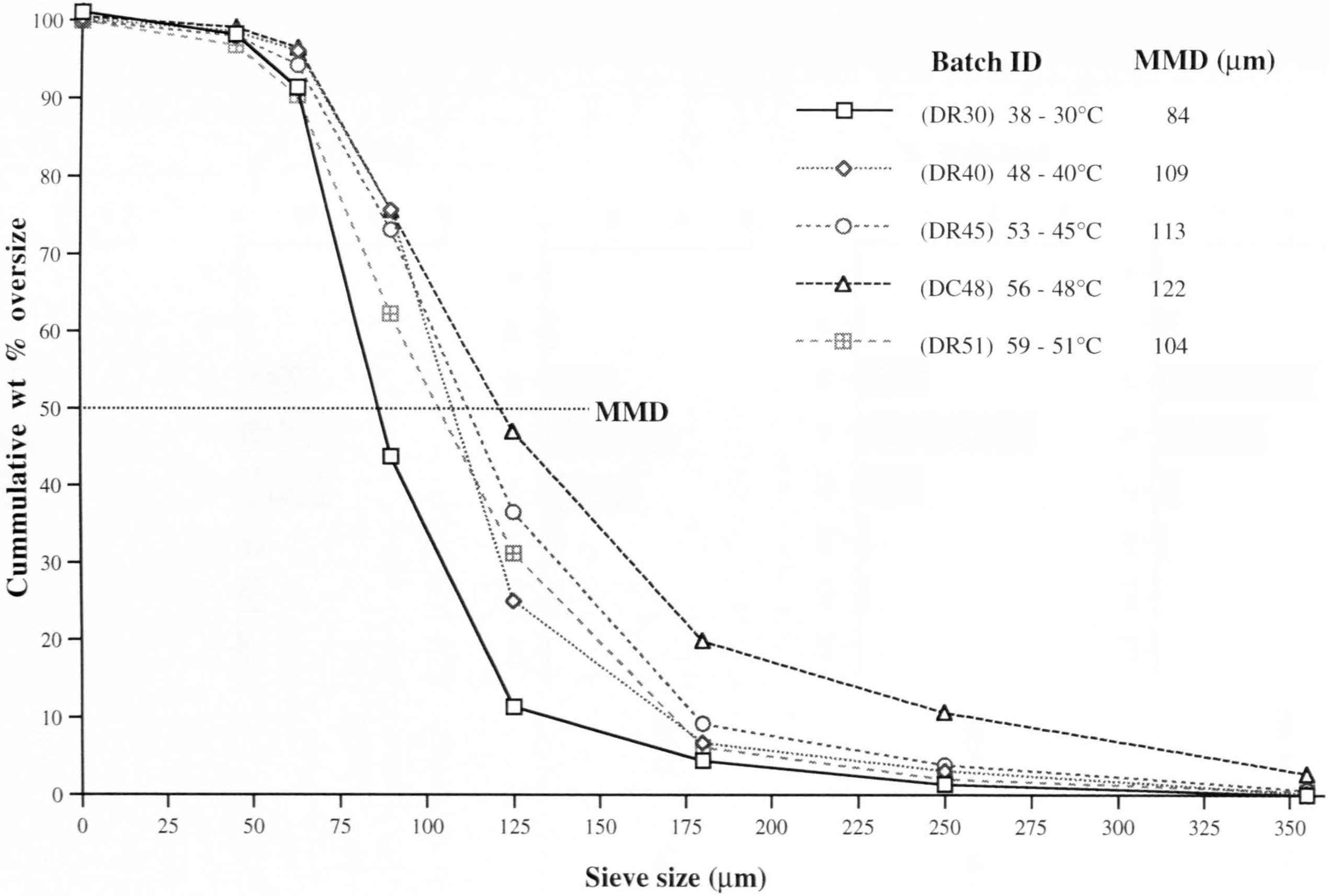

Figure 4.24 Effect of crystallisation temperature on the particle size distribution and mass median diameter (MMD) of dextrose (constant linear crystal growth rate)

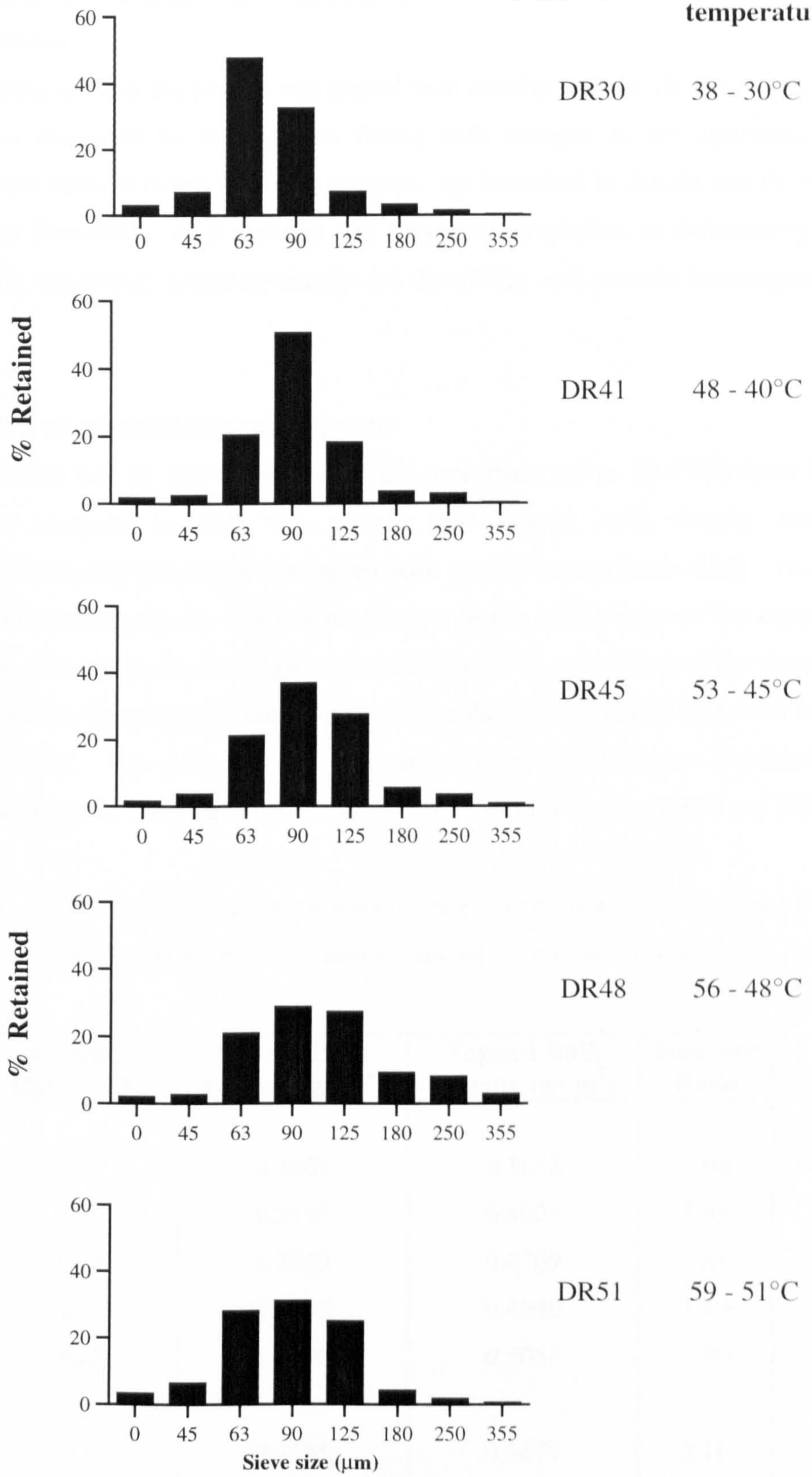

Figure 4.25 Effect of crystallisation temperature on the particle size distribution of dextrose (constant linear crystal growth rate)

4.8 Effect of crystallisation conditions on the bulk density and flowability of dextrose

The variability of both the poured and tapped bulk density and the flowability of the material (as measured by the Hausner Ratio) with changes in the crystallisation conditions are detailed in the following sections. As described in chapter one the bulk density and flowability of a material are important properties in determining its compression behaviour, affecting mainly the die filling and particle rearrangement stages.

4.8.1 Effect of crystallisation cooling rate

The data shows that by increasing the cooling rate from 0.5 to 50.0°C/h there is a progressive increase in both the poured and tapped bulk density values (with the effect being greater for the tapped bulk density value (Table 4.20). This is believed to be principally an effect of the change in the particle size of the crystals. These changes in the poured and tapped densities result in a lowering of the Hausner Ratio (increasing flowability) from 1.96 to 1.70 as the cooling rate is increased from 0.5 to 50.0°C/h. However even the lowest value of 1.7 indicates a cohesive, non-flowing material. The same trend was also observed for batches DS05 and DS50.

Table 4.20 Effect of crystallisation cooling rate on the poured and tapped bulk density values and the Hausner ratio of crystallised dextrose

Batch	Cooling Rate (°C/h)	Poured Bulk Density (g/cm^3)	Tapped Bulk Density (g/cm^3)	Hausner Ratio
D05	0.5	0.1863	0.3658	1.96
D1	1.0	0.2135	0.4025	1.88
D10	10.0	0.2629	0.4769	1.81
D30	30.0	0.2757	0.4949	1.79
D50	50.0	0.2970	0.5057	1.70
DS05	0.5	0.1796	0.3677	2.10
DS50	50.0	0.1861	0.3685	1.98

* Initial supersaturation ratio S = 1.5. In all other batches S = 1.3.

4.8.2 Effect of initial supersaturation ratio

Table 4.21 illustrates the influence of the initial supersaturation ratio on the poured and tapped bulk density values and the flowability of dextrose.

It is seen that an increase in the initial supersaturation ratio results in a lowering of the poured bulk density and an increase in the tapped bulk density. Consider for example batches D05, DS05 and DR30. As the initial supersaturation ratio is raised from 1.3 to 1.5 to 1.6, the poured bulk density decreases from 0.1863 to 0.1796 to 0.1757 g/cm^3 and the tapped bulk density increases from 0.3658 to 0.3477 to 0.3848 g/cm^3. This increasing gap between the poured and tapped density as the initial supersaturation ratio is increased results in an increased Hausner ratio. These effects are again thought to be mainly a result of changes in the particle size of the crystals produced. As the initial supersaturation ratio is increased, both the particle size and possibly the length to width ratio of the crystals were observed to decrease. The decrease in flowability with increasing supersaturation ratio may also indicate changes in the surface properties of the crystals, with rougher crystal faces resulting from the increased growth rates observed with higher levels of supersaturation.

4.8.3 Effect of crystal growth time

The effect of increasing the overall growth time of the crystals on the bulk densities and flowability of dextrose is show in Table 4.22. It was found that for both batches examined increasing the crystal growth time had no significant effect on the either the bulk densities or the flowability of the crystalline dextrose produced. This result is surprising as increasing the growth time caused a significant change in the particle size of the crystals. For all batches the relatively high Hausner Ratios (> 1.8) indicate cohesive materials with no inherent flow properties.

Table 4.21 Effect of initial supersaturation ratio on the poured and tapped density values and the Hausner ratio of crystallised dextrose

Batch	Saturation Ratio	Poured Bulk Density (g/cm^3)	Tapped Bulk Density (g/cm^3)	Hausner Ratio
D05	1.30	0.1863	0.3658	1.96
DS05	1.50	0.1796	0.3677	2.10
DR30	1.60	0.1757	0.3848	2.19
D50	1.30	0.2970	0.5057	1.70
DS50	1.50	0.1861	0.3685	1.98
DC40	1.30	0.2121	0.3824	1.80
DR40	1.50	0.2038	0.3961	1.94
DC45	1.30	0.2424	0.4245	1.75
DR45	1.40	0.2445	0.4328	1.77
DR51	1.10	0.4294	0.5926	1.38
DC51	1.30	0.5555	0.7402	1.30

* These batches were prepared at a cooling rate of 50°C/h. All other batches were prepared at a cooling rate of 0.5°C/h.

Figure 4.22 Effect of crystallisation growth time on the poured and tapped density values and the Hausner ratio of crystallised dextrose

Batch	Crystallisation Time (h)	Poured Bulk Density (g/cm^3)	Tapped Bulk Density (g/cm^3)	Hausner Ratio
D1	8.00	0.2135	0.4025	1.88
D1T	16.00	0.2139	0.4064	1.90
D30	0.27	0.2757	0.4949	1.79
D30T	16.00	0.2699	0.4885	1.81

4.8.4 Effect of seed crystal, particle size

The results shown in Table 4.23 represent the effect of altering the size of the seed crystals on the bulk densities and flowability of dextrose.

Change the seed size from less than 45 μm to between 63 and 90 μm resulted in the poured bulk density increasing from 0.1863 to 0.3471 g/cm^3 and the tapped bulk density increasing from 0.3658 to 0.4663 g/cm^3. These changes are again a result of the change in the particle size and size distribution of the crystals. The Hausner ratio was also significantly altered decreasing from 1.96 indicating a very cohesive material to 1.34 indicates a material with an acceptable degree of flow.

Figure 4.23 Effect of seed crystal, particle size on the poured and tapped bulk density values and the Hausner ratio of crystallised dextrose

Batch	Seed Size (μm)	Poured Density (g/cm^3)	Tapped Density (g/cm^3)	Hausner Ratio
D05	< 45	0.1863	0.3658	1.96
DX05	63-90	0.3471	0.4663	1.34

4.8.5 Effect of additives

The effect of including small amounts (2.5% w/w) of two other carbohydrates (lactose and sucrose) in the supersaturated solutions of dextrose on the bulk densities and flowability of the crystals produced is detailed in Table 4.24. Comparing the results with those for batch D05 which was crystallised under identical conditions but with no additives it is clear that inclusion of either lactose or sucrose causes an increase in both the poured and tapped bulk density values of crystallised dextrose. The larger increase being observed when the additive was sucrose. This effect cannot be attributed simply to changes in particle size and size distribution, as inclusion of lactose caused the particle size to decrease while the inclusion of sucrose caused the particle size to increase. This supports the previous findings that inclusion of either additive resulted in change to crystal habits (Figures 4.3 and 4.4).

Table 4.24 Effect of additives on the poured and tapped bulk density values and the Hausner ratio of crystallised dextrose

Batch	Poured Density (g/cm^3)	Tapped Density (g/cm^3)	Hausner Ratio
D05	0.1863	0.3658	1.96
DLac	0.2128	0.4084	1.92
DSuc	0.2990	0.5050	1.69

4.8.6 Effect of crystallisation temperature

The influence of crystallisation temperature on the poured and tapped bulk density values and the Hausner ratio of dextrose are shown in Table 4.25.

In both sets of batches (i.e. those with constant initial supersaturation ratios of 1.3 and those with the constant linear growth rate) an increase in the crystallisation temperature resulted in a raising of both the poured bulk density and the tapped bulk density. It also caused a gradual lowering of the Hausner ratio (indicating an increase in flowability), ranging from 1.96 for batch D05 representing a very cohesive material to a value of 1.30 for batch DC51 which is typical of a free flowing material.

The major mechanism by which crystallisation temperature influences these parameters is by the effect it has on the crystal habit of dextrose, changing it from the long needle-shape habit of dextrose monohydrate as seen for batch D05 in Figure 4.1 to the more prismatic habit of anhydrous dextrose, as illustrated in Figure 4.4 for batch DR51.

Table 4.25 Effect of crystallisation temperature on the poured and tapped bulk density values and the Hausner ratio of crystallised dextrose

Batch	Poured Bulk Density (g/cm^3)	Tapped Bulk Density (g/cm^3)	Hausner Ratio
D05	0.1863	0.3658	1.96
DC40	0.2121	0.3824	1.80
DC45	0.2424	0.4245	1.75
DC48	0.3833	0.5639	1.47
DC51	0.5555	0.7402	1.30
DR30	0.1757	0.3848	2.19
DR40	0.2038	0.3961	1.94
DR45	0.2445	0.4328	1.77
DC48	0.3833	0.5639	1.47
DR51	0.4294	0.0.5926	1.38

4.9 Concluding discussion

The data presented in this chapter clearly demonstrate the ability of the crystallisation process to modify a wide range of physicochemical properties of dextrose. It therefore illustrates the need for careful control of crystallisation process variables if consistent and reproducible excipients are to be obtained both from lot to lot and from source to source. It also demonstrates the potential of crystallisation as a tool for deliberately modifying material properties with the aim of optimising behaviour during pharmaceutical operations such as tableting.

CHAPTER FIVE

COMPACTION BEHAVIOUR OF DEXTROSE CRYSTALS

5.1 Introduction

This chapter presents the compaction data obtained from the compression of the various batches of dextrose using both a universal testing instrument (Monsanto T10) in compression mode (section 3.4.1) and a compaction simulator (section 3.6.1). In order to fully illustrate the effect of the various crystallisation conditions on the compression behaviour of dextrose the same batch of dextrose may be referred to in more than one section for the purposes of comparison.

The compression behaviour of the various batches was examined by application of the Heckel equation (equation 1.4) to the data obtained from compression of compacts. As discussed in chapter one, Heckel plots can be plotted either from data obtained during compression when the compact is still in the die ("at pressure") or from data obtained after the compact has been ejected from the die (zero pressure). Both approaches have been used in this work. Section 5.2 will present the post compression (ejected tablet) data while the zero pressure data will be discussed in section 5.3.

The degree of elastic recovery occurring within the compacts after compression was assessed by several methods and the data obtained is detailed in section 5.4.

The results from a limited study investigating the effect of compression speed on the consolidation of the various batches of dextrose are presented in section 5.5.

The mean yield pressure (section 1.2.8) which is a fundamental material property was obtained from the reciprocal of the slope of the linear portion of the Heckel plot using linear regression analysis of the data. The linearity of the slope was assessed by the correlation coefficient (CC), a value of 1.00 being obtained for a completely linear plot. Extrapolation of the linear portion of the Heckel plot to zero pressure intersected the Ln (1/1-D) axis at a point referred to as a relative packing fraction, D_A. This densification factor is known to be influenced only by the size and shape of the particles or crystals being compressed. Two other packing fractions, D_0 and D_B, which are a measure of particle packing due to filling and rearrangement respectively where also determined from the "at pressure" compaction data.

Several parameters, including punch dimensions, state of lubrication and speed of compaction have been shown to affect mean yield pressure values (York 1979; De Boer et al., 1978; Rees and Rue, 1978; Roberts and Rowe, 1985). It has thus been suggested that the mean yield pressure provides a relative measure of a material's tendency to deform by plastic deformation (low mean yield pressure) or by particle fragmentation (high mean yield pressure). As far as was possible experimental conditions were kept constant throughout the course of this work.

The ejected tablet (zero pressure) mean yield pressure is a measure of a materials ability to maintain the volume reduction caused by compression and is therefore a measure of its tendency to deform plastically. The tablet in die ("at pressure") mean yield pressure describes the ability of the material to deform during compression, but does not distinguish between elastic deformation, plastic flow or fragmentation. The difference between the ejected tablet mean yield pressure and the tablet in die mean yield pressures has also been used to evaluate the tendency of a material to undergo elastic recovery after compression (Paronen, 1987).

5.2 Post-compression (ejected tablet) Heckel plots and mean yield pressure values obtained from compression of dextrose

This section will detail the effect of the various crystallisation conditions on the Heckel plots, mean yield pressure and the relative packing fraction (D_A) of dextrose. The coefficient of variation for the mean yield pressure and the relative packing fractions were less than 5% in all cases.

For calculation of the Heckel data the axial and radial dimensions of the compacts (n=5) were determined no sooner than 48 hours after ejection. Heckel data was calculated and analysed using Microsoft Excel software.

5.2.1 Effect of crystallisation cooling rate

The post-compression Heckel plots constructed from the dimensions of compacts prepared using dextrose crystallised at a range of cooling rates are displayed in Figures 5.1 and 5.2.

The shape of the Heckel plots (section 1.2.8) appear to indicate that type A deformation behaviour as identified by Hersey and Rees (1971) was occurring. This type of behaviour was proposed to represent materials with different initial packing densities which consolidate firstly by particle slippage and rearrangement followed by plastic deformation.

As the data show (Table 5.1) changing the crystallisation cooling rate appeared to have no effect on the on the mean yield pressure and thus the deformation behaviour of dextrose crystallised from aqueous solutions. However, there is a definite effect on the relative packing fraction D_A. Increasing the crystallisation cooling rate from 0.5 to 50°C/h causes the densification factor D_A to steadily decrease, indicating that altering the crystallisation cooling rate has an affect on the size and/or the shape of the crystals produced. These findings support the results and observations reported in chapter four. Although the compacts were prepared from a single size range (63-90 μm) of crystals the distribution of sizes (even within a small range) were probably affected by changes to the crystallisation cooling rate. From microscopic observation it was also suggested that subtle changes to the shape (length to width ratio) of the crystals may have been occurring

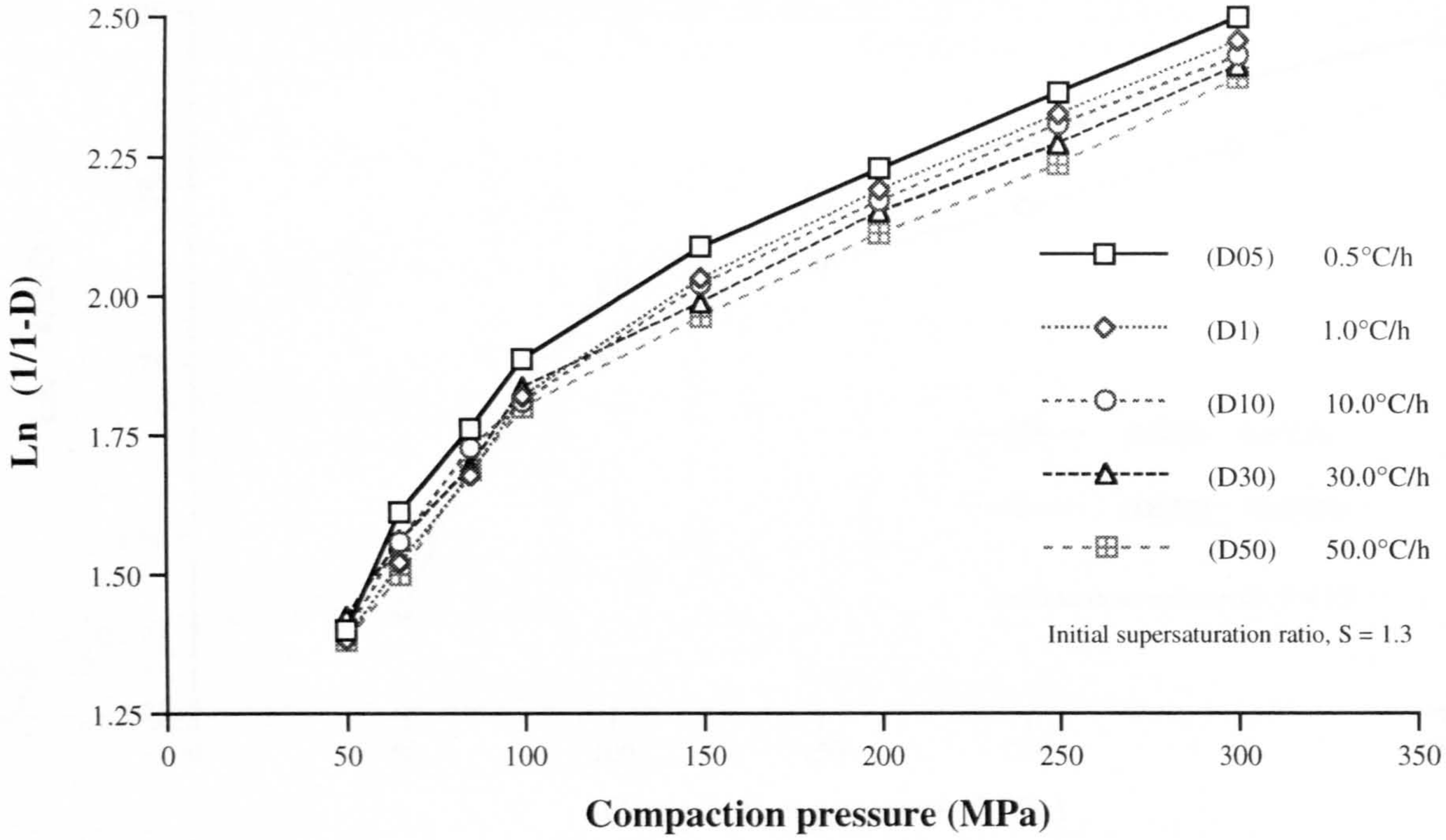

Figure 5.1 Effect of crystallisation cooling rate on the Heckel plots of dextrose

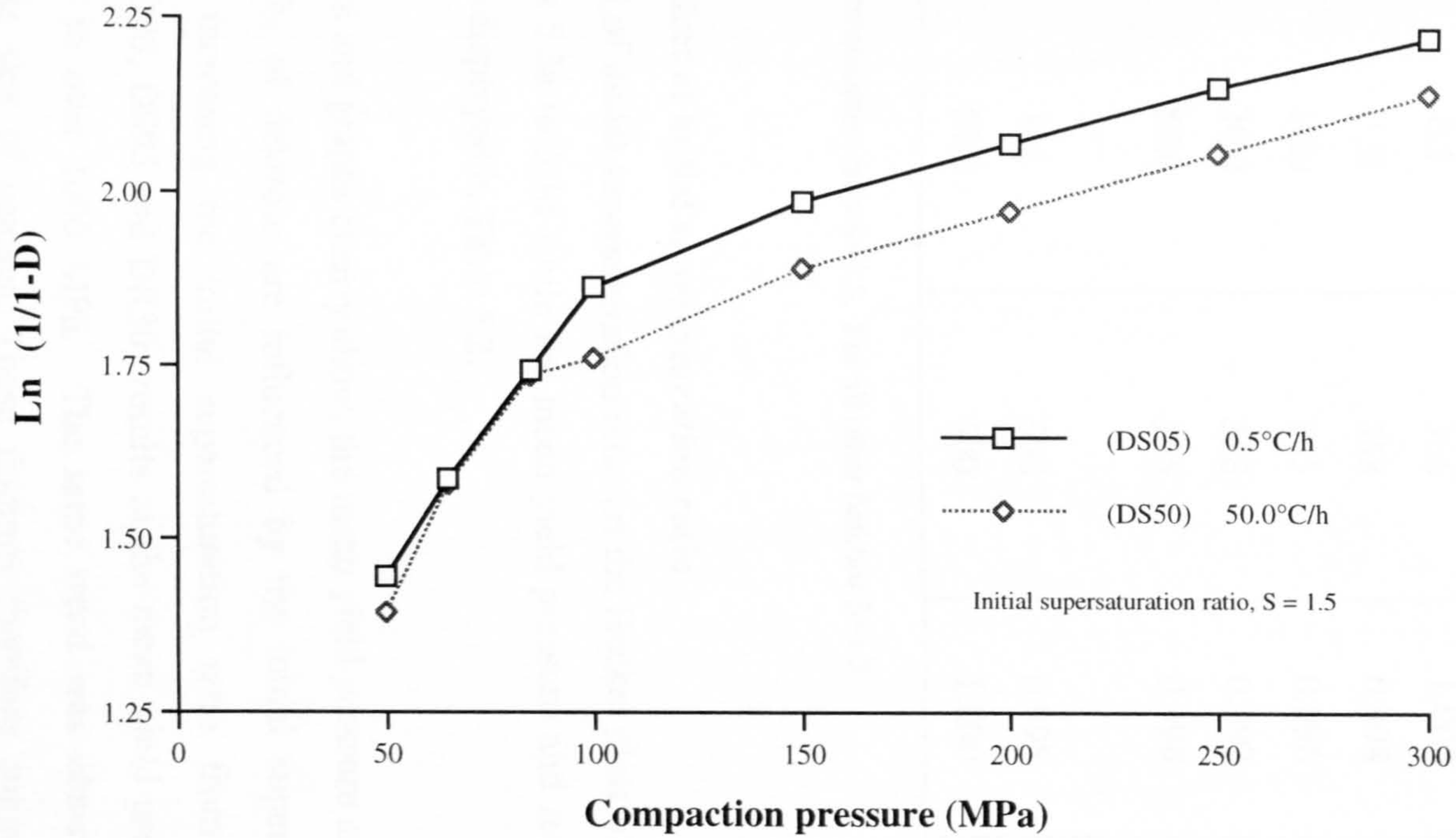

Figure 5.2 Effect of crystallisation cooling rate on the Heckel plots of dextrose

Table 5.1 Effect of crystallisation cooling rate on the mean yield pressure (ejected tablet) and relative packing fraction, D_A

Batch	Cooling Rate (°C/h)	Mean Yield Pressure (MPa)	CC	D_A
D05	0.5	366	1.000	1.682
D1	1.0	358	0.998	1.618
D10	10.0	365	0.998	1.600
D30	30.0	358	0.997	1.581
D50	50.0	355	0.998	1.544
DS05*	0.5	608	0.998	1.755
DS50*	50.0	600	1.000	1.640

*Initial supersaturation ratio S=1.5. For all other batches S=1.3.

5.2.2 Effect of initial supersaturation ratio

The effect of initial supersaturation ratio on the Heckel plots of dextrose is illustrated in Figures 5.3a to 5.3d while the mean yield pressure and relative packing fraction values are displayed in Table 5.2.

As the data and graphs clearly show, the mean yield pressure and the relative packing fraction D_A of dextrose are influenced by the initial supersaturation ratio. For example, increasing the initial supersaturation ratio from 1.3 through to 1.6 (batches D05, DS05 and DR30) results in the mean yield pressure increasing from 366 MPa to over 1000 MPa. The same trend was observed for all the other comparable sets of batches. These findings therefore suggest that as the initial supersaturation ratio of dextrose solutions is increased, so the tendency of the crystals to consolidate by a fragmentation mechanism also increases. Increasing the initial supersaturation ratio led to a progressive increase in the relative packing fraction (Table 5.2) indicating changes to the densification behaviour of dextrose. This again supports the observations reported in chapter four that the crystal size distribution,

bulk density, and possibly the crystal habit were all influenced by the initial supersaturation ratio.

Table 5.2 Effect of initial supersaturation ratio on the mean yield pressure (ejected tablet) and relative packing fraction D_A of dextrose

Batch	Supersaturation Ratio	Mean Yield Pressure (MPa)	CC	D_A
D05	1.30	366	1.000	1.682
DS05	1.50	608	0.998	1.755
DR30	1.60	1005	1.000	1.941
D50*	1.30	355	0.998	1.544
DS50*	1.50	600	1.000	1.640
DC40	1.30	337	0.997	1.616
DR40	1.50	686	1.000	1.810
DC45	1.30	319	0.998	1.526
DR45	1.40	479	0.998	1.663
DR51	1.10	284	0.999	1.330
DC51	1.30	442	0.998	1.514

* These batches were prepared at a cooling rate of 50°C/h. All other batches were prepared at a cooling rate of 0.5°C/h.

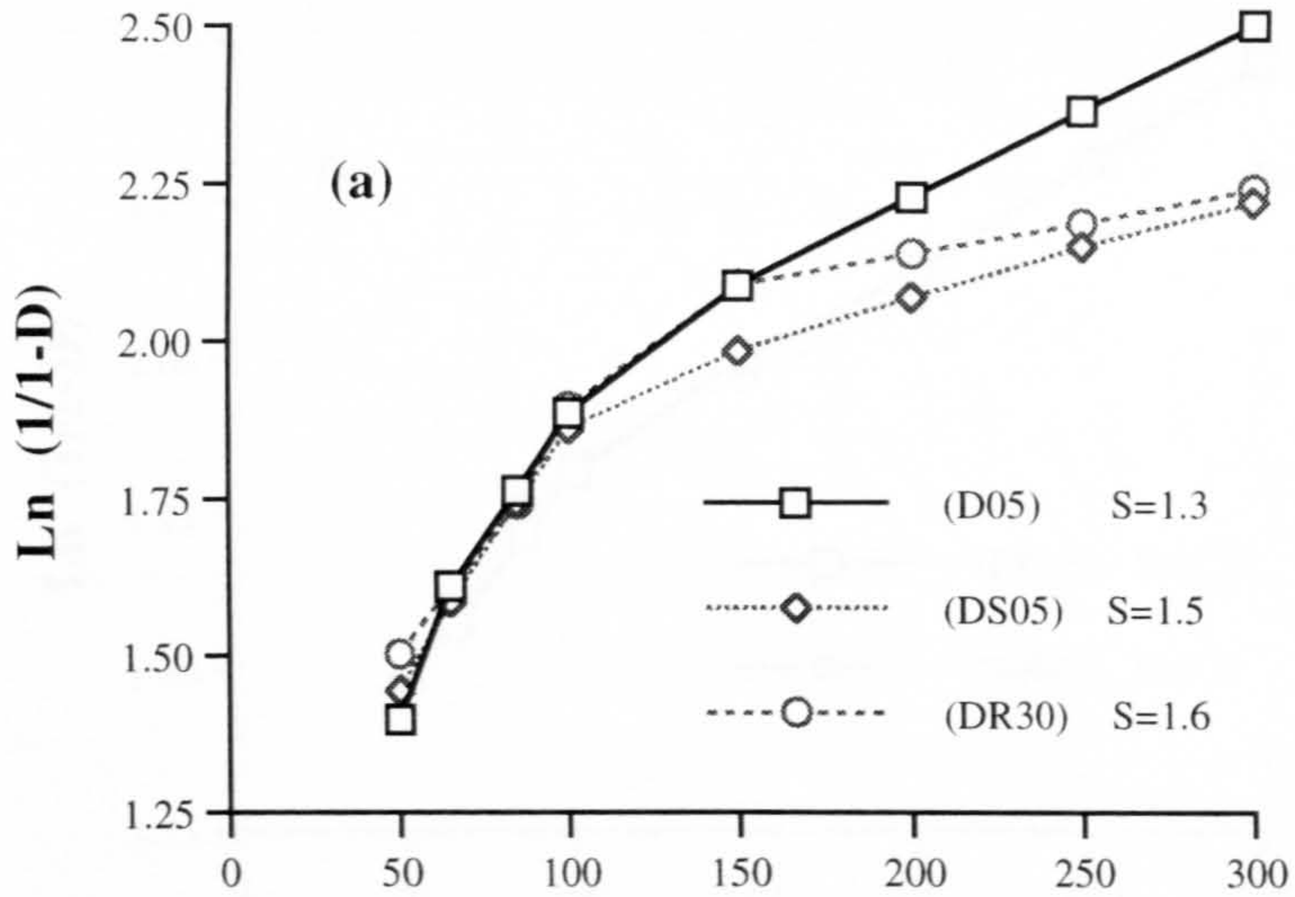

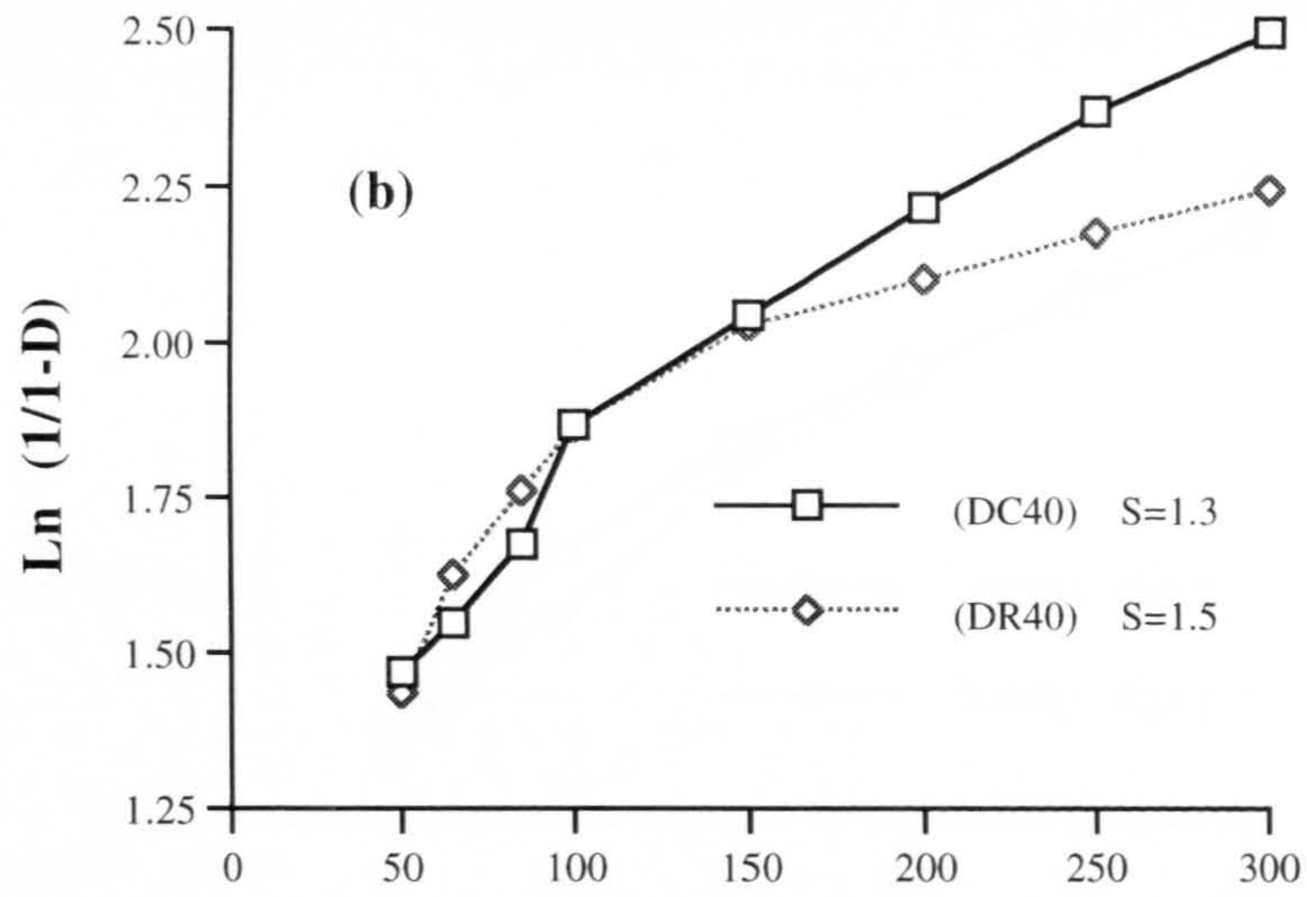

Figures 5.3a and 5.3b Effect of initial supersaturation ratio on the Heckel plots of dextrose

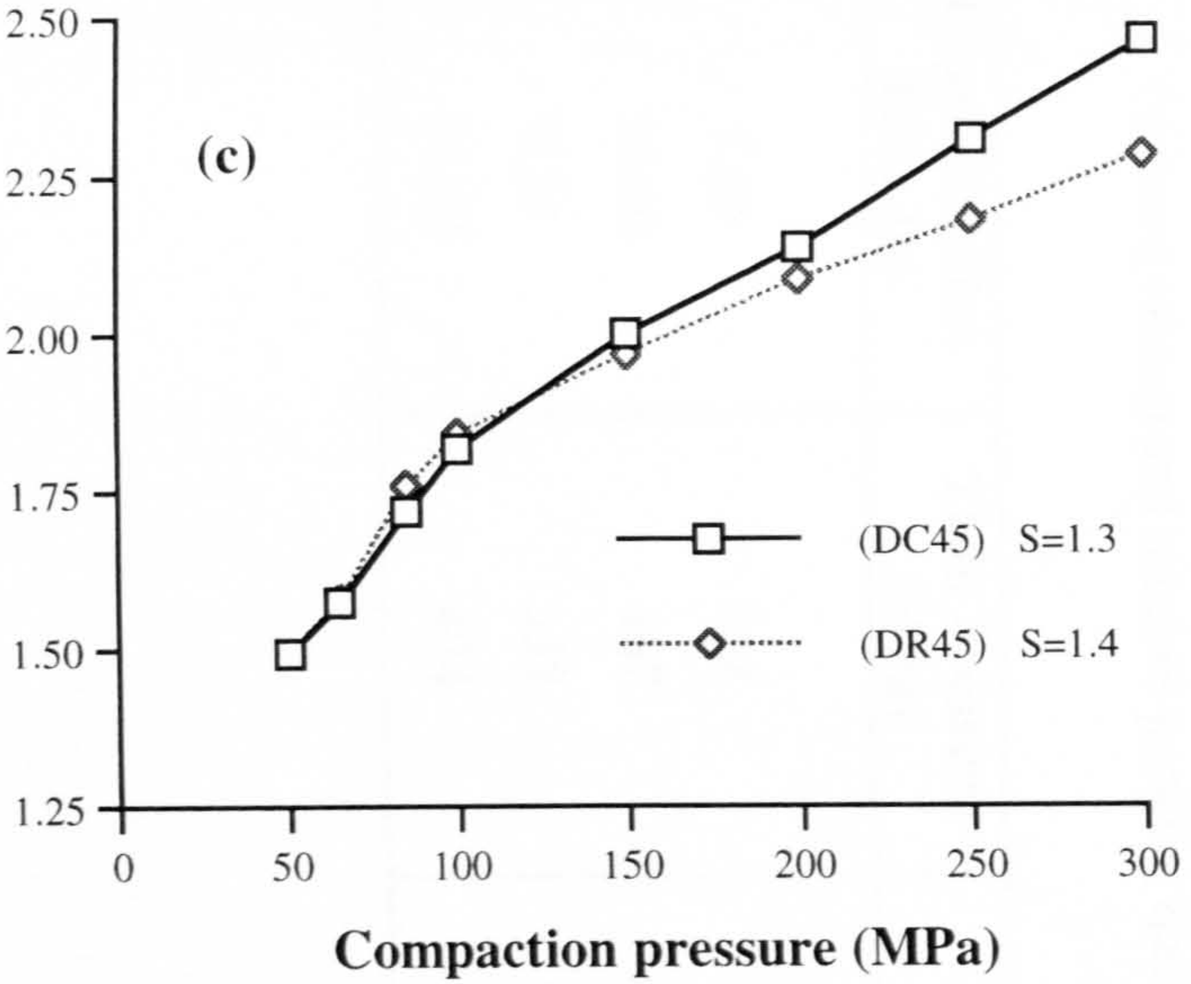

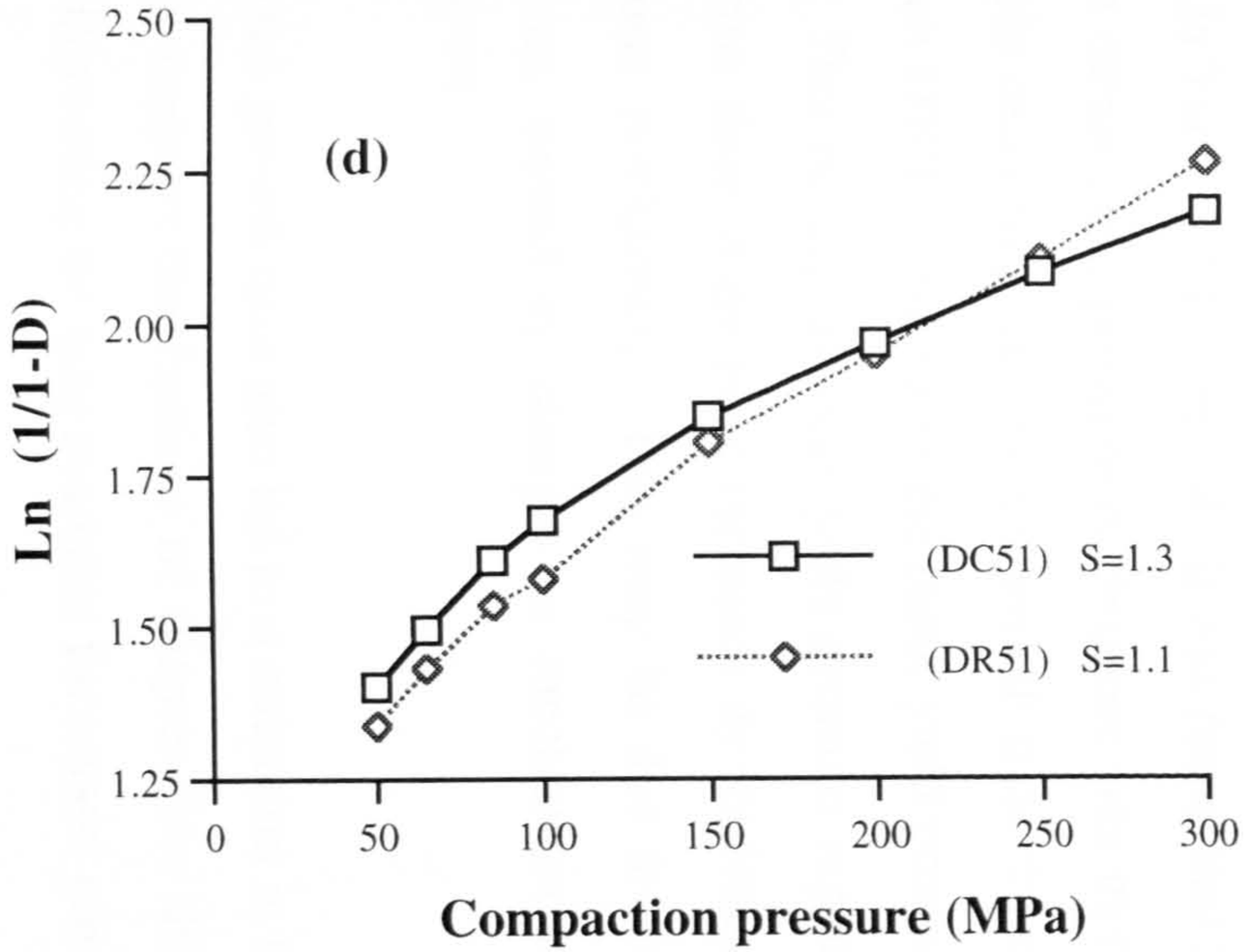

Figures 5.3c and 5.3d Effect of initial supersaturation ratio on the Hekel plots of dextrose

5.2.3 Effect of crystal growth time

The effects of extending the crystal growth time on the Heckel data for dextrose are illustrated in Table 5.3 Figure 5.4. It was found that by extending the time of crystal growth the mean yield pressure of dextrose was increased significantly (Table 5.3). For example extending the crystal growth time from 0.27 hours (batch D30) to 16 hours (batch D30T) resulted in the mean yield pressure being increased from 358 to 474 MPa. This raising of mean yield pressure suggests therefore that extending the crystallisation time of dextrose increases its tendency to deform predominately by a fragmentation mechanism. This may be due to the introduction of more lattice imperfections, caused by changes in mechanism of crystal growth as discussed previously [redacted].

Extending the growth time also led to a reduction in the relative packing fraction D_A. Again, this supports the findings of chapter four that particle size distribution was altered by increasing the time available for crystal growth.

Table 5.3 Effect of crystal growth time on the mean yield pressure (ejected tablet) and relative packing fraction ($D_{A)}$ of dextrose

Batch	Crystallisation Time (h)	Yield Pressure (MPa)	CC	D_A
D1	8.00	358	0.998	1.618
D1T	16.00	467	0.999	1.692
D30	0.27	358	0.997	1.581
D30T	16.00	474	0.998	1.663

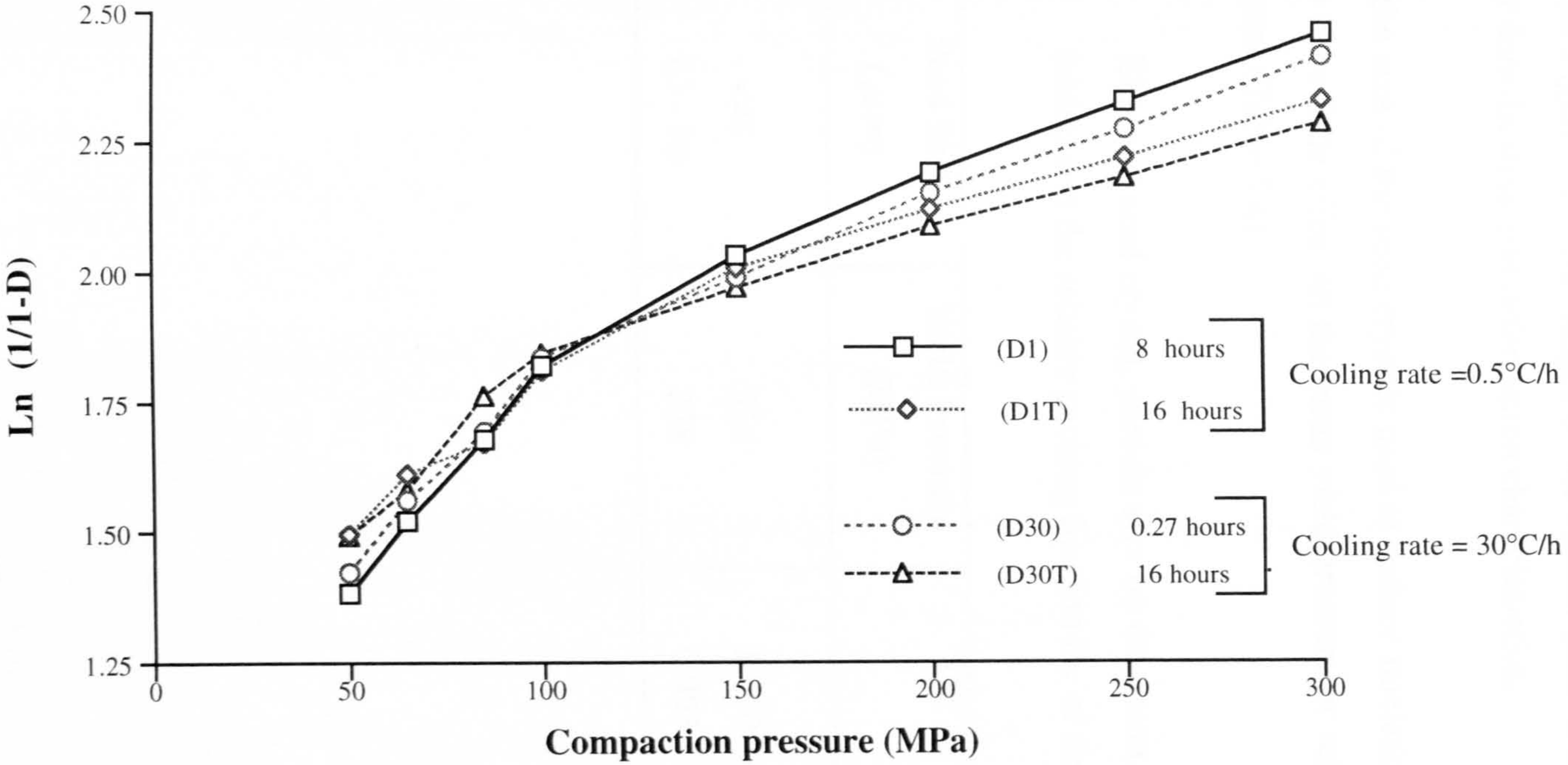

Figure 5.4 Effect of crystal growth time on the Heckel plots of dextrose

5.2.4 Effect of seed crystal, particle size

The influence of seed crystal size on the Heckel data for dextrose is illustrated in Table 5.4 and Figure 5.5. The shapes of the Heckel plots indicate that the materials have similar densification and deformation characteristics.

Increasing the size of the seed crystals used to induce nucleation and crystal growth appeared to have little effect on the mean yield pressure or relative packing fraction, D_A, of dextrose (Table 5.4).

Table 5.4 Effect of seed crystal, particle size on the mean yield pressure (ejected tablet) and the relative packing fraction D_A of dextrose

Batch	Seed Size (μm)	Yield Pressure (MPa)	CC	D_A
D05	<45	366	1.000	1.682
DX05	63 - 90	358	0.995	1.542

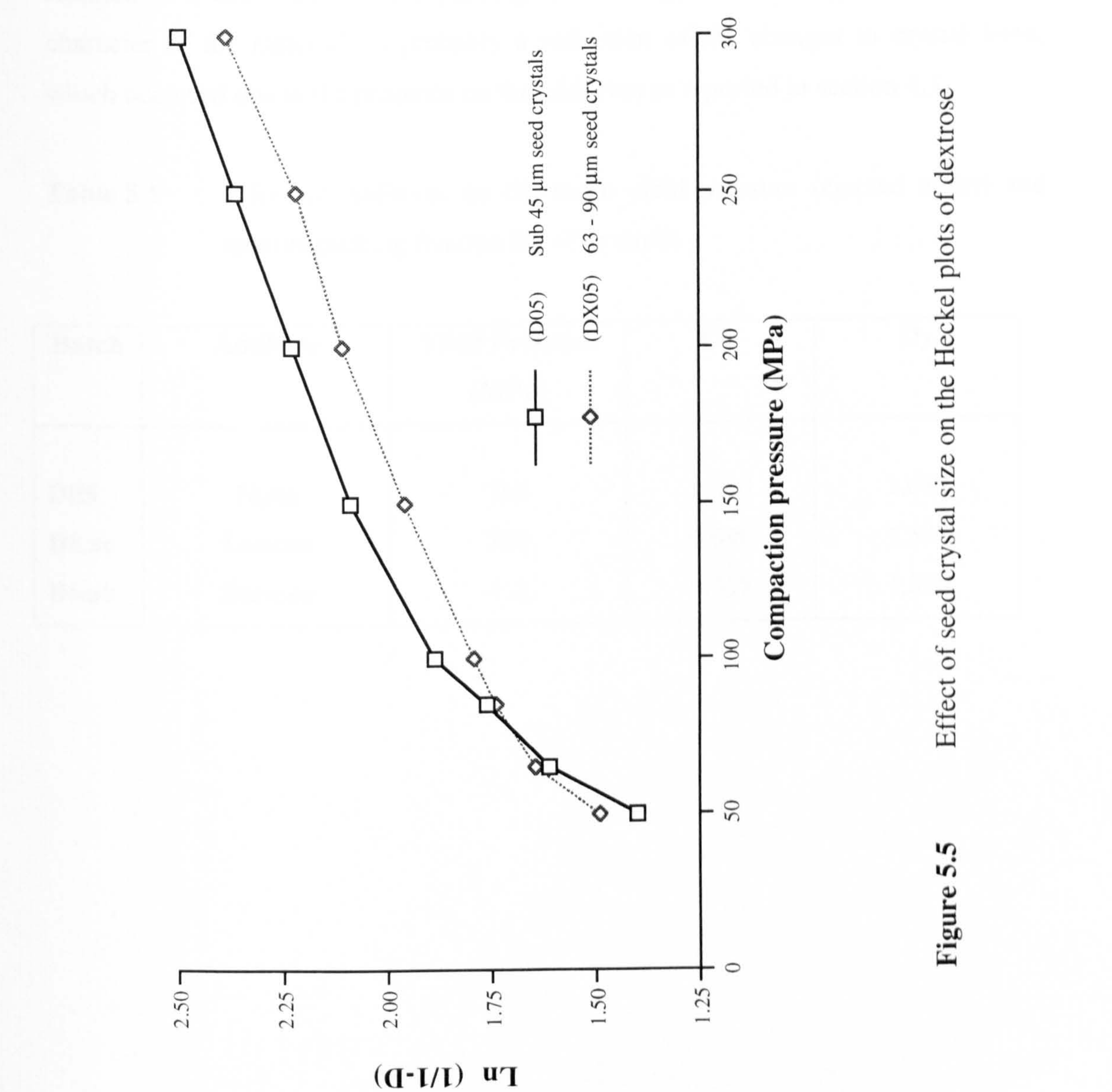

Figure 5.5 Effect of seed crystal size on the Heckel plots of dextrose

5.2.5 Effect of additives

Table 5.5 and Figure 5.6 illustrates the effect of additives (lactose or sucrose), on the Heckel data of dextrose. Inclusion of both lactose and sucrose are seen to cause a rise in the mean yield pressure of the final product (Table 5.5) indicating an increased tendency to deform by a fragmentation mechanism. Inclusion of either additive also resulted in a decreased relative packing fraction D_A. This change in the packing character of the materials is probably a reflection of the changes in crystal habit, which occurred due to the presence on the additives as reported in section 4.3.

Table 5.5 Effect of additives on the mean yield pressure (ejected tablet) and relative packing fraction D_A of dextrose

Batch	Additive	Yield Pressure (MPa)	CC	D_A
D05	None	366	1.000	1.682
DLac	Lactose	380	0.996	1.503
DSuc	Sucrose	418	0.998	1.516

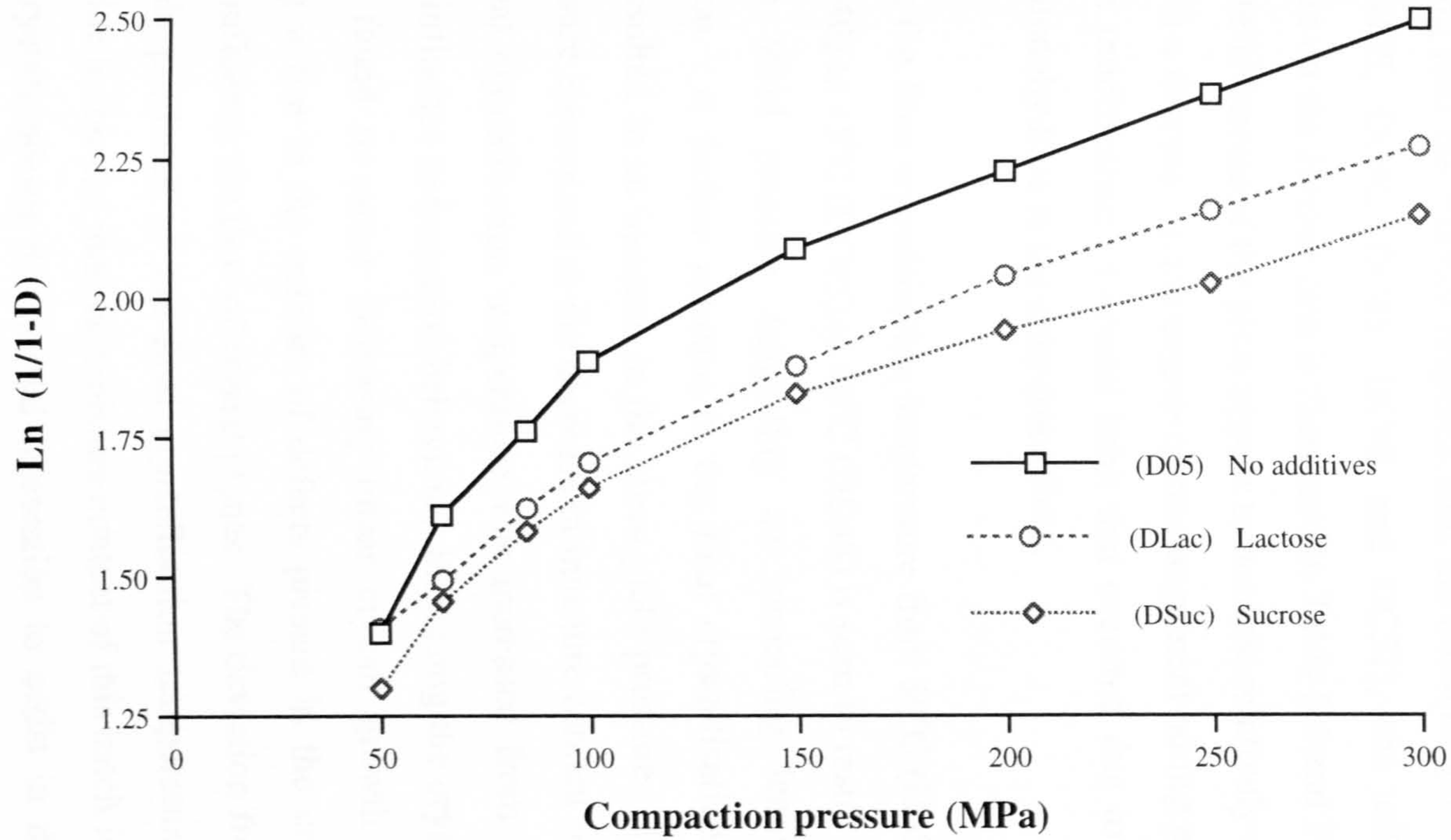

Figure 5.6 Effect of additives on the Heckel plots of dextrose

5.2.6 Effect of crystallisation temperature

As described previously, two sets of batches were crystallised at a range of temperatures. One set was crystallised from supersaturated solutions with a constant initial supersaturation ratio of 1.3, while the second set was crystallised with varied initial supersaturation ratios in order to produce batches with a constant linear crystal growth rate.

Considering first the batches prepared with the constant initial supersaturation ratio (batches D05, DC40, DC45, DC48 and DC51), the effect of crystallisation temperature on the Heckel data is illustrated in Table 5.6 and Figure 5.7. As the final temperature is increased the plots appear to become relatively more linear suggesting that there is a decrease in the degree of rearrangement taking place. This is probably due to the modification of crystal habit that occurred due to the crystals changing from the monohydrate to the anhydrous form.

Increasing the final crystallisation temperature from 30°C (D05) through the range to 40°C (DC40) to 45°C (DC45) to 48°C (DC48) is seen to result in a steady decrease in the mean yield pressure suggesting an increasing tendency towards plastic deformation. A further increase in the final crystallisation temperature to 51°C (DC51) resulted in an increase in the mean yield pressure. These changes in mean yield pressure correspond to the decrease in moisture content reported (section 4.6.1), as the final crystallisation temperature was increased from 30 to 48°C, which is known to influence deformation behaviour. Increasing the crystallisation temperature was also found to cause increasing linear crystal growth rates (section 4.2.6), suggesting a rise in the number of defects present in the crystal lattice, a factors known to influence the flow of crystal planes. The deviation from the trend shown by the crystals produced at the final crystallisation temperature of 51°C (DC51) is probably due to the fact that the moisture content of this batch is so low (less than 1%) that the crystals posses no internal lubrication to assist in the flow of the crystal planes.

As the final crystallisation temperatures are increased from 30 to 48°C there is a steady decrease in the relative packing fraction D_A corresponding to the changes in the size distribution and flowability of the crystals reported in chapter four. The value

then increases for the batch prepared above 51°C corresponding to its change from the monohydrate to the anhydrous crystal habit.

Considering now the batches prepared with the constant growth rate (batches DR30, DR40, DR45, DC48 and DR51). As the temperature is increased there is a steady decrease in the mean yield pressure (Table 5.6) going from 1005 MPa for batch DR30 to 284 MPa for batch DR51. Several factors are probably contributing to this increased tendency towards plastic deformation. As the temperature of crystallisation is increased, the initial supersaturation ratio and the moisture both decrease and the nature of the crystals change from the monohydrate form to the anhydrous form. A similar trend is observed for the relative packing fraction D_A reflecting the changes to the size distribution, bulk density and flowability of the batches as reported in chapter four.

Table 5.6 Effect of crystallisation temperature on the mean yield pressure (ejected tablet) and relative packing fraction D_A.

Batch	Crystallisation Temp (°C)	Mean Yield Pressure (MPa)	CC	D_A
D05	38 - 30	366	1.000	1.682
DC40	48 - 40	337	0.991	1.619
DC45	53 - 45	319	0.998	1.526
DC48	56 - 48	301	0.989	1.379
DC51	59 - 51	442	0.998	1.514
DR30	38 - 30	1005	1.000	1.941
DR40	48 - 40	685	1.000	1.810
DR45	53 - 45	479	0.998	1.663
DC48	56 - 48	301	0.989	1.379
DR51	59 - 51	284	0.995	1.338

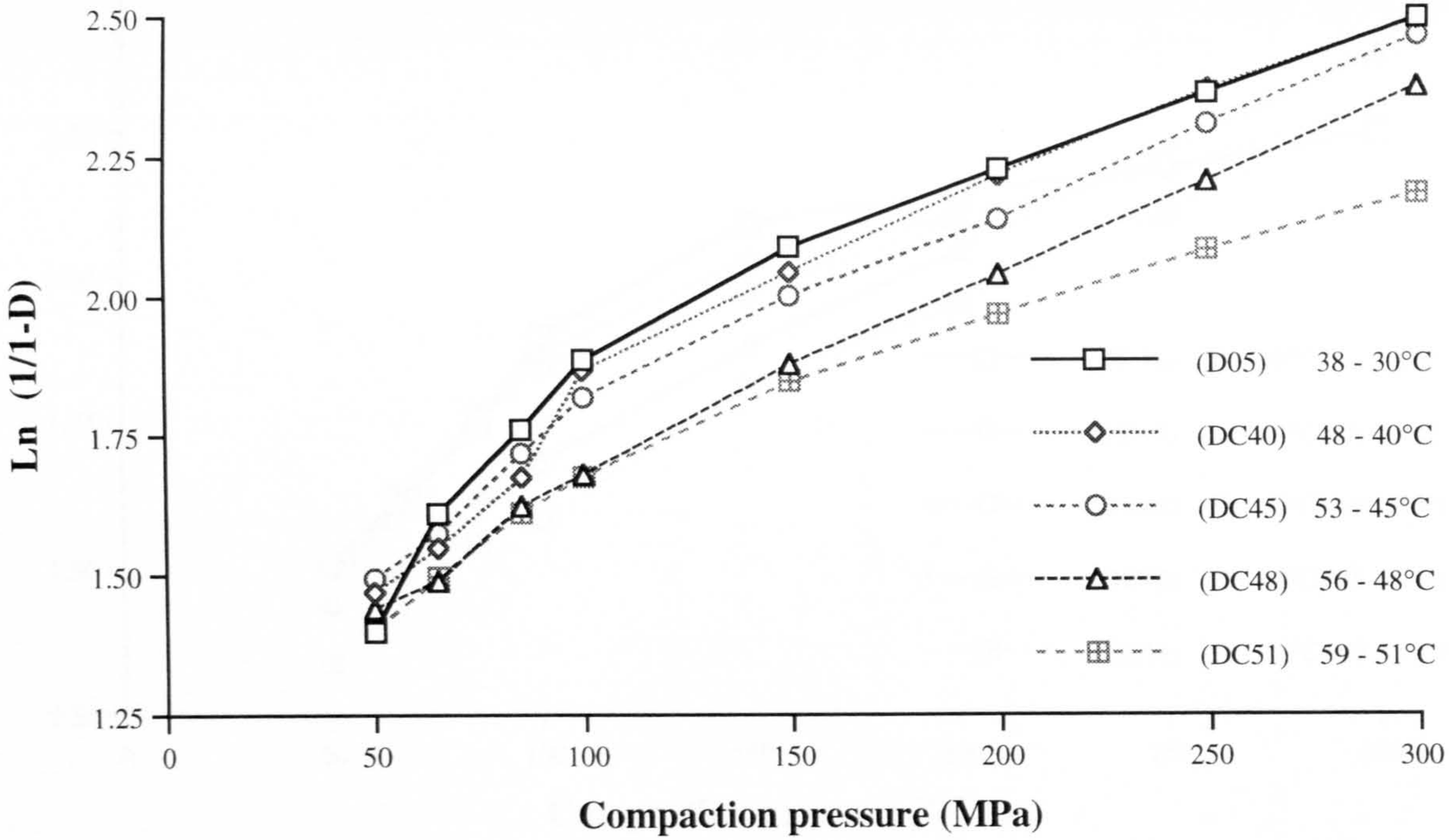

Figure 5.7 Effect of crystallisation temperature (at a constant initial supersaturation ratio of 1.3) on the Heckel plots of dextrose

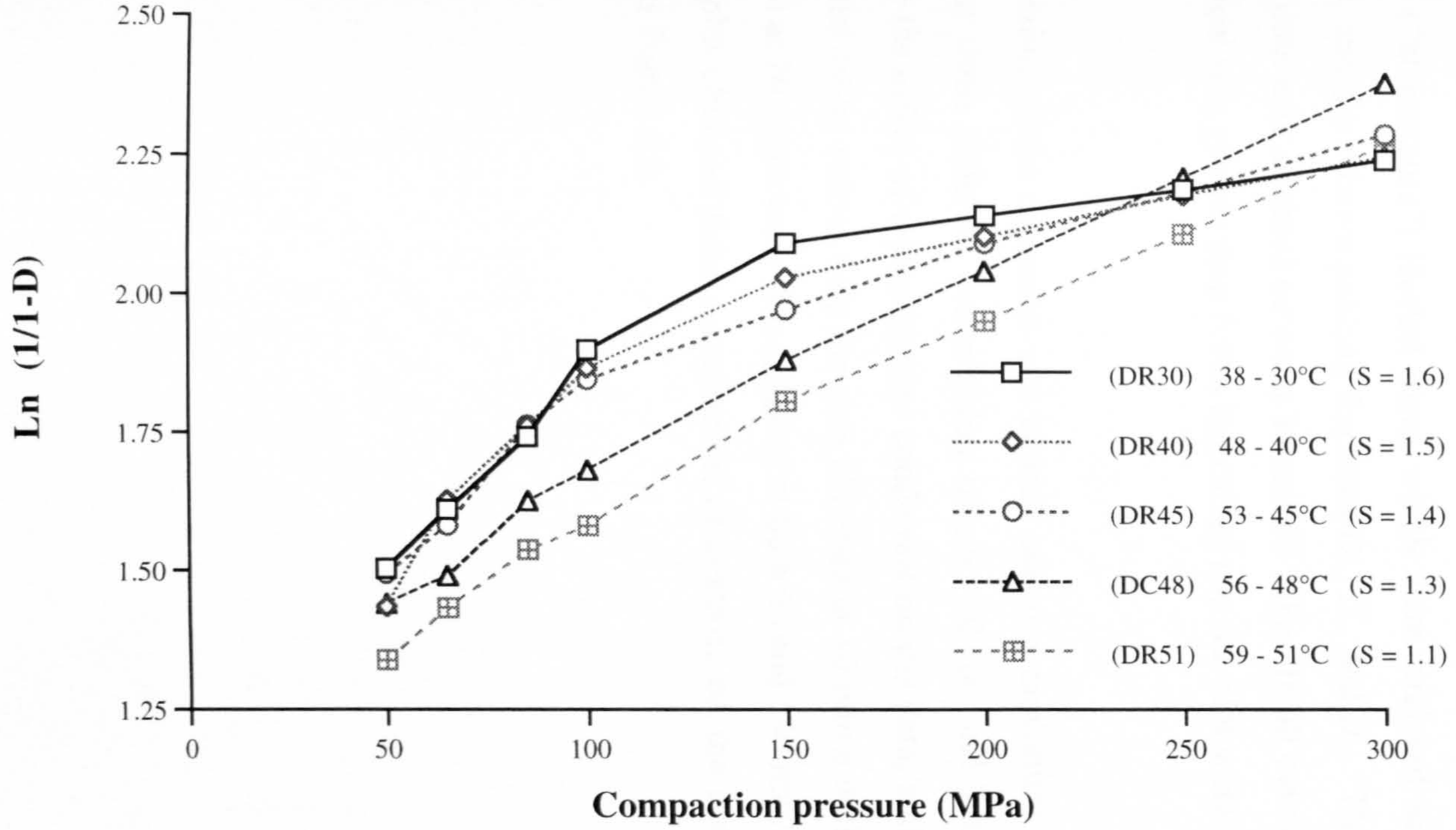

Figure 5.8 Effect of crystallisation temperature (at a constant linear crystal growth rate) on the Heckel plots of dextrose

5.3 Tablet in die ("at pressure") Heckel plots and mean yield pressure values obtained from compression of dextrose

This section will present the data obtained from the compression of compacts (n=4) using the compaction simulator (John Moores University, Liverpool) as described in section 3.6. The punch movement was continually monitored by load cells and the data store on a mainframe computer. The data was then converted and manipulated to produce ("at pressure") Heckel plots, which were analysed to give the mean yield pressure, and the relative packing fractions D_A, D_o and D_B. The linear portion of the Heckel plots was assessed between 30 and 65 MPa. In all cases the linear correlation co-efficient was greater than 0.988 indicating that the plot were linear over the chosen range.

Compression of the compacts was carried out to a maximum compression force of 10 kN at three different compression speeds; 10, 60 and 140 mm/s. In order to evaluate the effect of crystallisation conditions on the data, and for comparison with the ejected tablet values only the data obtained at 10 mm/s will be used. The trends observed at 10 mm/s were also apparent at both 60 and 140 mm/s. A typical complete Heckel plot obtained from compression of dextrose on the compaction simulator is shown in Figure 5.9.

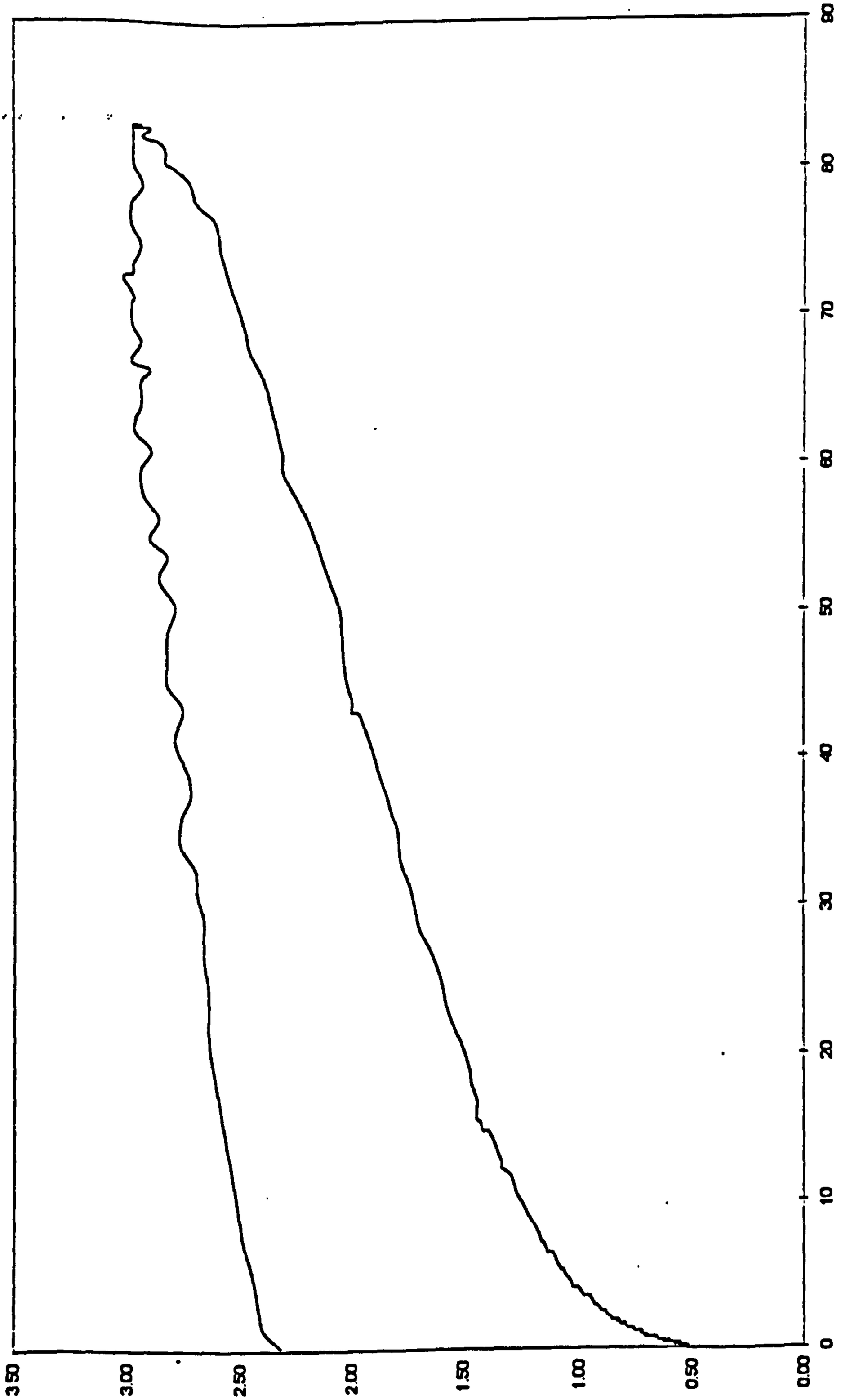

Figure 5.9 A complete Heckel plot obtained for dextrose (Batch D05) compacted on the compaction simulator

5.3.1 Effect of crystallisation cooling rate

As with the ejected tablet values, no major differences in the "at pressure" mean yield pressure was observed with changing crystallisation cooling rate (Table 5.7). However there was a decrease in D_B, (the packing fraction due to particle rearrangement) again indicating that there is a change in crystal size distribution, crystal shape, bulk density and flowability with changing crystallisation cooling rate.

Table 5.7 Effect of crystallisation cooling rates on the mean yield pressure ("at pressure") and the relative packing fractions D_A, D_o, and D_B.

Batch	Cooling Rate (°C/h)	Mean Yield Pressure (MPa)	D_A	D_O	D_B
D05	0.5	36.8	0.686	0.496	0.190
D1	1.0	37.6	0.668	0.489	0.179
D10	10.0	32.6	0.669	0.509	0.160
D30	30.0	36.3	0.665	0.535	0.130
D50	50.0	33.9	0.638	0.537	0.098
DS05*	0.5	45.9	0.697	0.497	0.205
DS50*	50.0	48.7	0.669	0.565	0.124

*Initial supersaturation ratio S=1.5. In all other batches S=1.3.

5.3.2 Effect of initial supersaturation ratio

As was observed for the results from the ejected tablet method, the mean yield pressure values obtained by the "at pressure" method are seen to rise with increasing initial supersaturation ratio (Table 5.8) suggesting a greater tendency towards fragmentation.

The packing fraction D_B, which is measure of the amount of rearrangement occurring in the die under low pressures, also increases with increasing initial supersaturation ratio. This reflects previous findings that particle size, crystal shape, surface

properties and bulk density could all be altered by changes in the initial supersaturation ratio.

Table 5.8 Effect of initial supersaturation ratio on the mean yield pressure ("at pressure") and relative packing fractions D_A, D_o and D_B

Batch	Supersaturation Ratio	Mean Yield Pressure (MPa)	D_A	D_O	D_B
D05	1.30	36.8	0.686	0.496	0.190
DS05	1.50	45.9	0.697	0.492	0.205
DR30	1.60	56.8	0.685	0.414	0.271
D50*	1.30	33.9	0.638	0.537	0.098
DS50*	1.50	48.7	0.669	0.565	0.124
DC40	1.30	36.8	0.666	0.483	0.183
DR40	1.50	55.3	0.680	0.415	0.265
DC45	1.30	32.5	0.687	0.501	0.186
DR45	1.40	53.2	0.637	0.428	0.209
DR51	1.10	50.4	0.607	0.502	0.105
DC51	1.30	57.4	0.663	0.526	0.137

* These batches were prepared at a cooling rate of 50°C/h. All other batches were prepared at a cooling rate of 0.5°C/h.

5.3.3 Effect of crystal growth time

Extending the crystal growth time appeared to have no effect on either the "at pressure" mean yield pressure or the packing fractions, indicating no change in the densification or deformation mechanism of batches crystallised for different lengths of time. This seems to contradict the ejected tablet results (section 5.2.3) which showed that the mean yield pressure values was raised with extended growth time. The results from the ejected tablet method are, however, calculated after the compact has undergone its elastic recovery and so are only a measure of a materials ability to deform plastically, while the tablet in die method, does not distinguish between the different types of deformation taking place. Therefore, the different trend in the results probably indicates a change in the degree of elasticity of dextrose with changing growth time.

Table 5.9 Effect of crystal growth time on the mean yield pressure ("at pressure") and the relative packing fractions D_A, D_o and D_B.

Batch	Crystallisation Time (h)	Yield Pressure (MPa)	D_A	Do	D_B
D1	8.0	37.6	0.668	0.489	0.179
D1T	16.0	36.4	0.662	0.489	0.173
D30	0.27	36.3	0.665	0.535	0.130
D30T	16.0	37.4	0.662	0.529	0.133

5.3.4 Effect of seed crystal, particle size

The data (Table 5.10) suggest that increasing the seed size from less than 45 μm to between 63 and 90 μm has little effect on the "at pressure" mean yield pressure or packing fraction of crystallised dextrose, and thus no change in the deformation behaviour would be expected. These results are in agreement with the ejected tablet results indicating no change in the elasticity of dextrose with increasing seed crystal size (section 5.2.4).

Table 5.10 Effect of seed crystal, particle size on the mean yield pressure ("at pressure") and relative packing fractions D_A, D_B and D_o

Batch	Seed Size (μm)	Yield Pressure (MPa)	D_A	D_O	D_B
D05	<45	36.8	0.686	0.496	0.190
DX05	63 - 90	40.6	0.658	0.472	0.186

5.3.5 Effect of additives

The influence of incorporating additives into the crystallisation system of dextrose on its compression behaviour in terms of Heckel derived data is detailed in Table 5.11.

Inclusion of both lactose and sucrose caused an increase in the "at pressure" mean yield pressure suggesting a greater tendency towards fragmentation. A similar effect was observed with the ejected tablet results (section 5.2.5).

The changes observed in the packing fractions are thought to be due to the modifications in crystal habit which occurred on the inclusion of the additives as reported in section 4.3.

Table 5.11 Effect of additives on the mean yield pressure ("at pressure") and the relative packing fractions D_A, D_o and D_B.

Batch	Additive	Yield Pressure (MPa)	D_A	D_O	D_B
D05	None	36.8	0.686	0.496	0.190
DLac	Lactose	48.2	0.752	0.452	0.273
DSuc	Sucrose	45.8	0.675	0.472	0.203

5.3.6 Effect of crystallisation temperature

The effect of crystallising dextrose over different temperature ranges, both at a constant initial supersaturation ratio and at a constant crystal growth rate, on the Heckel data is shown in Table 5.12.

For the batches prepared with the constant initial supersaturation ratio of 1.3 (i.e. D05, DC40, DC45, DC48 and DC51) the "at pressure" mean yield pressure is seen to gradually rise with increasing temperature, indicating a move towards a greater fragmentation tendency. This is, however, contrary to the ejected tablet, mean yield pressure results which decreased with increasing temperature. This difference would suggest that as the temperature is changed the degree of elastic recovery within dextrose compacts is also altered.

For the batches crystallised with a constant growth rate (batches. DR30, DR40, DR45, DC48 and DR51) the "at pressure" mean yield pressure shows steady decrease with increasing temperature indicating an increase in the plasticity of dextrose with increasing temperature. The same trend was also observed with the ejected tablet data. These results are probably due to a combination of several factors such as moisture content, crystal habit, and crystal structure.

Table 5.12 Effect of crystallisation temperature on the mean yield pressure ("at pressure") and relative packing fractions D_A, D_o and D_B.

Batch	Crystallisation Temp (°C)	Mean Yield Pressure (MPa)	D_A	D_o	D_B
D05	38 - 30	36.8	0.686	0.496	0.190
DC40	48 - 40	36.8	0.666	0.483	0.183
DC45	53 - 45	41.5	0.687	0.501	0.186
DC48	56 - 48	52.3	0.661	0.516	0.145
DC51	59 - 51	57.4	0.663	0.526	0.137
DR30	38 - 30	51.8	0.685	0.414	0.271
DR40	48 - 40	55.3	0.680	0.415	0.265
DR45	53 - 45	53.2	0.637	0.428	0.209
DC48	56 - 48	52.3	0.661	0.516	0.145
DR51	59 - 51	54.3	0.627	0.472	0.155

5.4 Elastic recovery and capping tendency

The amount of elastic recovery that takes place in a compact after removal of the compression load can have a significant effect on its integrity. The greater the degree of recovery, the more inter-particle bonds will be broken and thus the lower the tensile strength of the compact. In some cases, it may sufficient to cause the compact to cap or laminate. As discussed in chapter one, several methods have been used to evaluate elastic recovery. The following methods were used on the compacts prepared on the compaction simulator.

One of the most widely used methods utilises the equation proposed by Armstrong and Haines-Nutt (1972) to defined elastic recovery:

$$E_{(\text{"at pressure"})} = \frac{H_o - H_p}{H_o} \times 100 \qquad \text{(equation 1.1)}$$

where H_o is the thickness of the compact obtained after ejection (24 hours) and H_p is the minimum thickness obtained during compression. This equation was also applied to the compacts prepared using the Monsanto T10 tensometer (section 3.4.3). This will be referred to as $E_{(\text{zero pressure})}$.

Duberg and Nystrom (1986) and Paronen (1987) have used the decompression phase of Heckel plots to assess the fast elastic yield pressure or immediate elastic recovery (ER) of compacted materials. This was calculated as the relative percentage increase in the porosity of the compact that occurred during decompression.

By subtracting the slope obtained from the ejected tablet method from the slope of the tablet in die method (E_{Diff}) Paronen and Juslin (1983) and Paronen (1987) have defined a compact's tendency to cap.

Table 5.13 summarises the elasticity of the compacts prepared from the various batches of dextrose as assessed by the different methods.

Table 5.13 The elasticity of compacts prepared from dextrose (crystallised using a variety of conditions) as assessed by several methods

Batch	$E_{(zero\ pressure)}$ (%)	$E_{(“at\ pressure”)}$ (%)	ER (%)	E_{Diff} (MPa)
D05	1.65	16.75	186	329
D1	1.61	13.39	150	320
D10	1.52	12.86	145	322
D30	1.47	11.99	126	322
D50	1.41	11.63	75	321
DS05	1.38	16.34	202	562
DS50	1.48	11.94	96	551
D1T	1.25	13.92	152	431
D30T	1.47	12.14	130	437
DX05	1.71	11.72	101	317
DLac	1.15	15.04	172	332
DSuc	1.24	14.74	159	372
DC40	1.52	14.28	116	300
DC45	1.49	13.48	101	286
DC48	1.35	12.09	108	249
DC51	1.47	12.08	89	385
DR30	2.12	16.97	221	948
DR40	1.64	13.58	131	631
DR45	1.71	12.42	120	427
DR51	1.34	11.85	45	234

The trends observed between elastic recovery results and crystallisation conditions showed good agreement between the various methods. The value of elastic recovery $E_{(\text{zero pressure})}$ determined on the compacts prepared using the universal testing instrument was low in all cases and appeared to be unaffected by the crystallisation conditions used, indicating that most of the elastic recovery was occurring while the compact was still in the die (or at least before the dimensions of the ejected compacts could be measured). Therefore, only the elastic recovery determined from the compacts prepared on the compaction simulator will be discussed further.

There was a steady decrease in the degree of elastic recovery ($E_{(\text{"at pressure"})}$ and ER) with increasing cooling rates (batches D05, D1, D10, D30 and D50 and batches DS05 and DS50) but no difference in the relative capping tendency (E_{Diff}). The decrease in elastic recovery is possibly due to increased bonding surfaces being available for the batches prepared at the faster cooling rates due to the decrease in the particle size of the crystals.

Increasing the crystallisation time (batches D1/D1T and batches D30/D30T) appeared to have no effect on the amount of elastic recovery ($E_{(\text{"at pressure"})}$ and ER) of compacts but did result in an increased capping tendency (E_{Diff}).

Inclusion of lactose (DLac) and sucrose (DSuc) into the crystallisation system caused a reduction in the elastic recovery of compacts as compared to batch D05 but caused no change in the capping tendency.

Increasing the final crystallisation temperature (with constant initial supersaturation ratio and constant linear growth rate) caused the elastic recovery ($E_{(\text{"at pressure"})}$ and ER) compacts to decrease. This is in agreement with the findings reported in sections 5.2.6 and 5.3.6, which showed a different trend in the mean yield pressure values obtained by the two methods. In general, there was also a decrease in the capping tendency of the compacts with increasing crystallisation temperature. However batch DC51 deviated from the trend. This is possibly due to the low moisture content of batch DC51 reducing the bonding capacity of the dextrose.

5.5 Compression speed

The effect of compression speed on the deformation and consolidation properties of pharmaceutical materials has been widely studied (e.g. York, 1979; Armstrong, 1989; Roberts and Rowe, 1985) and it has been found that the effects are material dependent. In general terms, visicoelastic substances (i.e. those which undergo plastic flow) were found to have time dependent consolidation characteristics, their porosity decreasing and tensile strength increasing with decreasing compression rate (increased dwell time). Materials which are known to undergo brittle fracture and consolidate via fragmentation were found to be independent of compression rate.

Roberts and Rowe (1985) introduced the strain rate sensitivity (SRS) term (equation 1.9) to describe the change in yield pressure with compression speed.

A limited study on the effect of compression speed on the compacts of dextrose prepared at the various crystallisation conditions was carried out using the High-speed compaction simulator (John Moores University, Liverpool). Due to the constraints of time, it was possible to prepare compacts at only three speeds (10, 60 and 140 mm/s). The data generated were treated as described in section 3.6 in order to calculate the "at pressure" mean yield pressure. The elastic recovery of the compacts, prepared at the three compression rates, was also determined.

5.5.1 Effect of compression speed on the mean yield pressure of dextrose

The effect of the various crystallisation conditions on the mean yield pressure has been discussed already using the data generated at a compression rate of 10 mm/s. The same effects were noted at all compression speeds for each batch.

Four compacts from each batch of dextrose were compacted at each compression speed. The relative standard deviations, in the mean yield pressure values, obtained for each batch were between 2-8%.

Table 5.14 presents the mean yield pressure values obtained at each of the three compression rates.

Table 5.14 Effect of compaction speed on the mean yield pressure ("at pressure") of dextrose crystallised using a variety of process conditions

Batch	Compression Speed		
	10 mm/s	60 mm/s	140 mm/s
	Mean Yield Pressure (MPa)		
D05	36.8	35.4	36.1
D1	37.6	38.2	38.8
D10	32.6	33.4	31.9
D30	36.3	34.9	35.2
D50	33.9	35.1	35.4
DS05	45.9	47.2	47.6
DS50	48.7	46.5	47.2
D1T	36.4	36.8	38.2
D30T	37.4	38.4	38.1
DX05	40.6	39.6	41.2
DLac	48.2	49.4	46.1
DSuc	45.8	46.2	46.6
DC40	36.8	38.2	37.4
DC45	32.5	31.4	32.9
DC48	52.3	50.6	53.6
DC51	57.4	59.1	56.2
DR30	56.8	56.9	57.6
DR40	55.3	56.8	56.3
DR45	53.2	50.9	53.3
DR51	50.4	51.2	49.7

As the data indicates, no significant change in the mean yield pressure was detected with increasing compression speed indicating that all of the batches consolidated predominately by a fragmentation mechanism. It must be noted, however, that the three speeds used in this study did not cover the entire range usually employed for this type of investigation. Roberts and Rowe (1985) used a top speed of 330 mm/s while many studies have used speeds up to 1000 mm/s, which represent the speeds experienced on typical high-speed tablet presses. Often no change in the mean yield pressure is recorded over the range of speeds used in this study, but the values are altered when greater speeds are employed. Therefore, although these results would appear to suggest that all the materials are predominately compacting by a fragmentation process with no time dependency they cannot be considered conclusive.

5.5.2 Effect of compression speed on the elastic recovery of dextrose compacts

The elastic recovery of the compacts (Table 5.15) prepared at each speed were calculated using the equation of Armstrong and Haines-Nutt (1972) as detailed in section 5.4. However, increases in the elastic recovery were observed for many of the batches especially at the highest compaction rate of 140 mm/s. This suggests that as the rate of compaction is increased (dwell time decreased) more elastic energy is retained in the compacts. In some cases the compacts prepared at the highest speed capped on production (indicating a large degree of elastic recovery) and so no measurement could be made. The decrease in dwell time probably leads to a reduction in the amount of fragmentation which takes place at the higher compaction pressures and so reduces the number of new bonding surfaces created. Thus, the effect of elastic recovery is more noticeable as there are fewer bonds to overcome.

Table 5.15 Effect of compaction speed on the elastic recovery of compacts prepared from dextrose crystallised using a variety of process conditions

Batch	Compaction Speed		
	10 mm/s	60 mm/s	140 mm/s
	Elastic Recovery %		
D05	16.75	16.23	17.80
D1	13.39	13.39	14.30
D10	12.86	12.01	13.61
D30	11.99	11.89	12.61
D50	11.63	11.70	14.66
DS05	16.34	16.74	18.28
DS50	11.94	15.40	-
D1T	13.92	14.0	15.90
D30T	13.94	14.77	16.05
DX05	13.72	14.51	14.98
DLac	15.40	15.85	17.68
DSuc	14.74	14.77	16.66
DC40	13.28	13.54	14.12
DC45	13.48	13.34	13.74
DC48	12.09	11.48	13.74
DC51	12.08	12.21	14.64
DR30	16.97	18.57	-
DR40	13.50	14.68	16.89
DR45	12.42	13.03	12.96
DR51	11.85	12.03	11.91

5.6 Discussion

The results of the work in this chapter demonstrate that careful control and manipulation of crystallisation process variables can result in modified compaction behaviour of dextrose as indicated by changes in the mean yield pressure values obtained from Heckel plots. The degree of elastic recovery occurring within the compacts subsequent to compaction, was assessed by three different methods which showed good correlation and showed that certain crystallisation variables could be used to alter the values.

It should be noted that there is doubt over the validity of the "at pressure" Heckel data obtained as a different pressure range (as compared to the "ejected tablet" data) was investigated.

CHAPTER SIX

TENSILE STRENGTH OF DEXTROSE AND ITS COMPACTS

6.1 Introduction

The data presented in this chapter detail the influence of crystallisation conditions on the tensile strength of dextrose compacts and utilises these findings to indicate the effects on the fundamental tensile properties of dextrose crystals. The tensile strength of compacts is primarily a measure of the degree of inter particle bonding and elastic recovery which takes place during and after compression of the material respectively.

6.2 Effect of crystallisation conditions on the tensile strength of dextrose and its compacts

Compacts were prepared from the various batches of dextrose on the tensometer (as described in section 3.4.1). Their tensile strength was calculated by applying the equation of Fell and Newton (1968) to diametral crushing strength measurements obtained from compacts which failed in tension (see section 3.4.2).

In an attempt to give some indication the influence of crystallisation conditions on the fundamental tensile strength of dextrose, an extrapolated exponential equation (section 1.3.7) proposed by Ryskewitch (1962) was employed. This enabled the data obtained from the compacts to be extrapolated to zero porosity and so give an assessment of the fundamental material tensile strength.

6.2.1 Effect of crystallisation cooling rate

Figures 6.1 and 6.2 illustrate the effect of crystallisation cooling rate on the tensile strength of dextrose compacts. As expected, the tensile strength of compacts prepared from dextrose crystallised at all cooling rates is seen to increase with increasing compression pressures and thus decreasing porosity. All the samples showed a similar relationship between compression pressure and porosity reaching a porosity of approximately 7% at the maximum applied compression load of 300 MPa. It was not, however, possible to obtain tensile strength data for all the compacts, as those prepared above 200 MPa (150 MPa for the batch DS50 prepared at 50°C/h and S=1.5) tended to cap or laminated during the diametral crushing test, and thus were not considered to have failed in tension.

For those compacts which did fail in tension, an increase in the crystallisation cooling rate of the dextrose resulted in an increased compact tensile strength when compared

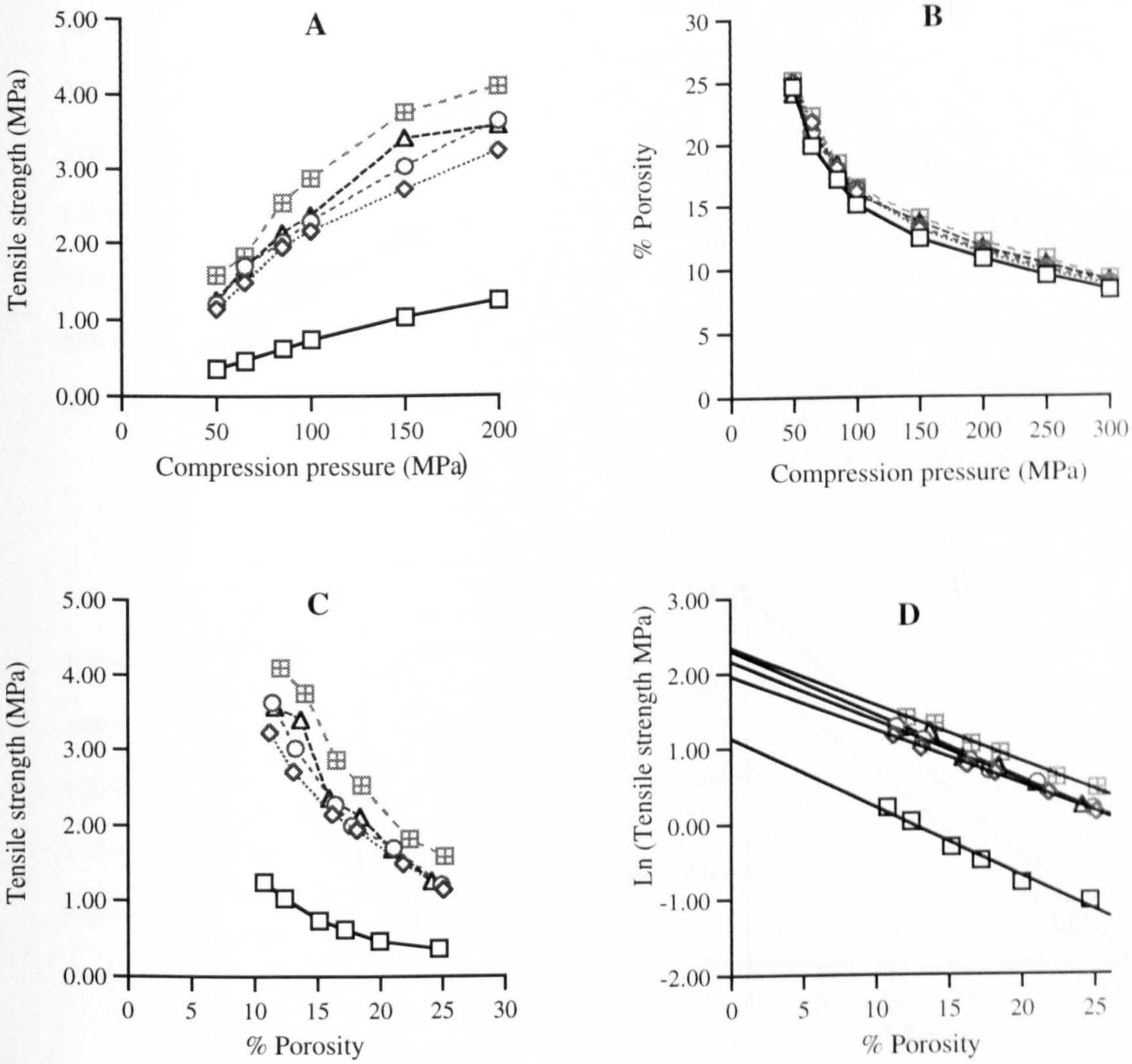

Figures 6.1 Effect of crystallisation cooling rate on the tensile strenght and porosity of dextrose compacts

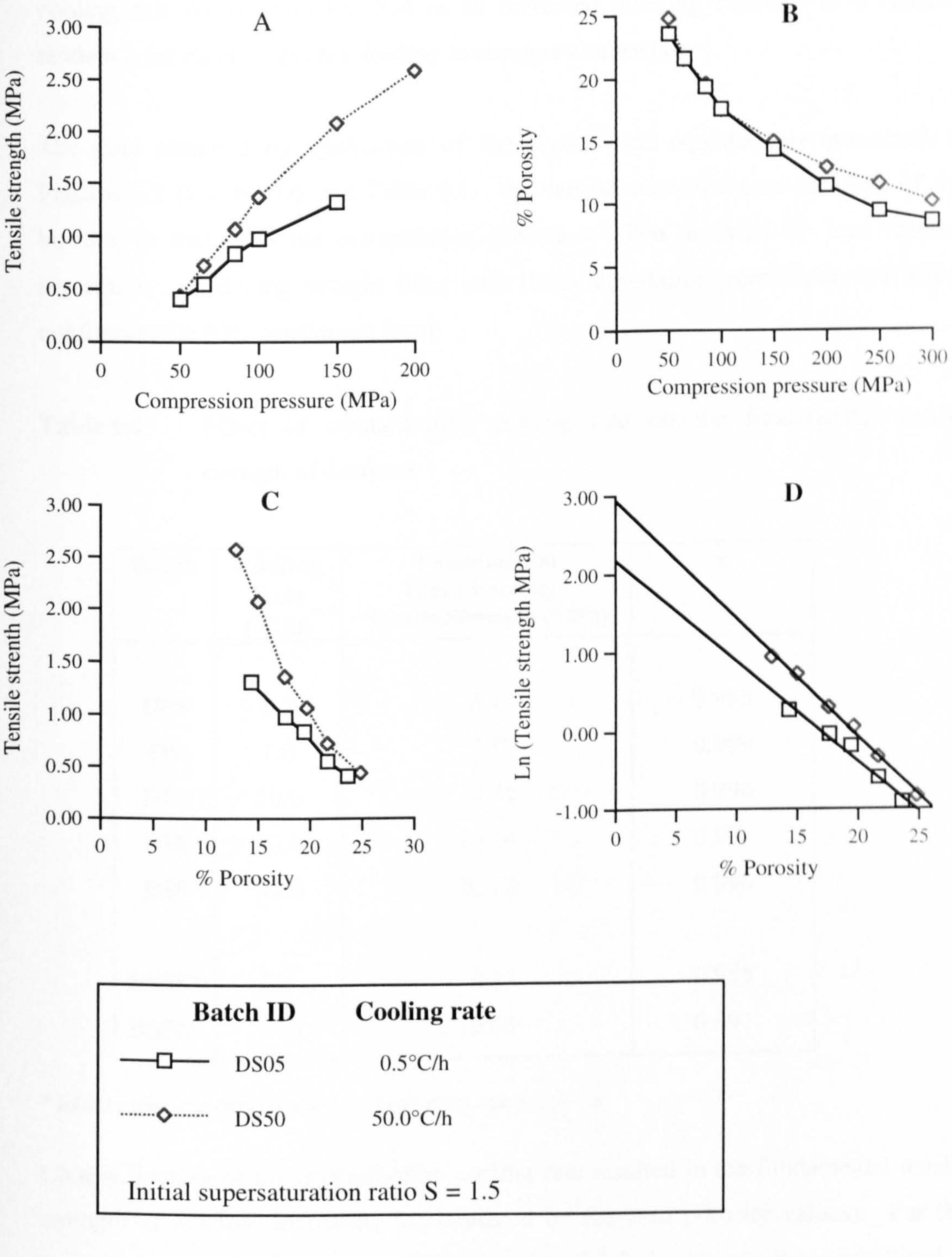

Figure 6.2 Effect of crystallisation cooling rate on the tensile strength and porosity of dextrose compacts

at equivalent porosity values. This would suggest that increasing the crystallisation cooling rate of dextrose resulted in an increased bonding capacity or a reduced tendency for elastic recovery, leading to stronger compacts.

The data obtained by application of the Ryskewitch equation are presented in Figures 6.1 (D), 6.2(D) and Table 6.1. As can be seen, the data for each of the batches fit well with the extrapolation procedure when assessed by least squares regression, producing straight lines with linear correlation coefficients (r) which conform at the 99% confidence level.

Table 6.1 Effect of crystallisation cooling rate on the fundamental tensile strength of dextrose

Batch	Cooling Rate (°C/h)	Fundamental (Zero Porosity) Tensile Strength (MPa)	r
D05	0.5	3.12	0.988
D1	1.0	7.17	0.999
D10	10.0	8.71	0.996
D30	30.0	10.10	0.990
D50	50.0	10.18	0.996
DS05*	0.5	8.83	0.985
DS50*	50.0	19.05	0.997

* Initial supersaturation ratio S=1.5. In all other batches S=1.3.

Clearly, increasing the crystallisation cooling rate resulted in the fundamental tensile strength of dextrose increasing (as indicated by the zero porosity values). For the batches prepared with a supersaturation ratio of 1.3, increasing the crystallisation cooling rate from 0.5 to 50.0°C/h increased the fundamental tensile strength from 3.12 to 10.18 MPa.

These results correspond with the trend observed in the true density results (section 4.4.1) which suggested that a subtle change in crystal structure took place with changing crystallisation cooling rate. As the cooling rate was increased the true density values decreased possibly indicating the presence of more crystal imperfections. This has previously been shown to increase the ability of a material to produce good compacts. The increase in tensile strength also corresponds to the increase in linear growth rate. This factor has also been shown to increase the defect density within a crystal lattice. These changes in crystal structure are probably also responsible for the increase in the fundamental tensile strength of dextrose with increasing crystallisation cooling rate (as observed from the zero porosity values) due to the presence of defects that disrupt the flow of slip planes along which deformation and fracture would normally take place.

6.2.2 Effect of initial supersaturation ratio

The effect of initial supersaturation ratio on the tensile strength of dextrose and its compacts was evaluated by comparison of batches which were crystallised under the same conditions except for differences in the initial supersaturation ratios.

For each set of comparable batches, the interrelationship between tensile strength porosity and compression pressure is illustrated in Figures 6.3, 6.4, 6.5 and 6.6. Increasing the initial supersaturation ratio is seen to cause a general increase in the tensile strength of dextrose compacts (especially at the higher compaction forces). As previously noted, there was again a maximum value of compression pressure above which compacts capped or laminated on testing and so a tensile strength value could not be calculated. This effect also appeared to be related to the initial supersaturation level. For example, considering batches D05, DS05 and DR30 with initial supersaturation ratios of 1.3, 1.5 and 1.6 respectively. The maximum compression pressure which produced compacts that subsequently failed in tension increased from 150 to 200 MPa with increasing initial supersaturation ratio, and the maximum tensile strength of the compacts increased from 1.25 to 2.90 MPa. This increase in tensile strength follows the same trend as the linear growth rates, which also increased with initial supersaturation ratio (section 4.2.2). It is therefore likely that the increased in tensile strength is due to an increased crystal defect density resulting from the faster growth rates experienced.

When the Ryskewitch equation was applied to the data, the linear correlation coefficients (r) obtained all confirmed linear correlation at the 99% confidence level. The calculated fundamental (zero porosity) tensile strength of dextrose crystallised at a series of initial supersaturation ratios is detailed in Table 6.2. In all cases, the fundamental tensile strength of dextrose is seen to increase with increasing initial supersaturation ratio. For example, by raising the initial supersaturation ratio from 1.3 (D05) to 1.6 (DR30) the fundamental tensile strength of dextrose is raised from 3.12 to 33.11MPa. This may be due to the fact that at different initial supersaturation ratios different growth mechanisms predominate and so changes in the crystal structure and defect density may occur resulting in modified deformation, consolidation and bonding behaviour.

Table 6.2 Effect of initial supersaturation ratio on the fundamental tensile strength of dextrose

Batch	Supersaturation Ratio	Fundamental (Zero Porosity) Tensile Strength MPa)	r
D05	1.30	3.12	0.988
DS15	1.50	8.83	0.985
DR30	1.60	33.11	0.993
D50*	1.30	10.18	0.996
DS50*	1.50	19.05	0.991
DC40	1.30	4.27	0.998
DR40	1.50	12.55	0.997
DC45	1.30	4.92	0.993
DR45	1.40	6.96	0.997
DR51	1.10	3.22	0.996
DC51	1.30	11.01	0.997

* These batches were prepared at a cooling rate of 50°C/h. All other batches were prepared at a cooling rate of 0.5°C/h.

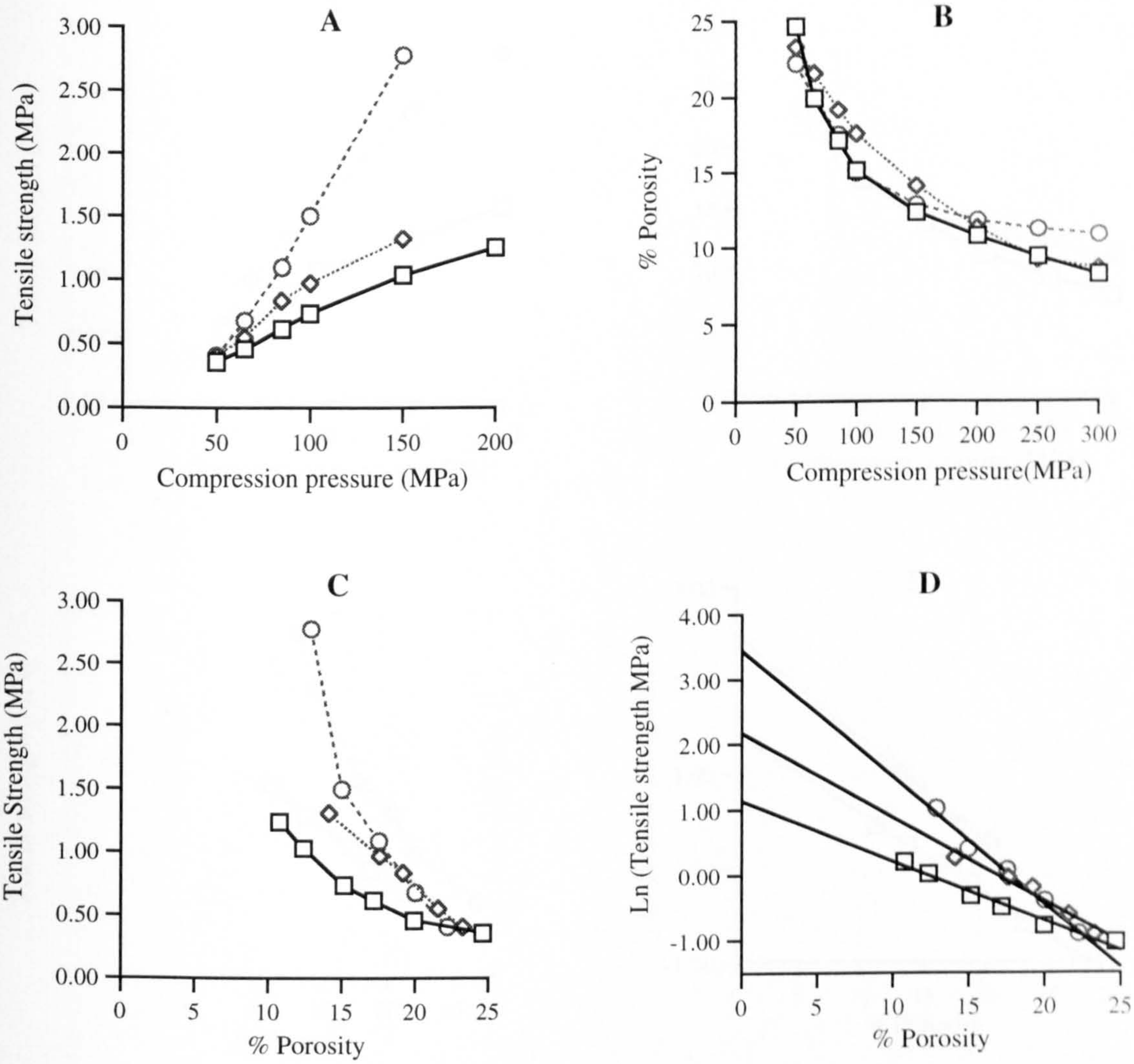

Figure 6.3 Effect of initial supersaturation ratio on the tensile strength and porosity of dextrose compacts

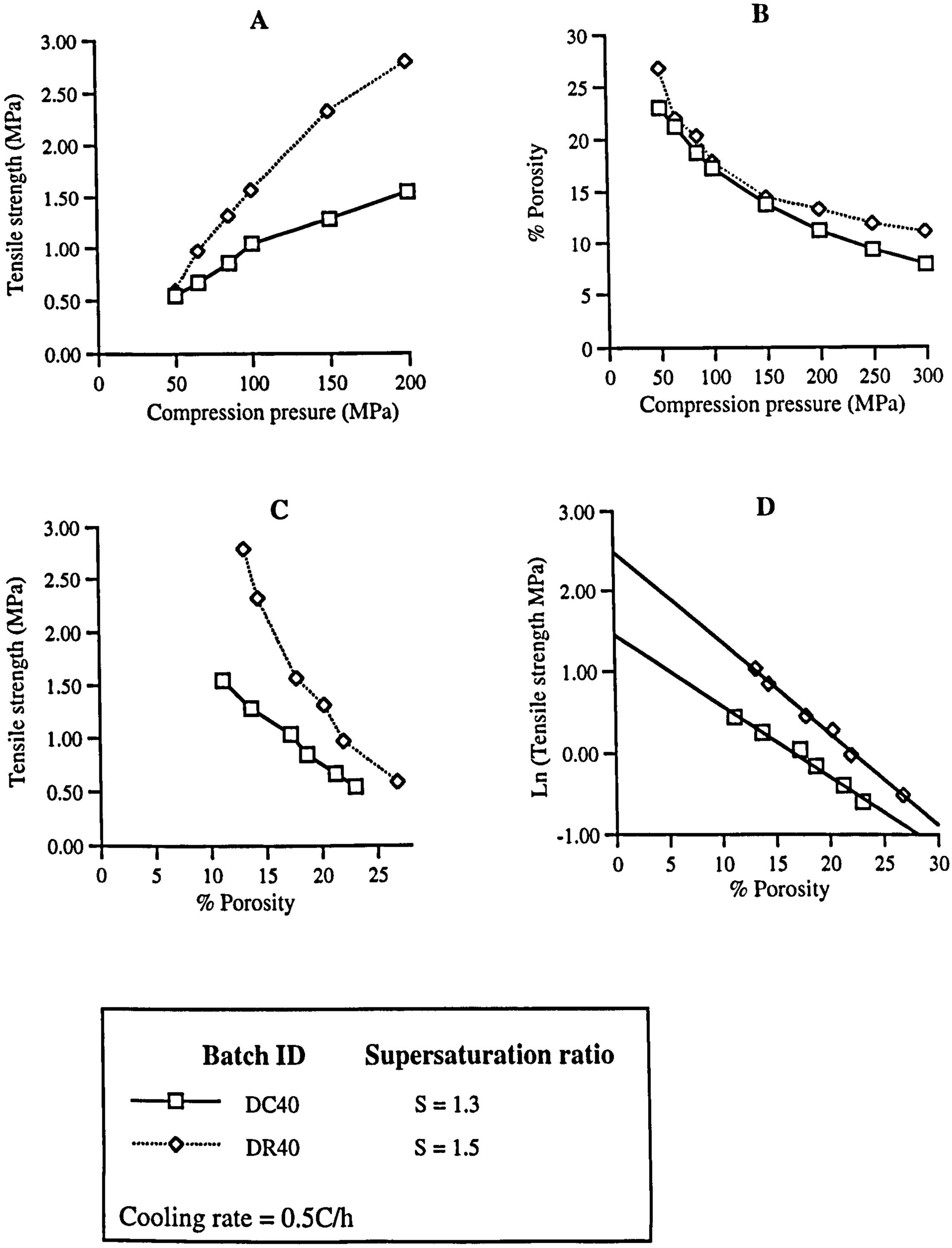

Figure 6.4 Effect of initial supersaturation ratio on the tensile strength and porosity of dextrose compacts

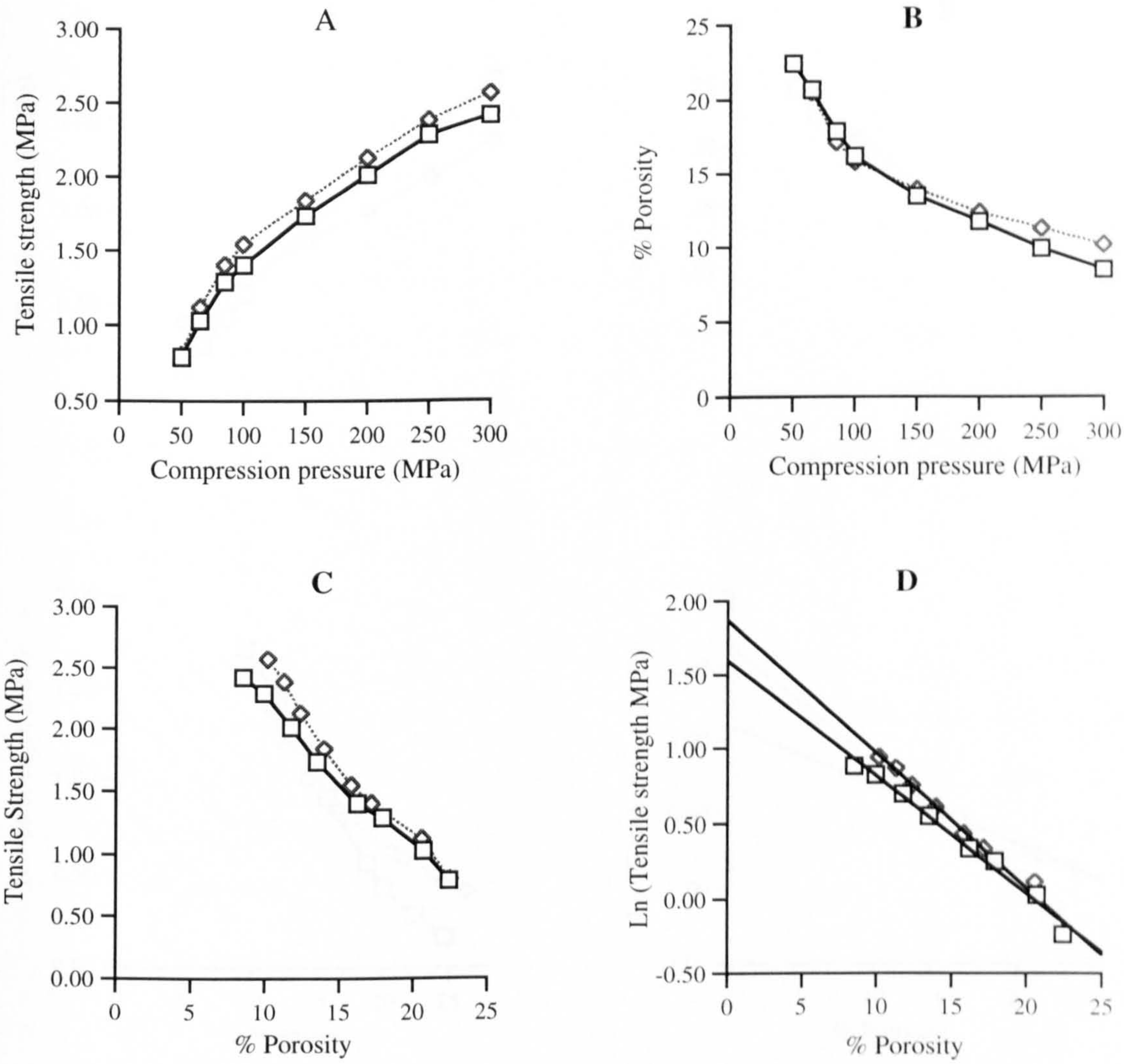

Figure 6.5 Effect of initial supersaturation ratio on the tensile strength and porosity of dextrose compacts

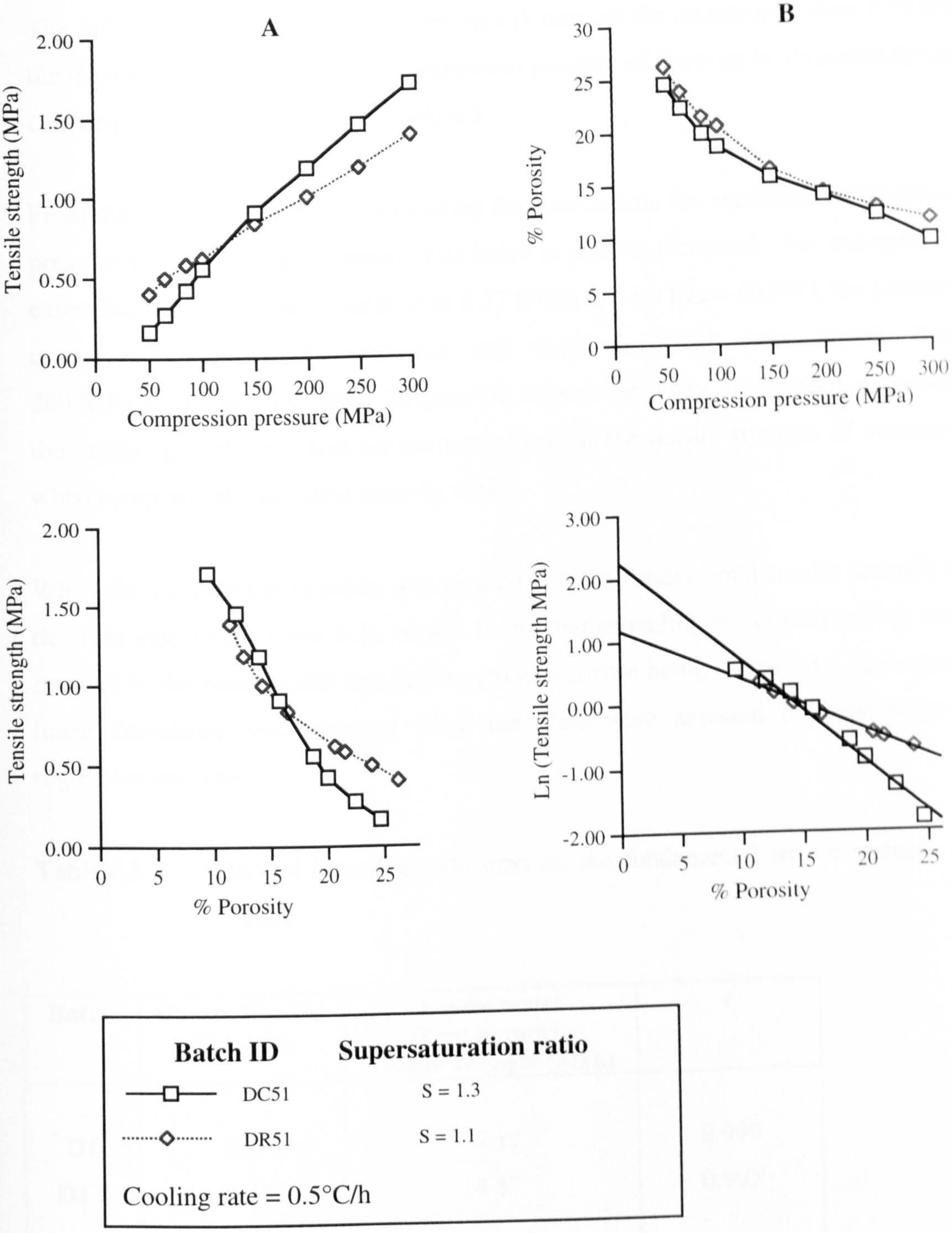

Figure 6.6 Effect of initial supersaturation ratio on the tensile strength and porosity of dextrose compacts

6.2.3 Effect of crystal growth time

The influence of increasing the crystal growth time on the interrelationships between the tensile strength, porosity and compression pressure of dextrose is illustrated by the data displayed in Figure 6.7 and Table 6.3.

From the data it is clear that by extending the growth time the maximum compression pressure which produced compacts that failed in tension increased. For example, by extending the crystallisation time from 0.27 (D30) to 16.0 hours (D30T), the pressure at which compacts that did not cap could be made was raised, from 200 MPa to at least 300 MPa. Despite the reduced tendency for capping, extending the crystal growth time had no positive effect on the tensile strength of compacts when compared at equivalent porosity values.

When the Ryskewitch equation was applied and the fundamental tensile strength of dextrose calculated (Table 6.3), it was found that extending the crystal growth time resulted in the fundamental tensile strength of dextrose being increased. Again good linear correlation was obtained when the plots were assessed by least squares regression analysis.

Table 6.3 Effect of crystal growth time on the fundamental tensile strength of dextrose

Batch	Crystallisation Time (h)	Fundamental (Zero Porosity) Tensile Strength (MPa)	r
D1	8.0	7.17	0.999
D1T	16.0	14.57	0.992
D30	0.27	10.10	0.990
D30T	16.0	19.10	0.997

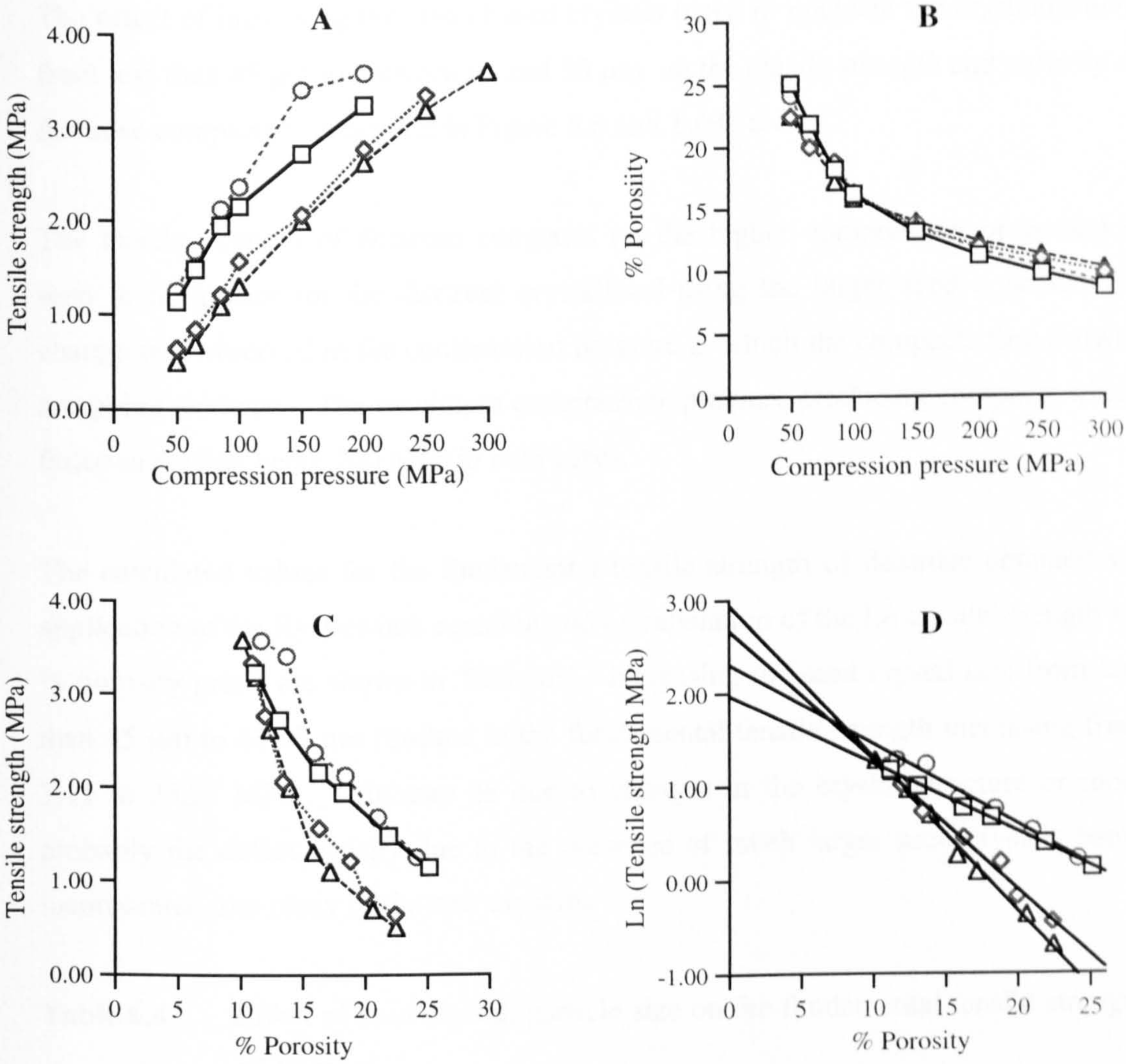

Batch ID		Crystallisation time	Cooling rate
—□—	D1	8 hours	1.0C/h
·····◇·····	D1T	16 hours	1.0°C/h
----○----	D30	0.27 hours	30.0°C/h
----△----	D30T	16 hours	30.0°C/h

Initial supersaturation ratio S = 1.3

Figure 6.7 Effect of crystal growth time on the tensile strength and porosity of dextrose compacts

6.2.4 Effect of seed crystal, particle size

The effect of increasing the size of seed crystals (used to nucleate the crystallisation) from less than 45 μm to between 63 and 90 μm on the tensile strength and porosity of dextrose compacts is presented in Figure 6.8 and Table 6.4.

The tensile strength of dextrose compacts (at the higher compression pressures) is seen to be greater for the dextrose crystallised using the larger seed crystals. No change was observed in the compression pressure at which the compacts first showed a capping tendency. The maximum compression pressure producing compacts which failed in tension being 200 MPa in both cases.

The calculated values for the fundamental tensile strength of dextrose obtained via application of the Ryskewitch equation and extrapolation of the Ln tensile strength vs. % porosity graph are shown in Table 6.4. Increasing the seed crystal size from less than 45 μm to 63-93 μm resulted in the fundamental tensile strength increasing from 3.11 to 25.27 MPa. This may be due to changes in the crystal structure or more probably the defect density due to the presence of much larger seed crystals being incorporated into many of the new crystals.

Table 6.4 Effect of seed crystal, particle size on the fundamental tensile strength of dextrose

Batch	Seed Size (μm)	Fundamental (Zero Porosity) Tensile Strength (MPa)	r
D05	> 45	3.11	0.988
DX05	63 - 90	25.27	0.997

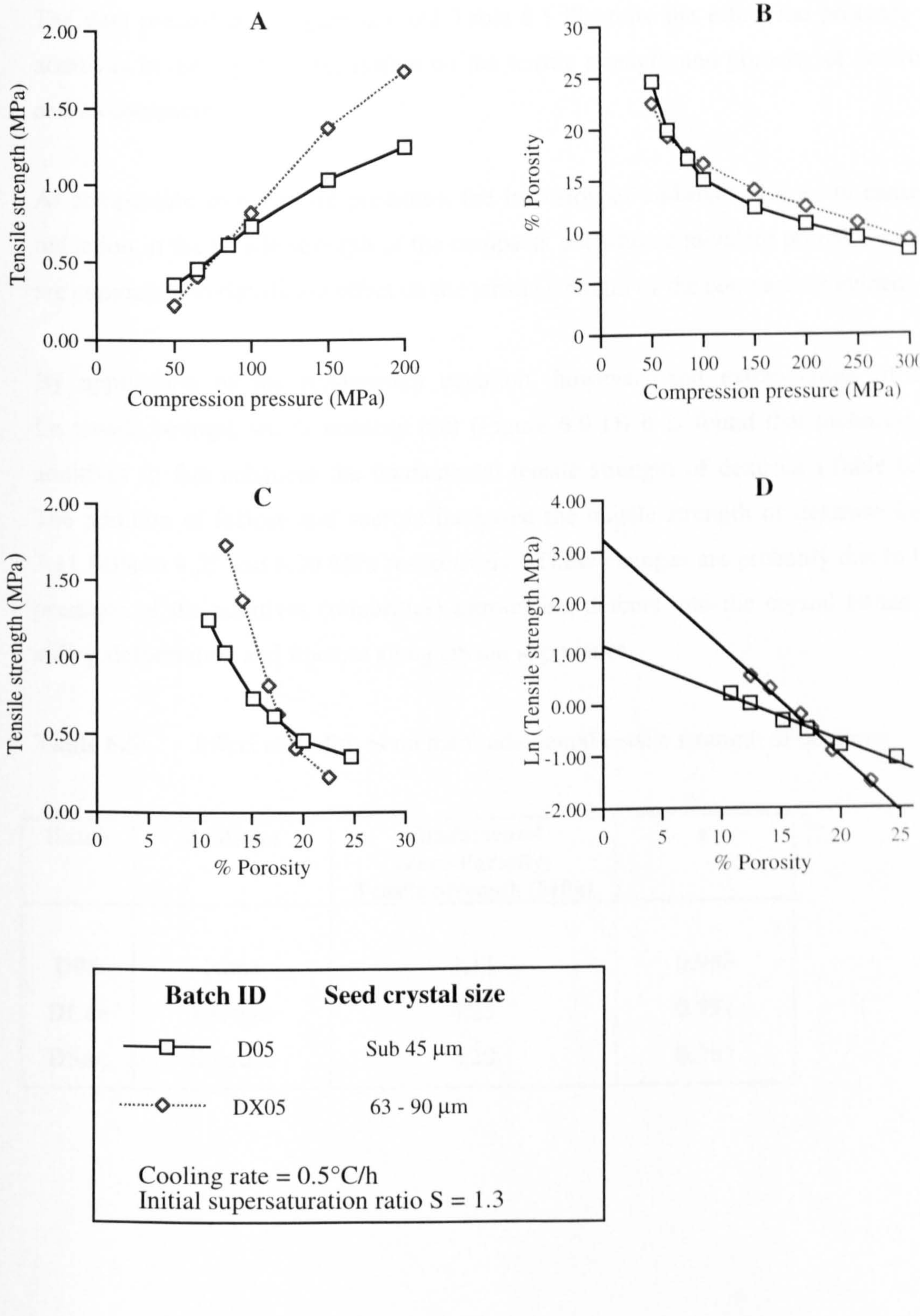

Figure 6.8 Effect of seed crystal particle size on the tensile strength and porosity of dextrose compacts

6.2.5 Effect of additives

The data presented in Figure 6.9 and Table 6.5 illustrate the effect the presence of additives in the crystallising system on the tensile strength and porosity of dextrose and its compacts.

At comparable compression pressures, the inclusion of additives is seen to cause a reduction in the tensile strength of the compacts but when equivalent porosity values are compared no significant effect on the tensile strength of the compacts is evident.

By application of the Ryskewitch equation, however, and extrapolation of the Ln tensile strength vs. % porosity plot (Figure 6.9 D) it is found that inclusion of additives in fact enhances the fundamental tensile strength of dextrose (Table 6.5). The addition of lactose and sucrose increased the tensile strength of dextrose from 3.11 MPa to 4.25 and 6.20 MPa respectively. These changes are probably due to the presence of the additives (impurities) introducing defects into the crystal lattice so aiding deformation and fracture along crystal slip planes.

Table 6.5 Effect of additives on the fundamental tensile strength of dextrose

Batch	Additive	Fundamental (Zero Porosity) Tensile Strength (MPa)	r
D05	None	3.11	0.988
DLac	Lactose	4.25	0.991
DSuc	Sucrose	6.20	0.987

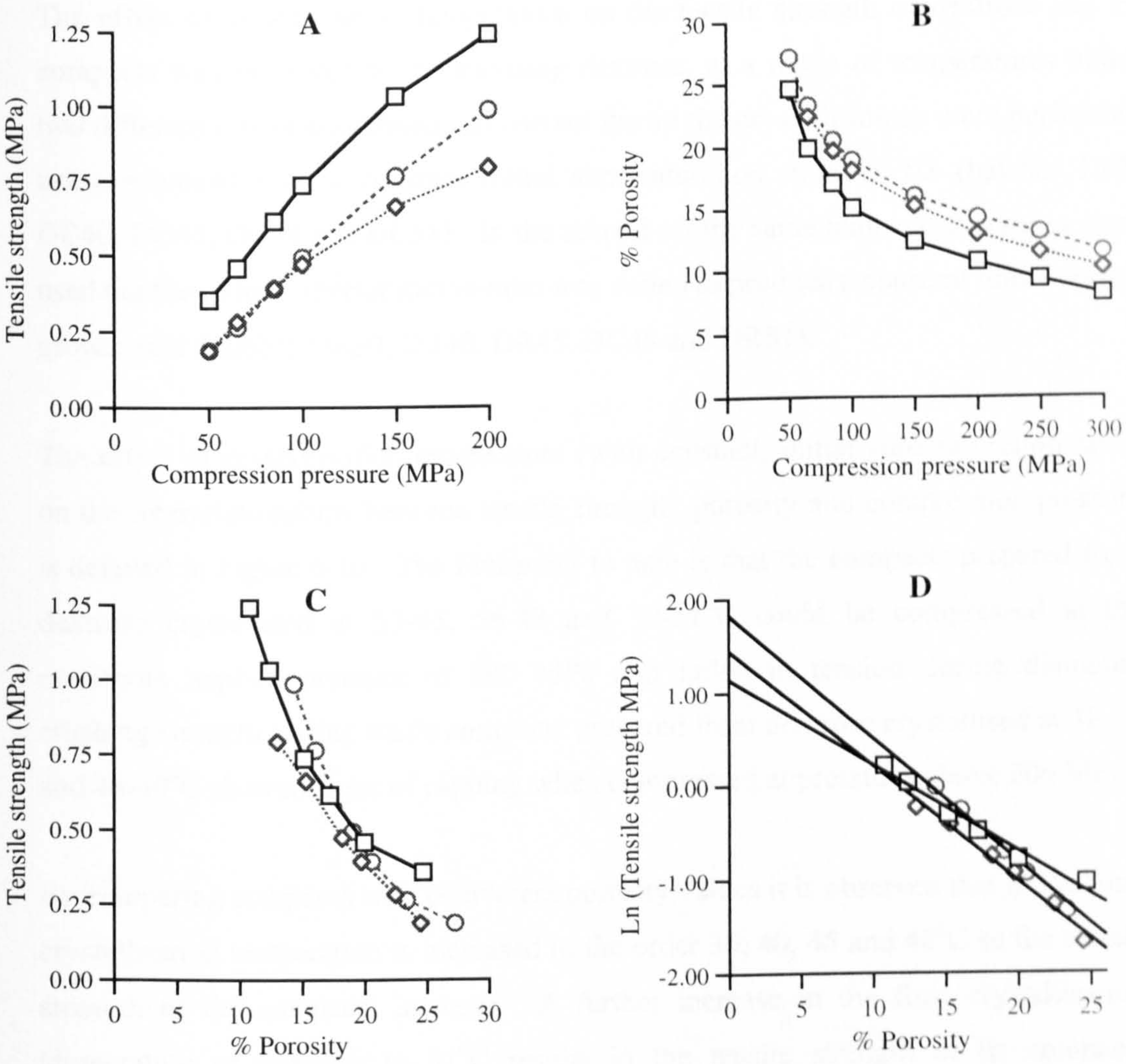

Figure 6.9 Effect of additives on the tensile strength and porosity of dextrose compacts

6.2.6 Effect of crystallisation temperature

The effect of crystallisation temperature on the tensile strength of dextrose and its compacts was evaluated by crystallising dextrose, at a range of temperatures under two different sets of conditions. In one set the all the crystallisations were performed using solutions with a constant initial supersaturation ratio of 1.3 (batches D05, DC40, DC45, DC48 and DC51). In the second set the same temperature ranges were used but the initial supersaturation ratio was varied to produce a constant linear crystal growth rate (batches DR30, DR40, DR45, DC48 and DR51).

The effect of crystallisation temperature (with constant, initial supersaturation ratio) on the interrelationships between tensile strength, porosity and compression pressure is detailed in Figure 6.10. The first point to note is that the compacts prepared from dextrose crystallised at 53-45, 56-48 and 59-51°C could be compressed at the maximum applied pressure of 300 MPa and failed in tension during diametral crushing strength testing while compacts prepared from dextrose crystallised at 38-30 and 48-40°C showed signs of capping when compressed at pressures above 200 MPa.

By comparing compacts with equivalent porosity values it is observed that as the final crystallisation temperature is increased in the order 30, 40, 45 and 48°C so the tensile strength of the compacts increase. A further increase in the final crystallisation temperature of dextrose to 51°C results in the tensile strength of its compacts decreasing again. By applying the Ryskewitch equation, however, and extrapolating the Ln tensile strength vs. % porosity plot it is revealed that the fundamental tensile strength of dextrose (crystallised at various temperature ranges) increases with increasing final crystallisation temperate for all the batches (Table 6.6). This increase in tensile strength corresponds to the increase in linear crystal growth rates (section 4.2.1) and the decrease in moisture contents (section 4.6.1) which were observed with increasing final crystallisation temperature.

Considering now the batches of dextrose crystallised at different temperatures but with a constant linear crystal growth rate. The variation of tensile strength, porosity and compression pressure is illustrated in Figure 6.11. As with the previous set of batches the capping tendency of compacts is reduced for the compacts prepared using dextrose crystallised at 53-45, 56-48 and 59-51°C. This corresponds to the batches

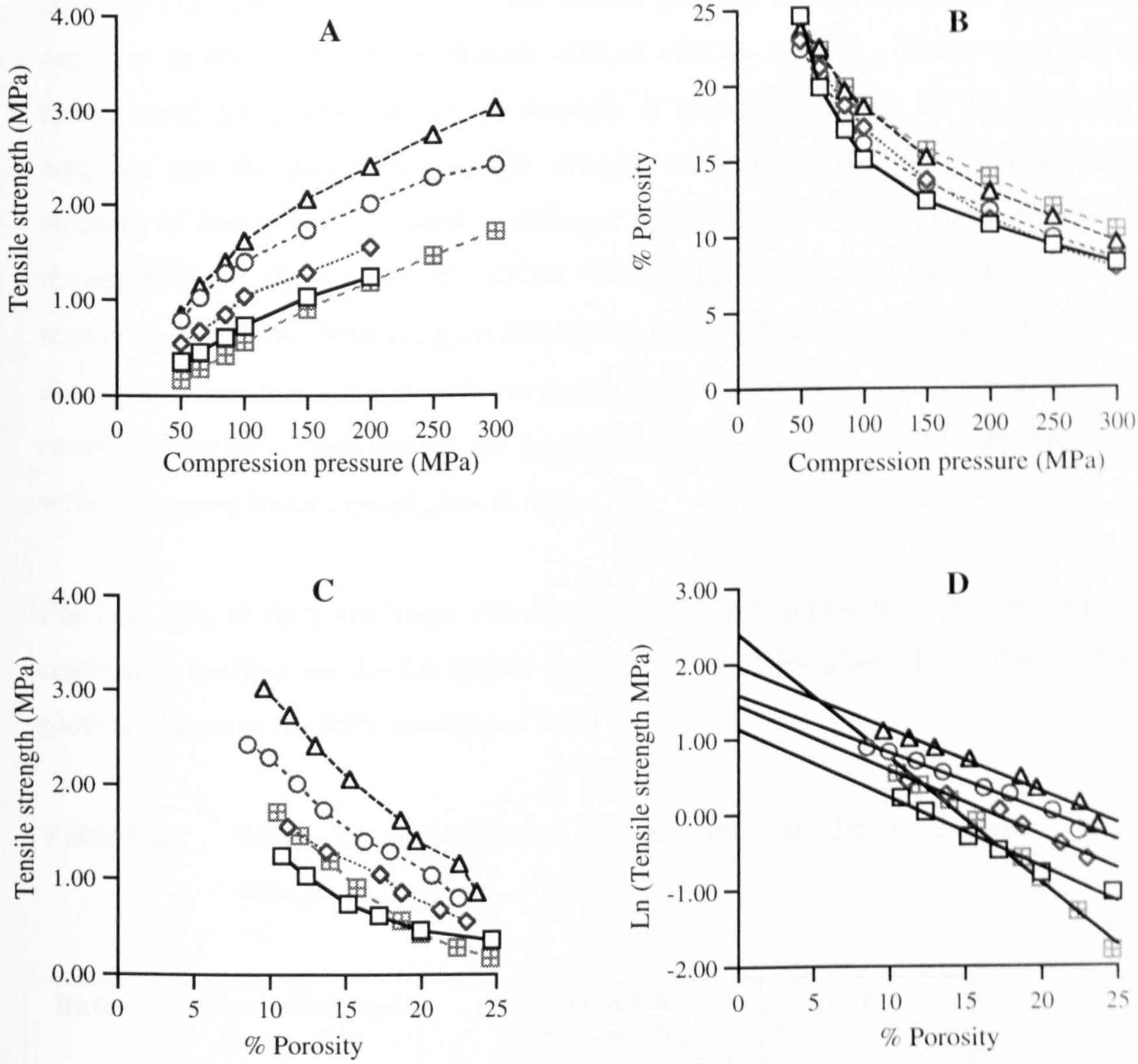

Batch ID	Crystallisation temperature range
D05	38 - 30°C
DC40	48 - 40°C
DC45	53 - 45°C
DC48	56 - 48°C
DC51	59 - 51°C

Cooling rate = 0.5°C/h
Initial supersaturation ratio S = 1.3

Figure 6.10 Effect of crystallisation temperature (constant initial supersaturation ratio) on the tensile strength and porosity of dextrose compacts

with the lowest moisture contents (section 4.6.1). When compacts of equivalent porosity (i.e. 10%) are compared the tensile strength of the compacts are seen to decrease in the order DR30 >DR40 >DR48 >DC45 >DR51. However when the fundamental (zero porosity) tensile strength is calculated by use of the Rystewitch equation and the plot of Ln tensile strength vs. porosity the fundamental tensile strength of dextrose crystallised at different temperatures is observed to decrease in the order DR30 >DR40 >DR45 = DC48 >DR51 (Table 6.6). This general decrease in tensile strength with increasing crystallisation temperature corresponds to the general decrease in moisture content with increasing temperature. This trend, however, is the reverse of the trend obtained for the dextrose crystallised at different temperatures but with increasing linear crystal growth rates.

For both sets of data, the linear correlation coefficients (r) obtained by least squares regression analysis on the Ln tensile strenght vs porosity plots all confirm that the plots are linear at the 95% confidence level

Table 6.6 Effect of crystallisation temperature on the fundamental tensile strength of dextrose

Batch	Crystallisation Temp (°C)	Fundamental (Zero Porosity) Tensile Strength MPa)	r
D05	38-30	3.12	0.988
DC40	48-40	4.27	0.998
DC45	53-56	4.92	0.993
DC48	56-48	7.13	0.987
DC51	59-51	11.01	0.997
DR30	38-30	33.11	0.994
DR40	48-40	12.55	0.998
DR45	53-45	7.06	0.997
DC48	56-48	7.13	0.987
DR51	59-51	3.22	0.996

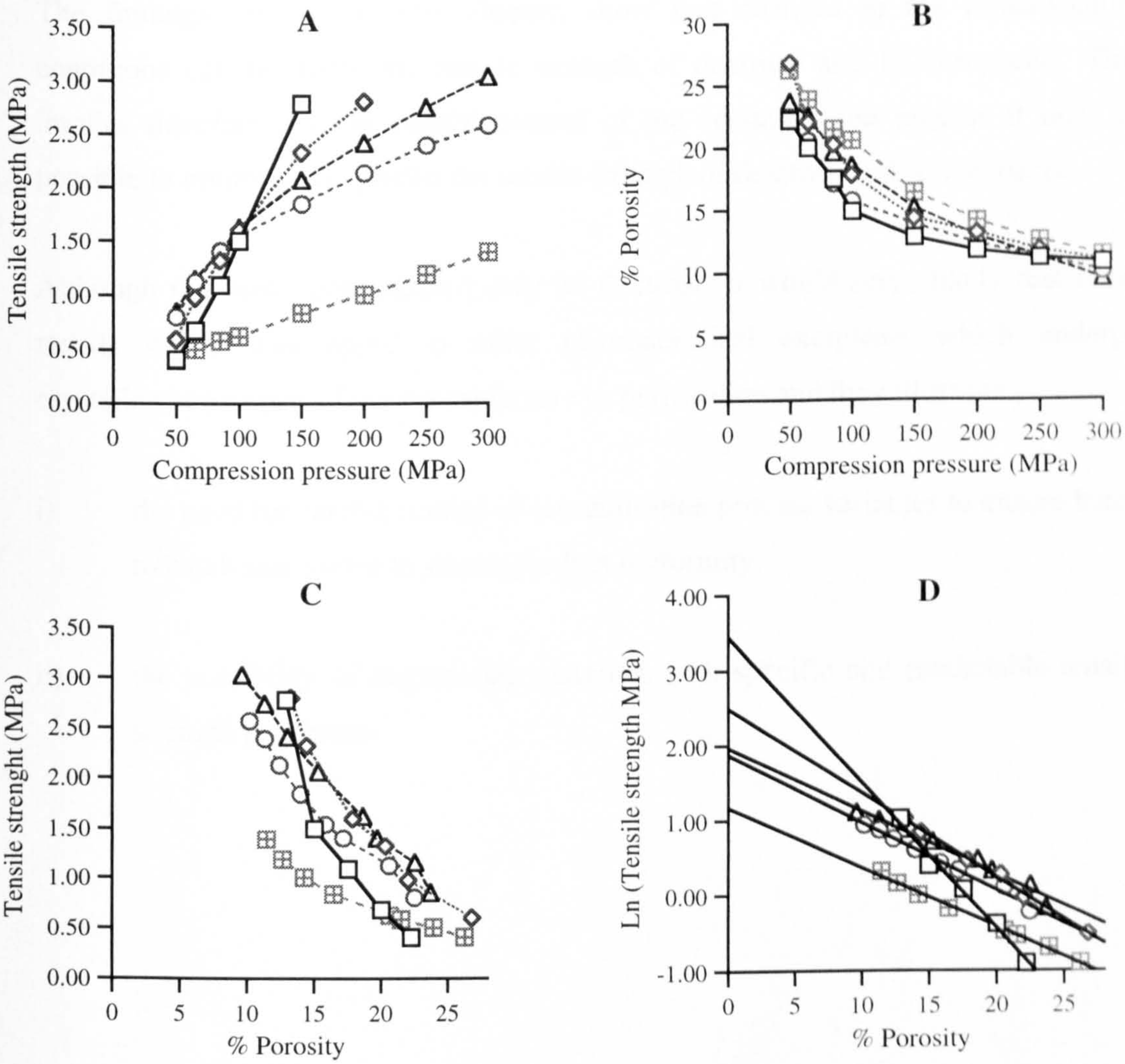

Batch ID		Crystallisation temperature range	Initial supersaturation ratio
—□—	DR30	38 - 30°C	S = 1.6
·····◇·····	DR40	48 - 40°C	S = 1.5
----○----	DR45	53 - 45°C	S = 1.4
----△----	DC48	56 - 48°C	S = 1.3
- - -⊞- - -	DR51	59 - 51°C	S = 1.1

Cooling rate = 0.5°C/h

Figure 6.11 Effect of crystallisation temperature (constant linear crystal growth rate) on the tensile strength and porosity of dextrose compacts

6.3 Discussion

The findings reported in this chapter, show that changes in the crystallisation conditions can influence the tensile strength of dextrose and its compacts. This implies therefore that by careful control of the crystallisation process it may be possible to optimise and predict the tensile strength of dextrose and its compacts.

Although this work concentrated only on dextrose, it would seem likely that these results would also apply to other pharmaceutical excipients which undergo crystallisation as part of their manufacture or purification and they illustrate:

i) the need for careful control of crystallisation process variables to ensure batch to batch and source to source product uniformity.

ii) the possibility of engineering materials with specific and predictable tensile strength properties.

CHAPTER SEVEN

BRINELL HARDNESS, ELASTIC MODULUS AND ELASTIC QUOTIENT OF DEXTROSE COMPACTS

7.1 Introduction

This chapter presents the mechanical data (i.e. Brinell hardness, elastic modulus and elastic quotient) obtained from the indentation studies performed on the compacts of dextrose, as described in Chapter 3. It focuses primarily on the effects of crystallisation variables on the above properties as determined directly from testing dextrose compacts. It also considers the effect of crystallisation conditions on the fundamental (zero porosity) Brinell hardness and elastic modulus of dextrose as calculated for each of the batches by application of an extrapolated exponential equation (Spriggs' equation) to the compact data, as described in section 1.3.7. The validity of using this equation to estimate the fundamental (zero porosity) material property was assessed by the linear correlation coefficient (r), a value of 1.0 corresponding to a completely linear relationship.

During indentation testing of the compacts it was found that both the Brinell hardness and elastic modulus steadily increased with increasing compression pressure (decreasing porosity) up to a specific point before they decreased again. It was observed that this apparent drop in the mechanical property from a maximum value always occurred for the compacts that did not fail in tension during diametrical crushing strength tests. It is believed that when the indenter tip was compressed onto these compacts the excess stored elastic energy (which caused the compacts to cap) resulted in a greater depth of indentation and thus falsely low hardness and elastic modulus values. Therefore, only those values obtained from compacts which failed in tension during the diametrical crushing strength testing were considered to be real and thus valid for use with the extrapolated exponential equation and for comparisons between the different batches. All the experimentally obtained data will be presented in the Figures of Brinell hardness vs. compression pressure and Brinell hardness vs. % porosity. The Brinell hardness data are considered in section 7.2 while the elastic modulus and elastic quotient results are discussed in section 7.3 and 7.4 respectively.

7.2 Effect of crystallisation conditions on the Brinell hardness of dextrose and its compacts

Hardness as measured by indentation is a way of evaluating a material's resistance to local deformation and is therefore a measure of its plasticity and is often used to characterise its compressibility. Brinell hardness has proved to be a suitable measure of the deformation resistance of tablets and pharmaceutical materials (Leuenberger et al., 1981). It must be remembered that it is the Brinell hardness of the compact that is being directly measured and thus the values obtained are a function not only of the material (dextrose) being compressed but also of the porosity (degree of consolidation) and the bonding within the compact resulting from the compression process.

The Brinell hardness (BH) of dextrose compacts was determined by indentation testing as described in section 3.4.9 and using equation 3.7:

$$BH = \frac{F}{\pi D h_1} \qquad \text{(equation 3.7)}$$

where h_1 is the depth of indentation, F is the applied force and D is the diameter of the indenter.

The Brinell hardness results quoted were calculated from the mean indentation depth recorded from 10 compacts. The relative standard deviations for each set of data ranged from 5 - 15% which appears to be large values considering the accuracy of the method. They are, however, typical of those reported by other workers and have been attributed to the problem of using a point method on a surface that in inherently heterogeneous and on a material which would be expected to anisotropic (have different properties on different crystal faces).

Throughout this section each Figure contains three graphs, A illustrates the variation of compact Brinell hardness with compression pressure, B presents the variation of compact Brinell hardness with compact porosity and C displays the data obtained using the extrapolated exponential equation.

7.2.1 Effect of crystallisation cooling rate

The Brinell hardness data obtained from compacts prepared using dextrose crystallised using various crystallisation cooling rates are illustrated in Figures 7.1 and 7.2. From both sets of data it is clear that the Brinell hardness values of compacts increases with increasing compression pressure (decreasing porosity). This is most likely to be due to the increasing densification of dextrose producing a more rigid and thus harder compact. In all cases the decline from the maximum value occurred for the compacts that did not fail in tension during the diametrical crushing strength testing (i.e. showed a tendency to cap or laminate) and so these values were not considered valid for use in comparing the various batches.

Comparing the results obtained at equivalent porosity values it is seen that increasing the crystallisation cooling rate of dextrose causes an increase in the Brinell hardness of the subsequent compacts. Initially this would appear to indicate that a greater degree of plastic deformation may be taking place with increasing crystallisation cooling rate. However this is not supported by the data from the Heckel plots (chapter 5) which showed that the mean yield pressure (and thus plastic deformation) was independent of the crystallisation cooling rate. Therefore, the increase in Brinell hardness must be due to increased bonding between the crystals within the compacts resulting in a greater resistance to deformation by the indenter. This is supported by the previous findings that tensile strength increased with increasing crystallisation cooling rate (section 6.2.1). A possible explanation for this may lie in the fact that the particle size distribution skewed towards the lower end of the 63-90 μm selected size range (section 4.7.1) with increasing crystallisation cooling rate, thus resulting in the availability of more bonding surfaces.

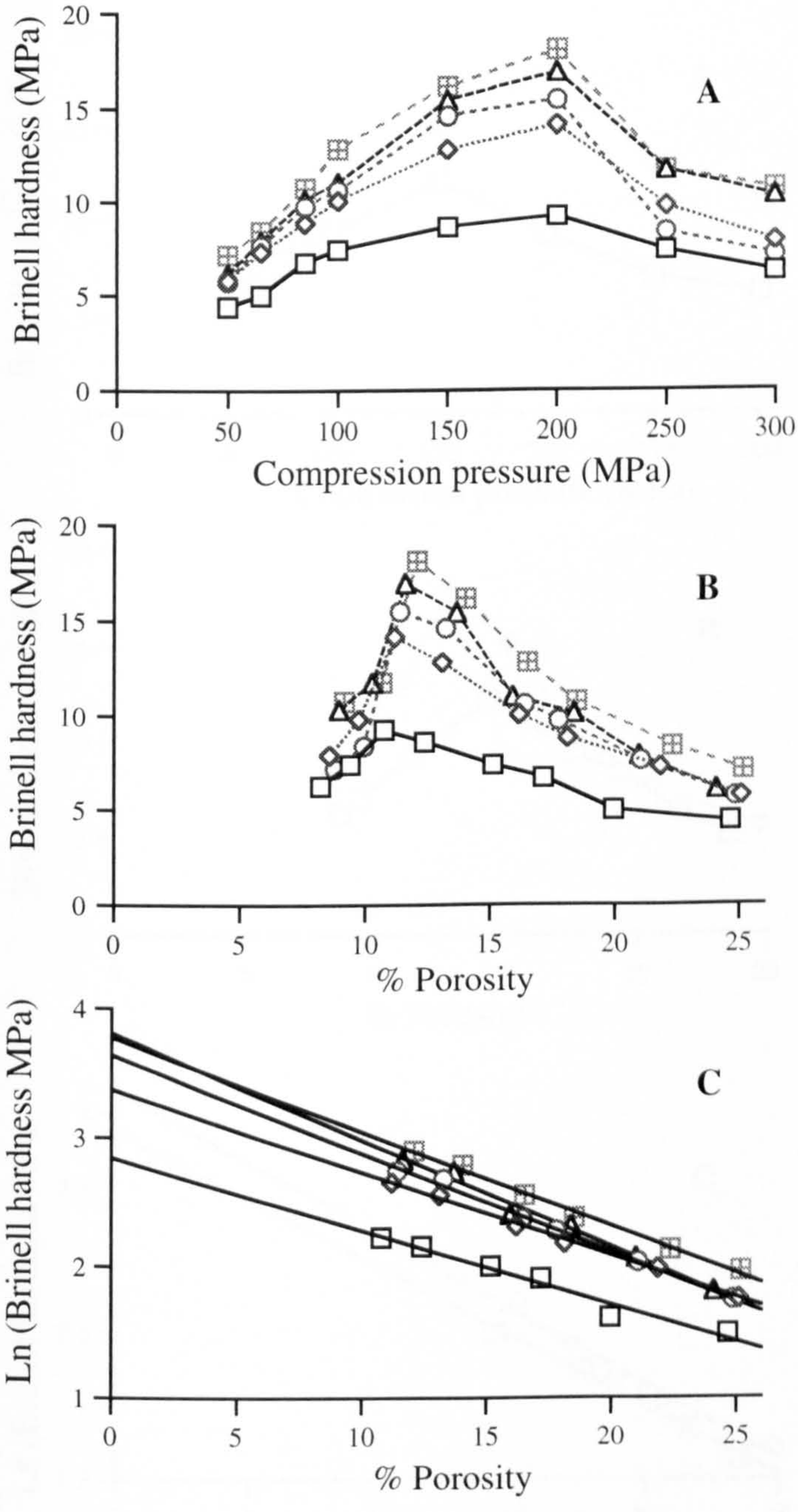

Figure 7.1 (A-C) Effect of crystallisation cooling rate on the Brinell hardness of dextrose compacts

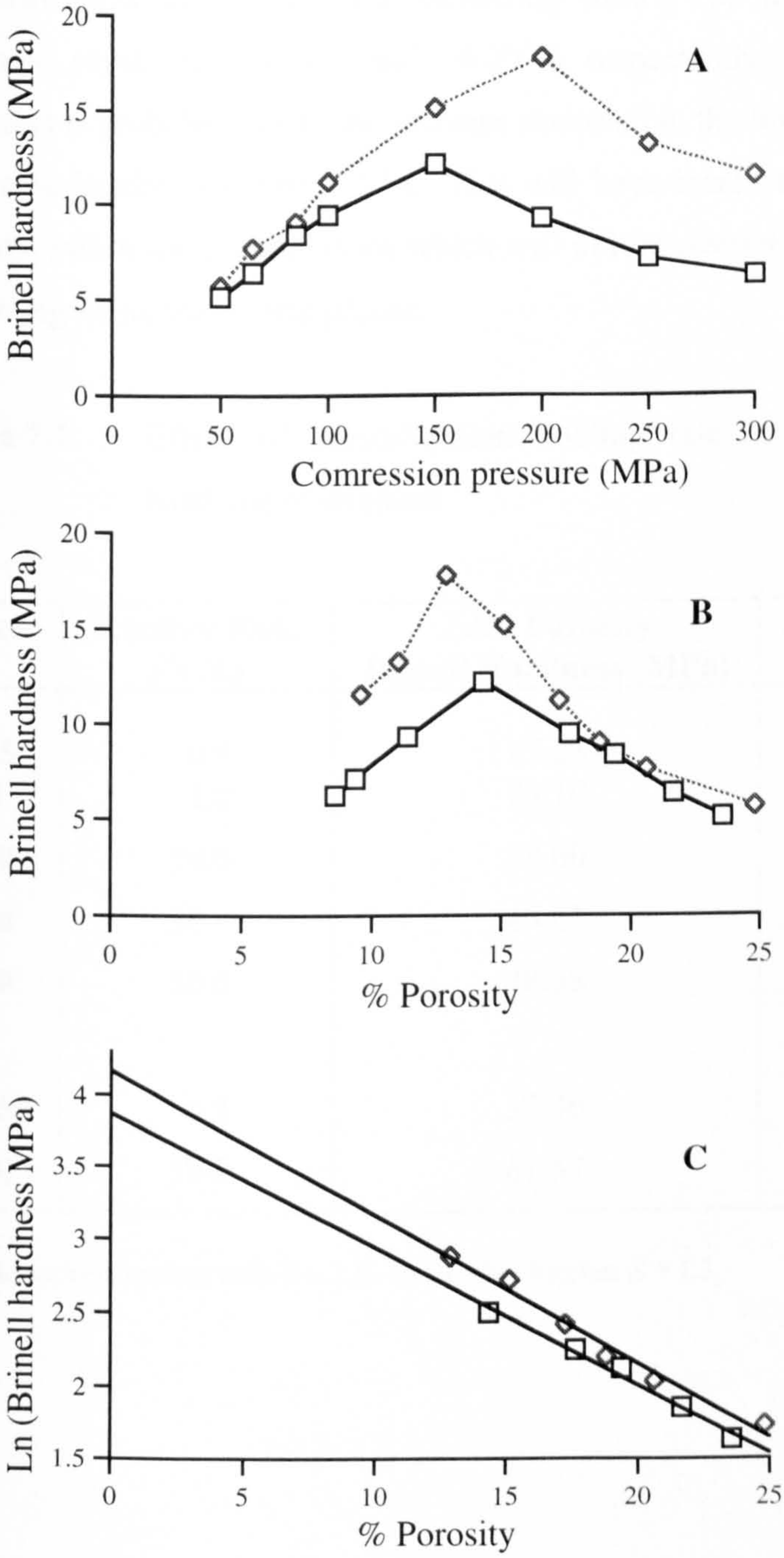

Figure 7.2 (A-C) Effect of crystallisation cooling rate on the Brinell hardness of dextrose compacts

The calculated fundamental (zero porosity) Brinell hardness values presented in Table 7.1 also show the same trend, increasing from 17.25 MPa to 48.38 MPa for the dextrose crystallised at 0.5 and 50.0°C/h respectively. This increase in Brinell hardness is probably due to the increase observed in the linear crystal growth rates for the same batches (section 4.2.1). This will have increased the dislocations (defect) density within the crystal lattice which will in turn restrict the amount of deformation occurring along the crystal planes.

Table 7.1 Effect of crystallisation cooling rate on the fundamental Brinell hardness of dextrose

Batch	Cooling Rate (°C/h)	Zero Porosity Brinell Hardness (MPa)	r
D05	0.5	17.25	0.984
D1	1.0	29.10	0.987
D10	10.0	38.00	0.990
D30	30.0	45.01	0.992
D50	50.0	48.38	0.992
DS05*	0.5	32.36	0.983
DS50*	50.0	61.57	0.989

* Initial supersaturation ratio S = 1.5. In all other batches S = 1.3.

7.2.2 Effect of initial supersaturation ratio

As the initial supersaturation ratio used to crystallise dextrose was increased so the Brinell hardness of the compacts, at comparable porosity values, was also seen to increase (Figures 7.3 - 7.6), the degree of the effect reflecting the difference in initial supersaturation ratio between samples. For example, raising the initial supersaturation ratio from 1.3 (D05) to 1.6 (DR30) caused an increase in the peak Brinell hardness of the compacts from approximately 8 to 16 MPa. As in the previous section these results would at first glance suggest an increase in plastic deformation with increasing initial supersaturation ratio. The Heckel data, however, (section 5.2.2) showed that increasing initial supersaturation ratio resulted in dextrose having a greater tendency to consolidate by fragmentation (lower mean yield pressure). This increased fragmentation would result in a greater number of bonding surfaces and thus increase the mechanical strength of the compacts. This view is supported by the tensile strength data (section 6.2.2). The Brinell hardness results are therefore a reflection of increased bonding capacity rather than of increased plastic deformation.

The data obtained from indentation studies on the compacts was used to plot a graph of Ln Brinell hardness vs % porosity and the fundamental (zero porosity) Brinell hardness value calculated by extrapolation of the graphs (Figure 7.3-7.6 C). All the data showed good linear correlation (Table 7.2). In every case increasing the initial supersaturation ratio resulted in the fundamental (zero porosity) Brinell hardness of dextrose being increased. This is therefore in agreement with the previous findings that increased initial supersaturation ratio increased the linear crystal growth rate (section 4.2.2) causing an increase in the amount of defects and dislocations present in the crystals. These defects can present an obstacle to deformation and may induce crack propagation (fragmentation).

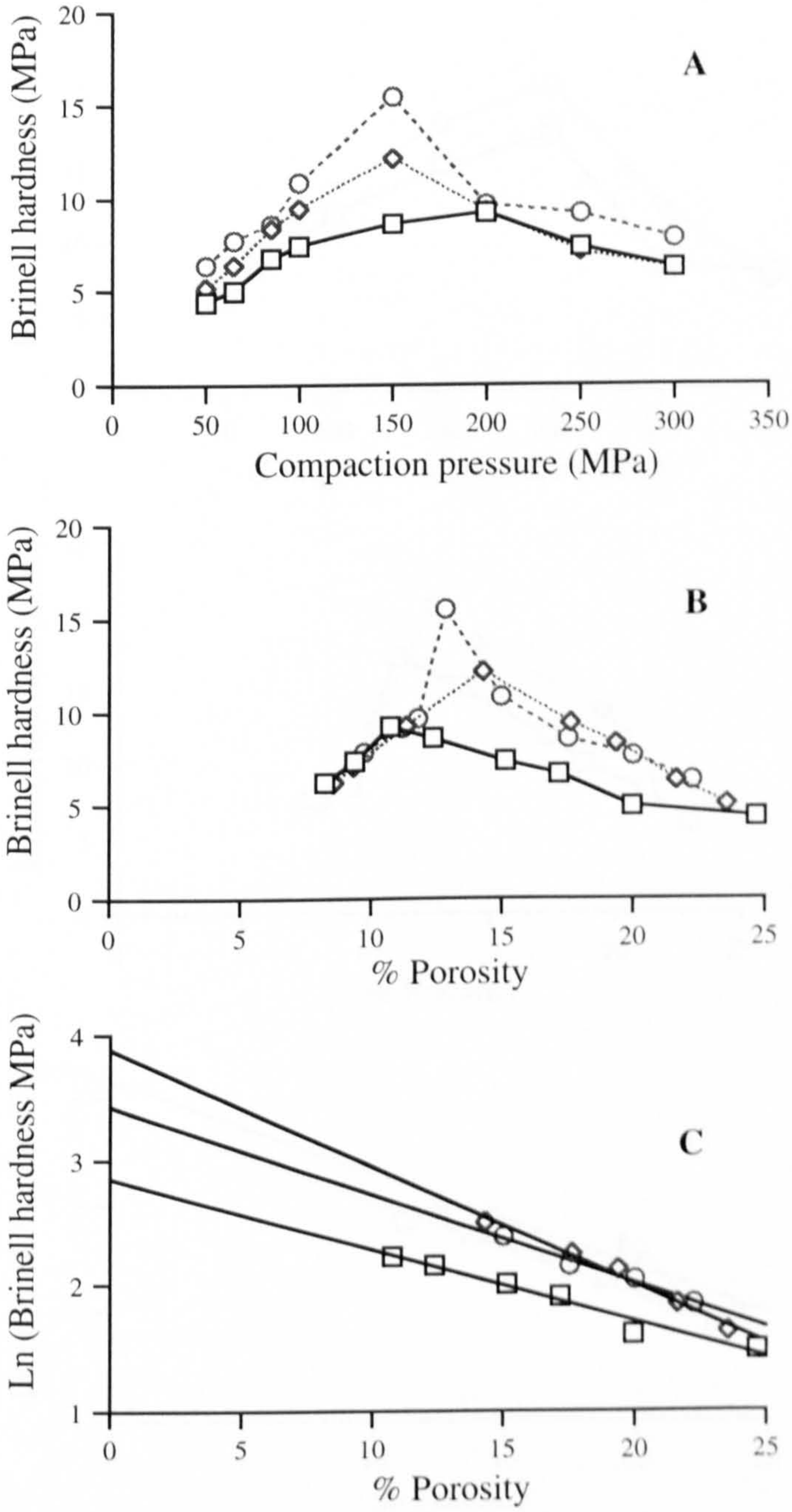

Figure 7.3 (A-C) Effect of initial supersaturation ratio on the Brinell hardness of dextrose compacts

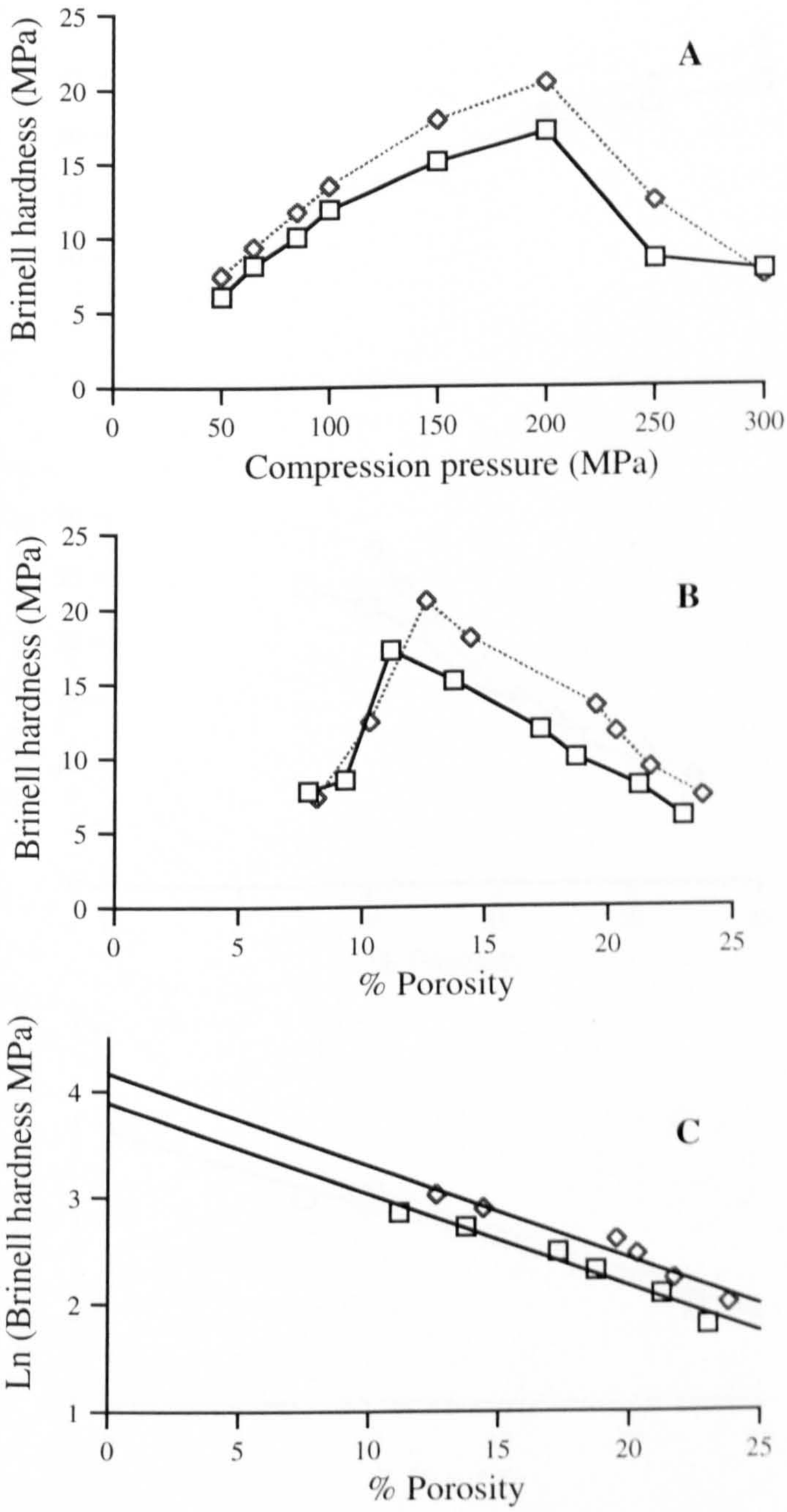

Figure 7.4 (A-C) Effect of initial supersaturation ratio on the Brinell hardness of dextrose compacts

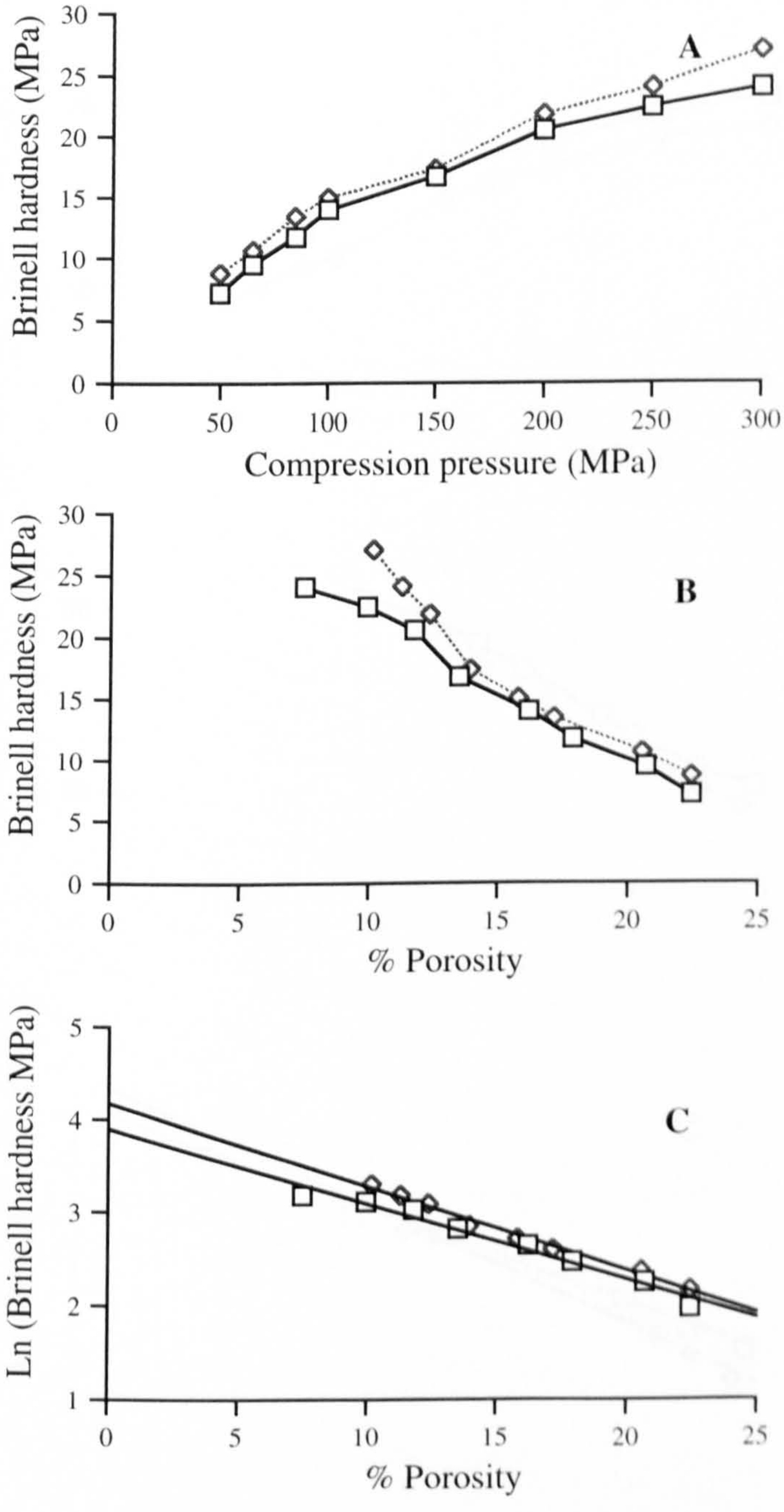

Figure 7.5 (A-C) Effect of initial supersaturation ratio on the Brinell hardness of dextrose compacts

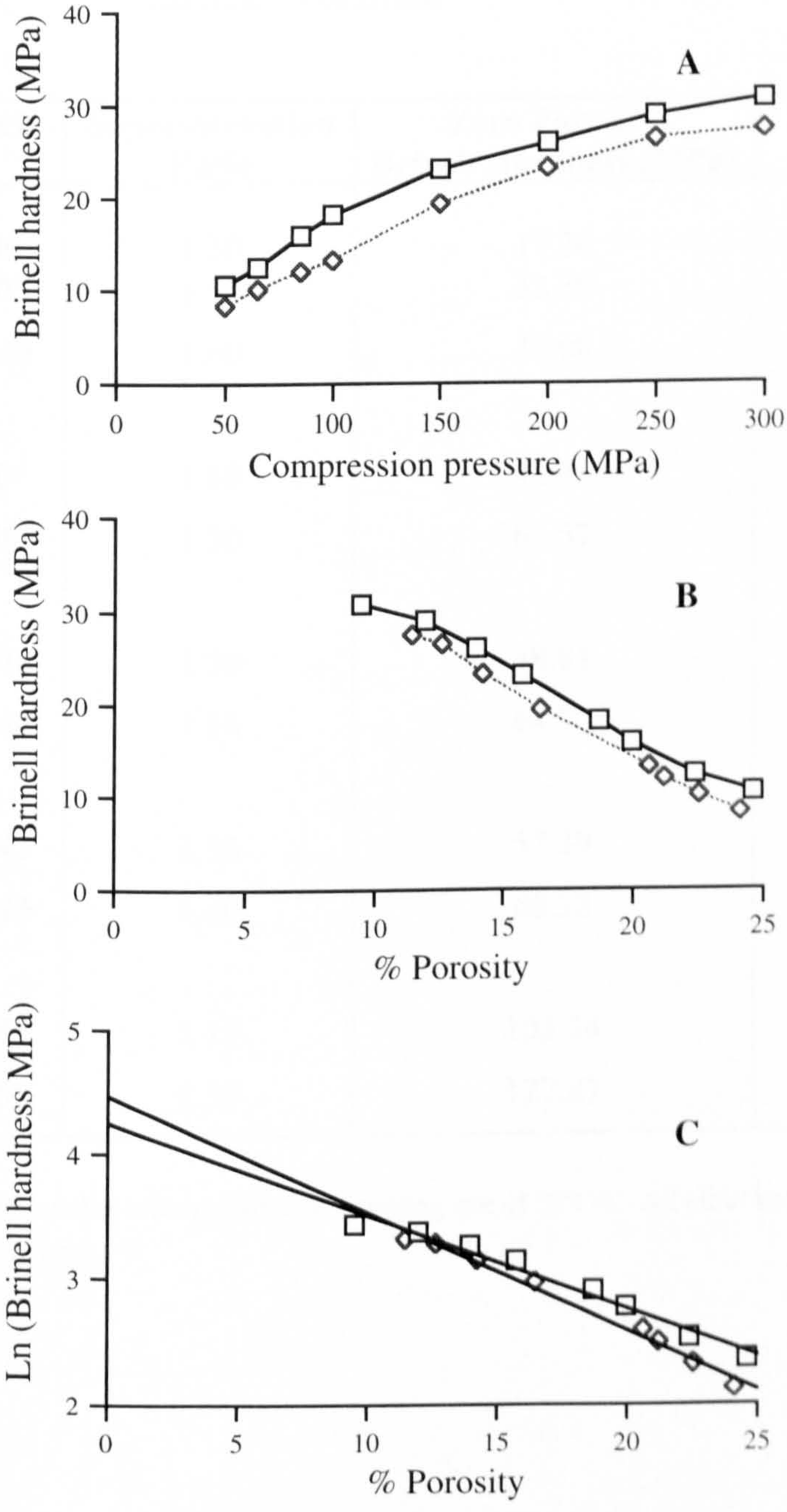

Figure 7.6 (A-C) Effect of initial supersaturation ratio on the Brinell hardness of dextrose compacts

Table 7.2 Effect of initial supersaturation ratio on the fundamental Brinell hardness of dextrose

Batch	Supersaturation Ratio	Zero Porosity Brinell Hardness (MPa)	r
D05	1.30	17.24	0.984
DS05	1.50	32.36	0.983
DR30	1.60	48.08	0.979
D50*	1.30	48.38	0.992
DS50*	1.50	61.57	0.989
DC40	1.30	48.81	0.986
DR40	1.50	64.70	0.981
DC45	1.30	57.39	0.980
DR45	1.40	66.22	0.984
DR51	1.10	103.34	0.982
DC51	1.30	127.87	0.976

* These batches were prepared at a cooling rate of 50°C/h. All other batches were prepared at a cooling rate of 0.5°C/h.

7.2.3 Effect crystal growth time

Figure 7.7 presents the Brinell hardness data obtained from the indentation studies on compacts prepared using batches of dextrose crystallised under similar conditions but with different total crystallisation times.

As with previous batches, the Brinell hardness increased with increasing compression pressure (due to greater densification) for the compacts that failed in tension during the diametrical crushing strength testing and decreased when compacts that did not fail in tension were studied. Only the Brinell hardness data from those compacts that failed in tension were considered to be valid for comparison and for use with the extrapolated exponential (Spriggs') equation.

From the data presented in Figure 7.7 B it appears that increasing the crystal growth time of dextrose has little effect on the Brinell hardness of the compacts when compared at equivalent porosity values. Also the apparent increase in the fundamental (zero porosity) Brinell hardness values with increased crystal growth times (Table 7.3) were found not to be significant when tested at the 95% confidence level (probably due to the relatively large scatter of indentation depths obtained experimentally). Therefore, it can be concluded that crystallisation time had no effect on the Brinell hardness of either dextrose crystals or dextrose compacts.

The Heckel data (section 5.2.3 and 5.3.3) showed that although extending the crystal growth time increased the tendency of dextrose to fragment and thus have a greater bonding capacity, a greater degree of elastic recovery was also in evidence thus cancelling out the effect. This view was supported by the findings that at comparable porosity values no change in the tensile strength of compacts was observed (section 6.2.3) when crystal growth times were increased. This substantiates the finding that increased crystal growth time has no effect on the Brinell hardness of dextrose compacts.

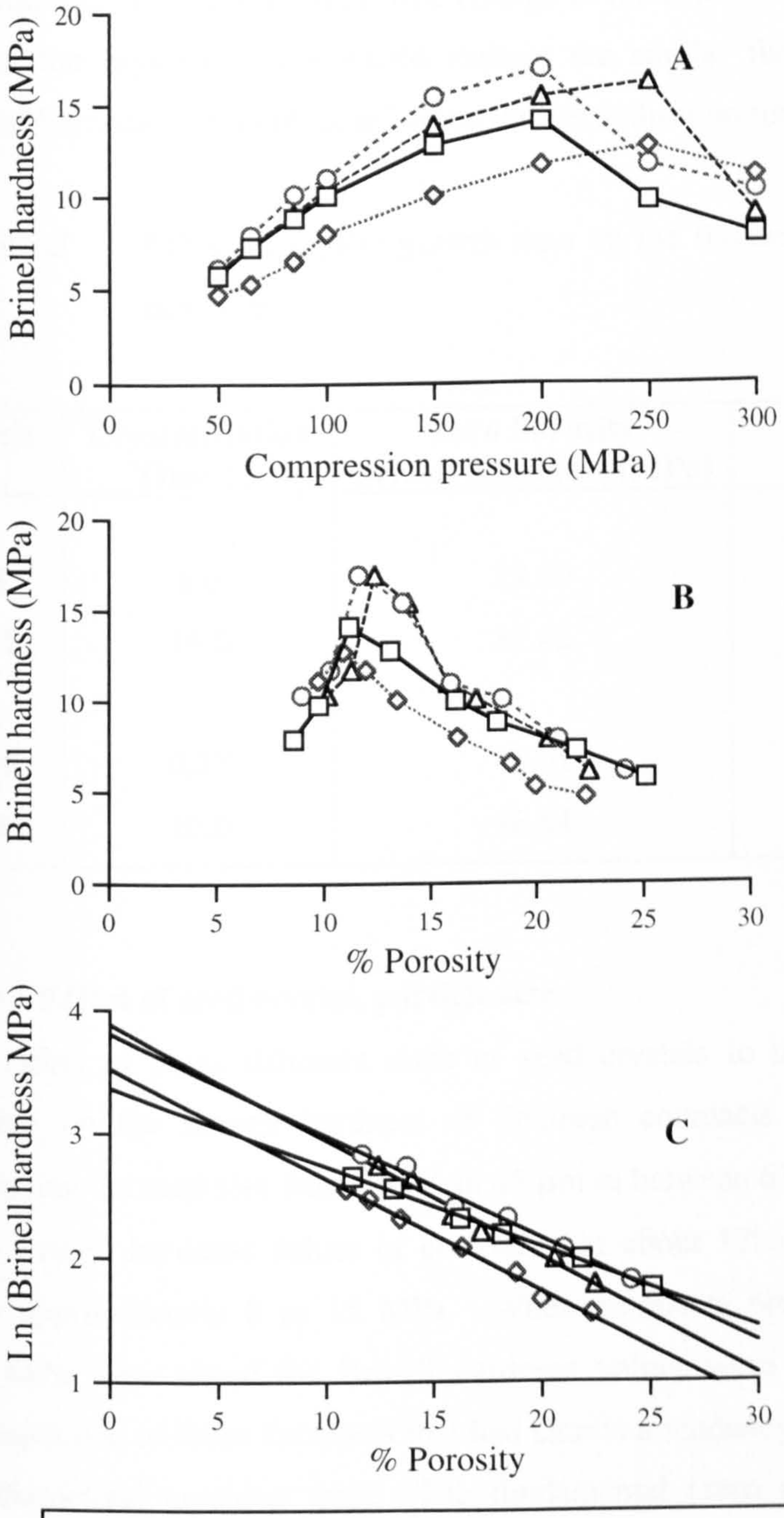

Figure 7.7 (A-C) Effect of crystal growth time on the Brinell hardness of dextrose compacts

Increasing crystal growth time had only a slight effect on the linear crystal growth rate (section 4.2.3) suggesting that little change in the density of dislocations and defects within the crystals. This would explain the similar fundamental (zero porosity) Brinell hardness values obtained when the crystallisation time was increased.

Table 7.3 Effect of crystal growth time on the fundamental Brinell hardness of dextrose

Batch	Crystallisation Time (h)	Zero Porosity Brinell Hardness (MPa)	C.C
D1	8.0	29.10	0.987
D1T	16.0	31.42	0.986
D30	0.27	45.01	0.992
D30T	16.0	46.84	0.984

7.2.4 Effect of seed crystal, particle size

The effect of using different sizes of seed crystals to nucleate the crystallisation process on the Brinell hardness of dextrose compacts is shown in Figure 7.8. Increasing the seed size from less than 45 μm to between 63 and 90 μm resulted in the peak Brinell hardness values of compacts (at about 12% porosity) being increased from approximately 8 to 15 MPa. When compacts prepared at pressures above 200 MPa were tested the Brinell hardness values were found to decrease. This corresponded to those compacts that had shown a tendency to cap or laminate during the diameteral crushing tests. The fundamental (zero porosity) Brinell hardness values (Table 7.4) of dextrose, as calculated by extrapolation of the Ln Brinell hardness vs. % porosity plot show that an increase from 17.14 to 41.51 MPa occurred when the crystal seed size was increased. The linearity of the plots is confirmed by the values of the correlation coefficients (r).

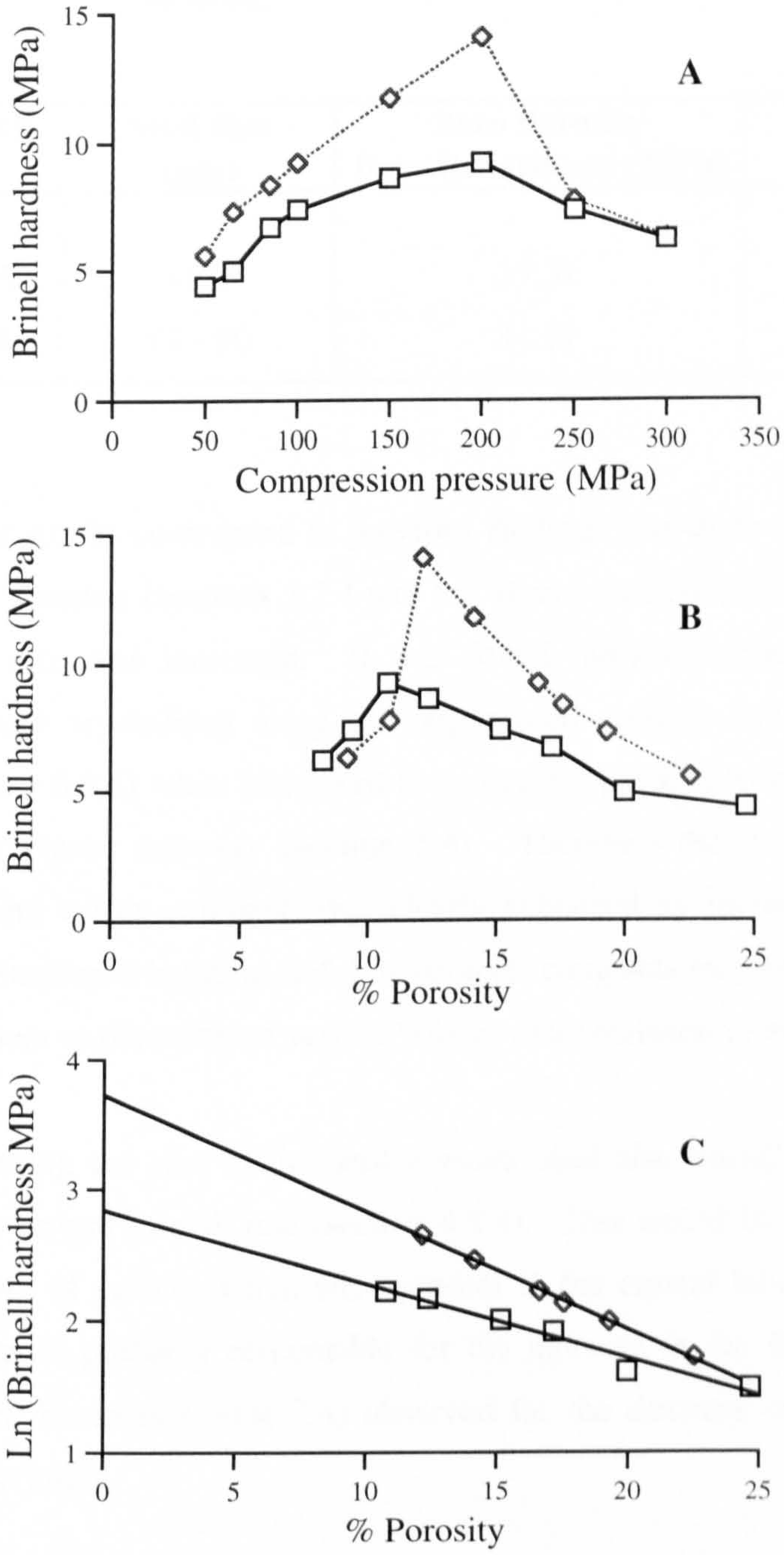

Figure 7.8 (A-C) Effect of seed crystal size on the Brinell hardness of dextrose compacts

Table 7.4 Effect of crystal seed size on the fundamental Brinell hardness of dextrose

Batch	Seed Size (μm)	Zero Porosity Brinell Hardness (MPa)	r
D05	< 45	17.31	0.983
DX05	63 - 90	41.51	0.989

These results correspond to previous findings that there was no change in the mean yield pressure (sections 5.2.4 and 5.3.4) and thus consolidation mechanism when the seed size was increased. It was found, however, that compacts prepared from dextrose crystallised using the larger seed crystals had a greater tensile strength (section 6.2.4) when compared at equivalent porosity values, probably as a result of lower elastic recovery (section 5.4). Therefore the degree of particle to particle bonding within compacts was clearly enhanced by increasing the seed crystal size. This increased bonding and thus stronger compacts may explain the increased Brinell hardness as the compact surface will be more resistant to indentation.

Increasing the size of the seed crystals used also brought about a reduction in the linear crystal growth rate (section 4.2.4). This would have caused a decrease in the number of defects which were present in the crystal lattice. This change in defect density is probably responsible for the increase in the fundamental (zero porosity) Brinell hardness (Table 7.4) observed for the dextrose crystallised using the larger seed crystals.

7.2.5 Effect of additives

The influence of including trace amounts other carbohydrates into the crystallisation system of dextrose on the Brinell hardness of its compacts is illustrated in Figure 7.9. As mentioned previously, only the data obtained from those compacts that failed in tension can be considered to be valid for the purpose of comparing the effect of crystallisation variables on the Brinell hardness of dextrose and its compacts. When

equivalent porosity values are compared it is seen that inclusion of either lactose or sucrose resulted in an increased Brinell hardness of the compacts.

Inclusion of either additive resulted in an increased mean yield pressure (section 5.3.5) indicating a move towards a more brittle and fragmenting material. As previously discussed, this increases the number of surfaces available for bonding and thus would be expected to result in stronger compacts. When the tensile strength of compacts (section 6.2.5) were compared, however, it was found that the presence of additives had no significant effect at comparable porosity values. The changes in crystal habit (section 4.3) due to the presence of additives did cause significant changes in the packing, rearrangement and consolidation characteristics of dextrose. Therefore the increased Brinell hardness of the compacts may not be due simply to increased bonding within the compacts.

Inclusion of either additive also caused an increase in the fundamental (zero porosity) tensile strength of dextrose (Table 7.5). Additives in the crystals of dextrose are seen as impurities (defects) and thus will disrupt the movement of crystal planes resulting in a greater resistance to deformation and thus harder crystals and possibly harder compacts.

Table 7.5 Effect of additives on the fundamental Brinell hardness of dextrose

Batch	Additive	Zero Porosity Brinell Hardness (MPa)	r
D05	None	17.24	0.984
DLac	Lactose	41.30	0.995
DSuc	Sucrose	24.48	0.995

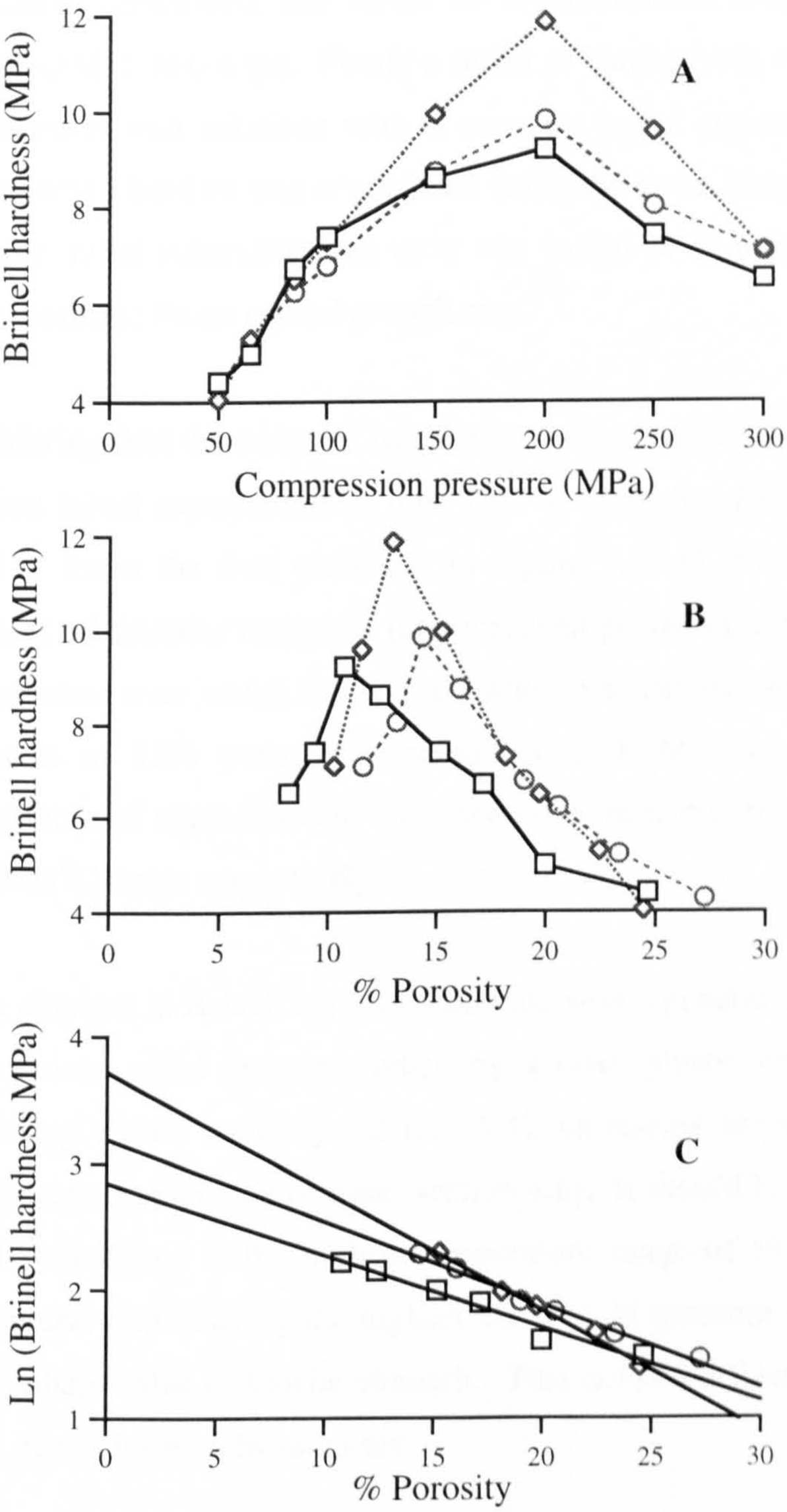

Figure 7.9 (A-C) Effect of additives on the Brinell hardness of dextrose compacts

7.2.6 Effect of crystallisation temperature

As already discussed, the effect of crystallisation temperature on dextrose was investigated in two ways. Firstly a series of batches was crystallised using a range of temperatures and solutions with a constant initial supersaturation ratio of 1.3. A second set of batches was crystallised using the same temperatures as before, but this time the initial supersaturation ratio was varied so as to produce a series of batches with a constant linear crystal growth rate.

Considering first the series of batches crystallised at different temperatures but with a constant initial supersaturation ratio (S) =1.3 (batches D05, DC40, DC45, DC48 and DC51). From the data presented in Figure 7.10 B it can be seen that the Brinell hardness of dextrose compacts (at equivalent porosity) is enhanced by increasing the temperatures over which the crystallisation was carried out. The Brinell hardness of compacts at 12% porosity increased from 8 MPa to over 30 MPa when the temperature of crystallisation was increased from the 38-30°C temperature range to the 59-51°C range respectively.

These changes in Brinell hardness coincide with a general trend of decreasing (ejected tablet) mean yield pressure indicating greater plastic deformation (section 5.2.6), decreasing elastic recovery (section 5.4), increasing tensile strength (section 6.2.6) and decreasing moisture content (section 4.6). It should be noted, however, that batch DC51 crystallised at the highest temperature range of 59-51°C often deviated from this general trend having the highest mean yield pressure (most fragmenting) and an intermediate value of tensile strength. This deviation from the general trend is most likely due to its anhydrous nature.

The increasing Brinell hardness of the dextrose compacts observed with increasing crystallisation temperature is likely to be a result of several factors. Initially the increased plastic deformation and decreased elastic recovery will have lead to stronger and thus harder compacts, while the very low (less than 0.5%) moisture content and changes in crystal structure and crystal habit of the batch crystallised over the 59-51°C temperature range resulted in its relatively high Brinell hardness value.

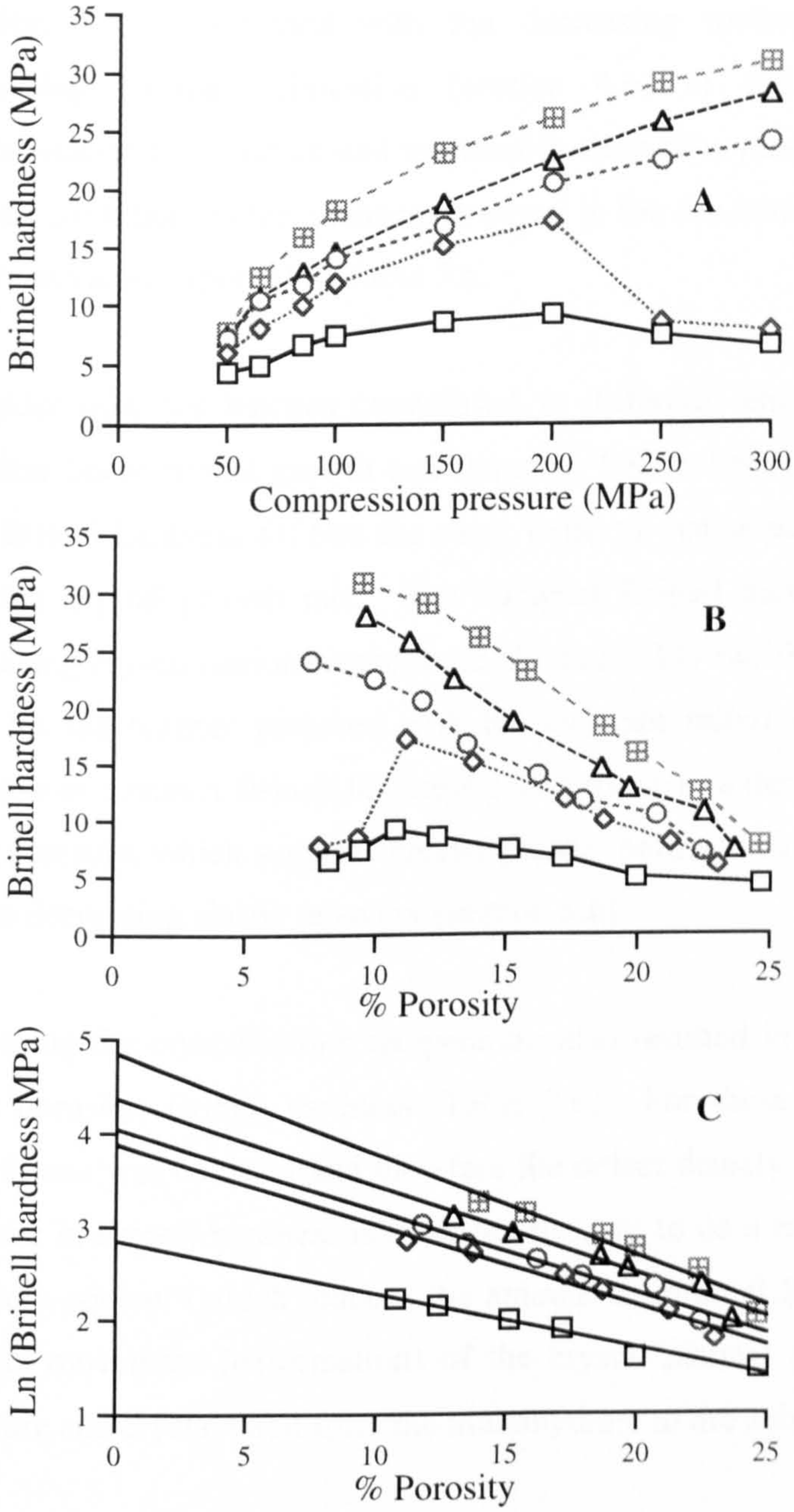

Figure 7.10 (A-C) Effect of crystallisation temperature (constant supersaturation ratio) on the Brinell hardness of dextrose compacts

The increasing linear crystal growth rate and thus increasing the defect density (section 4.2.6) combined with the decreasing moisture content and therefore decreasing internal lubrication (section 4.6) of the crystals with increasing crystallisation temperature and the modification of crystal structure and crystal habit will all contribute to the changes observed in the fundamental (zero porosity) Brinell hardness values reported in Table 7.6.

Consider now the batches crystallised at different temperature ranges but with a constant linear crystal growth rate (batches. DR30, DR40, DR45, DC48 and DR51). The Brinell hardness follows the same trend to that observed for the batches with a variable crystal growth rate. The compact Brinell hardness values increase with increasing crystallisation temperature (Figure 7.11) but the effects appear to be less than for the batches prepared with the constant initial supersaturation ratios. This increase in compact Brinell hardness corresponds to a decreasing ejected tablet mean yield pressure, which suggests greater plastic (permanent) deformation (section 5.2.6) and to decreasing elastic recovery (section 5.6).

Increasing the crystallisation temperature also resulted in an increasing fundamental (zero porosity) Brinell hardness (Table 7.6). For these batches, the linear crystal growth rate was constant and therefore the defect density should be unchanged. The increase in Brinell hardness is therefore thought to be a result of both the decreasing moisture content (which reduces the amount of internal lubrication available and so hinders movement (deformation) of the crystal planes) and the changes in crystal structure and crystal habit from the monohydrate to the anhydrous form.

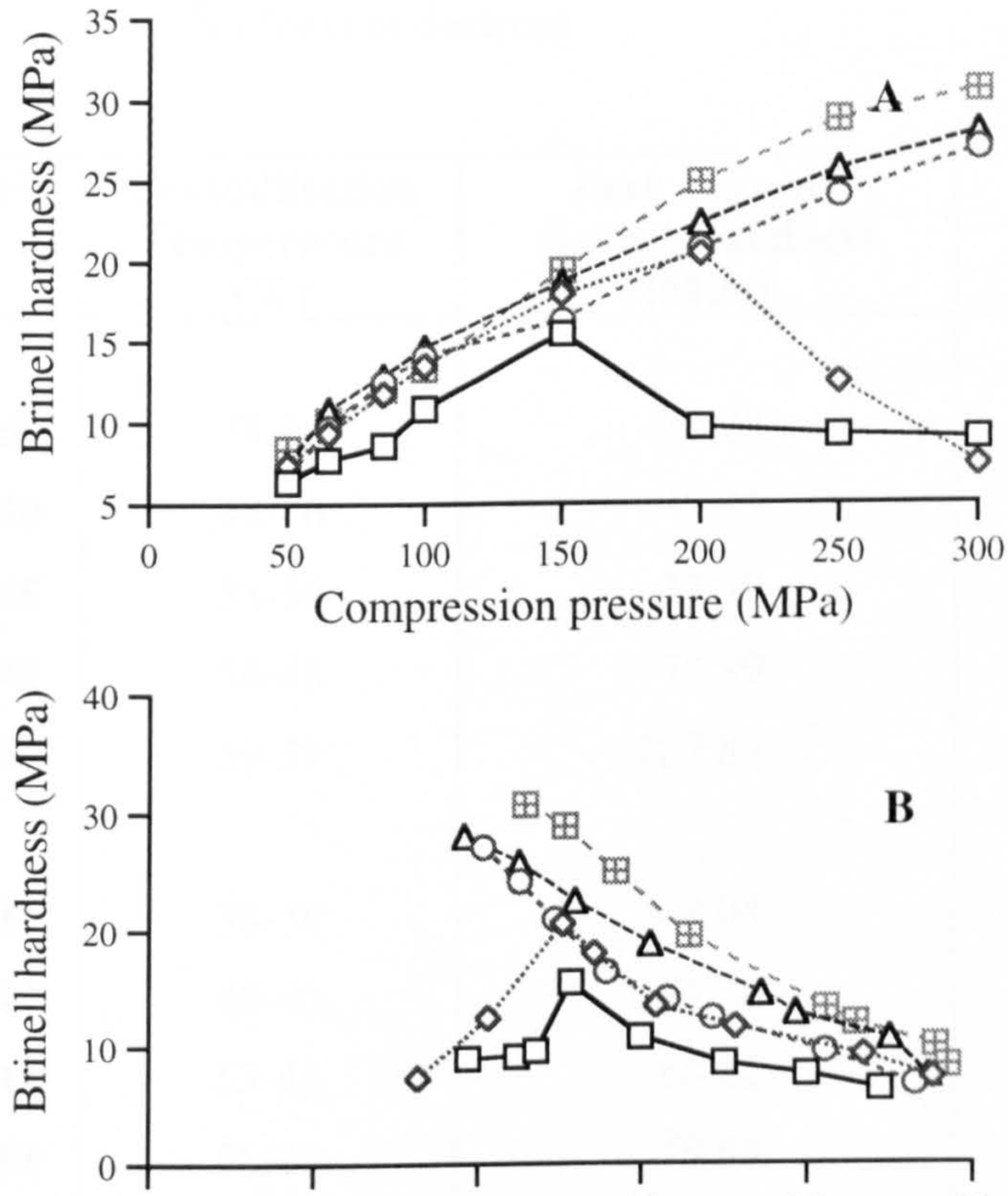

	Batch ID	Crystallisation Temperature Range	Supersaturation Ratio
—□—	DR03	38 - 30°C	S = 1.6
·····◇·····	DR40	48 - 40°C	S = 1.5
----○----	DR45	53 - 45°C	S = 1.4
----△----	DC48	56 - 48°C	S = 1.3
- - -⊞- - -	DR51	59 - 51°C	S = 1.1

Cooling rate = 0.5°C/h

Figure 7.11 (A-C) Effect of crystallisation temperature (constant growth rate) on the Brinell hardness of dextrose compacts

Table 7.6 Effect of crystallisation temperature on the fundamental Brinell hardness of dextrose

Batch	Crystallisation Temperature (^{o}C)	Zero Porosity Brinell Hardness (MPa)	r
D05	38-30	17.25	0.984
DC40	48-40	48.81	0.986
DC45	53-56	57.39	0.980
DC48	56-48	78.89	0.975
DC51	59-51	127.87	0.976
DR30	38-30	48.04	0.989
DR40	48-40	64.70	0.986
DR45	53-45	66.22	0.984
DC48	56-48	78.89	0.975
DR51	59-51	103.34	0.982

7.3 Effect of crystallisation conditions on the elastic modulus of dextrose and its compacts

Elastic modulus is a measure of the stiffness or rigidity of a material or a compacted specimen. The higher the elastic modulus the greater the stress required to strain the inter-molecular or inter-particle bonds (i.e. the test sample is less elastic/ductile). The elastic modulus values obtained from compacted specimens are a function of both the elasticity of the material and of the inter-particle bonding within the compact (Church, 1984a). The elastic modulus determined (or calculated using an extrapolated exponential equation) at zero porosity is a fundamental material property relating to the structure and inter-molecular bonding of its crystals independent of the effects of porosity.

Several methods have been employed to evaluate the elastic modulus of pharmaceutical materials but caution must be used when comparing results from different studies as different types of elastic modulus may have been measured. Tests such as beam bending and Vickers indentation studies measure a materials tensile elastic modulus (i.e. its resistance to tension) often referred to as the Young's Modulus of elasticity, while the elastic modulus determined via Brinell indentation studies is a compressive elastic modulus sometimes referred to as the bulk elastic modulus (Lum and Duncan-Hewitt, 1996).

The following section presents the (compressive) elastic modulus (E) data obtained when compacts prepared from dextrose crystallised employing a variety of process conditions were tested using the Brinell indentation testing technique as described in section 3.4.8.2 and equation 3.9:

$$E = K \times \frac{F}{\Delta h \sqrt{h_1}} \qquad \text{(equation 3.7)}$$

where F is the force applied to the indenter, h_1 is the depth of indentation, Δh is the amount of recovery recorded when the load is removed and K is a constant associated with the dimensions of the indenter. In this experiment the indenter used had a diameter of 1.55 mm and thus K had a value of 8.585 as shown in Appendix 1.

The elastic modulus results were calculated from the mean indentation depth and the mean recovery, after removal of the load, recorded during the indentation testing of ten compacts from each batch of material. In general the elastic modulus of compacts was seen to rise with increasing compression pressure and decreasing porosity due to greater densification and inter-particle bonding. However, when compacts that showed a tendency to cap or laminate (during diameteral crushing strength testing) were tested a dramatic decline in elastic modulus was observed. Therefore only the elastic modulus results obtained from those compacts that did fail in tension were considered valid for comparison between batches and for use with the extrapolated exponential equation to calculate the fundamental (zero porosity) elastic modulus values (E_o) of the various batches of dextrose. However all the experimental data are displayed in the Figures of elastic modulus vs. compression and elastic modulus vs. % porosity. The point at which the elastic modulus results of the compacts are compromised by the excess elastic energy can be clearly seen. Each figure has three separate graphs, A illustrates the variation of compact elastic modulus with compression pressure, B presents the variation of compact elastic modulus with compact porosity while C presents the extrapolated exponential data. The validity of using this exponential equation and extrapolating it to zero porosity is confirmed by the good linear correlation coefficients obtained throughout.

7.3.1 Effect of crystallisation cooling rate

The effect of crystallisation cooling rate on the elastic modulus of dextrose and its compacts is shown in Figures 7.12 and 7.13. The elastic modulus is seen to increase with increasing compression pressure and decreasing porosity (due to increased densification) up to point before it suddenly declines again. In every case this reduction in elastic modulus occurs for the compacts which did not fail in tension during the diameteral crushing strength tests and as mentioned previously these values of elastic modulus are not considered valid for comparing the results from various batches. Therefore, using only the data from those compacts which did fail in tension, it was observed that increasing the crystallisation cooling rate caused the elastic modulus of the compacts, at equivalent porosity, values to increase. For example increasing the crystallisation cooling rate from 0.5 to 50°C/h (batches D05 and D50) increased the peak elastic modulus value from approximately 7 to 18 MPa (Figure 7.12). This increase in the elastic modulus of the compacts indicates that the

compacts are becoming less elastic. This is in agreement with previous findings that increased crystallisation cooling rate resulted in greater compact tensile strength (section 6.2.1). This increased brittleness (or fragmentation tendency), however, was not reflected in the mean yield pressure values obtained from the Heckel plots (sections 5.2.1 and 5.3.1). Instead, the increased bonding was attributed to the fact that as the crystallisation cooling rate was increased the particle size distribution shifted towards the lower end of the 63-90 μm selected size range (section 4.7.1) thus increasing the number of inter-particle bonding surfaces available

By using the extrapolated exponential (Spriggs') equation the fundamental (zero porosity) material value of elastic modulus of each batch of dextrose was calculated (Table 7.7). Good linear correlation coefficients (r) were obtained for all the batches.

As the crystallisation cooling rate is increased the fundamental (zero porosity) elastic modulus also increases. This is likely to be a result of the increased crystal defect density induced by the rise in linear crystal growth rates (section 4.2.1) and confirmed by the changes in true density (section 4.4.1) with increasing crystallisation cooling rate. These defects disrupt the crystal structure hindering deformation of the crystal planes and also increase the number of flaws in the crystal structure providing more sites for the propagation of cracks and thus increase the brittleness (increased elastic modulus) of the dextrose crystals.

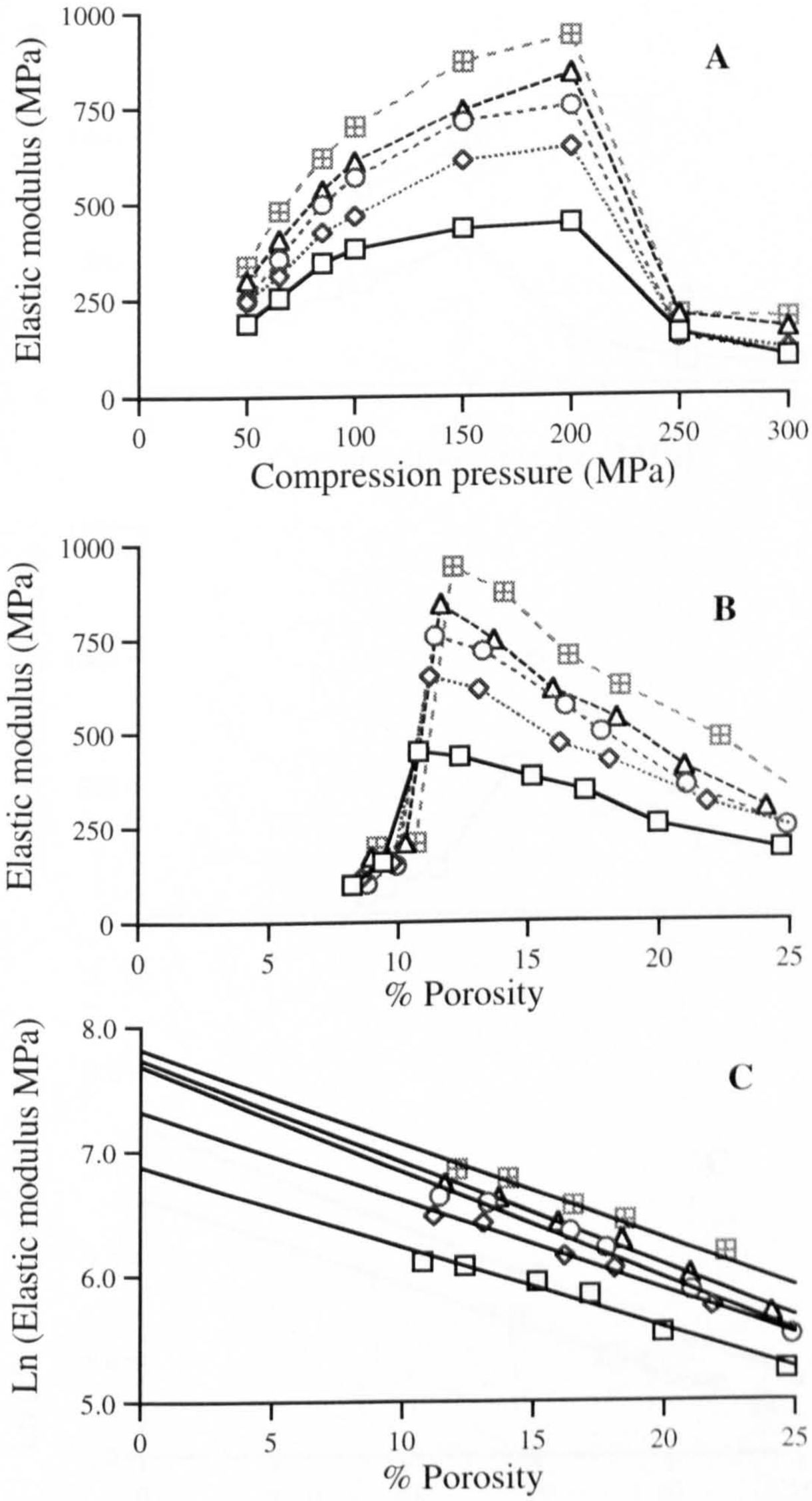

Figure 7.12 (A-C) Effect of crystallisation cooling rate on the elastic modulus of dextrose compacts

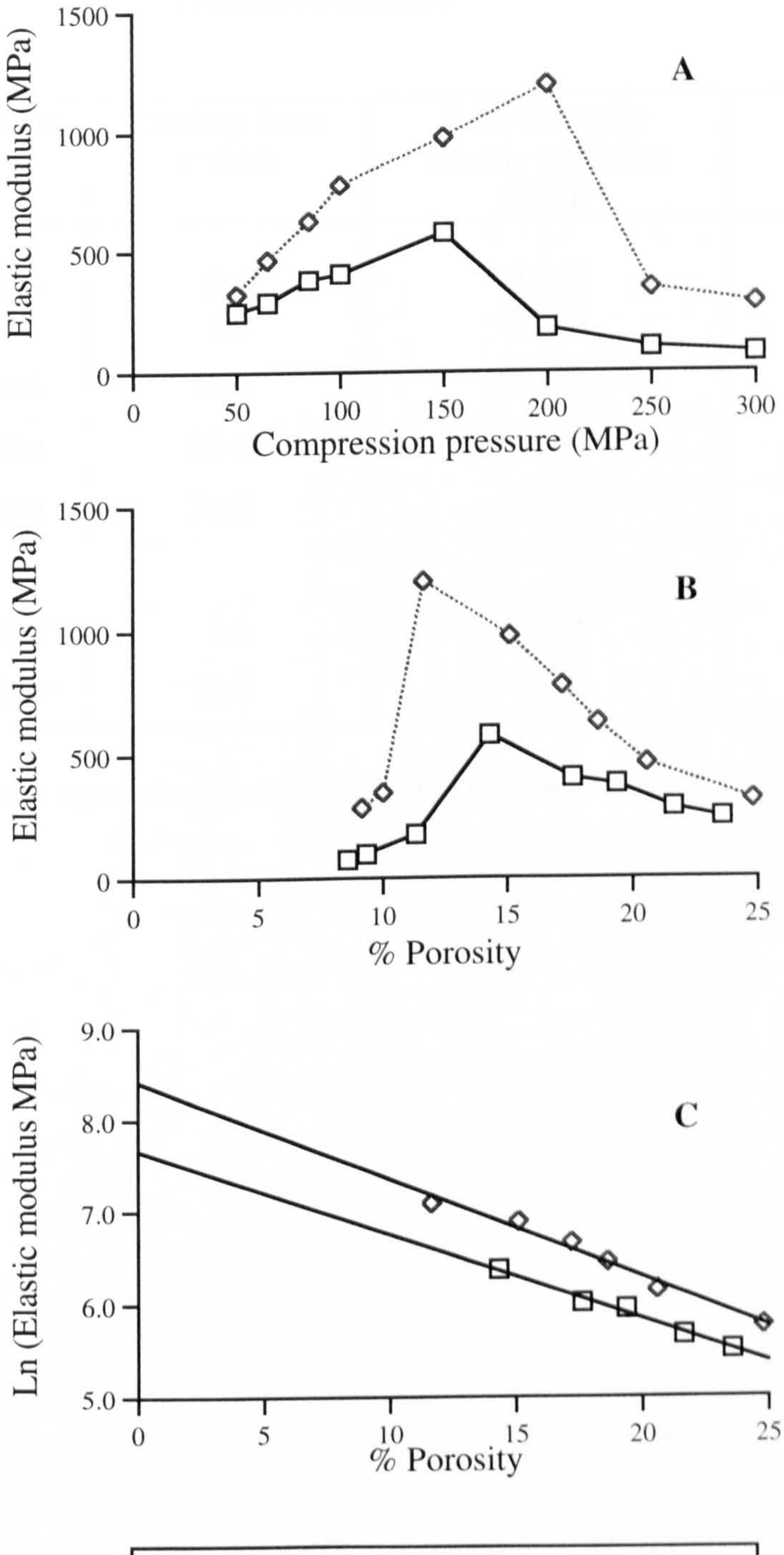

Figure 7.13 (A-C) Effect of crystallisation cooling rate on the elastic modulus of dextrose compacts

Table 7.7 Effect of crystallisation cooling rate on the fundamental elastic modulus of dextrose

Batch	Cooling Rate (°C/h)	Zero Porosity Elastic modulus (GPa)	r
D05	0.5	0.968	0.986
D1	1.0	1.516	0.997
D10	10.0	2.178	0.992
D30	30.0	2.296	0.995
D50	50.0	2.492	0.991
DS05*	0.5	2.298	0.994
DS50*	50.0	4.038	0.981

* Initial supersaturation ratio S = 1.5. All other batches S = 1.3.

7.3.2 Effect of initial supersaturation ratio

The effect of changing initial supersaturation ratio on the elastic modulus of dextrose compacts is illustrated in Figures 7.14 to 7.18. The elastic modulus increases as expected with increasing consolidation and as before some of the batches reach a maximum and then decrease again. The decrease coinciding with the point at which compacts no longer failed in tension during the diametral crushing tests and so these results were not used for comparisons between batches.

Comparing batches D05 (S=1.3), DS05 (S=1.5) and DR30 (S=1.6), increasing the initial supersaturation ratio resulted in an increased elastic modulus for compacts at equivalent compression force and equivalent porosity (Figure 7.14 A and B) and in the fundamental (zero porosity) elastic modulus of the three batches as detailed in Figure 7.14 C and Table 7.8.

Similar effects were also observed when batches D50/DS50 (Figure 7.15), batches DC40/DR40 (Figure 7.16) and batches DC45/DR45 (Figure 7.17) were compared, but the effect becomes less as the differences in the initial supersaturation ratio were reduced.

The increase in compact elastic modulus with increased initial supersaturation ratio implies that the compacts are becoming more rigid. This is probably due to the increased degree of bonding previously indicated by the increased tensile strength (section 6.2.2) which was attributed to the increased mean yield pressure and thus fragmentation tendency (sections 5.2.2 and 5.3.2). The increase in fundamental (zero porosity) elastic modulus is most likely a result of the increased linear crystal growth rates (section 4.3.2) and thus subsequent increased defect density which accompanied crystallisation with increased initial supersaturation ratios.

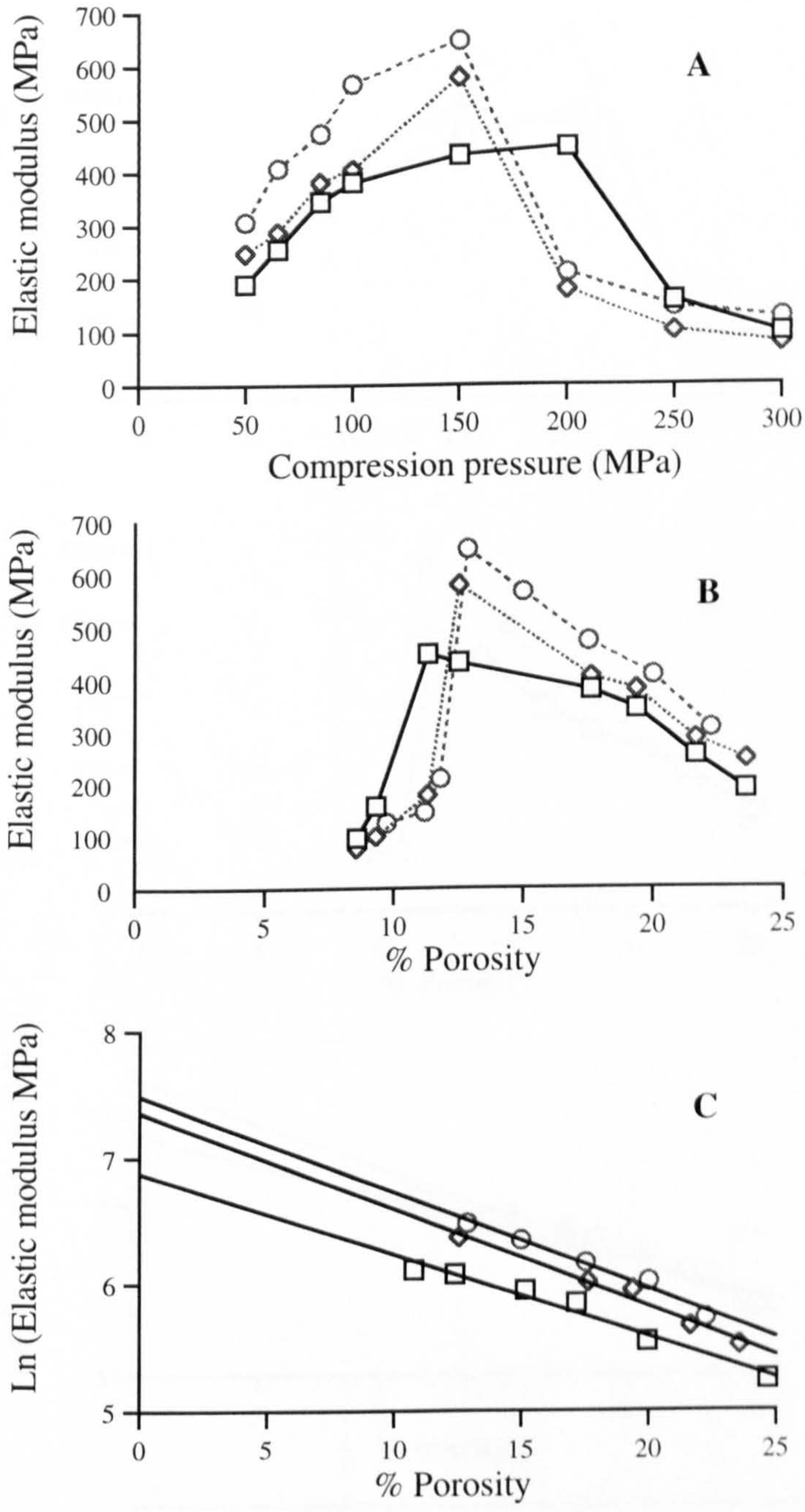

Figure 7.14 (A-C) Effect of initial supersaturation ratio on the elastic modulus of dextrose compacts

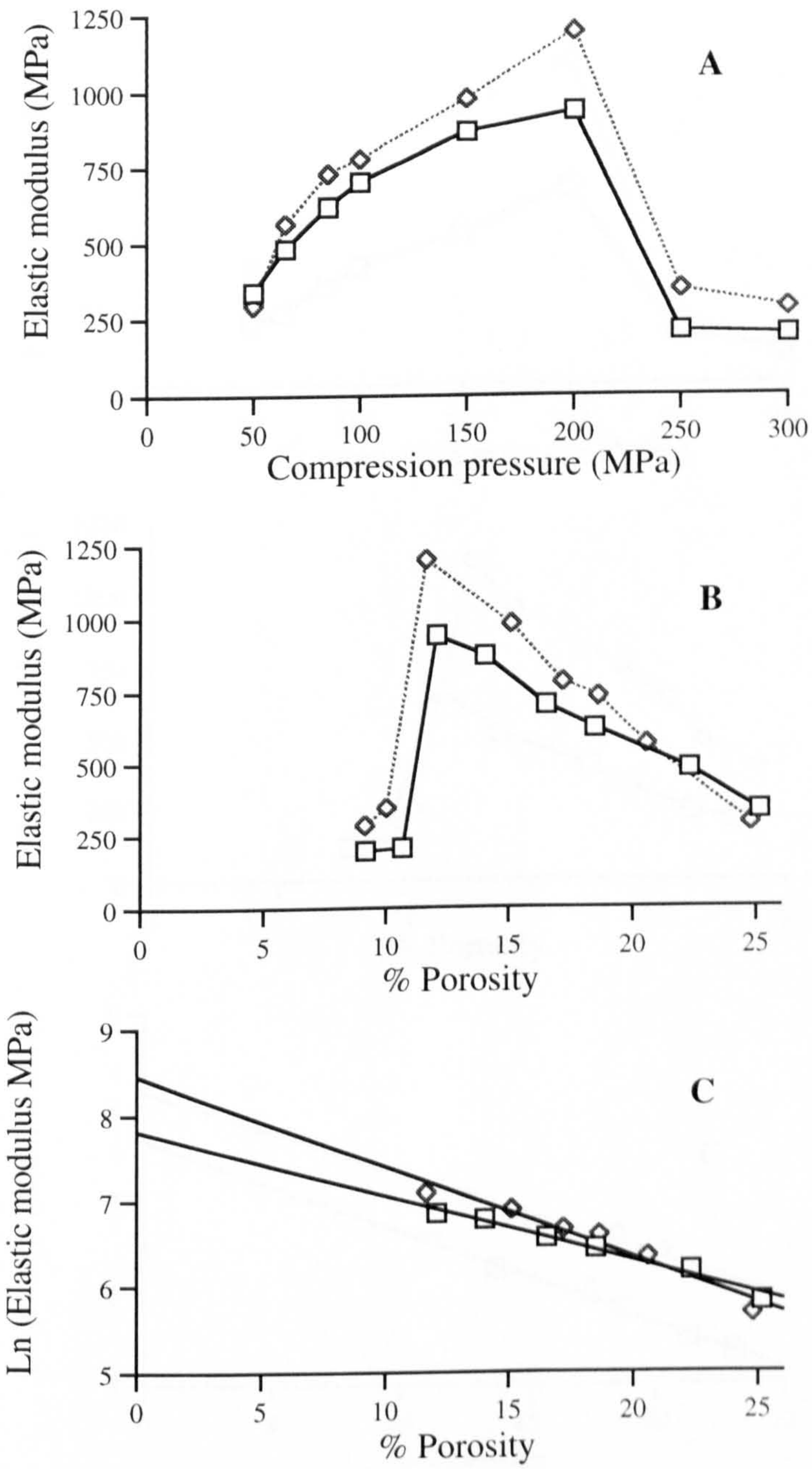

Figure 7.15 (A-C) Effect of initial supersaturation ratio on the elastic modulus of dextrose compacts

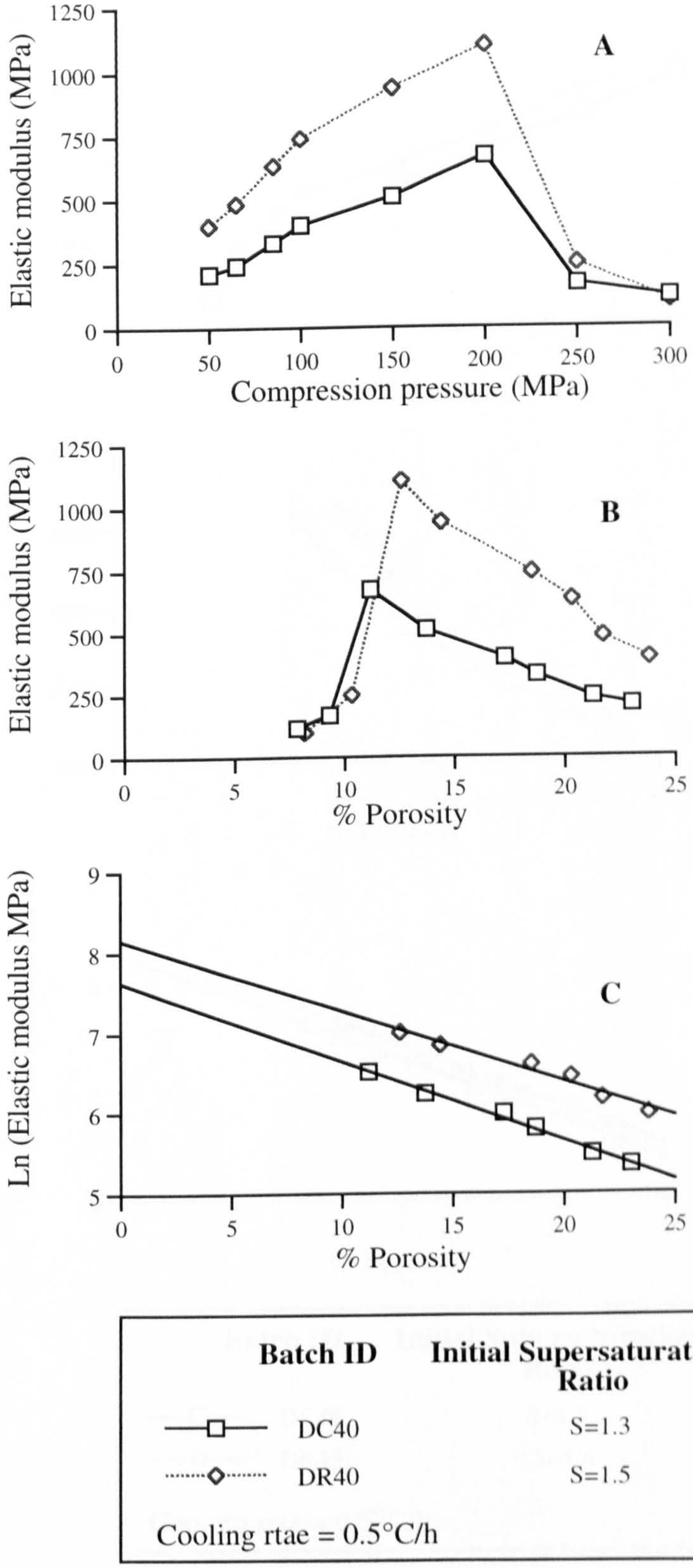

Figure 7.16 (A-C) Effect of initial supersaturation ratio on the elastic modulus of dextrose compacts

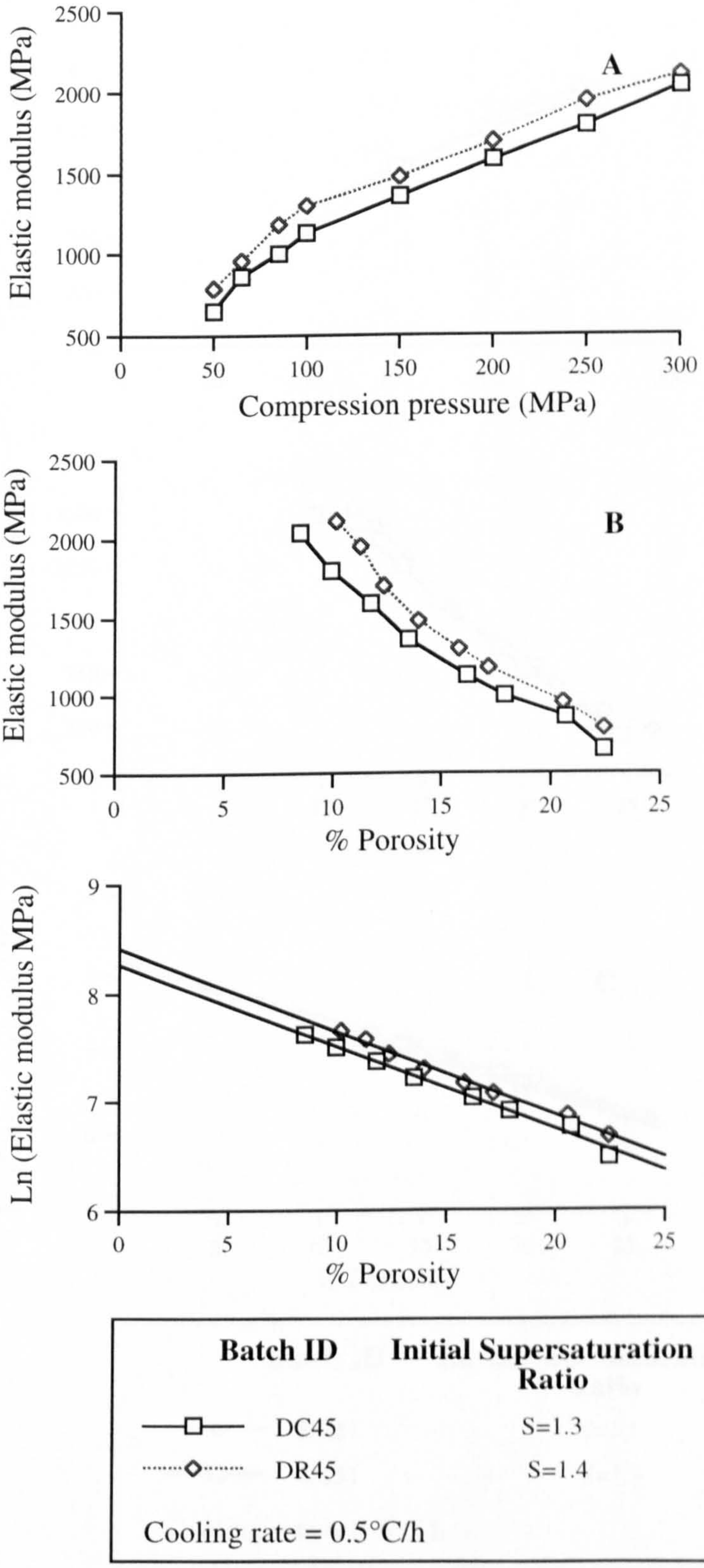

Figure 7.17 (A-C) Effect of initial supersaturation ratio on the elastic modulus of dextrose compacts

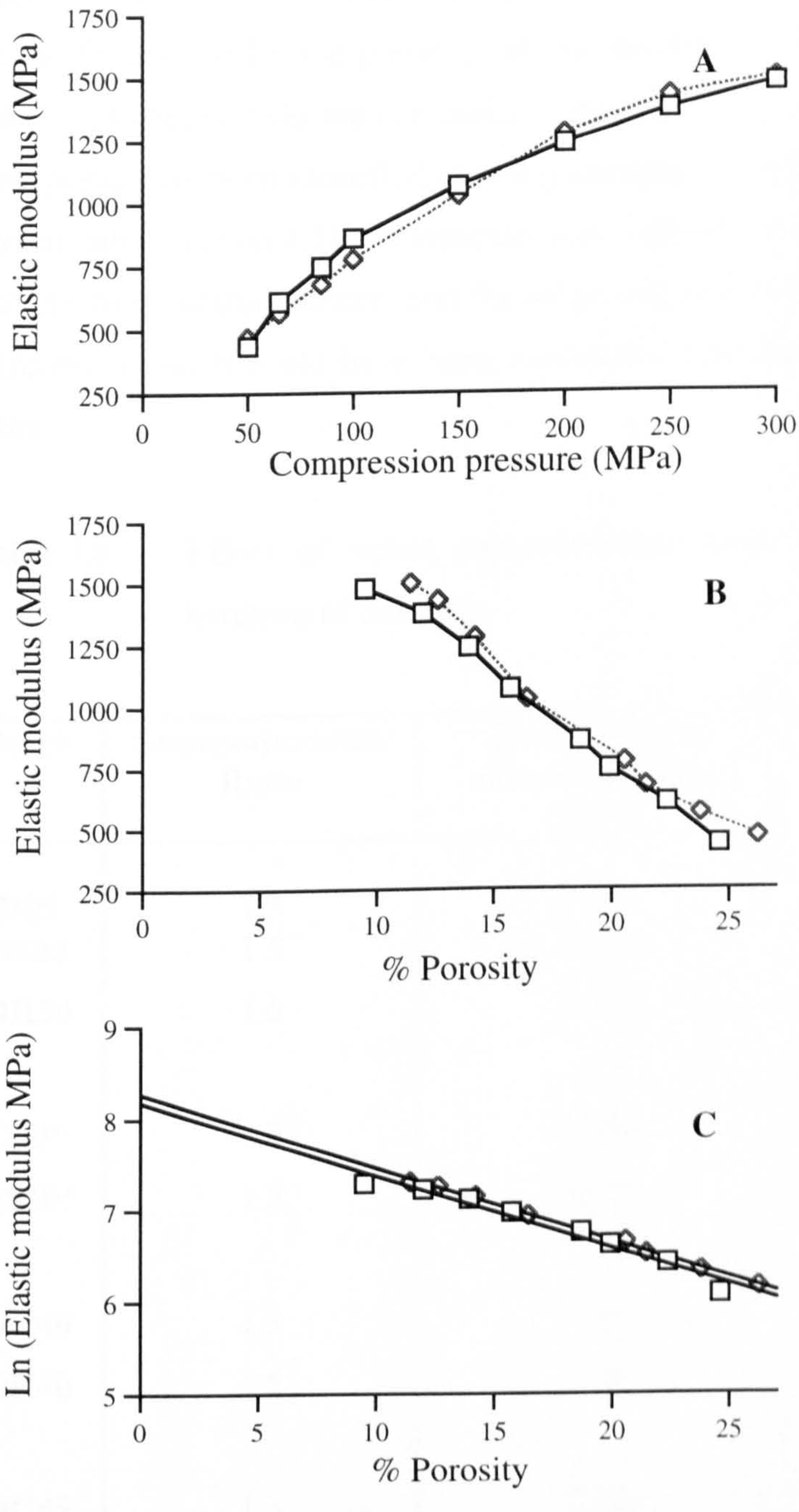

Figure 7.18 (A-C) Effect of initial supersaturation ratio on the elastic modulus of dextrose compacts

For batches DC51 and DR51, changes in the initial supersaturation ratio had no discernible effect on either the elastic modulus of compacts (Figure 7.18 A and B) or on the fundamental (zero porosity) elastic modulus of dextrose (Figure 7.18 C and Table 7.8) obtained via the extrapolated exponential equation. Both of these batches have previously been identified as being anhydrous in nature having the characteristic crystal habit (section 4.3) and typically low moisture content (section 4.6). It may be that this low moisture content and the anhydrous nature of both batches outweighs any differences which could have been attributed to the different initial supersaturation ratios.

Table 7.8 Effect of initial supersaturation ratio on the fundamental Brinell hardness of dextrose

Batch	Supersaturation Ratio	Zero Porosity Elastic Modulus (GPa)	r
D05	1.3	0.968	0.986
DS05	1.5	2.298	0.994
DR30	1.6	2.599	0.982
D50*	1.3	2.492	0.991
DS50*	1.5	4.038	0.981
DC40	1.3	2.067	0.978
DR40	1.5	3.484	0.985
DC45	1.3	3.901	0.995
DR45	1.4	4.536	0.990
DC51	1.3	3.575	0.981
DR51	1.1	3.916	0.995

*These batches were prepared with a cooling rate of 50°C/h. All other batches were prepared with a cooling rate of 0.5°C/h.

7.3.3 Effect of crystal growth time

Increasing the crystallisation growth time resulted in a lowering of the compact elastic modulus when compared at either equivalent compression forces or equivalent porosity values (Figure 7.19 A and B), indicating that the compacts had become more elastic. This corresponds with the previous findings that compact tensile strength was lower for the dextrose crystallised for the extended time especially at lower porosity values (6.2.3).

As indicated by the data presented in the Ln elastic modulus vs. % porosity graph (Figure 7.19 C) and in Table 7.9 the fundamental material (zero porosity) elastic modulus shows no change when crystallisation growth times are increased. It has already been reported that extending the crystal growth times caused no distinct changes in the moisture content (section 4.3) or the true density values (section 4.4.3) of dextrose and only a very slight change in the linear crystal growth rates (section 4.2.3). These factors all indicate that no change in crystallinity or crystal structure occurred when the crystal growth times were increased and so no change in the fundamental (zero porosity) material elastic modulus would be expected.

Table 7.9 Effect of crystal growth time on the fundamental elastic modulus of dextrose

Batch	Crystallisation Time (h)	Zero Porosity Elastic Modulus (GPa)	r
D1	8.0	1.516	0.997
D1T	16.0	1.498	0.991
D30	0.27	2.296	0.995
D30T	16.0	2.268	0.995

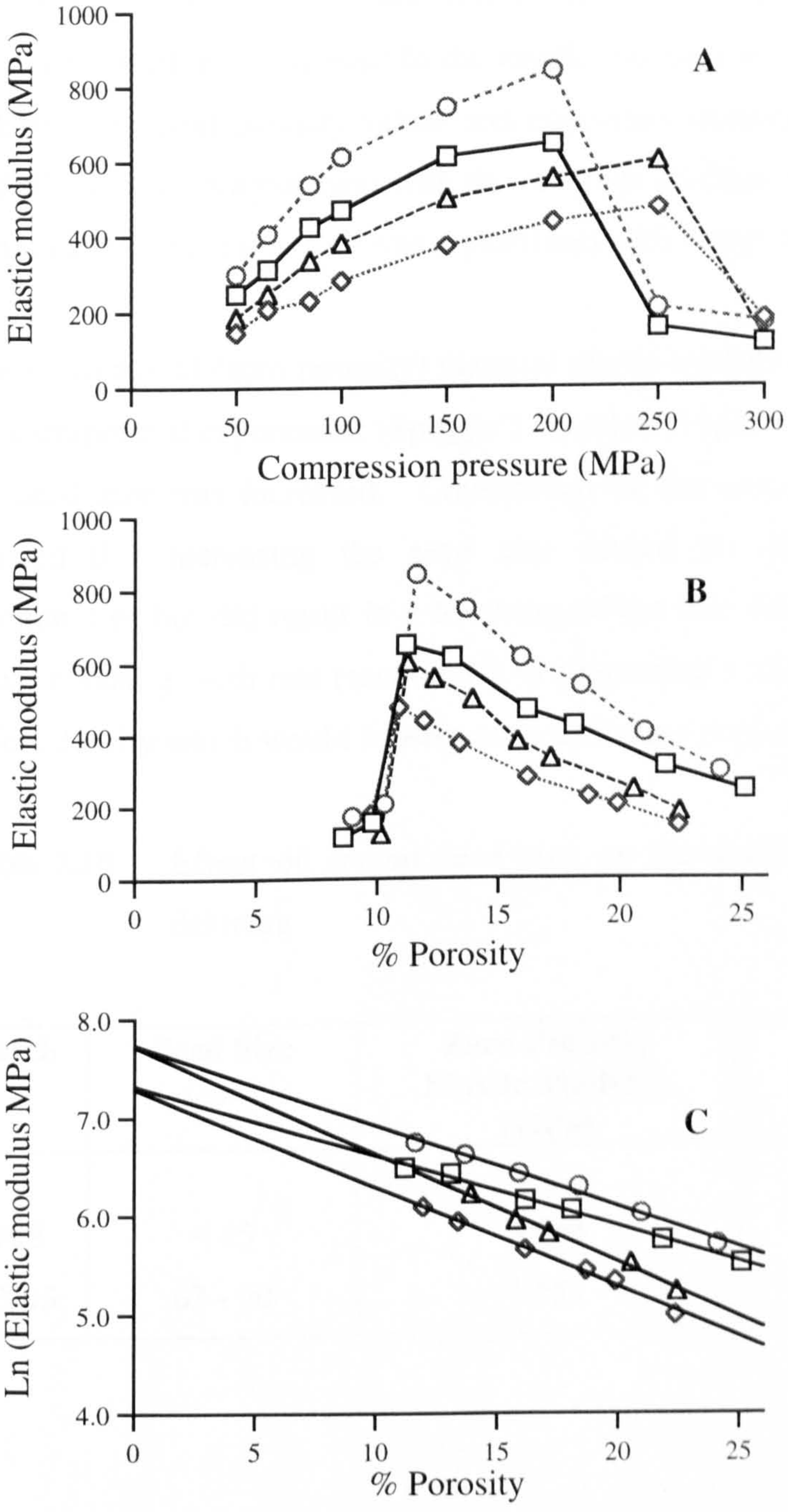

Batch ID		Crystallisation time	Cooling rate
—□—	D1	8hours	1.0°C/h
·····◇·····	D1T	16 hours	1.0°C/h
----○----	D30	0.27 hours	30.0°C/h
----△----	D30T	16 hours	30.0°C/h

Initial supersaturation ratio S = 1.3

Figure 7.19 (A-C) Effect of crystal growth time on the elastic modulus of dextrose compacts

7.3.4 Effect of seed crystal, particle size

Increasing the size of the seed crystals from less than 45 μm to between 63 and 90 μm resulted in an increase in the elastic modulus of dextrose compacts compared at both equivalent porosity values and equivalent compression forces (Figure 7.20 A and B). This is in agreement with the previous findings that compact tensile strength increased when the dextrose was crystallised with larger seed crystals (6.2.4).

The fundamental (zero porosity) material elastic modulus (Table 7.10) calculated via the extrapolated exponential (Spriggs') equation (Figure 7.20 C) also increased when the seed size was increased. Comparison of the same two batches in Chapter 4 showed that increasing the seed size caused no change in moisture content (section 4.6) but did result in a lowering of the true density (section 4.4.4) and the linear crystal growth rate (section 4.2.4) suggesting a change in crystal structure and defect density which would subsequently influence elastic modulus.

Table 7.10 Effect of crystal seed size on the fundamental elastic modulus of dextrose

Batch	Seed Size (μm)	Zero Porosity Elastic Modulus (GPa)	r
D05	< 45	0.968	0.986
DX05	63 - 90	1.551	0.994

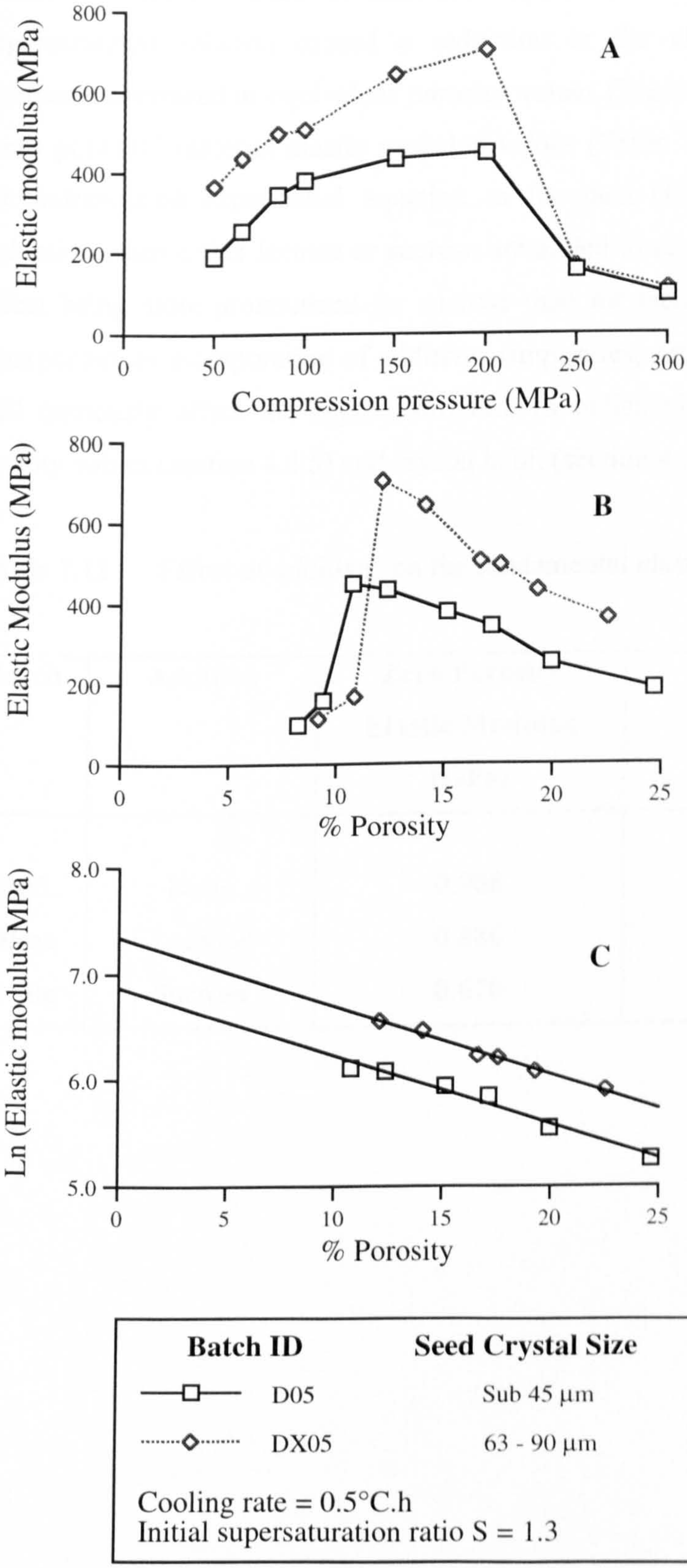

Figure 7.20 (A-C) Effect of seed crystal size on the elastic modulus of dextrose compacts

7.3.5 Effect of additives

Inclusion of trace amounts of other carbohydrates, namely lactose or sucrose, in the supersaturated solution caused a reduction in the elastic modulus of dextrose compacts compared at equivalent porosity values (Figure 7.21 B). The fundamental (zero porosity) material elastic modulus values (Table 7.11) calculated by applying the extrapolated exponential equation to the data (Figure 7.21 C) also show a reduction when either lactose or sucrose are added to the crystallisation system. The effect being more pronounced for sucrose than for lactose. These changes are not unexpected, as incorporation of additives (impurities) into the dextrose crystal lattice will obviously affect the crystal structure as indicated by the differences in true density values (section 4.4.5) and crystal habit (section 4.3).

Table 7.11 Effect of additives on the fundamental elastic modulus of dextrose

Batch	Additive	Zero Porosity Elastic Modulus (GPa)	r
D05	None	0.968	0.986
DLac	Lactose	0.886	0.997
DSuc	Sucrose	0.670	0.993

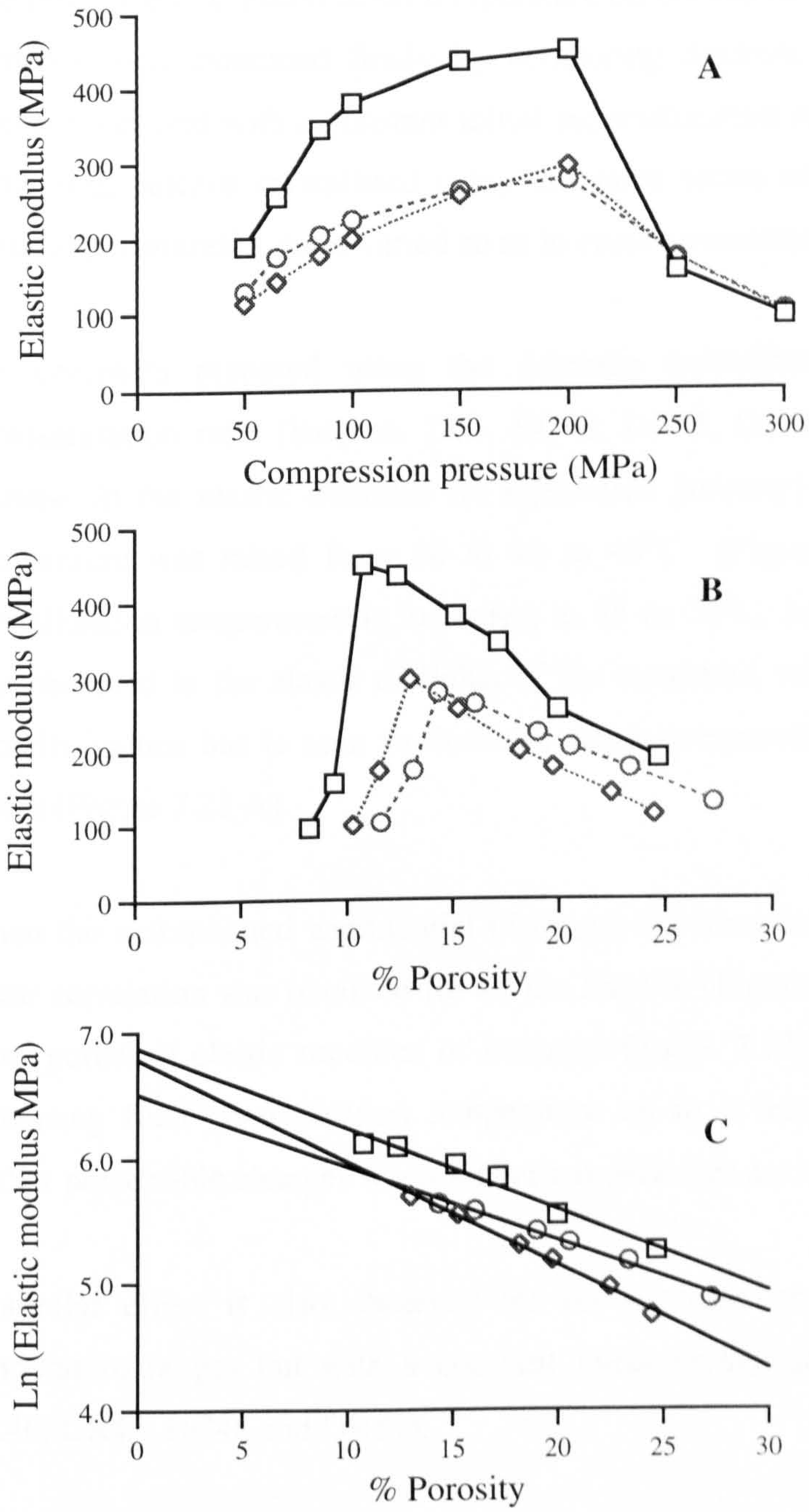

Figure 7.21 (A-C) Effect of additives on the elastic modulus of *dextrose compacts*

7.3.6 Effect of crystallisation temperature

The influence of crystallisation temperature on the elastic modulus of dextrose and its compacts was examined firstly by comparing dextrose crystallised at a series of temperatures and with a constant initial supersaturation ratio of 1.3, and secondly by comparing batches crystallised using the same series of temperatures but with the initial supersaturation ratio varied so as to ensure a constant linear crystal growth rate.

For compacts prepared using the dextrose crystallised with a constant initial supersaturation ratio (batches. D05, DC40, DC45, DC48 and DC51) there was an increase in the elastic modulus (at equivalent porosity) as the final crystallisation temperature was raised from 30 to 40 to 45°C (Figure 7.22 B). When the final crystallisation temperature is increased to 48 or 51°C, however, no further increase was observed in the elastic modulus of the compacts, when compared at equivalent porosity values but is seen to decrease when compared at equivalent compression forces (Figure 7.22 A).

When the extrapolated exponential (Spriggs) equation was applied to the data good linear correlation was obtained for all the batches (Figure 7.22 C). The fundamental (zero porosity) elastic modulus of dextrose (Table 7.12) is shown to increase with increasing final crystallisation temperature up to a temperature of 45°C, with no further perceptible changes when higher temperatures are used.

A similar effect is also observed for the dextrose crystallised over the various temperature ranges but with a constant linear crystal growth rate (batches DR30, DR40, DR45, DC48 and DR51).

As the data presented in Figure 7.23 B illustrate, increasing the final crystallisation temperature from 30 to 40 to 45°C resulted in the elastic modulus of compacts at equivalent porosity being raised, with no further real change taking place when final crystallisation temperatures of 48 or 51°C were used. However when the fundamental material (zero porosity) elastic modulus values (Table 7.12) are calculated using the extrapolated exponential (Spriggs') equation (Figure 7.23 C) it is seen to increase with increasing final crystallisation temperature up to 45°C but then decreases when higher temperatures of 48 and 51°C are used.

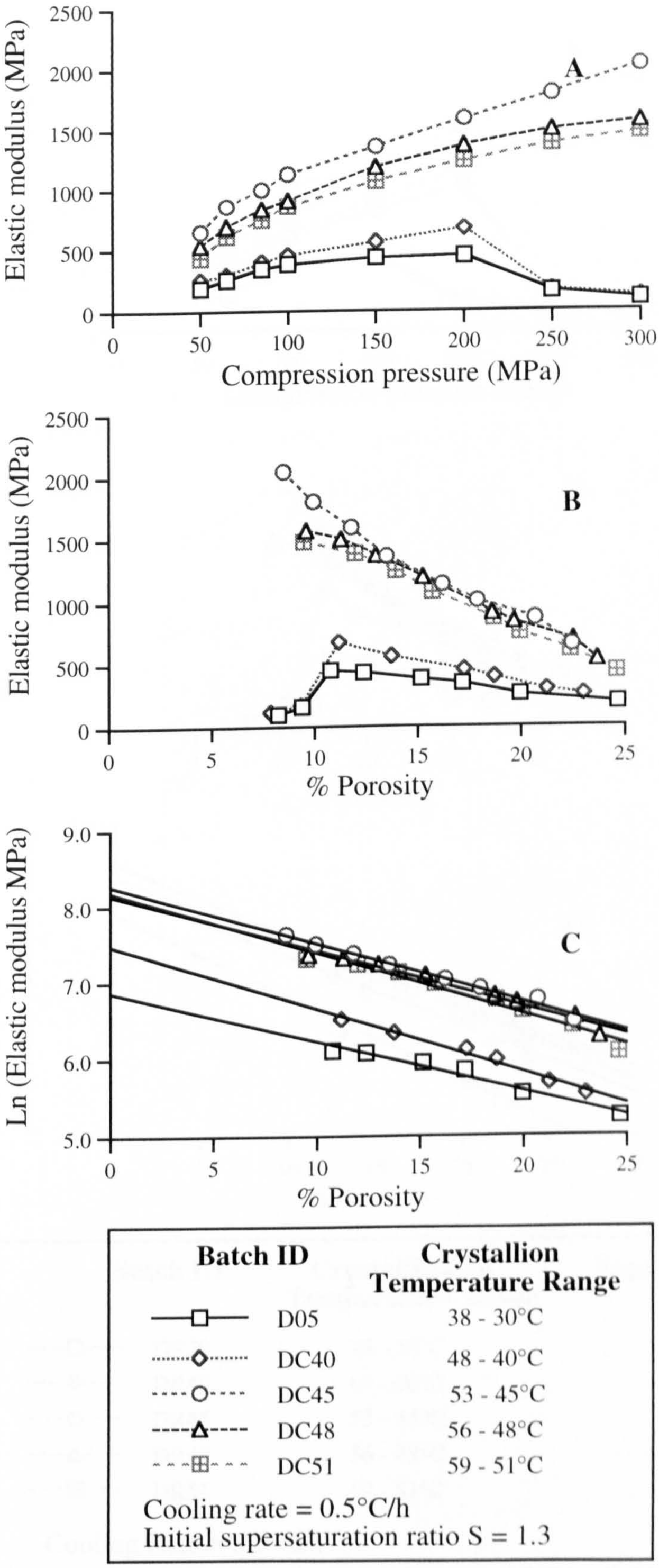

Figure 7.22 (A-C) Effect of crystallisation temperature (constant initial supersaturation ratio) on the elastic modulus of dextrose compacts

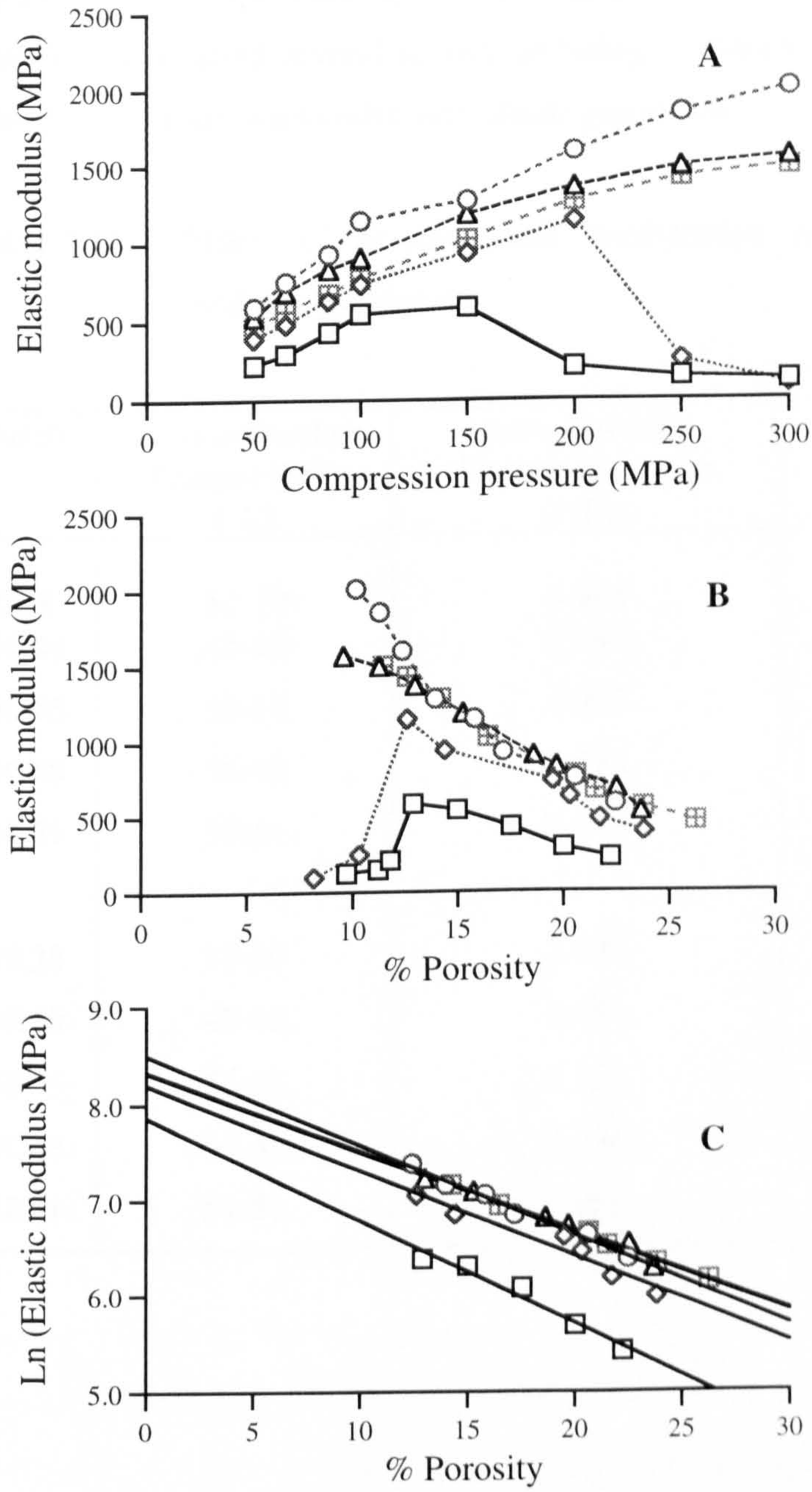

Batch ID		Crystallisation Temperature Range	Superaturation Ratio
—□—	DR30	38 - 30°C	S = 1.6
·····◇·····	DR40	48 - 40°C	S = 1.5
- - - -○- - - -	DR45	53 - 45°C	S = 1.4
----△----	DR48	56 - 48°C	S = 1.3
- - -⊞- - -	DR51	59 - 51°C	S = 1.1

Cooling Rate = 0.5°C/h

Figure 7.23 (A-C) Effect of crystallisation temperature (constant crystal growth rate) on the elastic modulus of dextrose compacts

These changes in both the compact and material elastic modulus of dextrose with crystallisation temperature agree with the previous observations that crystallisation temperature affected several factors including moisture content and crystal structure which are both known to influence elastic properties.

Table 7.12 Effect of crystallisation temperature on the fundamental elastic modulus of dextrose

Batch	Crystallisation Temperature (°C)	Zero Porosity Elastic Modulus (GPa)	r
D05	38-30	0.968	0.986
DC40	48-40	2.067	0.978
DC45	53-56	3.901	0.995
DC48	56-48	3.596	0.994
DC51	59-51	3.575	0.981
DR30	38-30	2.599	0.982
DR40	48-40	3.484	0.985
DR45	53-45	4.536	0.990
DC48	56-48	3.596	0.994
DR51	59-51	3.916	0.995

7.4 The effect of crystallisation conditions on the elastic quotient of dextrose compacts

Another measure of elasticity is the elastic quotient (EQ) defined by Aulton et al., (1974) as:

$$EQ = \frac{\Delta h}{h_1} \qquad \text{(equation 7.1)}$$

where Δ h is the amount of recovery after the load is removed and h_1 is the depth of indentation.

The elastic quotient was determined for those compacts prepared on the tensometer (section 3.4.1) at each compression pressure and are presented in Table 7.13. It was noted that for all the batches there was a general increase in the elastic quotient of the compacts as the compression pressure increased but the most significant change occurred for those compacts which had showed a tendency to cap or laminate Those compacts which did not fail in tension during diametral crushing testing are highlighted in bold type. From these results it is seen that an elastic quotient in excess of 39 % always occurred for compacts which capped or laminated.

7.5 Discussion

The data presented in this chapter shows clearly that modifications to the crystallisation conditions can have significant consequences for the mechanical properties (e.g. Brinell hardness and elastic modulus) of both dextrose and its compacts. Therefore it would seem likely that the crystallisation process could be used as a tool for the deliberate and predictable manipulation of pharmaceutical excipients (and drugs) with the specific aim of engineering materials with optimised mechanical behaviour. The data also confirms that the information gained from the relatively simple and inexpensive indentation apparatus is capable of measuring the mechanical properties of compacts and differentiating between materials which may have only slightly different properties. The application of an extrapolated exponential equation to the compact mechanical data in order to assess the fundamental material properties at zero porosity also appears to be confirmed the extremely good linear correlation obtained and its ability to differentiate between materials prepared using different crystallisation conditions in a way which can be explained by current thinking.

Table 7.13 Elastic quotient values for compacts of dextrose crystallised using a variety of conditions

Batch	Elastic quotient (%) at each compression pressure (MPa)							
	50	65	85	100	150	200	250	300
D05	15.6	17.24	18.3	19.5	22.0	22.6	**46.3**	**54.5**
D1	15.9	16.7	17.4	18.1	21.0	23.0	**55.6**	**54.5**
D10	15.5	17.2	18.3	19.5	22.0	22.6	**46.3**	**54.5**
D30	14.23	15.3	16.9	16.8	22.9	23.3	**54.7**	**54.8**
D50	13.85	14.23	15.9	16.25	21.07	22.85	**54.7**	**56.7**
DS05	10.1	20.4	23.7	26.4	29.4	**44.6**	**53.7**	**57.1**
DS50	14.3	18.3	17.7	19.9	22.7	23.3	**39.2**	**47.5**
D1T	14.7	20.6	22.3	23.8	28.9	33.1	34.8	**59.0**
D30T	22.3	23.6	23.0	24.6	25.5	31.9	34.4	36.1
DX05	14.57	15.3	15.7	15.9	17.7	21.1	**44.7**	**50.2**
DLac	20.1	24.0	26.1	27.8	34.7	36.9	**48.3**	**52.7**
DSuc	19.2	19.1	21.4	22.3	27.9	31.3	**37.1**	**51.12**
DC40	13.8	14.8	16.3	17.4	19.9	20.1	**41.7**	**52.1**
DC45	8.4	11.1	11.2	13.1	14.2	16.6	16.7	16.5
DC48	10.8	14.35	15.5	17.3	19.2	21.9	24.5	26.7
DC51	14.0	20.4	24.0	25.5	29.5	30.3	30.8	32.6
DR30	20.2	20.5	16.3	18.4	17.7	**40.1**	**53.7**	**60.9**
DR40	14.3	16.6	17.9	18.9	22.9	26.1	**49.8**	**56.9**
DR45	13.5	15.4	15.5	15.3	16.6	19.6	18.1	17.6
DR51	14.5	16.1	17.3	17.6	23.4	27.5	30.5	31.8

CHAPTER EIGHT

GENERAL DISCUSSION AND SUGGESTIONS FOR FUTURE WORK

8.1 General discussion

The aims of this thesis were to investigate the role of crystallisation conditions in controlling and manipulating the physicochemical and mechanical properties of dextrose and to elucidate the interrelationships which exist between the crystallisation process, and the fundamental material properties of dextrose and its compaction behaviour.

In an attempt to directly obtain fundamental mechanical data, work was performed in an effort to grow single crystals of dextrose of suitable perfection and size. Although a gel crystallisation technique was identified as a potential crystal growth medium, experiments to grow single crystals of dextrose had only limited success. Single crystals were obtained but they proved unsuitable for mechanical testing due to several reasons:

- their extremely fragile nature (due to the slender crystal habit) prevented handling and testing
- the rate of crystal growth was extremely slow making it difficult to obtain a sufficient number of crystals
- crystals could only be grown using a very limited set of conditions thus preventing an investigation into the effect of crystallisation conditions an the mechanical properties of the crystals.

Investigation into the effect of crystallisation conditions on the physicochemical, mechanical and compaction properties of dextrose produced by batch crystallisation proved much more successful. Batches of dextrose were crystallised using a range of process conditions believed to mimic those used in the commercial production of dextrose and most other pharmaceutical materials. The effect of modifying these crystallisation conditions on the physio-chemical properties of dextrose was assessed using X-ray diffraction studies and by measuring parameters such as true density, bulk density, flowability, moisture content and particle size. The various batches of crystalline dextrose were then compacted and the effect of altering the crystallisation conditions on the compression behaviour of dextrose and the mechanical properties

(i.e. yield pressure, tensile strength, Brinell hardness and elastic modulus) of its compacts evaluated.

The usefulness of the indentation technique to evaluate the mechanical properties of compacts and to differentiate between different materials was clearly demonstrated. It was considered that for this type of study the relatively simple and inexpensive apparatus described had advantages over more technical and more expensive indenters. For example the load used in this study produced indentations in the 5-30 μm range which are thought to avoid many of the problems of surface irregularities often associated with the use of micro and nano indentation techniques which typically produce indents of less than 5 μm.

The capability of assessing fundamental material properties such as elastic modulus from data obtained by testing compacts of dextrose was also illustrated.

The following discussion summarises the results obtained from this study and suggests areas for further research.

Increasing the crystallisation cooling rate resulted in:

- increasing linear crystal growth rates probably due to the maximum level of supersaturation being reached more quickly so increasing the thermodynamic driving force for nucleation and crystal growth
- decreasing true density values indicating a possible reduction in the degree of crystallinity (i.e. a greater number of lattice imperfections caused by the increased linear growth rate)
- a greater number of X-ray diffraction peaks indicating a less ordered system (i.e. more lattice imperfections)
- a reduction of particle size and a more scattered size distribution probably due to the reduction in the overall growth time
- increased poured and tapped bulk density values suggesting subtle changes in the packing characteristics and perhaps crystal habit) of the crystals
- no effect on moisture content

- no effect on the mean yield pressure obtained by either the "ejected tablet" or the "at pressure" methods, suggesting no change in deformation behaviour. Changes to the relative packing fractions were however, observed, indicating possible changes in the packing and rearrangement characteristics of the crystals.
- an increase in both the compact and fundamental mechanical properties (i.e. tensile strength, Brinell hardness and elastic modulus) inferring that bonding capacity was increased, elasticity was decreased and the presence of a greater number of lattice imperfections and defects.

Increasing the initial supersaturation ratio resulted in:

- an increased linear crystal growth rate due to the greater saturation potential and thus greater thermodynamic driving force which would in turn raise the degree of nucleation
- changes to the true density values indicating modification of crystal structure possibly due to different growth mechanism predominating
- no change in moisture content
- the particle size of the batch crystallised using the 59-51°C temperature range increasing while the particle size of the other batches decreased
- an increase in bulk density values of the batch crystallised using the 59-51°C temperature range while the bulk density values of the other batches decreased
- a decrease in the flowability (increased Hausner ratio) was also observed with increasing initial supersaturation ratio
- an increased mean yield pressure value being obtained from both the "ejected tablet" and the "at pressure" Heckel treatments. This implies that increased initial supersaturation resulted in a greater inclination towards consolidation via a fragmentation mechanism
- an increased degree of elastic recovery in the compacts after removal of the compression force and an increased difference between the "ejected tablet" and the "at pressure" mean yield pressures which often indicates a greater likelihood of capping
- an increased compact tensile strength probably due to the fact that a greater degree of fragmentation taking place which resulted in a greater number of bonding surfaces

- an increased fundamental material tensile strength most likely as a result of the increased number of crystal lattice defects which are a consequence of the faster linear crystal growth rates
- an increase in both the compact and fundamental material Brinell hardness and elastic modulus of dextrose. The increased compact properties are thought to be a result of the greater degree of inter-particle bonding while the increased fundamental properties of the crystals are probably a reflection of changes in the crystal structure and defect density due to the increased growth rates and possibly to changes in the dominant growth mechanisms.

Increasing the time available for crystal growth caused:

- no notable change the linear crystal growth rate and thus no change in crystal structure or defect density would be expected
- no marked changes in the true density of the dextrose batches, further indicating that crystal structure was unaffected
- no change in moisture content
- an increase in particle size due to the greater time available for crystal growth
- no effect on either the poured or tapped bulk density values or the flowability of the crystals
- an increase in the "ejected tablet" mean yield pressures signalling a greater degree of fragmentation during consolidation but no change in the "at pressure" mean yield pressure values. The different trends between the two methods suggests an increased degree of elasticity in the compacts with increased growth time. This is confirmed by the elastic recovery results
- no marked effect on the tensile strength of compacts. At higher porosity values the compact tensile strength is actually decreased probably due to the increased elastic recovery outweighing any benefits to the bonding capacity rising from the increased number of fragments (bonding surfaces)
- no substantial changes in either the compact or fundamental material Brinell hardness or elastic modulus values. This is thought to be a reflection of the fact that crystal growth time had no effect on crystal structure.

Increasing the seed crystal, particle size from less than 45 μm to between 63 and 90 μm caused:

- a reduction in the linear crystal growth rate possibly due to a reduction in the actual number of seed crystals available for growth
- a reduction in the true density of the dextrose crystallised, possibly due to a decrease in the number of lattice imperfection as a consequence of the slower growth rate
- no change in moisture content
- an increase in the particle size probably because there was fewer crystals competing for the same amount of solute
- an increase in both the poured and tapped bulk density values and an increase in the flowability of the material, changing from a cohesive material to a relatively free flowing one
- no substantial changes in the mean yield pressure values obtained from either the "ejected tablet" or the "at pressure" Heckel treatments demonstrating that deformation behaviour was unaffected. Elastic recovery, however, was reduced probably due to the changes in the particle rearrangement characteristics as indicated by the changes observed in the relative packing fractions
- an increase in both the compact and fundamental tensile strength. The increased compact tensile strength was probably a result of the decreased elastic recovery while the increased fundamental material tensile is likely to be a consequence of the reduced number of lattice imperfections arising from the decreased linear crystal growth rate
- an increase in both compact and fundamental Brinell hardness and elastic modulus. The increased compact properties are believed to be a result of increased interparticle bonding (tensile strength) arising from the decreased elastic recovery. The increased fundamental material properties are believed to be reflection of changes in the crystal structure such as the degree of crystallinity and defect density resulting from the slower growth rate seen for the dextrose crystallised using the larger seed crystals.

Inclusion of the trace amounts of additives such as lactose or sucrose resulted in:

- a slower rate of crystal growth due to the presence of impurities
- very different true density values reflecting a difference in crystal structure due to the presence of additive molecules in the crystal lattice
- no change in moisture content
- a change in the crystal habit probably due to the additive molecule selectively adsorbing onto particular crystal faces and retarding further growth of those faces
- a reduction in particle size due to the slower rate of growth
- an increase in the poured and tapped bulk density values of both batches and an increase in the flowability of the batch containing sucrose, thought to be a due to the changes in crystal habit
- an increase in the mean yield pressure values obtained by both the "ejected tablet" and the "at pressure" methods signalling a greater propensity towards a fragmentation mechanism for deformation. The relative packing fractions were also affected reflecting the changes in crystal habit.
- no marked change in the elastic recovery results
- no notable change in the compact tensile strength. This was surprising, as the greater fragmentation tendency would have been expected to increase the number of bonding surfaces. The presence of additives molecules may however, have reduced the interparticle attractive forces
- enhanced fundamental material tensile strength possibly as a consequence of the changes in crystal structure which could hinder deformation along particular crystal lattice planes.
- an increase in both compact and fundamental Brinell hardness and elastic modulus most likely as a result of the modified crystal structure being more resistant to deformation along its crystal lattice planes

Increasing the temperature range over which the crystallisations were performed was investigated in two ways. Firstly, the batches were crystallised with a constant, initial supersaturation ratio of 1.3, while a second series were crystallised with a constant linear crystal growth rate. Increasing the crystallisation temperature resulted in:

- increased linear crystal growth rate of those batches crystallised with a constant initial supersaturation ratio. This is believed to a result of the increasing supersaturation potential (i.e. the increasing difference between the saturation concentration and the concentration at the final crystallisation temperature)
- changes to the crystal habit. The batches crystallised over the 59-51°C temperature range were clearly different to those crystallised at the lower temperatures. The habit was identified as being typical of anhydrous dextrose crystals. The batches produced using the 56-48°C temperature range appeared to have some crystals typical of both the monohydrate and the anhydrous forms
- changing true density values, indicating modifications to the crystal structure and supporting the previous findings that crystal habit was altered. For the batches crystallised with a constant initial supersaturation ratio the true density increased steadily with increasing temperature, while for the other series crystallised to have a constant growth rate, no clear pattern was evident, possibly due to the fact that as temperature was increased the initial supersaturation ratio had to be decreased in order to achieve the constant crystal growth rate
- very different X-ray diffraction patterns. As the temperature of crystallisation was increased up to the batch crystallised using the 56-48°C temperature range so more diffraction peaks were observed whilst the batch crystallised using the 59-51°C temperature range had only one significant peak which was similar to that of the anhydrous dextrose reference material. It is thought that the increasing number of peaks in the other samples may be a reflection of the fact that some of the crystal growth occurred above the temperature / solubility transition point and some occurred below it. This resulted in a system containing either, crystals which began life as anhydrous but were latter transformed to the monohydrate form or a mixture of both monohydrate and anhydrous crystals

- moisture content gradually decreased with increasing crystallisation temperature going from a value of approximately 9.1% (typical of dextrose monohydrate) to a value of less than 1% (characteristics of anhydrous dextrose)
- the particle size and the size distribution were clearly influenced by the changes to crystallisation temperature probably as a reflection of the changes in crystal habit
- increasing poured and tapped bulk density values and a notably increase in the flowability of the crystals, going from a cohesive material to a free flowing one. Again this is believed to be a result of changes in the crystal morphology
- changing mean yield pressure values indicating a change in deformation behaviour. For both series of batches the "ejected tablet" mean yield pressure values decreased with increasing crystallisation temperature, suggesting a move towards a more plastic mechanism of deformation. The same trend was also observed for the "at pressure", mean yield pressure values although the effect was less notable. The elastic recovery of the compacts also appeared to decrease with increasing crystallisation temperature.
- a general increase in the tensile strength of compacts until the batch crystallised using the highest temperature range of 59-51°C was compacted. The tensile strength of the compacts prepared from this batch had the lowest tensile strength. These results are thought to be largely a consequence of the changing moisture contents with an optimum value probably being attained for the batch crystallised at the 56-48°C temperature range with a moisture content of approximately 4.7%. The fundamental material tensile strengths increased with increasing crystallisation temperature for the series crystallised with the constant initial supersaturation ratio, again probably as a result of the decreasing moisture contents but decreased for the series crystallised with the constant growth rate
- an increasing compact and fundamental material Brinell hardness for both series of batches probably due to a combination of factors such as crystal growth rates, defect density, crystal structure, growth mechanisms and most importantly moisture content

Clearly, changes to the crystallisation conditions can have a significant effect on a multitude of physicochemical and mechanical properties of dextrose which have serious implications for its use in pharmaceutical operations such as tableting. It

would therefore seem likely that similar interrelationships exist between the crystallisation conditions, material properties and the pharmaceutical application of many other excipients and drug substances.

This study illustrates the need for careful control of crystallisation conditions in order to produce a reproducible material and so eliminate many of the problems associated with the use of materials from different batches and different sources, which are often experienced in pharmaceutical development. This study has also demonstrated the ability of the crystallisation process to be used as a tool for the deliberate manipulation and engineering of materials whose properties could be optimised to suit their intended use. It may therefore be appropriate to consider the crystallisation process as an early step in formulation design rather than simply the final stage of a materials manufacture or purification.

From the crystallisation conditions used in this study it would appear that those used to produce batch DC48 (i.e. 0.5°C/h cooling rate, an initial supersaturation ratio of 1.3 and a crystallisation temperature range of 56-48°C) resulted in the material best suited to use as a direct compression tableting excipient. This material had good flow properties (low Hausner ratio) and produced compacts with good mechanical properties, such as tensile strength and Brinell hardness and showed no significant capping tendency.

8.2 Suggestions for future work

A more detailed study of the solid state properties of materials and their links with processing operations such as tableting would be extremely useful. Therefore a more comprehensive X-ray diffraction study combined with other techniques to determine crystallographic and molecular structural data may elucidate interrelationships which could be exploited in order to engineer materials with optimised material properties.

Important fundamental or intrinsic mechanical properties could be obtained if single crystals suitable for testing were obtained. There are many examples of techniques for growing single crystals and further research may identify a method capable of supporting the growth of single crystals of dextrose that was also flexible enough to

permit an investigation into the effects of changing crystallisation conditions. It should also be possible to employ micro- and nano-indentation which require only very small test specimens to evaluate fundamental mechanical properties. Caution must however, be exercised when using such data to interpret or predict bulk mechanical behaviour as it is likely that the crystallisation conditions used to produce the single crystals will not be those used to crystallise the bulk material and therefore the fundamental material properties of the bulk material.

This study concentrated solely on dextrose as a model material for use as a direct compression tableting excipient. It is envisaged, however, that this type of study could be performed on a range of pharmaceutical excipients and drug substances in order to collect enough data to enable pharmaceutical scientists to reproducibly and predictably modify and engineer materials with the intention of optimising their physicochemical and mechanical properties with respect to any particular pharmaceutical operation.

Appendix 1

Derivation of the equation for calculating elastc modulus from Brinell indentation studies and calculation of the constant K

In Brinell (spherical) indentation the change in the shape of the impression when the load is removed is illustrated in Figure 3.4 where r_1 and r_2 are the radius of the indentation under load, F and after the load is removed respectively. From the classical theory of Hertz (Tabor 1951) the following equation is derived:

$$d = 2.2\left\{\frac{F}{2}.\frac{r_1 r_2}{r_2 - r_1}\left(\frac{1}{E_1}+\frac{1}{E_2}\right)\right\}^{\frac{1}{3}} \qquad \text{equation 1}$$

where E_1 and E_2 are the elastic modulus of the test material and the indenter respectively. From this equation one can derive an equation which permits calculation of elastic modulus from indentation studies. The Poisson's ratios have been assumed a value of 0.3.

It can be seen from the geometry that provided $h < r$, then $h \approx d^2/8r$ (or $d = \sqrt{8hr}$)

and that $$\Delta h = h_1 - h_2 = \frac{d^2}{8}\left\{\frac{r_2 - r_1}{r_1 r_2}\right\} \qquad \text{equation 2}$$

where h_1 and h_2 are the depths of penetration with the load and after the load is removed respectively.

From equation 1 $$\frac{r_2 - r_1}{r_1 r_2} = \frac{2.2^3}{d^3}.\frac{F}{2}.\left(\frac{1}{E_1}+\frac{1}{E_2}\right)$$

where E_1 is the elastic modulus of the test material. E_2 the elastic modulus of the indenter is so large that $1/E_2$ is negligible.

Therefore $$\Delta h = \frac{2.2^{3}}{8d} \cdot \frac{F}{2} \cdot \frac{1}{E_i}$$

The radius of the indenter (r_1) = 7.5×10^{-4}

Thus $$\Delta h = \frac{10.648}{8\sqrt{8h_i 7.5x10^{-4}}} \cdot \frac{F}{2} \cdot \frac{1}{E_i}$$

substituting values $$\Delta h = \frac{10.648}{8 \times 2.828 \times 0.0274 \times h_i} \cdot \frac{F}{2} \cdot \frac{1}{E_i}$$

which leads to $$\Delta h = \frac{17.17}{h_i} \cdot \frac{F}{2} \cdot \frac{1}{E_i}$$

rearranging $$E_i = 8.585 \times \frac{F}{h_i \Delta h}$$

and so $$E_i = K \frac{F}{h_i \Delta h}$$

where K is a constant related to the size of the indenter.

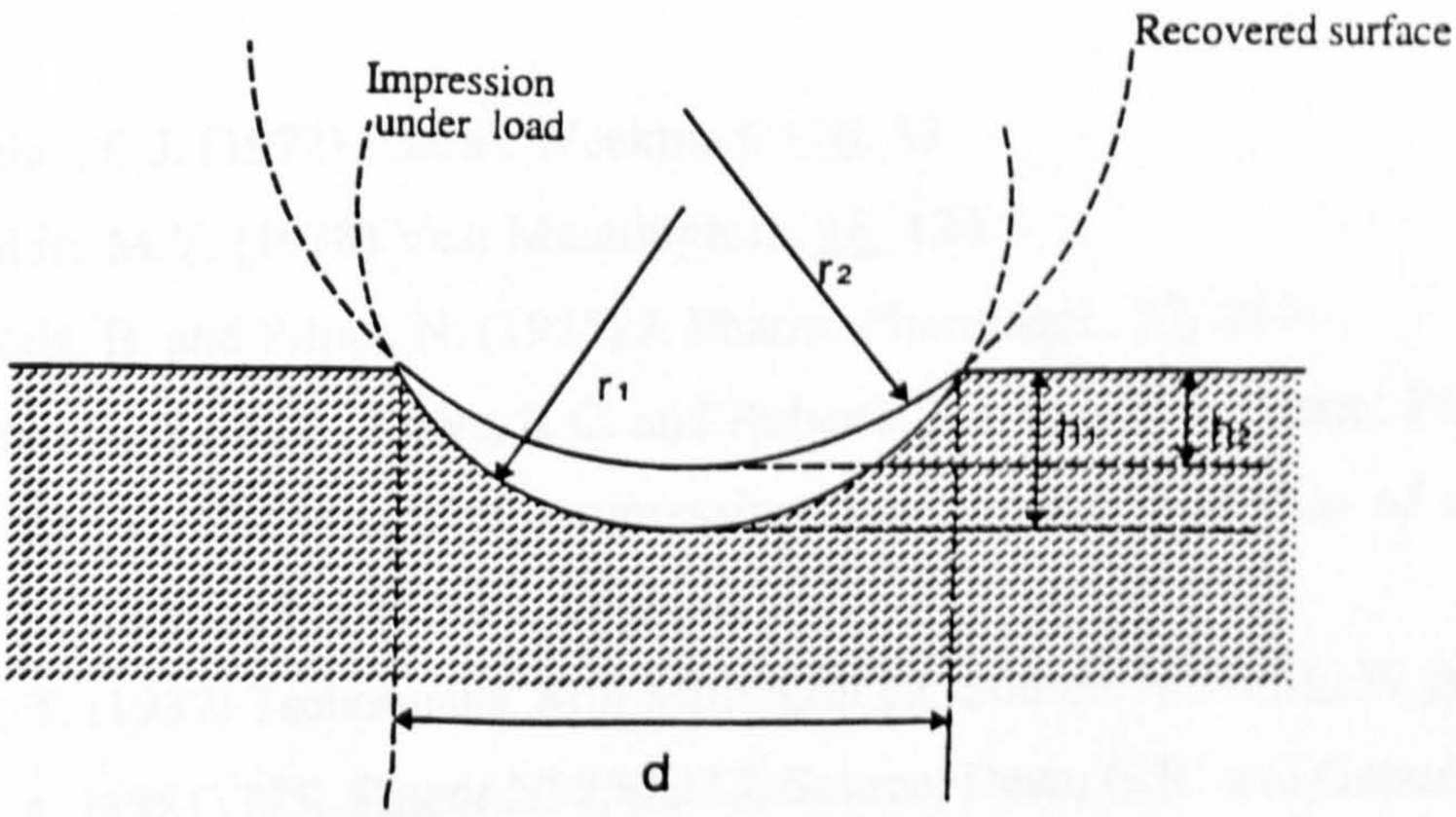

Figure 3.4 The geometry of spherical indentation

Under load the indenter, radius penetrates to a depth of h_1 giving an impression of diameter d. When the load is removed the curvature of the impression increases to r_2 and its depth to h_2.

References

A

Adolfsson, A and Nystrom, C. (1996) Int. J. Pharm., 132, 95

Alderborn, G. (1996) in " Pharmaceutical Powder Compaction Technology" Eds. Alderborn, G. and Nystrom, C., Marcel Dekker New York

Alderborn, G. Borjesson, E., Glazer, M. and Nystrom, C. (1988) Acta Pharm. Suec., 25, 31

Alderborn, G. and Nystrom, C. (1982) Acta Pharm. Suec., 19, 381

Alderborn, G., Pasanesk, K. and Nystrom, C. (1985) Int. J. Pharm., 23, 79

Amidon, G.E. and Houghton, M.E. (1995) Pharm. Res., 12 (6) 923

Armington, A.F. and O'Connor, J. (1968) J. Crystal Growth 4, 367

Armstrong, N.A. (1986) Manf. Chem. 57 (12), 29

Armstrong, N.A. (1989) Int. J. Pharm. 49 (1), 1

Armstrong, N.A. and Haines-Nutt, R.F. (1972) J.Pharm. Pharmacol., 24, suppl. 135P

Armstrong, N.A. and Patel, A.N. (1986) Drug Dev. and Ind. Pharm. 12 (11-13) 1885

Aulton, M.E., Tebby, H. and White, P. J. P. (1974) J. Pharm. Pharmacol., 26, Suppl. 59P

Aulton, M.E. (1981a) Pharm. Acta Helv. 56, 4

Aulton, M.E. (1981b) Pharm Acta Helv. 56, 12

Aulton, M.E., Celik, M. and Travers, D.N. (1984) Proc. 4th Pharm. Tech. Conf., 163, Edinburgh,

Aulton, M.E., Houghton, R.J. and Wells, J.I. (1985) Proc, 5th Pharm. Tech. Conf., Harrogate, 399

B

de Baley, C.J. (1972) Pharm. Weekblad. 106, 57

Bal'Shin, M.Y. (1938) Vest Metalloprom, 18, 124

Bangada, B. and Pilpel, N. (1985) J. Pharm. Pharmacol., 37, 289

Bassam, F., York, P., Rowe, R.C. and Roberts, R.J. (1988) J. Pharm. Pharmacol. 40,. 68P

Bateman, S., The effects of compression speed on the properties of compacts, Ph.D thesis (1988) Liverpool Polytechnic, England

Beck, T. (1939) Tschermaks. Min Miltergrguen: Source, Newkirk, W.B. (1939)

Behr, A. (1881) U.S. Patent N° 250,333, Source, Dean, G.R. and Gotterfried, J.B. (1974)

Bennema, P. and Gilmer, G.H. (1973) The Kinetics of Crystal Growth in "Crystal Growth" Ed. Hartman, P. North Holland, Amsterdam.

Berkovitch-Yellin, J. (1985) J. Am. Chem. Soc., 107, 8239

Bernabe, I., Martin, P., Joris, E., Guyot-Herman, A.M., Conflant, P., Drache, M. and Vanacker-trublin, F., (1997) Pharm. Tech. Eur. 9 (1), 42

Black, D.B. and Lovering, E.G. (1974) J.Pharm. Pharmacol., 11, 295

Blau, P.J. and Lawn, B.R. (1985) Eds. "Microindentation Techniques in Material Science", ASTM special technical publication

de Boer, A.H., Bolhuis, G.K. and Lerk, C.F. (1978) Powder Technol. 20, 75

Bolhuis, G.K. (1988) Manf. Chem., 59, 29

Bransom, S.H., Brown, D.E. and Watts, P., (1969) Proc. Symp. Inst. Chem. Eng., 24

Breenbaun, R. and Brodie, I. (1959) Br. J. Appl. Sci., 10, 281

Brethoud, A. (1912) J. Chim. Phys., 10 624

Burton, W.K., Cabrera, N and. Frank, F.C. (1951) Phil. Trans. Roy. Soc. A243, 299

C

Church, M.S. (1984a) Mechanical characteristics of pharmaceutical powder compacts. Ph.D thesis Nottingham University, England

Church, M.S. (1984) 4th Pharm. Technol. Conf., Edinburgh University, Vol. 1. 185

Chiou, W.L. and Kyle, L.E. (1979) J. Pharm. Sci., 68, 1224

Chow, A.H., Chow, P.K.K., Wang, Z. and Grant, D.J.W. (1985) Int. J. Pharm., 24, 239

Chow, K.Y., Go, J., Mehdizadeh, M. and Grant, D.J.W. (1984) Int J. Pharm., 20, 3

Cooper, A.R. and Eaton, L.E. (1966) J. Am. Ceramic Soc., 45, 97

D

Davey, R.J. (1982) Solvent effects in crystallisation processes, in "Current Topics in Material Science", Vol. 8, Ed. Kaldis, E., Elsevier Press, Amsterdam.

David, S.T. and Augsberger, L.L. (1977) J. Pharm. Sci., 66, 155

Dean, G.R. and Grotterfried, J.B. (1974) Carbohydrate Res., 34, 315

Duberg, M. and Nystrom, C. (1986) Powder Technol., 46, 67

Duncan Hewitt, W.C. and Grant, D.J.W., (1987) Powder Tech. 52, 17

Duncan Hewitt, W.C. and Weatherly, G.C. (1989a) Pharm. Res. 6 (5), 373

Duncan Hewitt, W.C. and Weatherly, G.C. (1989b) Pharm. Res. 6 (12), 1060

Duvall, R.N. and Joshy, K.T. (1965) J. Pharm. Sci. 54 (8) 1196

E

Edwards, L.W., (1982) US Patent No. 4,357,172

Eriksson, M. and Alderborn, G. (1995) Pharm. Res., 12 (7) 1031

Esezebo, S. and Pilpel, N. (1976) J. Pharm. Pharmacol. 28, 8

Etter, M.C., Jahn, D.A., Johnson, B.R. and Ojala, C. (1986) J. Crystal Growth 76, 645

F

Fairbrother, J.W. and Grant, D.J.W. (1978) J. Pharm. Pharmacol. 31, Suppl. 27P.

Fell, J.T. and Newton, J.M. (1968) J. Pharm. Pharmacol., 20, 675

Fell, J.T. and Newton, J.M. (1970) J. Pharm. Sci., 59, 688

Fell, J.T. and Newton, J.M. (1971) J.Pharm. Sci., 60, 1428

Frank, F.C., (1949) Disc. Faraday Soc. 5, 48

G

Gibbs, J.W. (1928) "Collected Works" Longmans Press, London

Gordon, R.E. and Amin, S.I., European Patent N° 0120587

Gonda, I., Abd El Khalik, A.F. and Britten, A.Z. (1985) J. Pharm, Pharmacol., 37, Suppl. 17P.

Grant, D.J.W. and York, P. (1986) Int. J.Pharm., 30, 161

Garti, N. and Tibika, F. (1980) Drug Dev. and Ind. Pharm. 6, 379.

Grerrta, M.K. and Berglund, K.A. (1989) J. Crystal Growth 102, 869

Criffiths, R.V. (1969) Manf. Chem. and Aerosol News, 40 (9) 29

H

Haleblian, J.K. (1975) J. Pharm. Sci., 64 (8) 1269

Haleblian, J.K and Mc Crone, W., (1969) J.Pharm. Sci., 58, 911

Hanoka, J.I. (1969) J. Appl. Phys., 40 (7) 2694

Hardman, J.S. and Lilley, B.A. (1973) Proc. Roy. Soc. A333 183

Hassen, D. (1970) Pharm. Ind. 32, 97

Hartman, P. "Crystal Growth", (1973) North Holland, Amsterdam.

Hatschek, E. (1970) Kolloid Zeitschrift 8, 13: Source Henisch, H.K. (1970)

Heckel, R.W. (1961a) Trans Metall. Soc. A.I.M.E., 221, 671

Heckel, R.W. (1961b) Trans. Metall. Soc. A.I.M.E., 221, 1001

Henderson, N.L. and Brono, A. J. (1970) J. Pharm. Sci 59 (9) 1336

Henisch, H.K., Dennis, J. and Hanoka, J.I. (1965) J. Phys. Chem. Solids 26, 493

Henisch, H.K. (1968) Helv. Phys. Acta., 41, 888.

Henisch, H.K. (1970) "Crystal Growth in Gels", Pennsylvania Univ. Press, London.

Henisch, H.K. (1971) Govt. Rep. Announcement . U.S., 71 (8) 204.

Hersey, J.A., Bayraktar, G. and Shotton, E. (1967) J. Pharm. Pharmacol., 19, Suppl. 24S

Hersey, J.A. and Rees, J.E. (1970) Particle Size Analysis Conf. Bradford Englang,

Hersey, J.A. and Rees, J.E. (1971) Nature, 230, 96

Hersey, J.A, Cole, E.T. and Rees, J.E. (1973) Proc. 1st Int. Conf. on the Compaction and Consolidation of Particulate Material Brighton England

Hess, H. (1978) Pharm. Tech. Int., 2, (9) 38

Heywood, H. (1947) Inst. Chem. Eng., 25, 14.

Hiestand, E.N. (1978) Int. Conf. on Powder Tech. and Pharmacy, Basel, Switzerland.

Hiestand, E.N., Amidon, G.E., Smith, D.P. and Tiffany, B.D. (1981) proc. Int. Powder Bulk Handling and Processing Conf., 1981, Posemount Illinois

Hiestand, E.N. and Smith, D.P. (1984) Powder Tech., 38, 145

Holmes, H.N. (1926): Source Henisch, H.K., (1970)

Humbert-Droz, R., Dolker, E., Gurny, R., and Mardier, P., (1982) Int. J. Pharm. Tech. Prod. Mfr., 4, 29

Huttenrauch, R. (1977a) Pharmazie, 32, 130

Huttenrauch, R. (1977b) Proc. 1st Int. Conf. Pharm. Tech. APGI Paris, Vol. 4, 114

Huttenrauch, R. (1978) Acta. Pharm. Technol., Suppl. 6, 55

Huttenrauch, R. (1983) Pharm. Ind., 45, 435

Huffine, C.L. (1962) Journal Am. Inst. Chem Engrs., 8 (4), 490

Higuchi, T., Nelson, E. and Busse, L.W. (1954) J. Am. Pharm. Assoc. Sci. Edn., 43 (6), 344

I

Ichikawa, J., Imagawa, K. and Kanesiwa, N. (1988) Chem Pharm. Bull. 36, 2699.

Imaizumi, *H.*, *Nambu*, N. and Nagai, T. (1977) Chem. Pharm. Bull., 28, 2565

J

Jackson, F. and Silbee, C.G. (1922) Natl. Bur. Stands. (U.S.) Sci Papers N° 437 17, 715

Jackson, K.A. (1968) "Solidification and Crystal Growth" Macmillan Press, New York.

Jaffe, J., and Foss, N.E. (1959). J. Am. Pharm. Assoc. (Sci. Edn) 48, 26

Jetzer, W., Leuenburger, H. and Sucker, H. (1983a) Pharm. Tech. April 33

Jetzer, W., Leuenburger, H. and Sucker, H. (1983a) Pharm. Tech. Nov 31

Jones, T.M. (1977) Pharm. Ind., 39 (5) 469

Jones, T.M. (1981) Int. Pharm. Tech. and Prod. Manf., 2 (2), 17

Jones, W.D. (1937) Principles of Powder Metallurgy. Ed. E. Arnold. London

K

Kaneniwa, N. Imagawa, K. and Otsuka, M. (1985) Chem. Pharm. Bull. 33, 802

Kawakita, K. and Tsutsumi, Y. (1966) Bull. Chem Soc . Japan, 39, 1364

Kerridge, J.C. and Newton, J.M. (1986) J. Pharm. Pharmacol., 38, Suppl. 78P

Khan, F., Pilpel, N. and Ingham, S. (1988) Powder Technol. 54, 161

Kirchoff, G.S.C. (1811) Academic Memoires, St. Pettesbourg. Source Dean, G.R. and Grotterfried, J.B. (1974)

Kossel, W. (1934) Annln. Phys. 21, 457

Krycer, I. and Pope, D.G. (1982) Drug Dev. and Ind. Pharm., 8 (3), 307

L

Leaucheaux, F., Roberts, M.C. and Manghi, E. (1981) J. Cryst. Growth, 51, 551

Leaucheax, F., Roberts, M.C. and Manghi, E. (1982) J. Cryst. Growth, 56, 141

Leuenberger, H., Hiestand, E.N. and Sucker, H. (1981) Chem. Eng. Tech. 53, 45

Leuenberger, H. (1982) Int. J. Pharm., 12, 44

Leuenberger, H. (1986) Pharm. Res., 3 (2), 12

Lindley, D.V. and Scott, W.F., (1995) 'New Cambridge Statistical Tables' 2nd Edn., Cambridge Univ. Press

Luangtana-Anan, M. and Fell, J.T. (1990) Int. J. Pharm. 60, 197

Ludlam-Brown, I. (1989) Ph.D.thesis Bradford University, England

Ludlam-Brown, I. (1990) 4th AAPS Meeting, Las Vegas U.S.A.

Lum, S.K. and Duncan Hewitt, W.C. *(1996) Pharm.* Res. 13, (11) 1739

M

Marc, K. (1908) Z. Physik Chem. 61, 385

Marsh, D.M. (1964). Proc. Royal Soc. Chem., London A279, 420

Marshall, P.V. and York, P. (1989) Int. J. Pharm., 55, 257

Marshall, P.V. and York, P. (1991) Int. J. Pharm., 67, 59

Martino, P., Martella, S, Guyot-Herman, A.M. Drache, M. and Conflant, P. (1993) Pharm. Sci. 3, 436

Mashadi, A.B. (1988) Mechanical properties of compacted powders, Ph.D thesis University of London, England

Mashadi, A.B. and Newton, J.M. (1987a) J.Pharm. Pharmacol. 39, 961

Mashadi, A.B. and Newton, J.M. (1987b) J.Pharm. Pharmacol. 39, Suppl. 67P

M^{C} Kenna, A. and M^{C} Cafferty, D.F. (1982) J. Pharm. Pharmacol., 15, 412

Metha, S.C., Bernado, P.D., Higuchi, W.I. and Simonelli, A.P. (1970) J. Pharm. Sci., 59, (5) 638.

Michaels, A.S. and Colville, A.R. (1960) J. Crystal Growth, 64, 13

Miers, H.A. (1904) Phil. Trans. Royal Soc., A202, 492

Milosovich, G. (1963) Drug and Cosmet. Ind., 92, (5) 557, 656, 662

Mulhearn, T.O. (1959) J. Mech. Phys. Solids, 7, 85

Mullin, J.W. (1979) in "Industrial Crystallisation " Eds. Jong, E.J. and Jancic, S.J. (1979) North Holland Publishing Company, Amsterdam

Mullin, J.W. (1993) "Crystallisation", Third edition, Butterworth, London

Mullin, J.W. and Jones, A.G. (1974) Chem. Eng. Sci., 29, 1383

N

Nakai, Y, Fukuke, E., Nakajima, S. and Morita, M. (1982) Chem. Pharm. Bull., 30, 1811

Nernst, W. (1904) Z. Physik Chem., 47, 52

Neumann, B.S. (1953) "Powders" in "Flow properties of disperse systems" Ed. Hermans, J.J., North Holland Publishing Co., Amsterdam

Newkirk. W.B. (1924) Ind. Eng. Chem. 16 (11) 1173

Newkirk, W.B. (1925) U.S. Patent N° 1,521,830

Newkirk, W.B. (1939) Ind. Eng. Chem. 31 (1) 18

Nickl, H.J. and Heinsch, H.K. (1969) J. Electrochem. Soc., 116, 1258

Noyes, A.A. and Whitney, W.R. (1897) J. Am. Chem. Soc. 19, 930

Nutter-Smith, A. (1949) Pharm. J. Sept 10th, 46

Nyvlt, J. (1971) "Industrial Crystallisation from Solutions", Butterworth, London.

O

Ostwald, W. (1897) Z. Physik Chem., 22, 289

Otsuka, M. and Kaneniwa, N. (1984) Chem. Pharm. Bull., 32 (3) 1071

P

Pamplin, B.R. (1980) "Crystal Growth" Pergamon Press. Oxford, England

Paronen, P. (1987) in "Pharmaceutical Technology" Ed. Rubinstein, M. H., 139

Paronen, P. and Juslin, M.J. (1983) J. Pharm. Pharmacol., 35, 627

Patel, A.N. (1986) "The influence of water on the compressional properties of some solids" Ph.D thesis, Welsh School of Pharmacy, University of Wales

Patel, A.R, and Roa, V. (1970) J. Crystal Growth 38, 285

Patel, A.R. and Roa, V. (1978) J. Crystal Growth 43, 351

Pikal, M.J., Lukes, A, Lang, J.E. and Gaines, K. (1978) J. Pharm Sci., 67, 767

Prost,C.E.J., and Mumford, N.V.S. (1924) Ind. Eng. Chem., 14, 217

Pollock, A.A. (1973) Non destructive testing 6 (5) 264

Pollock, A.A. (1981) Int. Adv. N.D.T., 7, 215

Pollock, A.A. (1992) ASM Handbook 18

R

Randloph, D., (1970) Chem. Eng. 4th May 80

Rankell, A.S. and Higuchi, T. (1968) J.Pharm. Sci. 57, 574

Rees, J. E., Hersey, J. A . and Cole, E.T. (1970) J. Pharm. Pharmacol. 22 , Suppl. 64S

Rees, J.E. and Rue, P.J. (1978) Drug Devl. Ind. Pharm. 4, 131

Ridgway, K., Shotton, E. and Glasby, J. (1969a) J. Pharm. Pharmacol., 21, Suppl. 19S

Ridgway, K., Glasby, J. and Rosser, P.H. (1969b) J. Pharm. Pharmacol., 21, 245

Ridgway, K. and Aulton, M. E. (1971) J. Pharm. Pharmacol. 23, Suppl. 111S

Ridgway, K., Aulton, M.E., and Rosser, P.H. (1970) J. Pharm. Pharmacol., 22, Suppl. 70S

Ridgway, K. and Shotton, J.B. (1970) J. Pharm. Pharmacol. 22, 24S

Roberts, R.J. and Rowe, R.C. (1985) J. Pharm. Pharmacol., 34, suppl. 25P

Roberts, R.J. and Rowe, R.C., (1986) J. Pharm. Pharmacol. 36, 567

Roberts, R.J. and Rowe, R.C. (1987a) Int. J. Pharm., 36, 205

Roberts, R.J. and Rowe, R.C. (1987b) Chem. Eng. Sci., 42 (4), 903

Roberts, R.J. and Rowe, R.C. (1989) Int. J. Pharm. 37, 15

Roberts, R.J. and Rowe, R.C. (1991) Powder Tech. 65, 139

Roberts, R.J. and Rowe, R.C., (1995) "Mechanical Properties" in Pharmaceutical powder compaction technology, Eds. Alderborn, C. and Nystrom, C., Marcel Dekker, New York.

Rigway Watt, P. (1981) Manf. Chem. 54, 42

Rubinsteien, M.H. (1987) Pharmaceutical Technology (tableting technology), Vol. 1

Rue, P. J and Rees, J.E. (1978) J. Pharm. Pharacol. 30, 642

Ryan, J.A. (1986) J.Pharm. Sci., 75, 805

Ryskewitch, E. and Duckworth, W. (1962) J Am. Ceram. Soc. 4 (5), 97

S

Samuels, L.E., in "Microindentation Techniques in Material Science and Engineering" Eds. Blau and Lawn (1985) ASTM publication

Schubert, H. (1971) Proc. 3rd Eur. Symp. on Comminution, I9, Source Wong (1988)

Seelig, R.P. and Wulff, J. (1946) Trans. Am. Inst. Min Metall. Engrs., 185, 561

Seth, P.L. (1959) Pharm. Ind. 21, 9

Shaw, M.C. and DeSalvo, G.J. (1970) Trans. Am. Soc. Mech. Engrs. B92, 480

Shell, J.W. (1963) J. Pharm. Sci., 52 (1) 100

Sheik-Salem, M. and Fell, J.T. (1982) Acta Pharm. Seuc. 19, 391

Shlanta, S. and Milosovich, G. (1964) J. Pharm. Sci., 53, 562

Shotton, E. and Ganderton, D. (1961) J. Pharm. Pharmacol., 13, Suppl. 144T

Shotton, E., and Rees, J.E. (1966) J.Pharm. Pharmacol., 18, Suppl. 1605T

Shotton, E. and Obiorah, B. (1973) J. Pharm. Pharmacol., 25, Suppl. 37S

Shukla, A.J. and Price, J.C. (1991) Pharm. Res. 8 (3) 336

Suryanarayanan, R. and Mitchell, A.G. (1985) Int. J. Pharm. 24, 1

Stanley, P. (1985) Postgraduate School on Production Processes in Tablet Manufacture School of Pharmacy, University of London

Spengler, H. and Kaelin, A. (1945) Pharm. Acta. Helv., 20 (7), 239

Spriggs, J.M. (1961) J. Am. Ceram. Soc., 44, 628

Springenberg, K. (1934) Handb. der Naturwiss., 362

T

Tabor, D. (1951) "The Hardness of Metals" Clarendon Press, Oxford

Train, D. (1956) J. Pharm. Pharmacol., 8, 745

Train, D. and Lewis, C.L. (1962) Trans. Inst. Chem. Engrs., 40, 235

Turba, E. and Rumpf, H. (1964) Chem. Eng .Tech., 36, 230

V

Valeton, J.J.P (1924) Z. Kristallogr., 60, 1

Van der Voots Maarschalk, K and Bolhuis, G.K. (1998) Pharmaceutical Technology Europe 10 [9 and 10] pages 30 and 28

Van Kamp, H.V, Bolhouis, G.K. and Lerk, C.F. (1986) Int. J. Pharm., 28, 229

Vere, A.W. (1978) "Crystal Growth: Principles and Progress" Plenum Press, New York.

Volmer, M. (1939) Source Mullin, J.W. (1993)

Vromans, H., de Boer, A.H., Bolhuis, G.K., Lerk, C.F., Kussendrager, K.D. and Brosh, H. (1985) Pharm. Weekblad Sci. Ed. 7, 186

W

Wagner, T. (1906) U.S. Patent N° 835,145: Source, Dean, G.R. and Gottfried, J.B. (1974)

Walker, E.E. (1924) Trans. Faraday Soc., 19, 23

Walker, E.E. (1924) Trans. Faraday Soc., 19, 73

Walker, E.E. (1924) Trans. Faraday Soc., 19, 614

White, P.J.P. and Aulton, M.E. (1980) J. Phys. Eng. Sci. Instrum. 13, 380

Whitter, E.O. and Gould, S.P. (1930) Ind. Eng. Chem., 23 (6) 670

Woodhead, P. J. and Newton, J.M. (1984) J. Pharm. Pharmacol. 36, 573

Wong, L.W., and Pilpel, N. (1990) J. Pharm. Pharmacol., 52, 145.

Wong, D.Y.T. (1988) "The deformation of single crystals of lactose" Ph.D thesis Leicester Polytechnic, England

Wong, D.Y.T. and Aulton, M.E. (1987) J. Pharm. Pharmacol., 39, Suppl. 124P

Wray, P.E. (1992) Drug Dev. and Ind. Pharm. 18 (6&7), 627

Wulff, G. (1901) Z. Kristallcyr. 34, 449: Source Wong (1988)

Y

York, P. (1978) J. Pharm. Pharmacol., 30, 6

York, P. (1979) J. Pharm. Pharmacol., 31, 244

York, P. (1983) Int. J. Pharm., 14, 1

York, P. (1992) Drug Dev. and Ind. Pharm., 18 (6&7), 675

York, P. and Grant, D.W.J. (1985) Int. J. Pharm., 25, 57

York, P. and Grant, D.W.J. (1985) Int. J. Pharm. 25, 57

York, P. and Pilpel. N. (1972) J.Pharm. Pharmacol. 24, suppl. 47P

York, P. and Pilpel, N. (1973) J.Pharm. Pharmacol., 25, suppl. 1P

Young, D. (1957) J. Phys. Chem. 61, 616